THE STUDY AND SYNTHESIS OF GROUP 4 TRANSITION METAL COMPLEXES IN ZIEGLER-NATTA CATALYSIS

By

Jonathan P. Corden

A thesis submitted as part requirement for the degree of

Doctor of Philosophy

Department of Chemistry

University of Warwick

August 1997.

CONTENTS

List of Figures, Tables, Schemes and Equations

Tables

Schemes

Equations

Tables

Tables

ACKNOWLEDGEMENTS

The author would like to thank the following people for their help during the course of this work.

Professor M. G. H. Wallbridge and **Professor P. Moore**, for their invaluable advice, guidance and support throughout the past three years.

Dr I. R. Little, of BP Chemicals, for his assistance and help throughout this work.

Dr W. Errington, for his invaluable help and tuition in the art of X–ray crystallography.

Dr J. Hastings, for his assistance in obtaining some of the N.M.R. spectra reported in this work.

Mr I. K. Katyal, for his help by recording most of the mass spectra presented in this thesis.

All the technicians in the Chemistry Department at the University of Warwick especially John Haslop and Harry Wiles.

To the people on the third floor, especially Paul P, Damian and Jase from C304; Steve, Sue and Satty from C303. Further thanks to Steve and Sue for their help with the molecular modelling. To the 5th floor coffee people including Stevie D, Hutch, Rob and Terry and finally to the chemistry football and cricket teams.

A very special thankyou to my wife Sally for all her support and encouragement as well as a wonderful three years.

Finally BP Chemicals and the EPSRC for providing the funding for this work.

DECLARATION

All of the work described in this thesis is original and was, except where otherwise indicated, carried out by the author.

Jonathan Paul Corden

August 1997

Some of the work described in Chapter 2 of this thesis has been published in the following references:

2,2–Dimethyl–1,3–bis(N–salicylideneimine)propane
J. P. Corden, W. Errington, P. Moore and M. G. H. Wallbridge, *Acta Crystallogr.*, *Sect C*, 1996, **52**, 125.

2–[1–[(2–Amino–4,5–dimethylphenyl)imino]ethyl]phenol
J. P. Corden, P. R. Bishop, W. Errington, P. Moore and M. G. H. Wallbridge, *Acta Crystallogr.*, *Sect C*, 1996, **52**, 2777.

Two Schiff Base Ligands Derived from 1,2–Diaminocyclohexane
J. C. Cannadine, J. P. Corden, W. Errington, P. Moore and M. G. H. Wallbridge, *Acta Crystallogr.*, *Sect C*, 1996, **52**, 1014.

Two Schiff Base Ligands Derived from 2,2–Dimethyl–1,3–propanediamine
J. P. Corden, W. Errington, P. Moore and M. G. H. Wallbridge, *Acta Crystallogr.*, *Sect C*, 1996, **52**, 3199.

Two Schiff Base Ligands Derived from 1,2–Diaminoethane
J. P. Corden, W. Errington, P. Moore and M. G. H. Wallbridge, *Acta Crystallogr.*, *Sect C*, 1997, **53**, 486.

ABBREVIATIONS

Bu	butyl
bipy	bipyridine
acac	pentane-2,4-dione
Cp	cyclopentadienyl
THF	tetrahydrofuran
IR	Infra–red
MAO	methylaluminoxane
N.M.R.	Nuclear Magnetic Resonance
ppm	parts per million
δ	chemical shift in ppm
^{13}C	carbon 13 (δ)
^{1}H	proton (δ)
py	pyridine
Mes	mesityl (2,4,6–CH_3–C_6H_2)
Me	methyl
Et	ethyl
Ph	phenyl
Bz	benzyl
CO	carbon monoxide
Å	Angstrom (1Å = 1 x 10^{-10} m)
br	broad
m	multiplet
d	doublet
t	triplet
q	quartet
qu	quintet
M.W	molecular mass
EI	Electron Impact Ionisation
CI	Chemical Ionisation

FAB	Fast Atom Bombardment
nm	nanometres (1nm = 1 x 10^{-9} m)
λ	wavelength in nm
M	metal
TMA	trimethyl aluminium
R, R'	alkyl group
L, L'	ligand
X	halide
DMSO	dimethylsulphoxide
F.T.	Fourier Transform
H_2tmtaa	5,7,12,14–tetramethyldibenzo[b,i][1,4,8,11]–tetaazacyclotetradecine
H_2omtaa	2,3,6,8,11,12,15,17–octamethyl–5,14-dihydro-5,9,14,18-tetraazadibenzo-[a,h]-tetaazacyclotetradecine
H_2SALEN	N,N'-Ethylenebis(salicylideneimine)
H_2SLPNDM	2,2–Dimethyl–1,3–bis(N–salicylideneimine)propane
H_2Hpy	3,7,11,17-Tetraazabicyclo[11.3.1]heptadeca-1(17),13,15-triene

SUMMARY

In this thesis a study of Group 4 transition metal complexes and their possible use as Ziegler–Natta catalysts for alkene polymerisation is described.

Several tetradentate Schiff base ligands have been synthesised and characterised, including some previously unreported examples. The products obtained from the reactions of Group 4 transition metal halides with the disodium salts of these ligands have been isolated and identified. The stereochemistry of these complexes is important for their use as Ziegler-Natta catalysts, and several complexes have been characterised by X-ray crystallography. [Ti(DMSALEN)Cl_2], [Ti(PhSALEN)Cl_2], [Ti(SLPNDM)Cl_2] and [Zr(SLPNDM)Cl_2(THF)] have a *trans*- geometry at the metal, and the complex [Ti(EtCycH)Cl_2] has a *cis*- geometry. The remaining complexes have been studied by molecular modelling to establish a likely stereochemistry.

The reactions of these dichloro complexes with trimethyl aluminium have been studied to gain insight into the chemistry involved in the polymerisation reactions. These reactions proceed with retention of the two chlorine atoms yielding complexes of the type [M(L)Cl_2($AlMe_3$)$_2$] (M = Ti, Zr; L = Schiff base). Side reactions also occur and the by-products [AlMe(EtSALEN)Al(Me)$_2$][$AlMeCl_3$] and [($AlMe_2$)$_2$($AlMe_3$)$_2$(EtSALEN)] have been isolated, and characterised by X-ray crystallography.

Work was also carried out on the synthesis of complexes of the type [MCl_2L] (M = Ti, Zr; L = tetra–azamacrocycle) by the reactions of MCl_4 with the dilithium salt of the ligand. These complexes have been fully characterised and the molecular structure of the complex [Zr(omtaa)Cl_2] determined by X-ray crystallography.

Finally all these complexes have been tested as Ziegler-Natta catalysts for ethene polymerisation. A few selected complexes were also tested for their use in styrene polymerisation and found to be inactive.

Ligands within this thesis

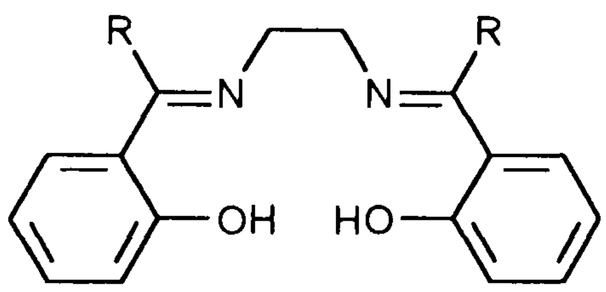

R = Me = H_2DMSALEN
R = Et = H_2EtSALEN
R = Ph = H_2PhSALEN

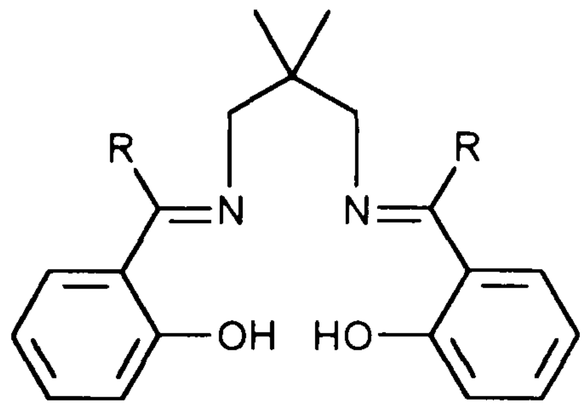

R = H = H_2SLPNDM
R = Me = H_2DMSLPMDM
R = Et = H_2EtSLPNDM
R = Ph = H_2PhSLPNDM

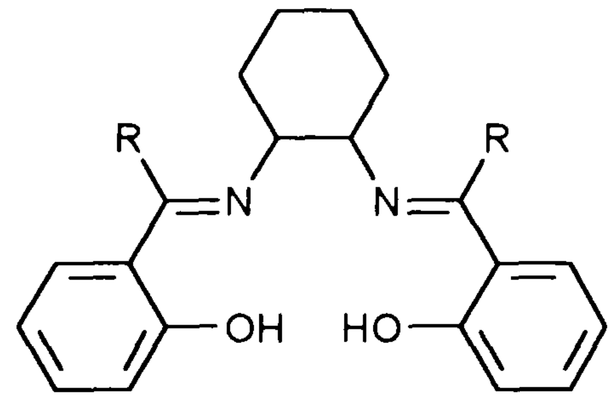

R = H = H_2CycH
R = Me = H_2DMCycH
R = Et = H_2EtCycH
R = Ph = H_2PhCycH

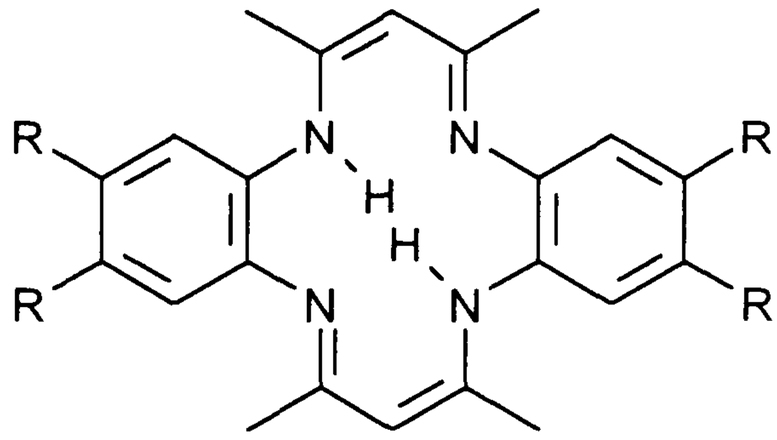

R = H = H_2tmtaa
R = Me = H_2omtaa

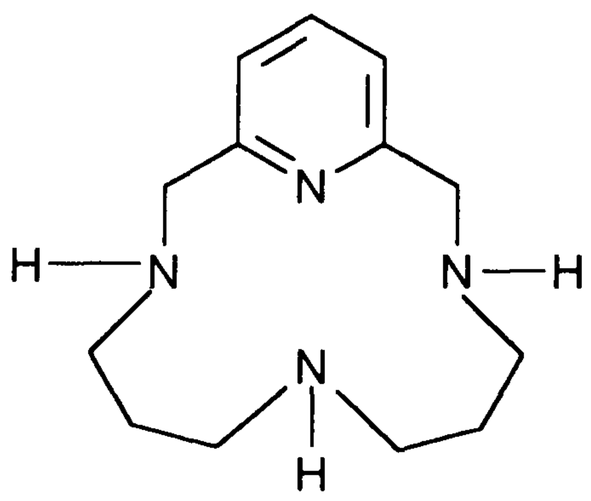

Hpy

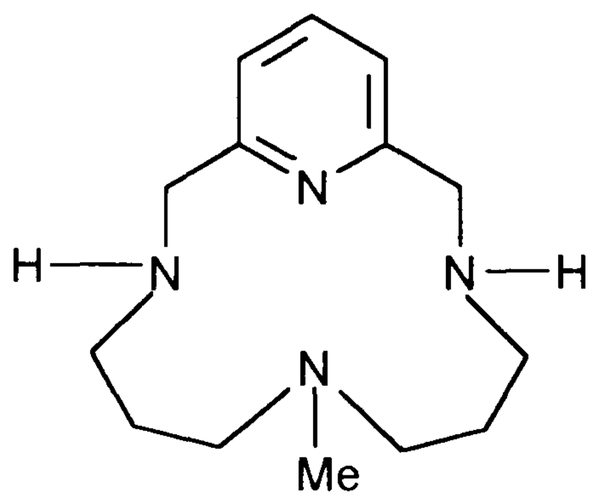

H_2Mepy

CHAPTER 1

INTRODUCTION

CHAPTER 1

Introduction

The general objectives and aims of this research are to find compounds which might act as homogeneous Ziegler–Natta catalysts, initially for the polymerisation of ethene. These aims will be discussed in more detail later in the introduction (see p.28). Also discussed later are alternative compounds to the well-developed *ansa*–metallocene homogeneous Ziegler–Natta catalysts (see p.22). These *ansa*–metallocene complexes are considered to be an 'idealised' model for a catalyst with regard to both steric and electronic effects at the metal centre. With this in mind, ligand systems have been designed and synthesised so that upon complexation with a metal the resulting stereochemistry at the metal centre is similar to that of the *ansa*–metallocene complexes.

The compounds which have been synthesised and discussed in this thesis are mainly Group 4 transition metal complexes, and usually halide-containing compounds. What follows is a general introduction to Group 4 transition metal chemistry followed by an introduction to Ziegler–Natta catalysis and the reasoning behind the work described in this thesis.

Group 4 Transition Metals

The Group 4 metals, titanium, zirconium and hafnium , are d–block elements, each with four valence electrons. For example, titanium has the electronic structure $[Ar]3d^2 4s^2$. The most stable and most common oxidation state of these elements, +4, involves the loss of all these electrons. Titanium can also exist in a range of lower oxidation states, most importantly Ti(III), (II), (0) and (–1). Zirconium and hafnium show a similar range of oxidation states, but the tervalent states are much less stable relative to the quadrivalent state compared with titanium. As a result, the coordination chemistry of zirconium and hafnium is dominated by the oxidation state IV, with only a small number of Zr(III) and Hf(III) complexes being known. Almost all of the latter are metal–trihalide adducts with simple Lewis bases, and only a few

are well characterised. One Zr(III) complex which has been characterised by X–ray crystallography is the chlorine bridged dimer $[\{ZrCl_3(PBu_3)_2\}_2]$.[1]

Table 1.1 Some properties of Group 4 metals.

Property	Titanium	Zirconium	Hafnium
Atomic number	22	40	72
Atomic weight	47.88*	91.22	178.49*
Number of natural isotopes	5 (^{48}Ti; 73.9%)	5 (^{90}Zr; 51.5%)	6 (^{180}Hf; 35.2%)
Electronic configuration	$[Ar]3d^24s^2$	$[Kr]4d^25s^2$	$[Xe]5d^26s^2$
* Atomic weight reliable to ±3 in the last digit.			

The most common coordination number of titanium is six (recognised for all oxidation states of the metal), although compounds exist where the coordination number is four, five, seven or eight. Titanium compounds in the III or lower oxidation states are readily oxidised to the IV state, and titanium compounds can also be hydrolysed to compounds containing Ti–O linkages.

Zirconium and hafnium prefer the higher coordination numbers, especially eight. This preference for Zr(IV) and Hf(IV) follows from the relatively large size and high charge of the +4 ions. These ions have the electronic configuration d^0 and as a result there are no stereochemical preferences due to a partly filled d shell, which results in a variety of coordination geometries. The oxidation states and stereochemistries associated with zirconium and hafnium are summarised in Table 1.2.

Table 1.2 Oxidation states and stereochemistry of zirconium and hafnium.

Oxidation state	Coordination number	Geometry	Example
M^0	6	Octahedral	$[Zr(bipy)_3]$
M^I (d^3)	Complex sheet and cluster structures		
Zr^{II} (d^2)	Complex sheet and cluster structures		
M^{II}	8		$[CpZrCl(dmpe)_2]$
M^{III} (d^1)	6	Octahedral	$[HfI_3]$
M^{IV} (d^0)	4	Tetrahedral	$[Zr(CH_2C_6H_5)_4]$
	6	Octahedral	$[Zr(acac)_2Cl_2]$
	7	Pentagonal bipyramidal	$Na_3[MF_7]$
	7	Capped trigonal prism	$(NH_4)_3[ZrF_7]$
	8	Dodecahedral	$[Zr(C_2O_4)_4]^{4-}$
	8	Square antiprism	$[Zr(acac)_4]$

The following section of this introductory chapter will aim to highlight some of the chemistry and structural features of the Group 4 metals, especially titanium. The topics discussed will, by necessity, be selective, and directed towards the chemistry discussed in this thesis.

Titanium(IV) Halides and their chemistry

The tetrahalides, especially the tetrachloride and tetrabromide, are all powerful Lewis acids and form an extensive series of addition compounds with neutral donors (Lewis bases).[2] Most research on the tetrahalides has centred around $TiCl_4$, but it has been found that TiF_4, $TiBr_4$, and TiI_4 form addition compounds that

are often isostructural to those of the tetrachloride. Titanium tetrachloride is a very important starting material for much of the chemistry of titanium, especially in the organometallic chemistry of the element. Titanium tetrachloride is, for example, used for the synthesis of the organometallic compound bis–cyclopentadienyl titanium dichloride [Cp_2TiCl_2] by reaction with sodium cyclopentadienide.

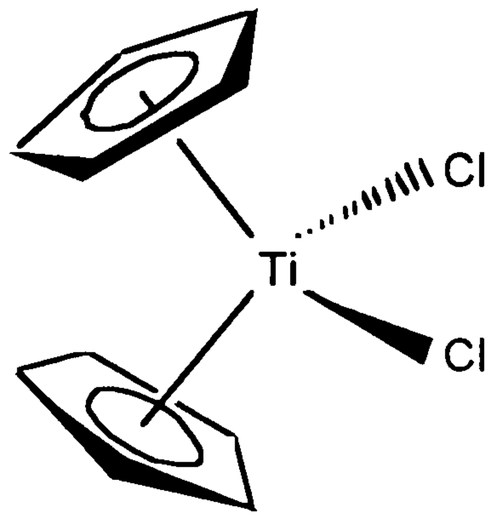

Figure 1.1 Bis-cyclopentadienyl titanium dichloride [Cp_2TiCl_2]

[Cp_2TiCl_2] is a red, crystalline solid[3] and is the principal starting material for much of the reported organometallic chemistry of titanium. The organometallic chemistry of titanium has been covered in several detailed reviews.[4]

Titanium tetrachloride is prepared in a number of ways, one way being the treatment of titanium dioxide with chlorine gas in the presence of carbon.[5]

$$TiO_2 + 2\ Cl_2 + 2\ C \xrightarrow{1000\ ^oC} TiCl_4 + 2\ CO$$

The remaining halides can be prepared from titanium tetrachloride and the appropriate hydrogen halide.[2]

$$TiCl_4 + 4\ HX \longrightarrow TiX_4 + 4\ HCl$$

$$(X = F, Br, I)$$

All the tetrahalides are extremely moisture sensitive, with $TiCl_4$ fuming copiously in air, and reacting vigorously with water to produce titanium dioxide.

$$TiCl_4 + 2\,H_2O \longrightarrow TiO_2 + 4\,HCl$$

Due to this hydrolysis, reactions carried out using titanium tetrahalides must be performed under a dry atmosphere. Some properties of the titanium tetrahalides are shown in Table 1.3.

Table 1.3 Physical properties of titanium tetrahalides

Compound	Colour and physical state	m.p(°C)	b.p(°C)	Structure*
TiF_4	White crystalline solid	–	284(subl)	Fluorine bridged polymer
$TiCl_4$	Colourless liquid	–24.1	136.45	Tetrahedral monomer
$TiBr_4$	Orange crystalline solid	38.25	233.45	Tetrahedral monomer
TiI_4	Dark brown solid	155	377	Tetrahedral monomer
* Data from ref 6				

Addition Compounds of Titanium Tetrachloride.

When discussing the addition compounds of the Group 4 metals thought should be addressed to the ligand donor atom and the metal centre. In oxidation state 0; Ti^0, Zr^0 and Hf^0 are soft acids and as such would be expected to form adducts with soft bases such as CO, PR_3, R_3As, R_2S, etc. An example of one such complex is $[Ti(CO)_2(PF_3)(dmpe)_2]$. When in oxidation state +4, these metal centres are hard acids and therefore would be expected to form addition compounds with hard bases e.g. OH^-, RO^-, NH_3, RNH_2, F^-, Cl^-, etc. Many examples of such compounds are

known e.g. $[TiCl_6]^{2-}$ and $[Ti(acac)_2Cl_2]$. However, even these hard M^{4+} centres can also form adducts with soft bases e.g. $[TiCl_4(diars)_2]$ and $[TiCl_4.2PMe_3]$.

Thus $TiCl_4$ forms adducts with oxygen, nitrogen, sulphur, phosphorus and arsenic donor ligands. In most of these addition compounds the titanium is in an octahedral environment, although coordination numbers of 5, 7 and 8 have also been cited.[2]

$TiCl_4$ Adducts with Monodentate Donor Ligands.

1:1 Adducts Giving $[TiCl_4.L]$ (L = monodentate ligand)

These compounds are well documented and a large number of these have been fully characterised by X–ray diffraction. In these compounds the titanium is often in an octahedral environment by dimerisation through halogen bridges. This can be seen in the THF adduct.

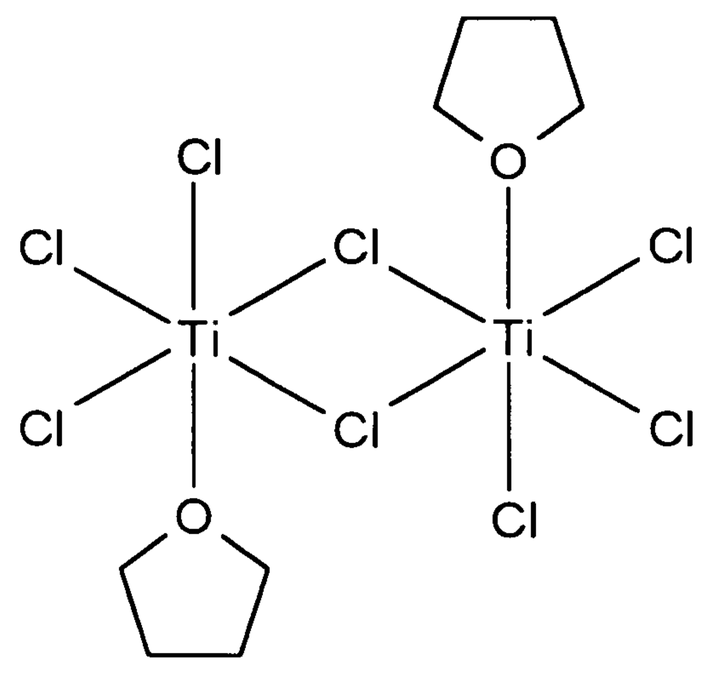

Figure 1.2 A diagrammatic representation of the dimeric 1:1 adduct $[TiCl_4.THF]$

Two types of metal–chlorine stretching vibrations are evident in the IR spectra of these compounds. These are Ti–Cl terminal stretches (in the region 450–350cm^{-1}) and Ti–Cl–Ti bridging vibrations (in the region 300–200cm^{-1}).

One notable, and interesting, exception to the dimeric formulation is the trimethylamine adduct $[TiCl_4.NMe_3]$. This is monomeric, containing five–coordinate trigonal bipyramidal titanium.[7]

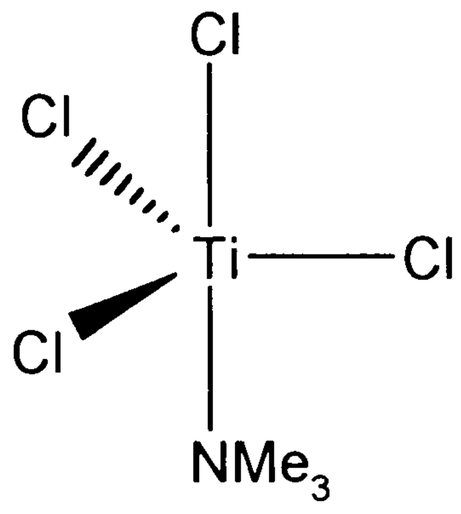

Figure 1.3 A diagrammatic representation of the monomeric [$TiCl_4.NMe_3$] adduct

Since this work Everhart and Ault[8] have studied the reactions of $TiCl_4$ with NH_3 and $(CH_3)_3N$. Cryogenic thin film experiments with these reaction products followed by subsequent warming have led to the formation of interesting amido and imido complexes.

1:2 Adducts Giving [$TiCl_4.2L$] (L = monodentate ligand).

Several of these adducts have been characterised by X–ray diffraction to reveal monomeric, hexa–coordinate titanium species with the donor ligands in a *cis*-configuration, for example where *L* = $POCl_3$, MeCN, and Et_2O.[9,10,11]

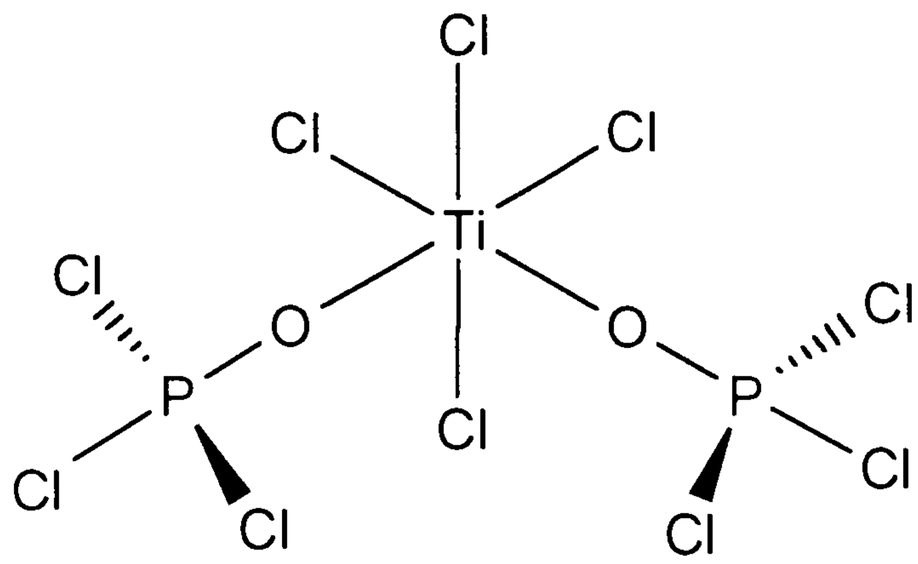

Figure 1.4 A diagrammatic representation of *cis*–[$TiCl_4.2POCl_3$]

The bis–THF adduct [$TiCl_4$.2THF] is a yellow crystalline solid which is relatively easy to prepare.[12] [$TiCl_4$.2THF] is a convenient alternative to $TiCl_4$ as a starting material in the synthesis of many titanium complexes.

Although the *cis*-configuration is seen in the majority of cases, the *trans*-structure is also possible. Research with more sterically hindered ligands has shown that the possibility of forming the *trans*- form tends to increase as the steric bulk of the ligand increases.

Two complexes which have been isolated and characterised as having the octahedral geometry with *trans*-donor ligands are [$TiCl_4$.2$PhCO_2Et$][13] and [$TiCl_4$.2C_5H_5N].[14]

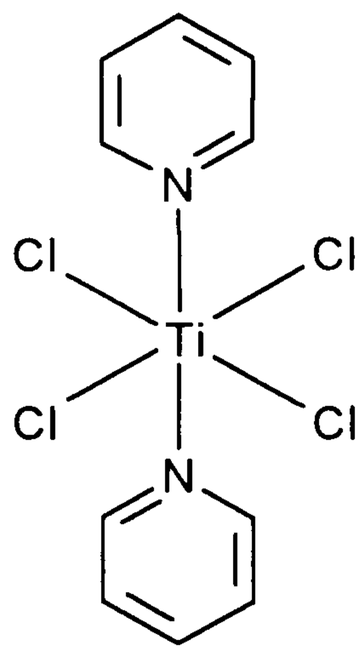

Figure 1.5 A diagrammatic representation of *trans*-[$TiCl_4$.2C_5H_5N]

Certain ligands, such as $POCl_3$[15,9] and EtOAc,[16] may produce 1:1 and 1:2 adducts depending on the reaction conditions. The 1:2 adducts are prepared by distilling $TiCl_4$ into a flask in which excess ligand has been introduced, and any unreacted ligand is then distilled off after the reaction has been stirred for one hour. The 1:1 adducts are prepared by mixing (e.g. EtOAc and $TiCl_4$) in a 1:1 molar ratio at liquid nitrogen temperatures; on warming crystals of the 1:1 adduct are formed. Other ligands such as ketones and acid halides appear to form 1:1 adducts exclusively. It is clear that there is a fine balance between both steric and electronic effects which influence the stoichiometry, and also the structure, in the formation of 1:1 and 1:2 adducts.[17] It is relevant to note here that the possibility of the existence of cationic titanium species in some reactions cannot be overlooked. Indeed there are

many well-characterised cationic species, such as $[CpTi(MeCN)_5][SbCl_6]_3.2MeCN$,[18] and although they will not be discussed in detail here, reference to them will be made as appropriate in the various parts of the thesis.

$TiCl_4$ Adducts with Bidentate Donor Ligands.

1:1 Adducts giving $[TiCl_4.B]$ (B = Bidentate Ligand)

The resulting adduct is generally monomeric with the titanium in an octahedral environment. This has been shown using X–ray crystallography, with ligands such as B = $Me_2C(COMe)_2$[19] and *o*–$C_6H_4(CO_2{}^iBu)_2$.[20]

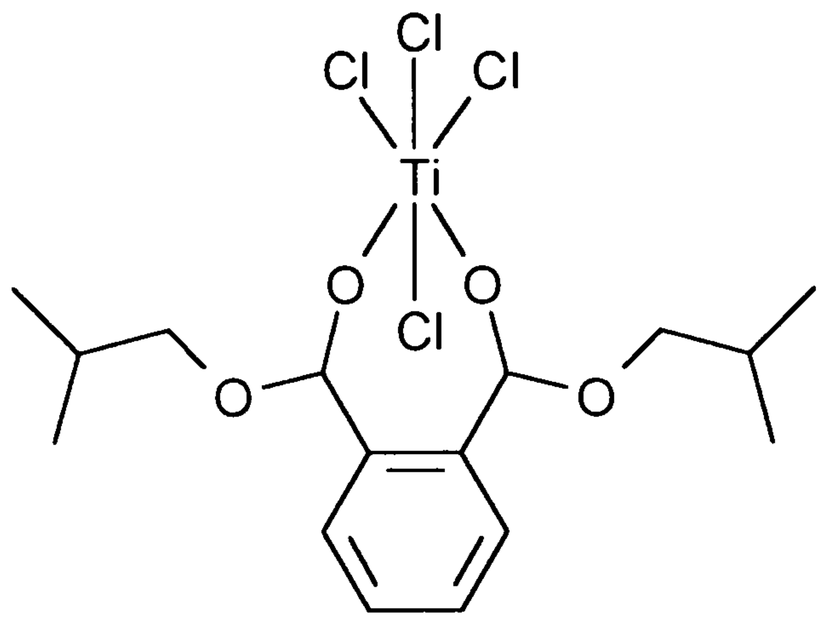

Figure 1.6 A diagrammatic representation of [*o*–$C_6H_4(CO_2{}^iBu)_2.TiCl_4$]

Titanium(IV) Compounds from $TiCl_4$

Titanium(IV) Alkoxides.

As well as forming neutral adducts, $TiCl_4$ reacts with a variety of compounds with the replacement of one or more chlorine atoms. The best studied of these compounds are the titanium(IV) alkoxides. A detailed review of this chemistry has been reported by Bradley.[21] There are two general preparative routes for titanium(IV) alkoxides available:

$$(a)TiCl_4 + 4\ NaOR \xrightarrow{\text{alcohol}} [Ti(OR)_4] + 4\ NaCl$$

$$(b)TiCl_4 + 4\ ROH + 4\ NH_3(\text{anhydrous}) \longrightarrow [Ti(OR)_4] + 4\ NH_4Cl$$

(R = alkyl, aryl)

Method (b) is normally employed because in the absence of a reagent that will remove the HCl, the reaction will only proceed as far as the $[TiCl_2(OR)_2]$ derivative.

Several alkoxy systems have been isolated and structurally characterised, for example $[Ti(OMe)_4]$,[22] $[Ti(OEt)_4]$[23] and $[Ti(OMe)(OEt)_3]$.[24] They exist as tetramers in the solid state and have a $[Ti_4O_{16}]$ framework which demonstrates the preference of titanium for six fold coordination.

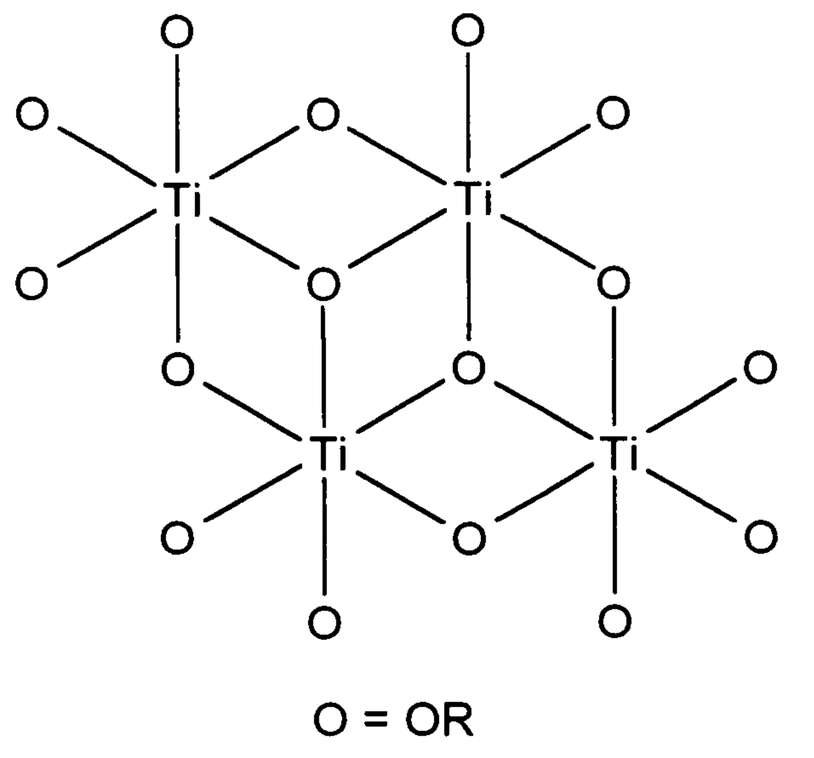

Figure 1.7 The tetrameric $[Ti_4O_{16}]$ framework in $[Ti(OR)_4]$ compounds

In solution, the lower alkoxides have been found to be trimeric. However they are proposed to be monomeric if sterically hindered by a bulky alkyl group. Due to the steric bulk of the phenoxides, $[Ti(OPh)_4]$, such species readily form 1:1 adducts whereas the sterically unhindered methyl and ethyl alkoxides $[Ti(OR)_4]$ (R = Me, Et) do not form 1:1 adducts.[25] This difference in behaviour towards Lewis bases is related to the monomeric, and therefore coordinatively unsaturated, nature of the phenoxides in solution, in contrast to that of the alkoxides.

The lower chain alkoxides are readily hydrolysed by moist air. However, the higher homologues, and the phenoxides are much less susceptible to hydrolysis. With carefully controlled conditions it is possible to isolate polymerisation intermediates. Klemperer and co–workers have carried out controlled hydrolysis reactions to give the polyalkoxides $[Ti_7O_4(OEt)_{20}]$, $[Ti_8O_6(OPh)_{20}]$ and$[Ti_{10}O_8(OEt)_{24}]$ which have been characterised by X–ray diffraction.[26]

A variety of $[TiX_{4-n}(OR)_n]$ (R = alkyl, aryl, alkenyl; X = halogen; n = 1, 2, 3) species are known. All of these compounds are hygroscopic. The compounds $[TiCl_2(OPh)_2]$[27] and $[TiCl_2(OEt)_2]$[28] have been structurally characterised by X–ray crystallography. This reveals that both compounds are dimeric containing penta–coordinate titanium in a trigonal bipyramidal environment. These compounds are generally prepared by direct reaction between the parent tetra–alkoxide and the appropriate molar proportion of the tetrahalide.

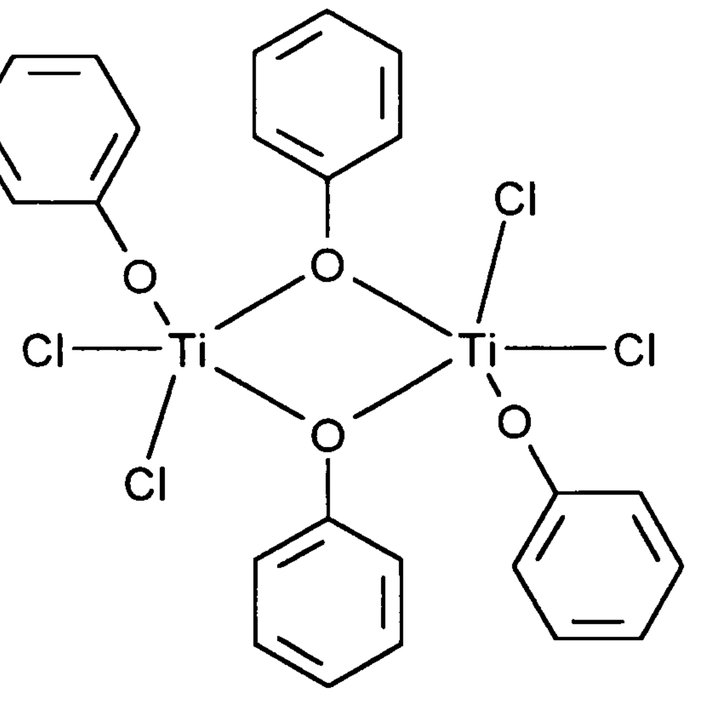

Figure 1.8 A diagrammatic representation of $[TiCl_2(OPh)_2]$

Titanium tetrahalides react with a variety of compounds which contain the hydroxide (OH) group. One class of ligand which will be discussed at length within this thesis, the Schiff base ligand, is an hydroxide containing ligand. Below, the chemistry of other hydroxide containing compounds with TiX_4 will be briefly discussed.

Titanium(IV) Carboxylates

$TiCl_4$ reacts with both aryl and alkyl monocarboxylic acids to produce substituted species with the elimination of hydrogen chloride gas. Ideally the addition of stoichiometric amounts of acid to the reaction system should allow all four substituted titanium compounds to be prepared by the successive replacement of chloride ions by carboxylate ligands. This is shown in the equation below

$$TiCl_4 + x\ RCO_2H \longrightarrow [TiCl_{4-x}(O_2CR)_x] + x\ HCl$$

(R = alkyl, aryl; x = 1, 2, 3, 4)

From the equation we see that the first product arising from the elimination of one mole of hydrogen chloride is $[TiCl_3(O_2CR)]$. Further work is required to establish whether the further substituted products can be obtained, since competing oxygen abstraction reactions can also occur.

Titanium(IV) β–Diketonates

Another type of ligand which contains an OH group are the β–diketonates. Of this class of bidentate chelate ligands the most commonly used is pentane–2,4–dione (acetylacetone,acac). This forms an anion as a result of enolisation and ionisation, as shown in the scheme below, and it is the enolate form which forms very stable complexes with most metals.

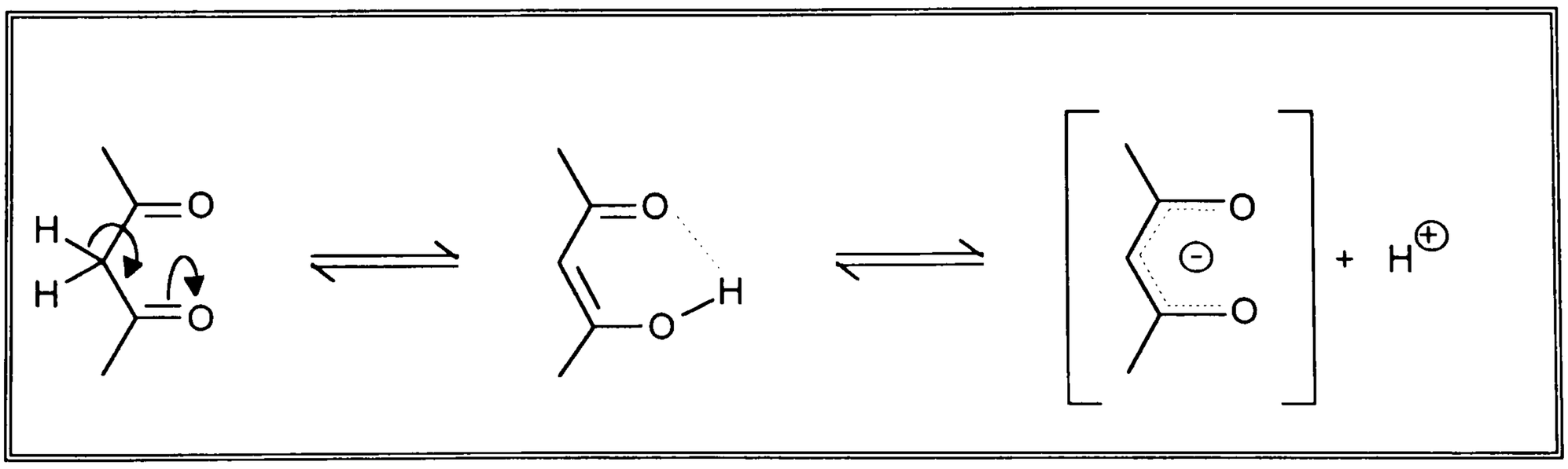

Scheme 1.1 The enolisation and ionisation of pentane–2,4–dione (acetylacetone)

The complex trichloro(pentane–2,4–dionato)titanium(IV) has been fully characterised by X–ray crystallography.[29] In the solid state it is dimeric and is prepared by the direct reaction of $TiCl_4$ with acetylacetone in a 1:1 molar ratio. The disubstituted product $[TiCl_2(acac)_2]$ has also been prepared, and has been assigned as having the *cis*-configuration of the $TiCl_2$ (terminal) group.

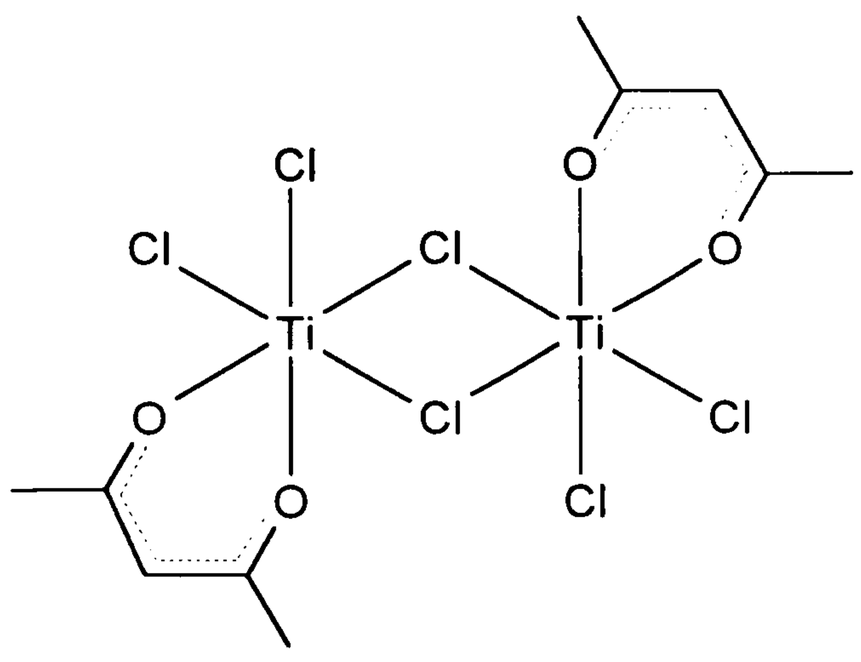

Figure 1.9 The dimeric structure of $[TiCl_3(acac)]$

The organometallic chemistry of the Group 4 metals is very extensive. Many organometallic compounds have been isolated with most of them containing the cyclopentadienyl (Cp, C_5H_5) ligand. This subject is of major importance owing to the facility with which certain organo-Group(IV) compounds catalyse the polymerisation of α–olefins using Ziegler–Natta catalysis.[30] This general topic will now be discussed in more detail in view of its relevance to the work researched within this thesis.

Ziegler–Natta Catalysis

Just over forty years ago Karl Ziegler (1955) noticed that during experiments to synthesise long-chain aluminium alkyls by treating aluminium triethyl with ethene under pressure ('*Aufbau reaction*') transition metal halides had a dramatic effect on the course of the reaction.[31] He discovered that nickel salts led to the dimerisation of ethene to butene, and more importantly that $TiCl_4$ catalysed the polymerisation of ethene to give a relatively high melting linear polymer. Guillo Natta then applied this catalytic system to propene and discovered that it promoted the stereoselective polymerisation of propene.[32] This use of metal halides activated by aluminium alkyls to polymerise alkenes (Ziegler–Natta catalysis) is now one of the most important industrial processes.

Polyethylene, as produced by Ziegler–Natta catalysis, is made up of long chains of CH_2 units which contain very few of the branches typical of polyethylene made using free radical catalysts. However, with polypropylene three structural types are possible

Isotactic

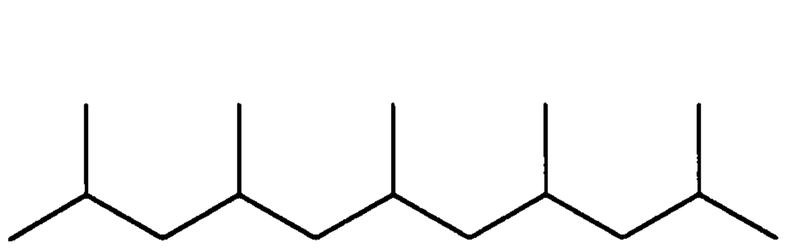

Syndiotactic

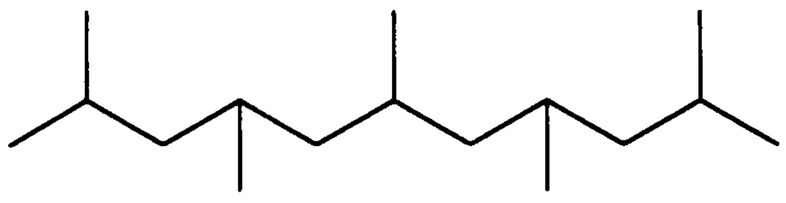

Atactic

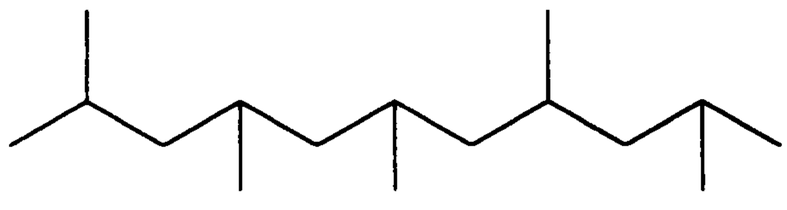

Figure 1.10 Isomers of polypropylene

These different isomers of polypropylene polymer have different properties. Industrially it is desirable to have a polymer with a stereoregular structure (i.e. isotactic or syndiotactic), and Ziegler–Natta catalysts are specifically designed to produce these specific stereoregular types.

The mechanism of Ziegler–Natta Catalysis.

Since the initial discovery of this important class of catalysts, the precise reaction pathway of the process has still not been fully established. It is generally believed that the polymerisation process involves the formation of a complex between the alkene and the active site of the catalyst, followed by a propagation step where the added alkene extends the polymer chain.

The main belief is that propagation occurs at a metal–alkyl bond which could be the transition metal alkyl, the activator alkyl, or an alkyl group which is bridging between these two components. The Cossee–Arlman mechanism[33] is now commonly accepted as the mechanism for alkene polymerisation; the active species is a metal alkyl with a vacant coordination site in a *cis*–position to the alkyl ligand:

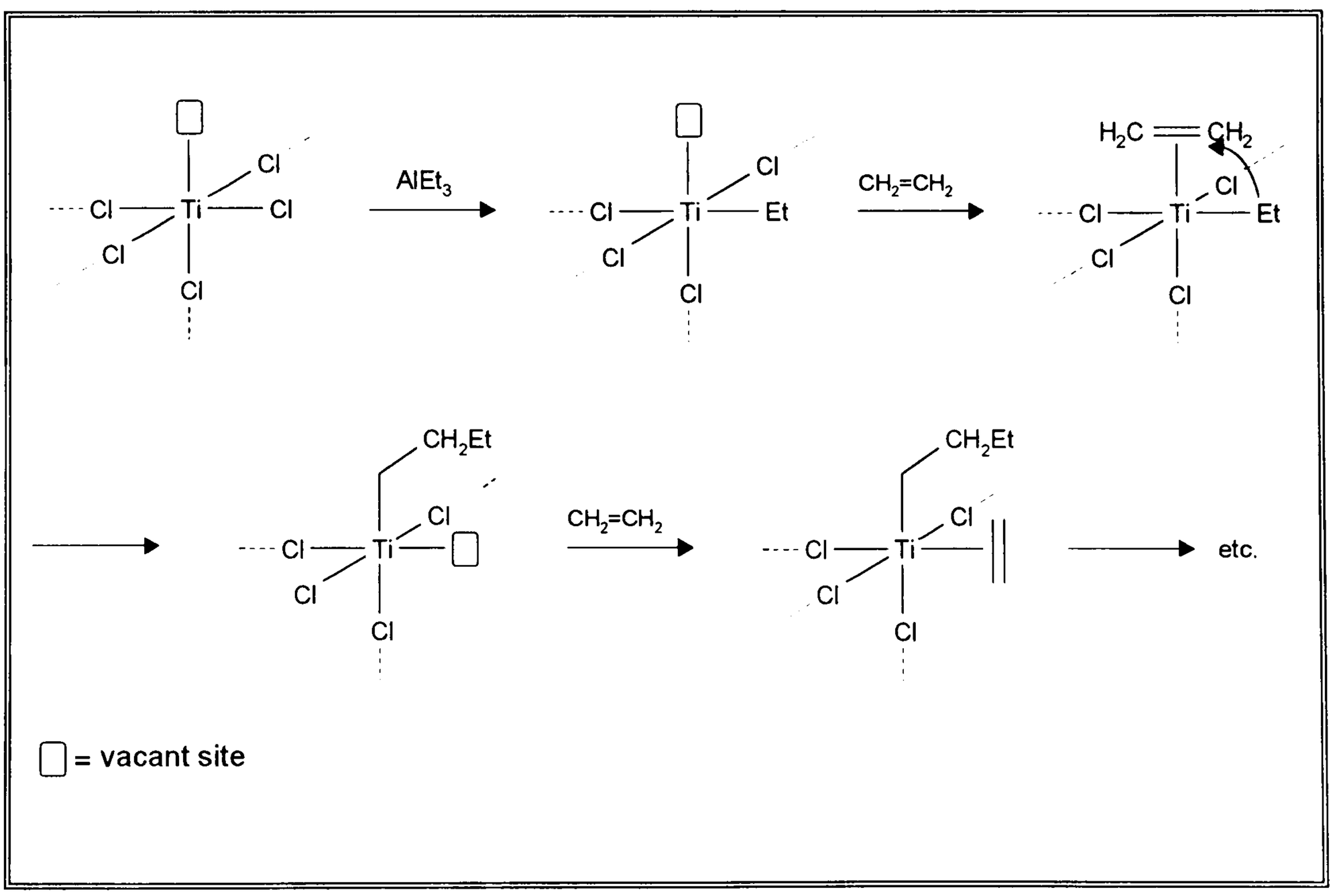

Figure 1.11 The Cossee–Arlman mechanism

The alkene monomer coordinates to the transition metal at a vacant site. The π-coordination of the alkene monomer to the transition metal is shown in Figure 1.12.

This bonding was first developed by Dewar, Chatt and Duncanson where the perpendicular orientation of the alkene situates the filled π and empty π* orbitals properly for overlap with metal orbitals.

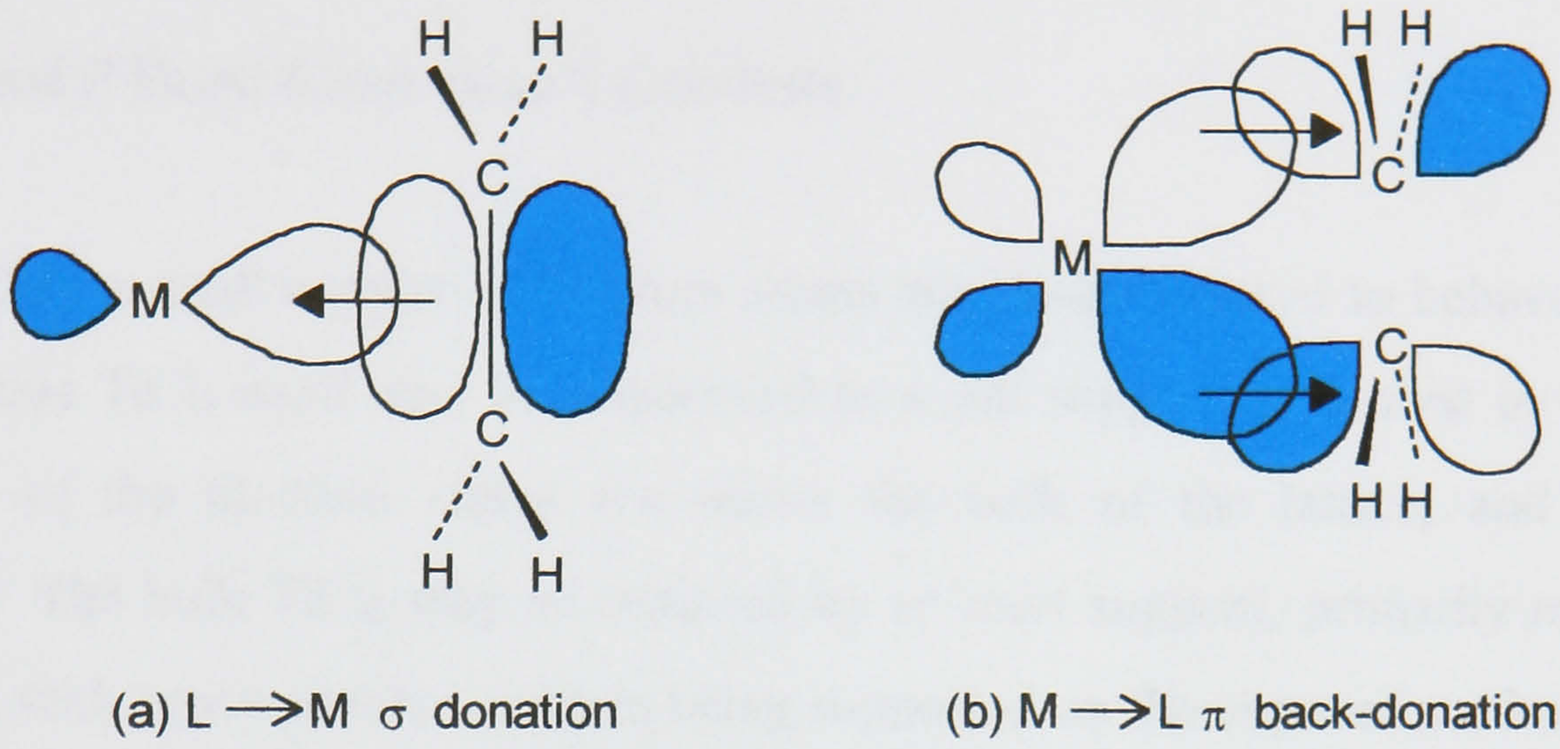

Figure 1.12 The Chatt-Dewar-Duncanson picture of bonding in a metal-olefin complex (Arrows show the direction of electron flow)

The alkyl group is then transferred to the bound alkene, where upon the resulting alkyl group forms a σ-bond to the transition metal atom. The complex then returns to the initial state by exchange of the polymer chain and the vacant site, allowing the polymerisation process to be repeated. The method of alkyl migration/transfer has been studied in detail in metallocene complexes and these results are discussed in more detail in this section (p.19).

Stereoregulation in Propene Polymerisation Catalysts

A successful catalyst in propylene polymerisation is dependent upon its ability to control the stereochemistry of the growth step, so that a crystalline, isotactic polymer can be produced. The history of development of these heterogeneous stereospecific catalysts falls into two main periods. The first period encompasses the $TiCl_3$–based catalysts originally developed by Natta and co–workers ('first generation' catalysts), along with a large number of 'second generation' catalysts based on $TiCl_3$ and modified with organic ligands which behave as Lewis bases. The second period produced the highly stereospecific and productive 'third generation'

catalysts. These latter catalysts involve the use of an inert support (such as magnesium chloride) which stems from the observations that the bulk of the titanium sites within the $TiCl_3$ lattice are inactive.

Supported ('Third Generation') Catalysts.

Only a small number of titanium atoms are ideally situated to behave as active sites. Thus $TiCl_3$ itself may be considered as a self supported catalyst in which the majority of the titanium atoms are within the bulk of the lattice, and therefore inactive. The bulk $TiCl_3$ may be replaced by an inert support, primarily magnesium chloride, with active titanium centres being supported on the exposed surfaces.

The choice of components of a successful supported catalyst for the polymerisation of propene is limited, and in practice a titanium(IV) compound is used instead of $TiCl_3$. Typically, these types of catalyst comprise of magnesium chloride, an aromatic ester (e.g. ethyl benzoate), and titanium tetrachloride which is used in conjunction with a trialkylaluminium compound combined with another aromatic ester (e.g. $AlEt_3$ with ethyl anisate).

Milling of the magnesium chloride increases the surface area and creates disorder and defects in the lattice. Titanium tetrachloride is then absorbed onto the surface giving a monolayer of active titanium sites. No other support for $TiCl_4$ functions as well as $MgCl_2$ which is probably a consequence of the comparability of the ionic radii of Ti^{4+} and Mg^{2+} which are very similar at 0.68 and 0.65Å respectively.

If a Lewis base is present when the $MgCl_2$ is milled, the surfaces are rapidly complexed, thus preventing the reagglomeration of the $MgCl_2$ particles and increasing the activity of the system even further. Although this may be achieved with a variety of Lewis bases, high stereospecificity is only achieved by aromatic esters. The most successful results have been obtained with the use of methyl and ethyl esters of benzoic, toluic or anisic acids. The reason for this remains obscure but may well be associated with their ability to impose a favourable steric and electronic arrangement at the titanium centre.

Group 4 Metallocene Complexes and Catalysis.

Since the discovery of the $TiCl_4/AlEt_3$ Ziegler–Natta catalysts, the polymerisation of α–olefins has developed into a major industry. Industrial processes often use heterogeneous (or supported) catalysts which have been specifically designed to be highly selective and efficient. However, as the catalysis takes place on the edges and at dislocations of the support system, coupled with the titanium centre, the resulting polymer has a broad molecular weight distribution.[30] The properties of these catalysts and the coordination geometry of the reaction centres is uncertain due to the non-uniformity of active sites, and the limited information available on their structural detail.[34]

As a result it was hoped that homogeneous organometallic catalysts capable of stereoselective α–olefin polymerisation would allow direct observations on the active site involved, and hence the mechanisms of polymer growth and its stereochemical control to be both determined and controlled.[35]

After the synthesis of the first Group 4 metallocenes by Wilkinson *et al*,[36] it was reported that homogeneous reaction mixtures of dicyclopentadienyl titanium dichloride [Cp_2TiCl_2] (Figure 1.1) and diethyl aluminium chloride could be used as homogeneous Ziegler catalysts, and these catalysts do indeed possess moderate activity.[37,38] However these homogeneous catalysts did not show any activity for polymerisation with propene. Another problem which was found to exist with these catalysts was that they were easily reduced to an inactive Ti(III) species and as a result were unable to compete with the highly active heterogeneous catalysts.

A major advantage with these metallocene based catalysts was their solubility, since this allowed better kinetic data to be obtained, leading to proposals of the possible reaction pathway. As explained previously such studies involving heterogeneous catalysts are understandably less well defined. Consequently numerous studies were aimed at the identification of reaction intermediates and reaction mechanisms of these homogeneous catalysts. Breslow and Newburg[39] suggested that in their [Cp_2TiCl_2] / [Et_2AlCl] system alkylation of the transition metal is first achieved, to form [Cp_2TiRCl] by ligand exchange with the alkyl aluminium

cocatalyst. This then forms a halide–bridged binuclear complex that has the ability to react with ethene.

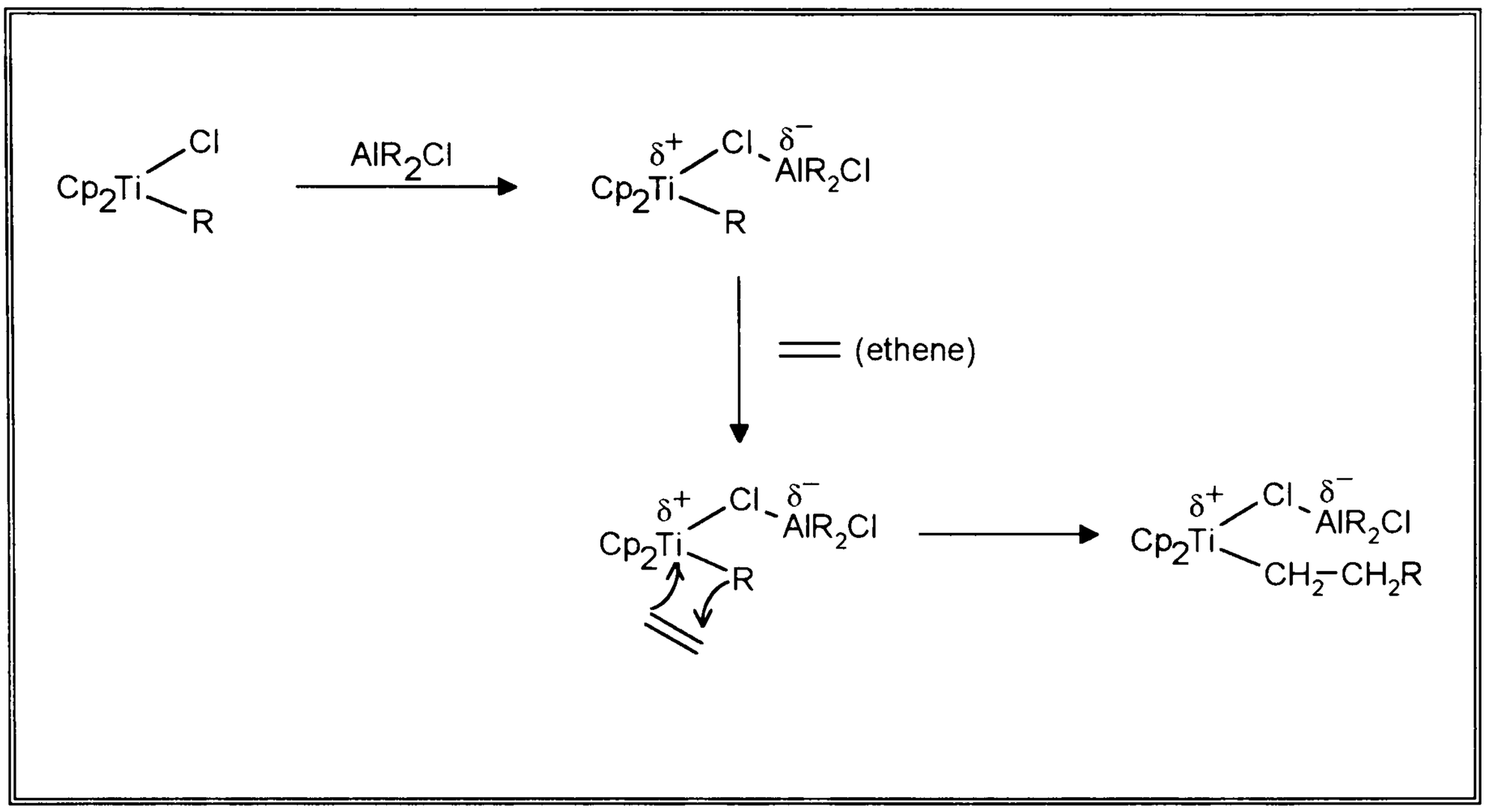

Figure 1.13 The pathway of polymerisation suggested by Breslow and Newburg

It was envisaged that there was polarisation of the molecule with a partial positive charge on the titanium and negative charge on the aluminium. This early metallocene work by Breslow, and subsequent studies by Chien,[40] contributed to the verification of the ideas put forward in the Cossee–Arlman mechanism for heterogeneous Ziegler–Natta catalysis.[33] These studies did not however resolve the nature of the active species. One possibility is that alkene insertion occurs into a bimetallic species, in which an alkyl group or halogen bridges the titanium and aluminium centres.[41-44] Another suggestion requires the formation of a truly ionic species $[Cp_2TiR]^+$ by abstraction of a halide anion and its incorporation into an anion $[R_xCl_{4-x}Al]^-$.[45] There was no direst evidence for the existence of such a species until Eisch *et al*[46] discovered that $PhC \equiv C\text{-}SiMe_3$ reacted with $[TiCl_2Cp_2]$ in the presence of $AlCl_2Me$ to give the cationic titanium vinyl complex (Figure 1.14).

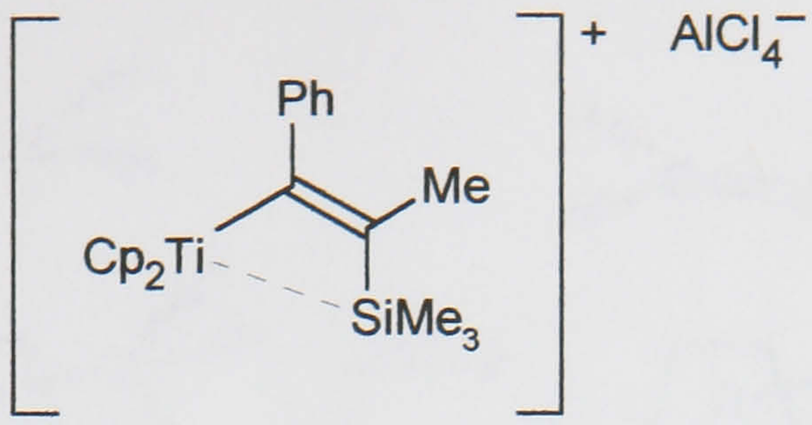

Figure 1.14 The cationic titanium vinyl complex.

Subsequent studies by Jordan *et al*[47] isolated the tetraphenyl borate salts of cations such as $[Cp_2ZrCH_3.THF]^+$ and $[Cp_2ZrCH_2Ph.THF]^+$ which polymerised ethylene without the addition of any activator. These and related findings in the groups of Bochmann,[48] Teuben,[49] and Taube[50] established that (alkyl)metallocene cations are crucial intermediates in homogeneous polymerisation catalysis. Such a complex has two low lying unoccupied orbitals d_π and d_σ (Figure 1.15)[51] where the d_σ orbital acts as the acceptor for the incoming alkene molecule.

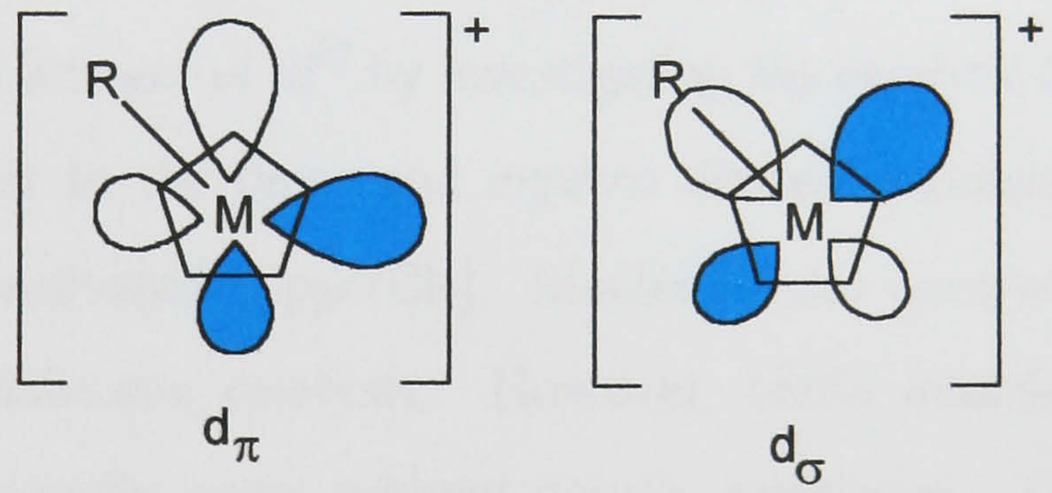

Figure 1.15 Showing the two low lying unoccupied orbitals dπ and dσ

The chain growth mechanism as well as the structure of the transition state in the polymerisation reaction have attracted considerable attention. Brookhart *et al*[52] suggested that the insertion of an olefin into the metal-alkyl bond is facilitated by an agostic interaction of one of the α-H atoms of the metal-bound alkyl chain with the metal centre of the Ziegler-Natta catalyst (Figure 1.16).

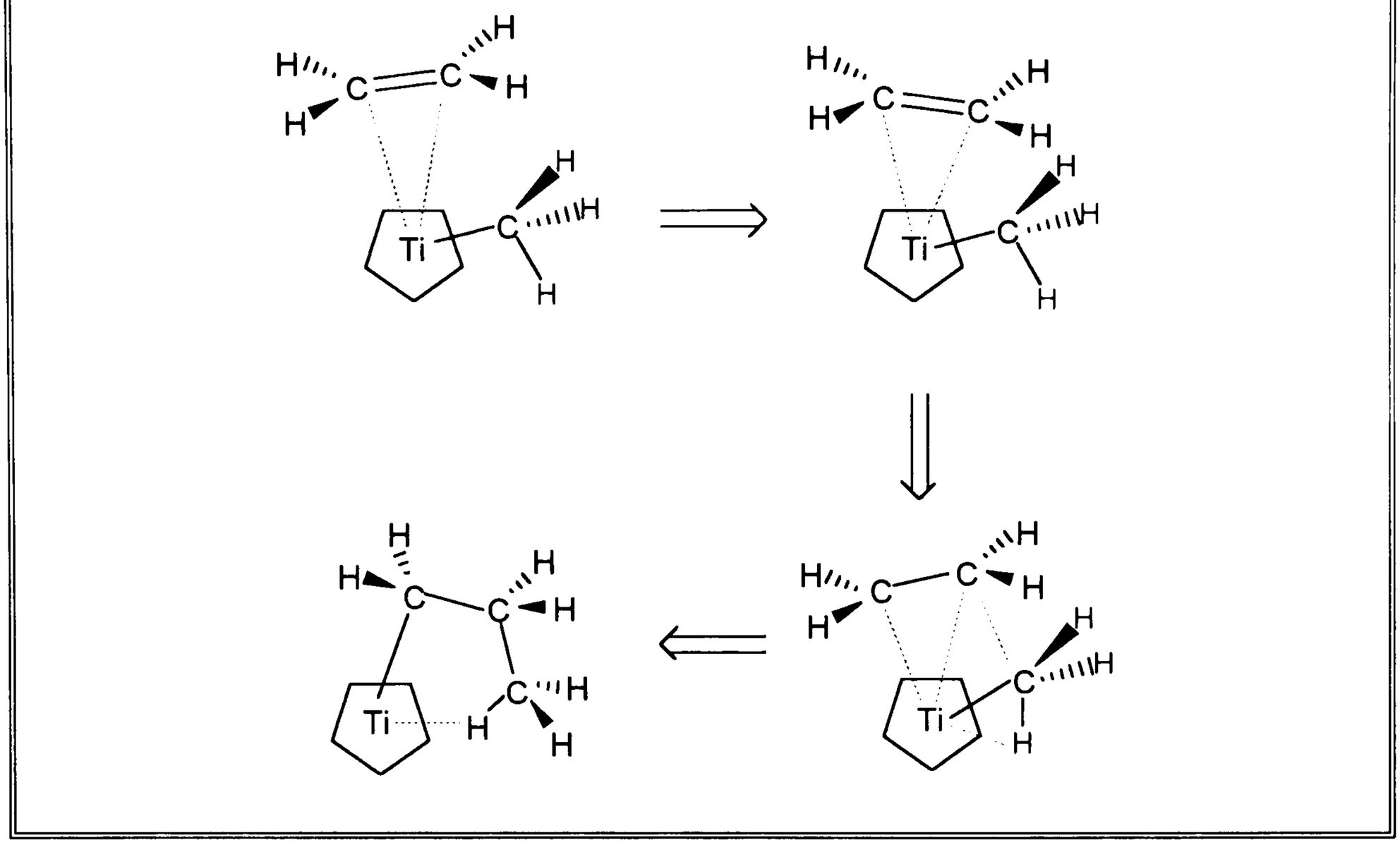

Figure 1.16 Showing the insertion step facilitated by an agostic interaction

The participation of an α-agostic interaction during the chain growth process was demonstrated by Brintzinger *et al*[53] by investigating the catalytic hydrodimerisation of α-deuterated hexanes to the *threo* and *erythro* diastereoisomers of 5-CH_2D-6-[D]-undecane by MAO-activated [Cp_2ZrCl_2]. Similar results were obtained by Piers and Bercaw[54] using scandocene catalysts. However, olefin insertions into metal-alkyl species might occasionally occur without agostic assistance. There have also been numerous theoretical studies on olefin insertion into the metal-alkyl bond of a cationic metallocene complex of the type $[Cp_2MMe(olefin)]^+$ (M = Ti, Zr).[55] Most of these studies concur with the view that in the insertion transition state one α-H atom of the migrating M-CH_2R group is in close proximity to the metal centre and that this M-H interaction is due to an α-agostic bond.

MAO cocatalysts.

The next major development came with the unexpected discovery that although these catalysts are very sensitive to hydrolysis, traces of water were found to

increase the rate of polymerisation in titanocene catalysts. The partial hydrolysis of the aluminium alkyl component to form aluminoxanes was postulated for the increase in activity.[56,57]

Sinn and Kaminsky, whilst studying the inactive system $[Cp_2ZrMe_2]/AlMe_3$ noticed that upon the addition of water the system became highly active towards ethene polymerisation.[58] This was attributed to the partial hydrolysis of $AlMe_3$ to give methylaluminoxane (MAO), and they found that the partial hydrolysis of $AlMe_3$ to MAO before the addition of the transition metal complex ($[Cp_2ZrCl_2]$ or $[Cp_2ZrMe_2]$) gave exceedingly active catalysts for the polymerisation of ethene.[59] Further support for the formation of MAO was established by its direct synthesis and characterisation as oligomers of the approximate composition $[(MeAlO)_n]$.

MAO is a polymeric glassy substance which consists of linear, cyclic and cross–linked compounds, probably mainly consisting of complexes with four coordination aluminium centres and some $OAlMe_2$ end groups.[60]

Sinn and Kaminsky[58] also showed that MAO activated homogeneous metallocene dihalide catalysts, in contrast to catalysts activated with aluminium alkyl halides, and these were capable of propene polymerisation. These simple homogeneous zirconocene catalysts however lack the stereoselectivity of the heterogeneous Ziegler–Natta catalysts. In order to achieve a high activity with these catalysts the MAO has to be used in a large excess, typically Al:Zr ratios 10^3–10^4:1, making the MAO the most costly consideration in these catalytic systems. Despite this, MAO is widely used as an activator even on an industrial scale.

Ansa–metallocenes

The discovery that these homogeneous metallocene dihalide catalysts were capable of polymerising propene and higher α–olefins revived the question of whether it would be possible to induce stereoregular homogeneous polymerisations to produce isotactic polymer by using specifically designed metallocenes

A significant development came with the synthesis of complexes where the two cyclopentadienyl ligands are tethered by an interannular bridge and behave as bis(pentahapto) chelates in metallocene complexes, the so–called *ansa*–metallocenes.

This interannular bridge restricts the normally free rotation of the cyclopentadienyl rings.

The first examples of *ansa*–metallocenes $[TiCl_2\{(CH_2)_n(C_5H_4)_2\}]$ (n = 1, 2) were reported by Brintzinger and co–workers in 1979.[61] The standard method of preparation of *ansa*–metallocenes is the reaction of the dilithium salt of the bridged bis(cyclopentadienyl) dianion with $TiCl_3$ or $TiCl_3(THF)_3$ followed by hydrolysis with HCl and atmospheric oxidation.

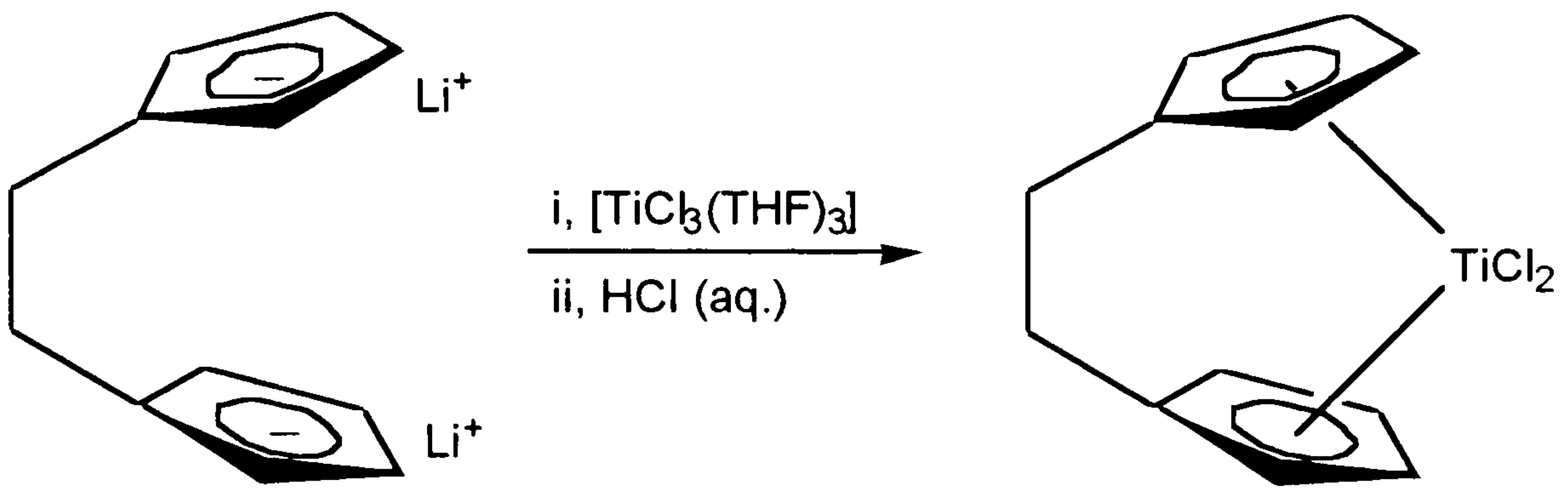

Equation 1.1 The preparation of *ansa*–metallocenes

It was the introduction of further substituents onto each cyclopentadienyl ring of the bridged ligand producing chiral metallocene complexes which became of great interest as potential catalysts for stereospecific alkene polymerisations.

The introduction of chirality into the *ansa*–metallocene results in the formation of two isomers i.e. *rac* and *meso*. The *rac*:*meso* ratio of products formed from the synthesis reaction varies depending on the substituent used, and this ratio can be affected by the addition of substituents on the bridge. The chirality within the metallocenes can be introduced in several ways producing the *rac* and *meso* isomers. The ways in which chirality in *ansa*–metallocenes can be achieved are the introduction of alkyl groups on the cyclopentadienyl rings, the introduction of conformationally restrained bis(indenes) and by the addition of substituents onto the interannular bridge.

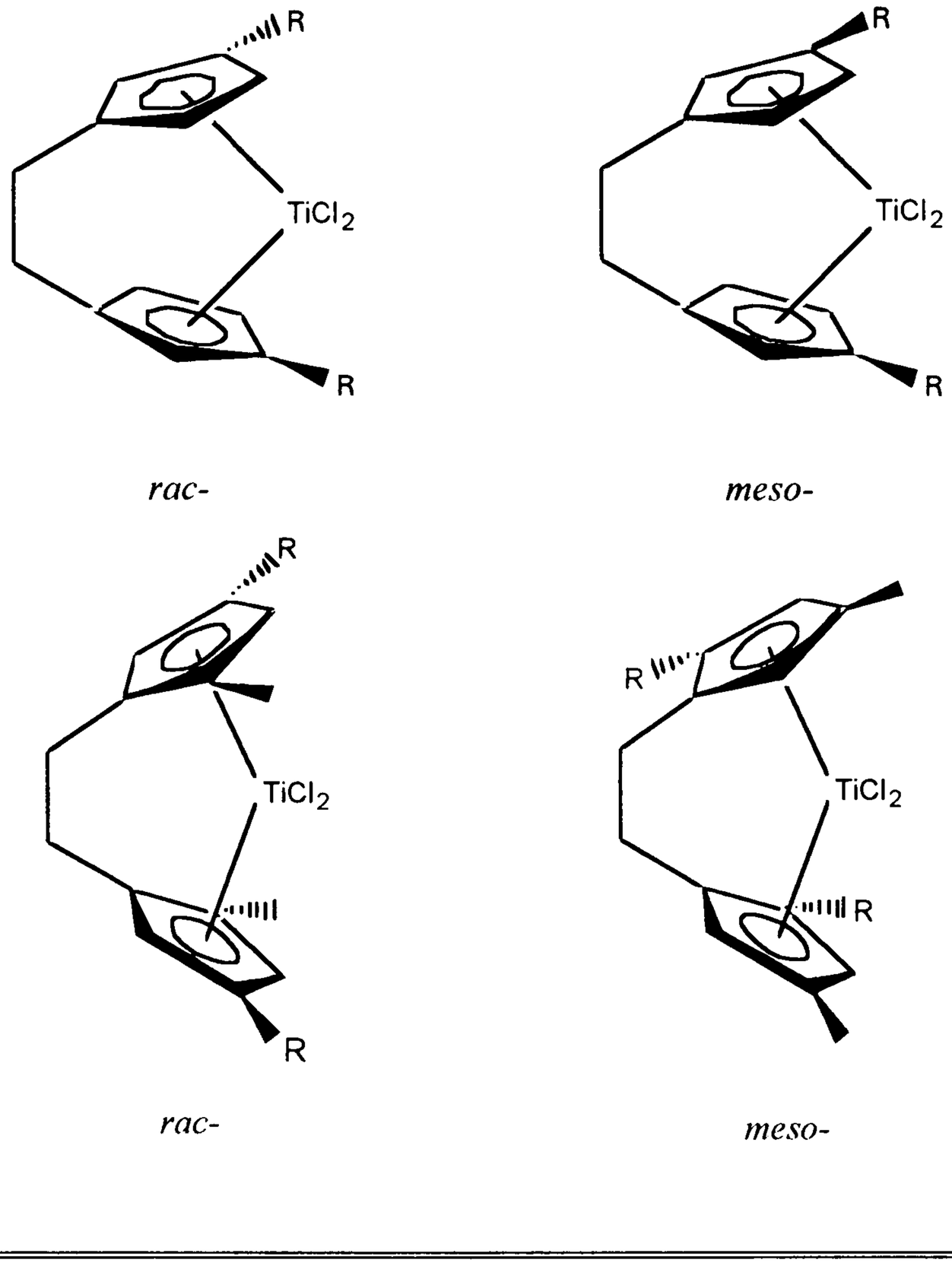

Figure 1.17 Showing *rac* and *meso* isomers of *ansa*–metallocenes

Using ethylene bridged ligands[62] Wild and Brintzinger[63] obtained ethylenebis(indenyl)– and ethylenebis(tetrahydroindenyl)-titanium complexes, [*rac*–(en–ind)$_2$TiCl$_2$] and [*rac*–(en–thind)$_2$TiCl$_2$], and their zirconium analogues. The conformationally constrained indenyl– and tetrahydroindenyl- ligands give these complexes chiral structures. It was expected that this chirality would be retained even under catalytic conditions. Two independent studies discovered that when activated with MAO, these *ansa*–metallocenes [(en–thind)$_2$TiCl$_2$][64] and [*rac*–(en–thind)$_2$ZrCl$_2$][65] were found to polymerise propene and other α–olefins to give highly isotactic polymers. The polypropylene produced from the *ansa*–zirconocene [*rac*–(en–thind)$_2$ZrCl$_2$]/MAO had a similar isotacticity to that produced by heterogeneous

Ziegler–Natta catalysts. These discoveries led to an extensive research effort into the exploration of the mechanisms by which these catalysts control the stereochemistry of the polymer growth, and into the effects of different metallocene structures on the tacticities and other properties of the polymer produced.

When steric restrictions are imposed on a reaction making it stereoselective, the rate of reaction is normally expected to decrease. However, the studies on propene polymerisation with the chiral *ansa*–zirconocene catalyst [*rac*–(en)(thind)$_2$ZrCl$_2$]/MAO showed its catalytic activity to be substantially higher than that of the unsubstituted, stereochemically unselective catalyst [Cp$_2$ZrCl$_2$]/MAO.[65] Even more sterically congested chiral catalyst systems were also shown to produce polypropylene at a higher rate than [Cp$_2$ZrCl$_2$]/MAO.[66,67]

Research has also shown that the structure of the metallocene has a marked effect on catalytic behaviour. The structure of the metallocene affects not only the activity of the catalyst but the tacticity of the polymer produced. These results find that both polymer activity and stereoselectivity are sensitive to both electronic and steric effects.

The size of the linking bridge has a significant effect on catalytic activity. Research has shown that zirconocenes with the one atom bridge Me$_2$Si unit yield more active catalysts than otherwise comparable complexes with the two atom bridge C$_2$H$_4$.[68,69] Zirconocenes with three or four–atom bridges have been found to be practically inactive for propene polymerisation in the presence of MAO.[70,71,72]

Different ring substituents also have an effect on catalytic activities with electron donating groups in the metallocene generally giving enhanced activity. Annelation of further six–membered rings in metallocenes results in three– to four-fold increases in productivity. These activities are most likely due to steric or electron shielding of the cationic reaction centre against coordination of MAO–bound anions or other metallocene units by the extended annelated rings. However, the knowledge about the effects of electronic factors on catalyst activities is limited.[73,74]

Activities of chiral zirconocene catalysts are also affected by MAO concentrations. There is an increase in activation as the ratio Al:Zr increases from 1 to 5000:1. Inhibition of the activity is then seen at higher Al:Zr ratios.[75,76] Catalyst activities have also been shown to be dependent on monomer concentration, with

polymerisation rates observed to increase more than linearly with alkene concentrations.[77,78]

As discussed previously when these chiral *ansa*–metallocene complexes are synthesised a mixture of *rac* and *meso* isomers are produced. Research has shown that these two isomers also have very different catalytic properties. *Meso*–isomers generally produce atactic polymers whereas *rac*–isomers tend to produce polymers which are highly isotactic. These findings result in the synthesis of *ansa*–metallocenes being geared towards the production and separation of the *rac*–isomers rather than the *meso*–isomer.

Alternative Catalysts and Ligand systems.

Despite the apparently almost ideal catalytic properties of metallocene complexes, increasing efforts are being focused on the potential of alternative metal–ligand complexes as Ziegler–Natta catalysts. Reasons for this are to find a ligand system to rival or even better the cyclopentadienyl ligand, and to develop neutral analogues of cationic complexes to eliminate the complications of a counteranion.

In this quest for good or better alternatives to *ansa*–metallocene catalysts, a variety of ligands have been synthesised and studied, some of which still contain substituted cyclopentadienyls.

For example, the chelating cyclopentadienyl–amide ligands as in Figure 1.18 have proved to be successful in a range of polymerisations and also with co–polymerisations.[79,80]

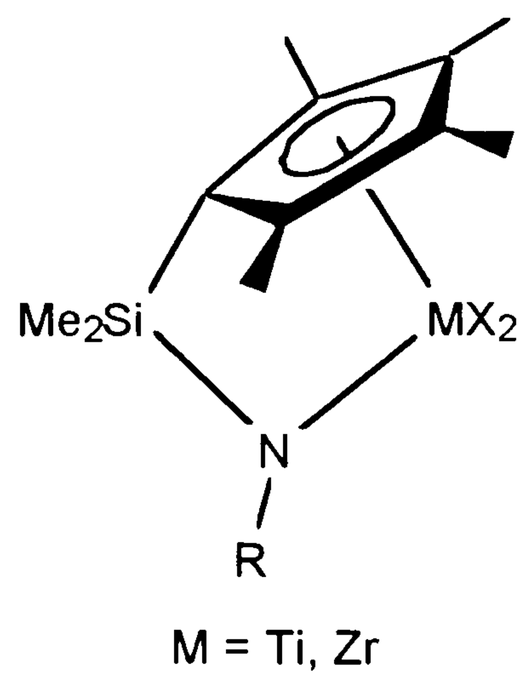

Figure 1.18 A cyclopentadienyl–amide ligand catalyst

Other Cp containing ligands like the benzamidinato complexes (Figure 1.19) have been found to catalyse the polymerisation of ethene, but are less active towards the polymerisation of propene.[81]

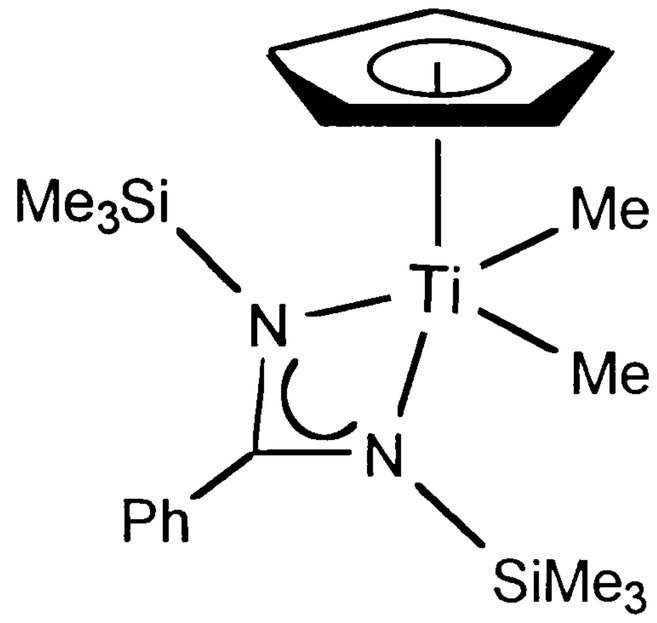

Figure 1.19 A titanium-benzamidinato complex

A radical departure away from the cyclopentadienyl ligand theme has seen the study of other ligands (Figure 1.20) which include macrocycles (a,b),[82] Schiff bases (c),[83] bidentate aryloxides (d,e), tridentate amides (f),[84] and bidentate β–diketiminate ligands (g).[85] Unlike the metallocene compounds these complexes have so far been found to be at best moderately active catalysts for ethylene polymerisation, and very poorly or non–active towards propene polymerisation. Unlike the metallocene complexes, these complexes have also been shown to give polymers with rather broad molecular weight distribution. It is also not certain whether the identity of the complexes remains intact under the polymerisation conditions.[86]

(a)

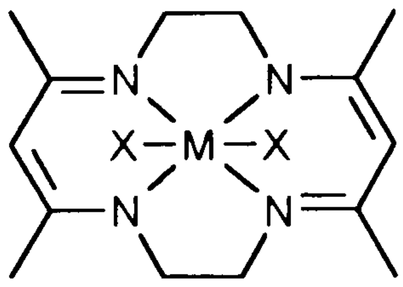

M = Ti, Zr

(b)

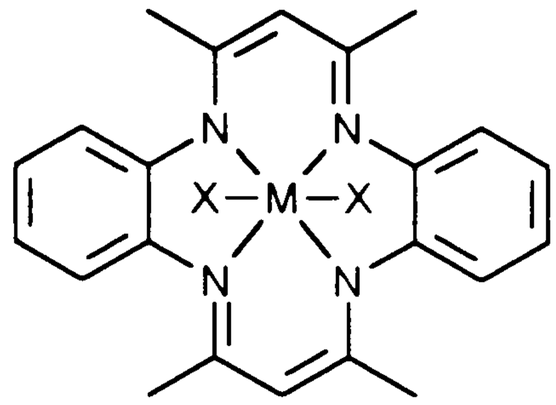

M = Ti, Zr

(c)

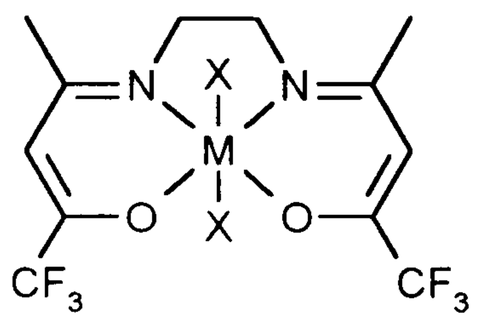

M = Ti, Zr

(d)

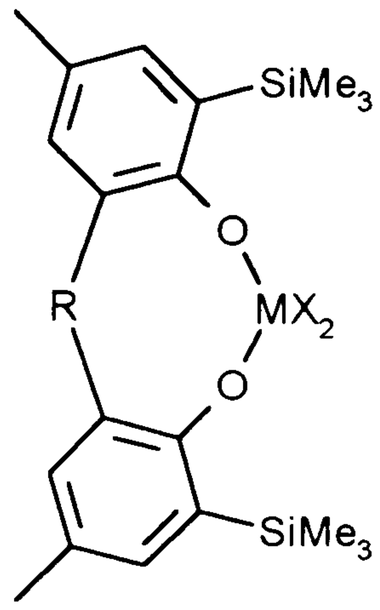

M = Ti, Zr

(e)

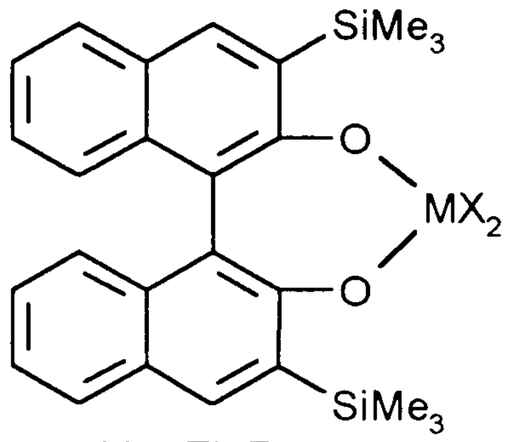

M = Ti, Zr

(f)

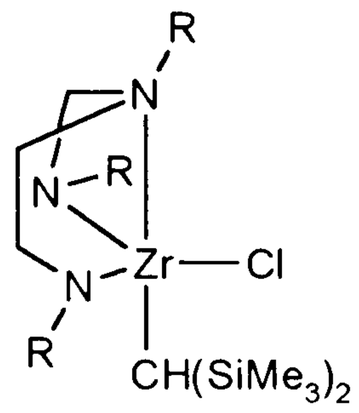

(g)

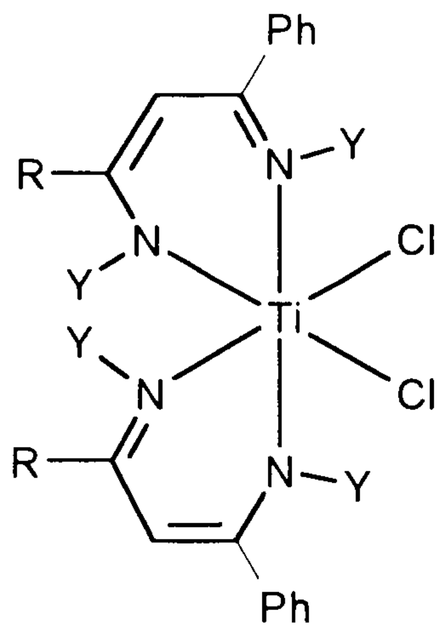

Y = $SiMe_3$

R = Ph, ^tBu

Figure 1.20 Alternative ligand systems for α–olefin polymerisation

The overall aim of the research described in this thesis is to synthesise and characterise a series of new compounds, and to examine initially their potential for use as ethylene polymerisation catalysts. The *ansa*–metallocenes were taken as the

"ideal model" for a Ziegler–Natta polymerisation catalyst i.e. a rigid ligand framework with a *cis*-- dihalide or alkyl configuration at the metal centre.

It was anticipated at the onset of this work that this could be achieved using both macrocyclic and Schiff base ligands. As will be discussed in the following introductory sections these types of ligands are potentially useful compounds, and possess many special properties which make them attractive for the preparation of potential new catalysts. As with the ansa–metallocene compounds these ligands are easily modified by the addition of substituents at various positions within the ligand structure to influence steric and/or electronic properties at the metal centre. The addition of substituents can also be used to introduce chirality within the complex formed. This versatility within these ligands was seen as vital, so that the potential to use ligand design to control catalyst active site performance in a predictable manner was available.

Macrocyclic Ligands.

A macrocycle is a cyclic ligand which has a minimum of nine constituent atoms, of which at least three must be donor atoms (e.g. N, S, or O), capable of coordinating to a metal centre. The macrocycle framework is made up of carbon atoms which can be saturated or unsaturated while the donor atoms can vary. The use of macrocyclic ligands is attractive because of the high stability of many of the complexes they form. They can also be used to control metal ion stereochemistry.

There have been a number of reviews covering the synthesis of macrocycles.[87–92] In the synthesis of any macrocycle the aim is to produce a cyclic system in which few or no unwanted side products are formed, and the macrocycle is synthesised in good yield. The synthetic routes to macrocycles can be split into three main categories which are the high dilution method, Richman–Atkins ring closure, and template synthesis. These methods are now briefly reviewed.

High dilution.[93]

This method involves the synthesis of open chain precursor molecules followed by a ring closure step which is carried out in a highly dilute solution. This has the effect of reducing the number of side reactions. The main problem with this method is the low yield which is often obtained. The yield can be improved significantly by using motor driven syringe pumps to control the rate of addition of the reactants. Yields of up to 25% are then possible.

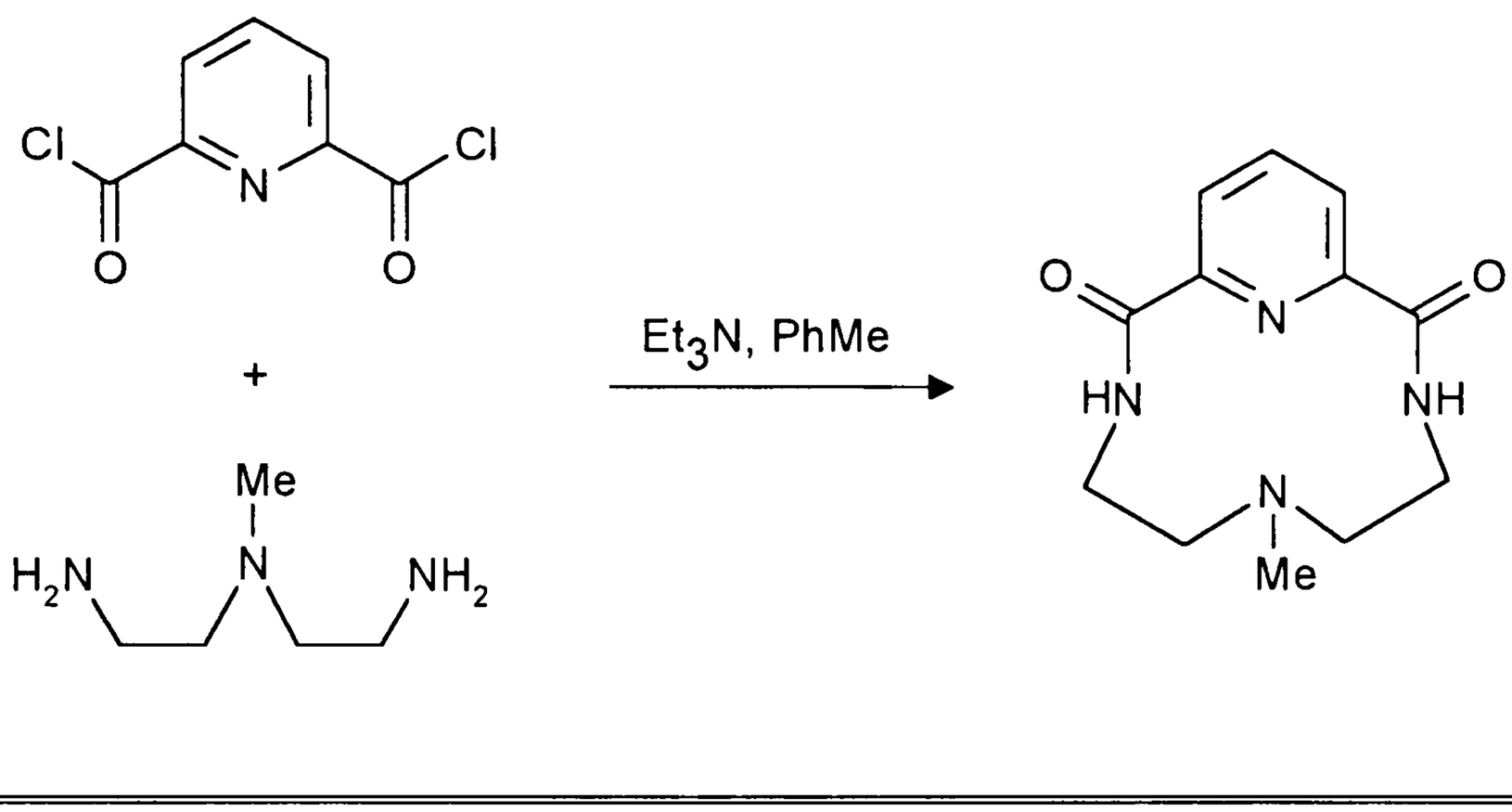

Figure 1.21 Example of a high dilution preparation.

Richman–Atkins Ring Closure.[94]

This technique involves the formation of tosylated derivatives of open chain amines, which are deprotonated and reacted to form the fully tosylated macrocycle. This technique is widely used for the preparation of aza–macrocycles, and provides a much higher yield than the high dilution method. The yields obtained by this method are typically 40–50 %. Ring closure of deprotonated tosylated amines is possible in dimethylformamide at 100 °C without the need of high dilution. The reason for this is steric, the bulky tosyl groups reduce the number of conformational degrees of freedom of the reactants and intermediates thus enhancing cyclisation.

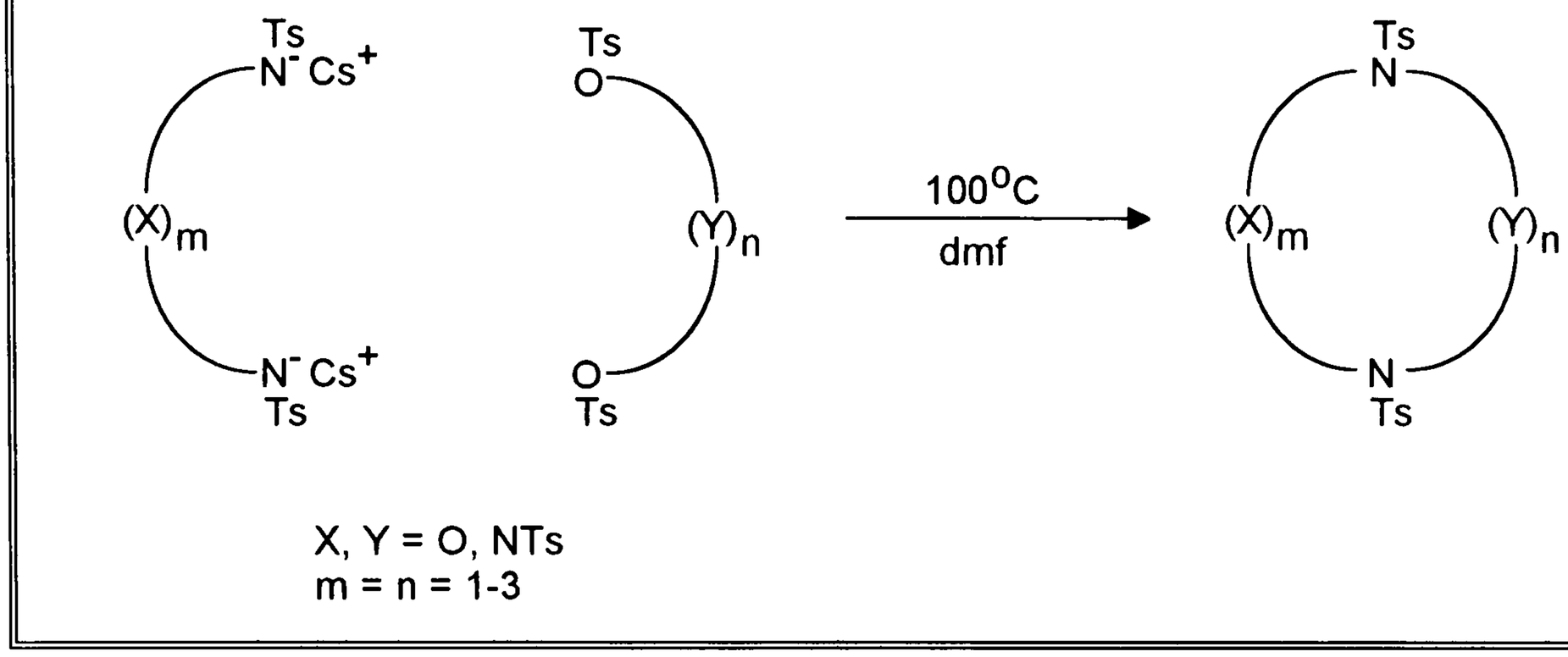

Figure 1.22 An example of the Richman–Atkins method

Template Synthesis.[90]

This method involves the synthesis of the macrocycle with a metal present to hold the reactants in a set stereochemistry. This results in the formation of the required ligand. The metal ion template controls the reaction and often increases the yield of cyclisation reactions.

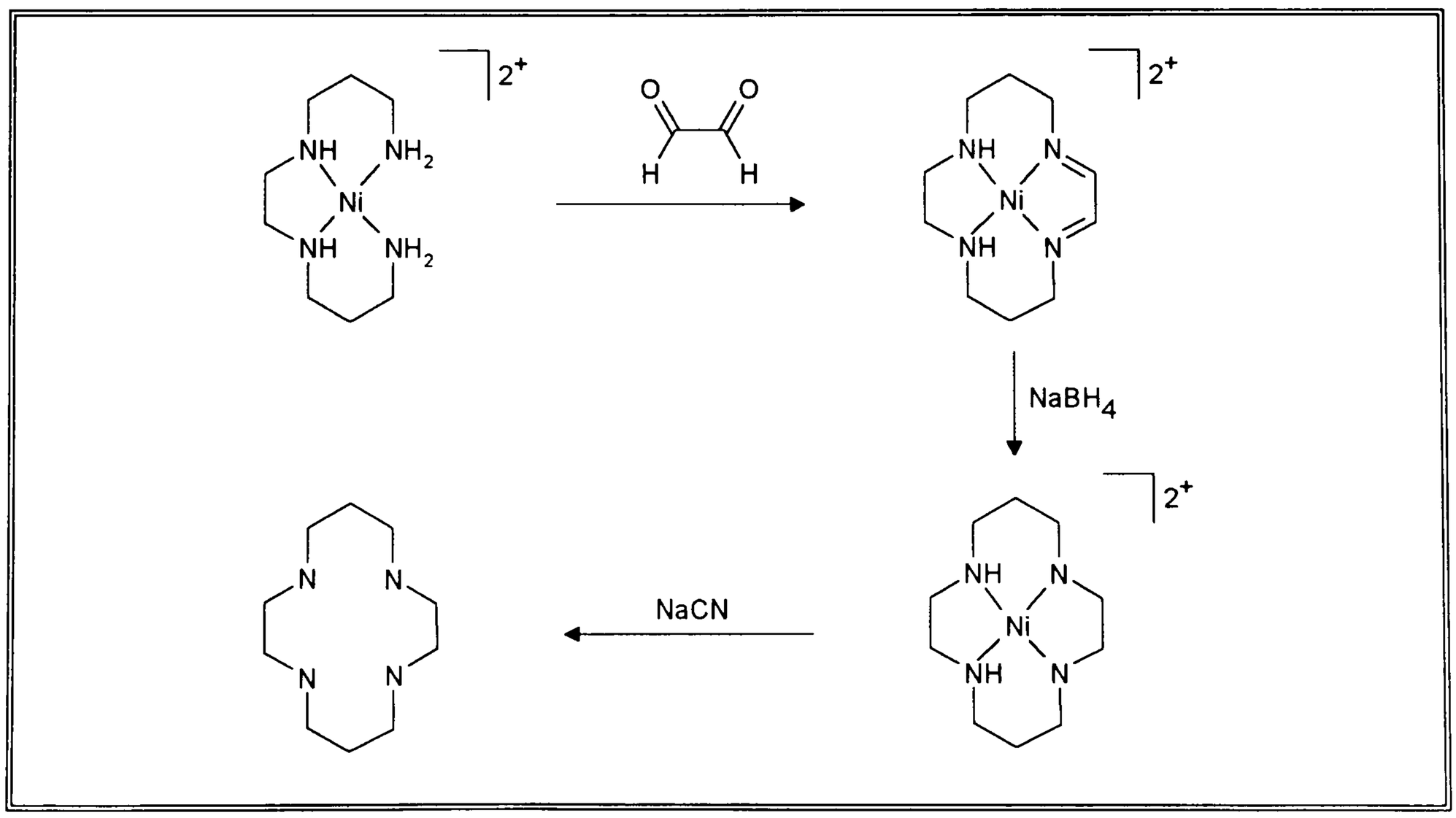

Figure 1.23 An example of a template synthesis

Properties of macrocyclic ligands.

The advantages that macrocyclic ligands have over their open chain analogues arise from two features. Firstly, macrocyclic ligands form metal complexes which are considerably more stable than those of their open chain congeners. This extra stability is attributed to the so called macrocyclic effect.[95] Work by Magerum[95] on cyclic tetraamine ligands found that the macrocyclic effect is about ten times larger than the chelate effect observed for copper(II) complexes with multidentate open chain analogues. This was also found to be the case in cyclic polyethers.[96] The enhanced stability of macrocyclic compounds is believed to arise from both enthalpy and entropy terms, and it was concluded that the relative magnitude of the enthalpy contribution is critically dependent on the match between cation and ligand cavity sizes for transition metals.[97,98] These conclusions show that the macrocyclic effect is not simply defined, and that different systems may respond differently to stabilising factors. Secondly, macrocycles can select specific metal ions when forming complexes, a feature which is a consequence of the cavity size of the molecule. Some metals are too large to fit without causing the ring to strain, whereas others are too small to be bonded within the cavity. This can be extremely important when designing a macrocycle to accept a certain metal. The relative stabilities associated with various metal ions in combination with macrocyclic ligands is a well developed area of chemistry.

Schiff base ligands.

Schiff's bases are a class of compounds containing the imine (azomethine) –RC=N– group and have been known for over one hundred years. Similarly, the coordination chemistry of these ligands has also been known for a long time. The imine (C=N) group is produced by the condensation between an amine and an active carbonyl group.

Their synthesis was first reported by Schiff,[99] and the most common method of obtaining a Schiff base is shown in Figure 1.24.

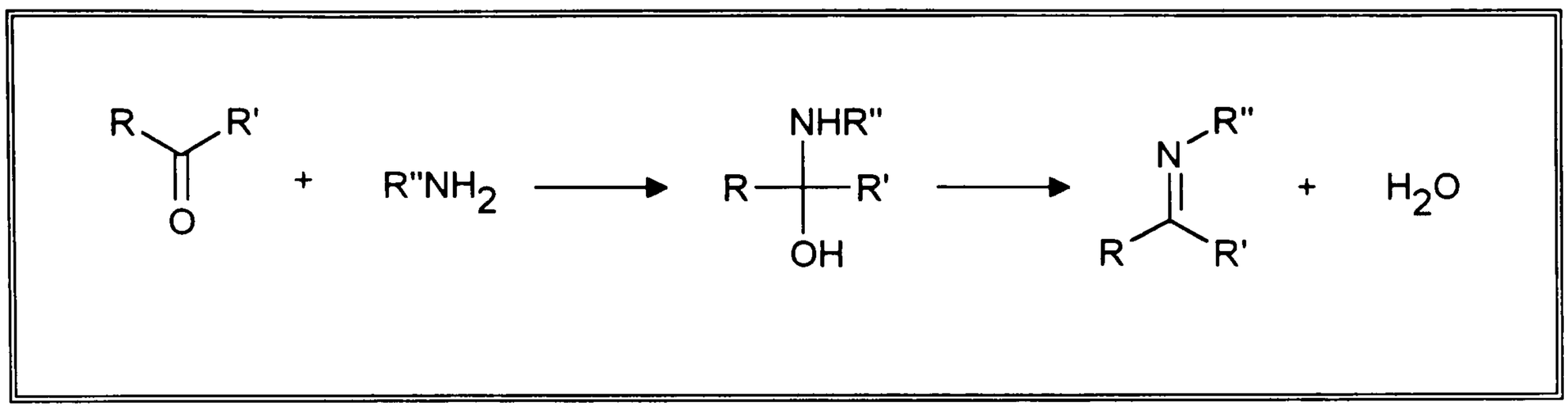

Figure 1.24 The general method for Schiff base synthesis

Schiff base ligands can be monodentate, bidentate, tridentate, tetradentate and multidentate. The donor atoms of the ligand are usually a combination of nitrogen and oxygen donor atoms. The ligands studied in this thesis are the tetradentate Schiff base ligands with an N_2O_2 donor set.

Tetradentate Schiff base ligands.

Tetradentate Schiff base ligands with the N_2O_2 donor set have been widely studied for their ability to coordinate to metal ions. The properties of these metal complexes are determined by the electronic nature of the ligand and its conformational behaviour.

The free ligands have been studied both in solution and the solid state to gain an insight into their structure, as well as to provide a comparison for the metal complexes. Various spectroscopic techniques have been used to investigate the keto–enol equilibrium and the nature of the hydrogen bonding within these molecules. The tautomeric equilibrium of a typical Schiff base ligand (H_2SALEN) can be represented as shown in Figure 1.25.

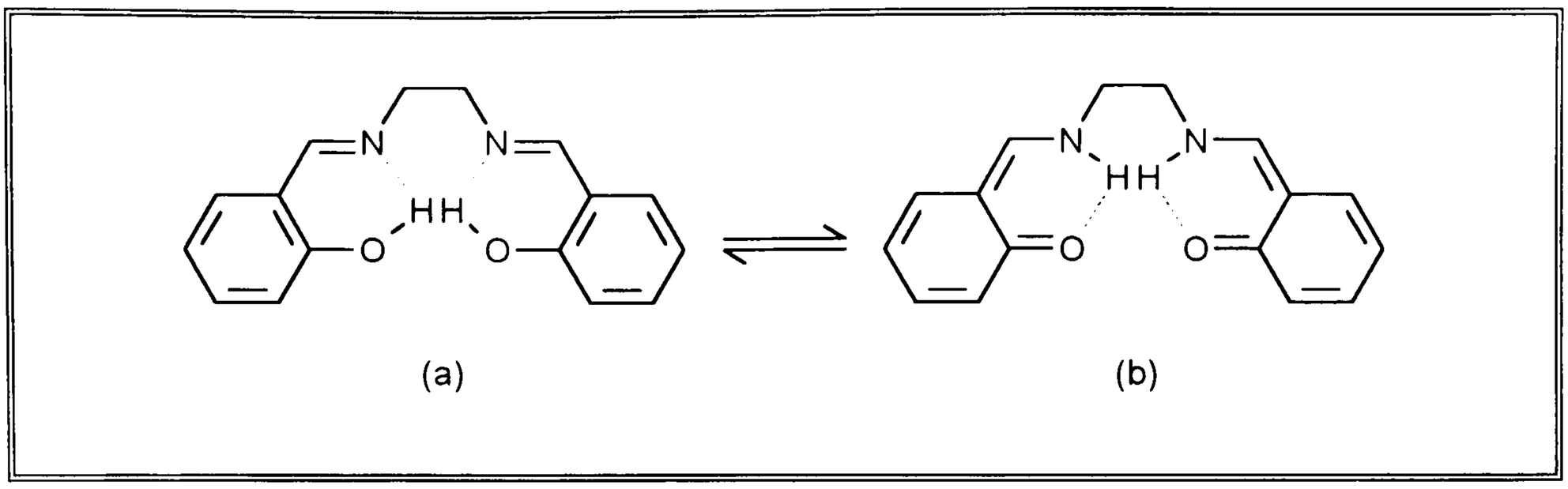

(a) (b)

Figure 1.25 The enolimine tautomer (a), and the ketoamine tautomer (b) of H_2SALEN

For the two possible tautomeric structures of these compounds, ^1H N.M.R and IR spectroscopy shows that the predominant structure for these ligands is the enolimine form (a). This enolimine structure has been confirmed by single crystal X–ray crystallography for the ligand H_2SALEN which shows the enolimine form with intramolecular hydrogen bonding.[100]

Ligand properties and conformational changes.

For most metal complexes with tetradentate Schiff base ligands derived from salicylaldehyde and the appropriate diamine, the ligand is in its ionised form. The phenolic protons are quite acidic because they are adjacent to a delocalized ring system, and as a result the proton can be readily removed by a base to give an O^- site. If enough base is used both acidic protons can be removed to give an $N_2O_2^{2-}$ donor set.

$$H_2SALEN \xrightarrow[OH^-]{base} [SALEN]^{2-} + 2\,H_2O$$

These ligands, $[SALEN]^{2-}$,are relatively flexible and this allows distortions of the Schiff base according to the metal atom nature and size, as well as to the bulkiness of axial or apical ligands. These properties of Schiff base ligands produce three possible arrangements for their metal complexes.

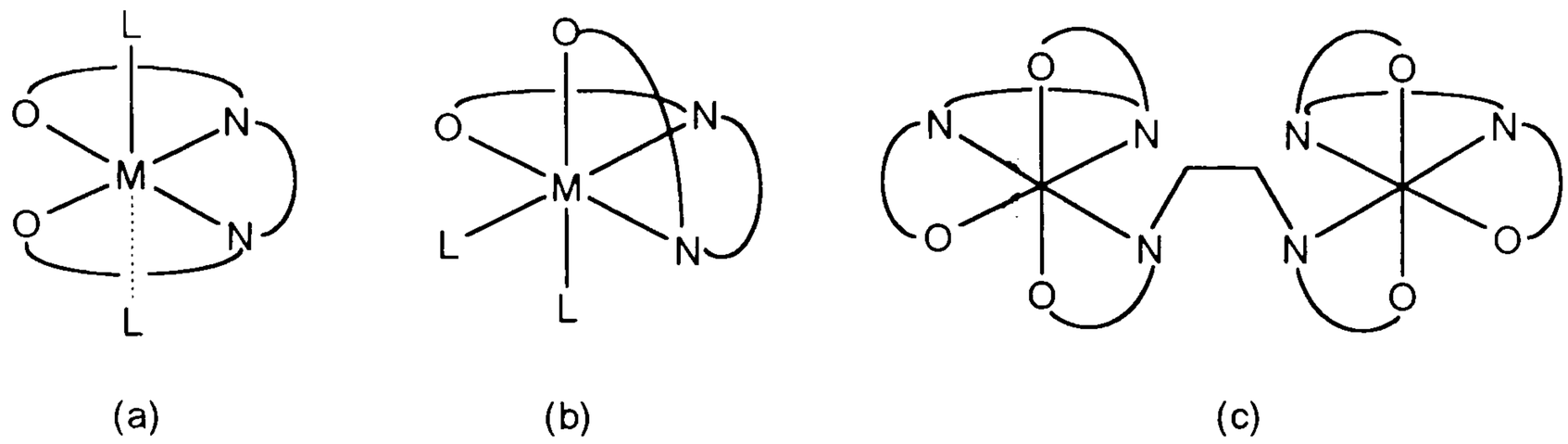

Figure 1.26 Possible arrangements of tetradentate Schiff bases in metal complexes.

The most common arrangement is shown in Figure 1.26 (a) where the four donor atoms are nearly coplanar producing a *trans* octahedral configuration, or a square–pyramidal geometry at the metal centre.

Earlier discussion has shown that the arrangement shown in Figure 1.26 (b) (i.e. where the ligand has folded to produce a *cis* configuration at the metal centre), would be the probable desired stereochemistry at the metal centre for the optimum structure as a potential homogeneous Ziegler–Natta catalyst. Therefore, it is necessary to study the factors which influence the stereochemistry of Group 4 early transition metal complexes leading to the folded *cis* structure.

Tetradentate Schiff base complexes of transition metals.

There has been substantial research carried out on the complexation of various Schiff base ligands with transition metals. The following section will describe some of the transition metal complexes synthesised with tetradentate Schiff bases, and the uses which have been found for these complexes. Then a detailed study of the work carried out with Group 4 transition metals and tetradentate Schiff base ligands will be discussed. Early work with tetradentate Schiff base ligands and transition metals was focused on the coordination chemistry of the complexes produced. Many transition metal Schiff base complexes have been synthesised, mainly using simple symmetrical ligands such as H_2SALEN[101,102] and H_2SALOPHEN.[103,104] In the majority of

complexes the ligand species is the dianionic form of the Schiff base, namely $[SALEN]^{2-}$ etc.

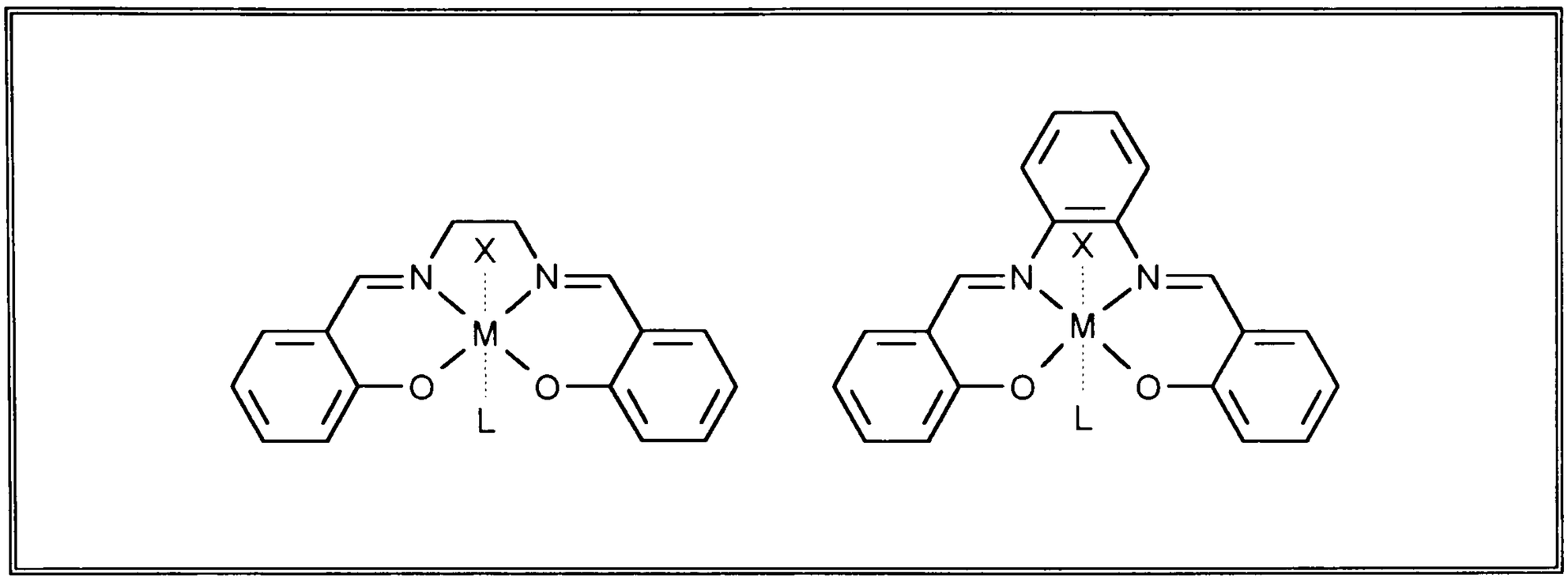

Figure 1.27 A representation of complexes formed with H_2SALEN and H_2SALOPHEN

Unsymmetrical tetradentate Schiff base ligands have also been synthesised and their reaction with transition metals studied. The reaction of these unsymmetrical ligands with copper and nickel produced asymmetric complexes which were used as models for the irregular binding of peptides.[105]

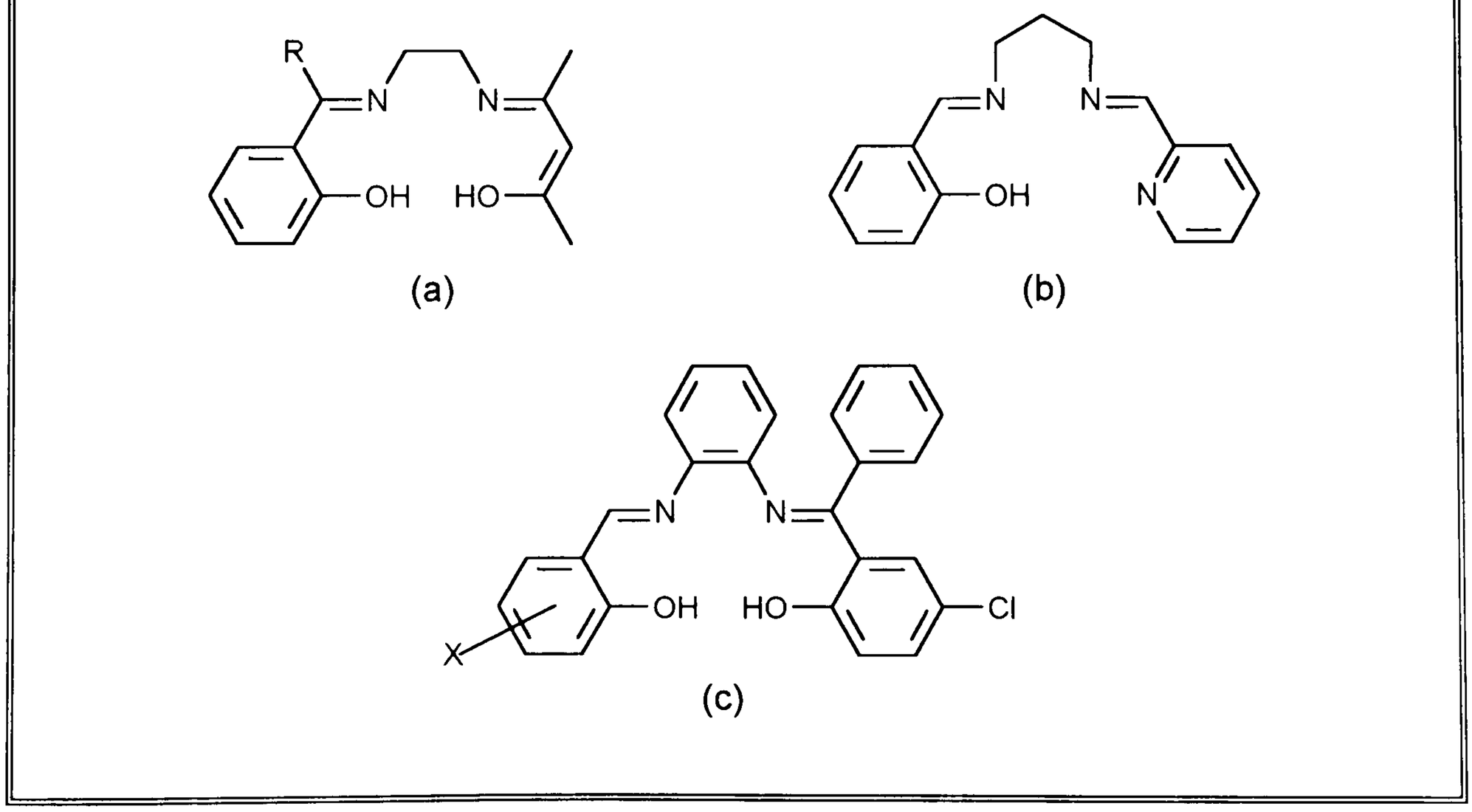

Figure 1.28 Examples of unsymmetrical tetradentate Schiff base ligands

Recently a great deal of interest and effort has been focused on the production of chiral metal Schiff base complexes for asymmetric catalysis in organic synthesis. This resulted from the discovery that manganese(III) complexes of chiral tetradentate Schiff base ligands are capable of catalysing the epoxidation of unfunctionalised alkenes in excellent enantiomeric excesses, exemplified by Jacobsen's catalyst.[106]

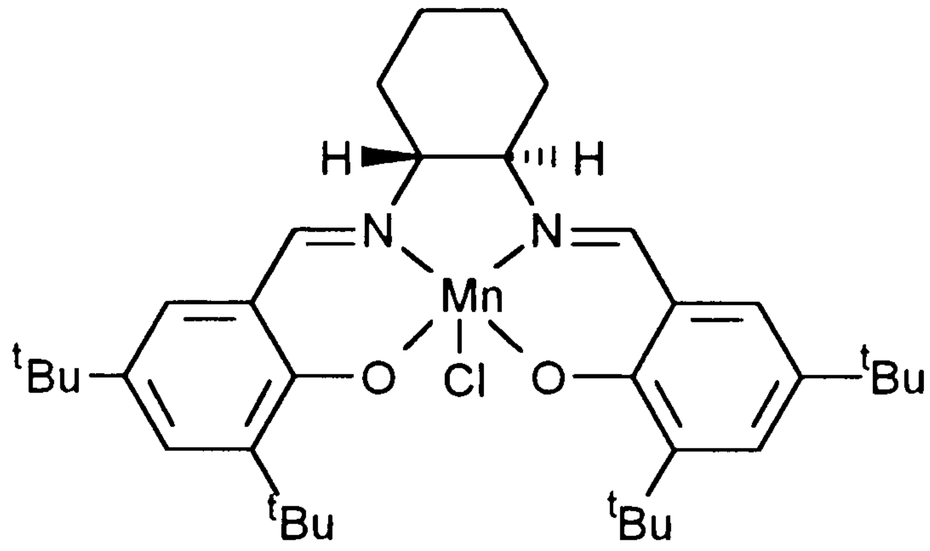

Figure 1.29 Jacobsen's catalyst

Group 4 tetradentate Schiff base complexes.

Reactions of the Group 4 metals, especially titanium, with a selection of tetradentate Schiff base ligands have been studied. The preparation of titanium(IV) complexes with the ligands H_2SALEN and H_2SALOPHEN were reported in 1971 by Biradar and Kulkarni.[107] These complexes [Ti(SALEN)Cl_2] and [Ti(SALOPHEN)Cl_2] had been prepared by the addition of the Schiff base to a solution of titanium(IV) chloride in absolute alcohol with heating to temperatures between 150 and 180 °C. However, no structural data was obtained on these complexes to elucidate the nature of the coordination at the metal centre.

The first structural information on Group 4 tetradentate Schiff base complexes came in 1972 when Gilli, Cruickshank *et al*[108] published the structure of [Ti(SALEN)Cl_2]. The structure revealed that the titanium atom is approximately octahedrally coordinated, with the two chlorine atoms in a *trans* configuration, with a Cl–Ti–Cl bond angle of 168.7(1)°, and with two *cis* oxygen atoms and two *cis* nitrogen atoms.

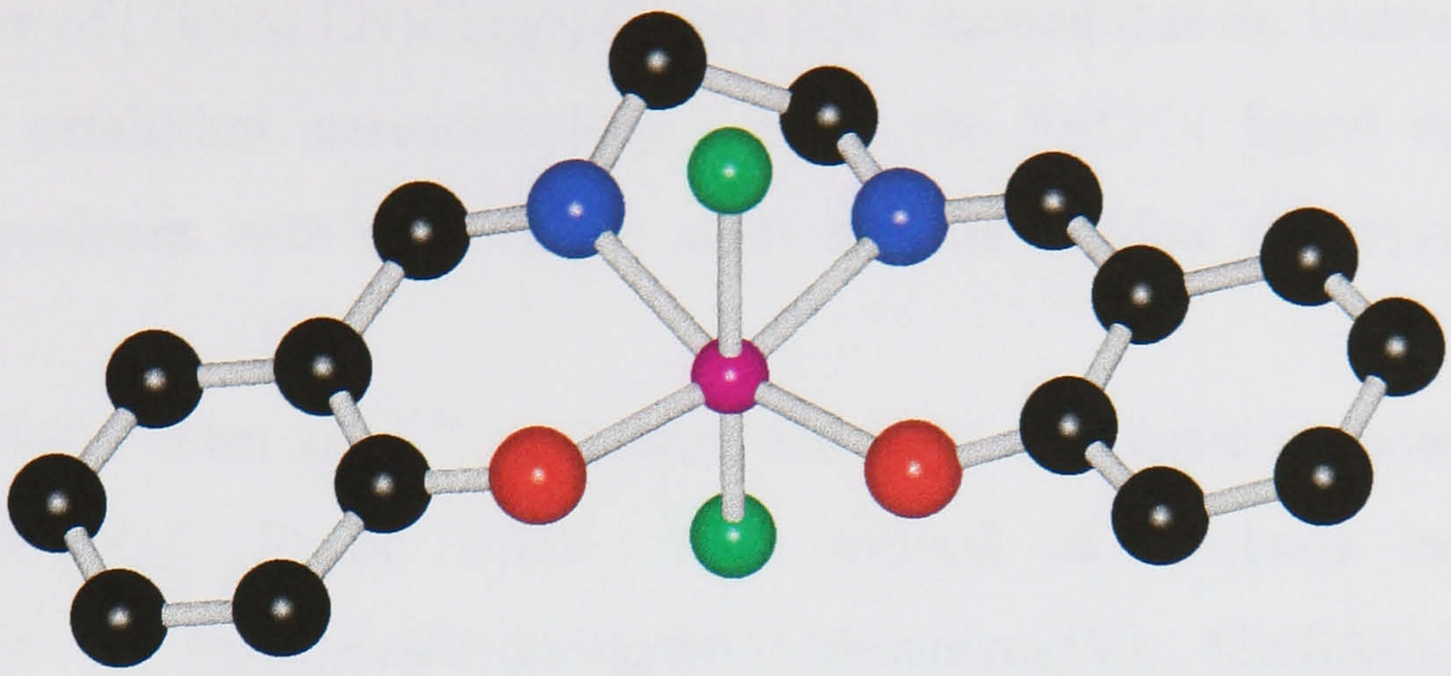

Figure 1.30 The molecular structure of [Ti(SALEN)Cl_2]

In 1978 Floriani *et al*[109] studied the reduction of [Ti(SALEN)Cl_2] with zinc dust in tetrahydrofuran to give the dimeric Ti(III) complex [{Ti(SALEN)(THF)}$_2$][$ZnCl_4$]. When a solution of this dimer is treated with pyridine (py) the production of the extremely air–sensitive Ti(III) complex [Ti(SALEN)Cl(py)] is formed.

$$2\ [Ti(SALEN)Cl] + Zn \xrightarrow{THF} [\{Ti(SALEN)(THF)\}_2][ZnCl_4].nTHF$$

$$2\ [Ti(SALEN)Cl] + Zn \xrightarrow{py\ /\ THF} 2\ [Ti(SALEN)Cl(py)].THF$$

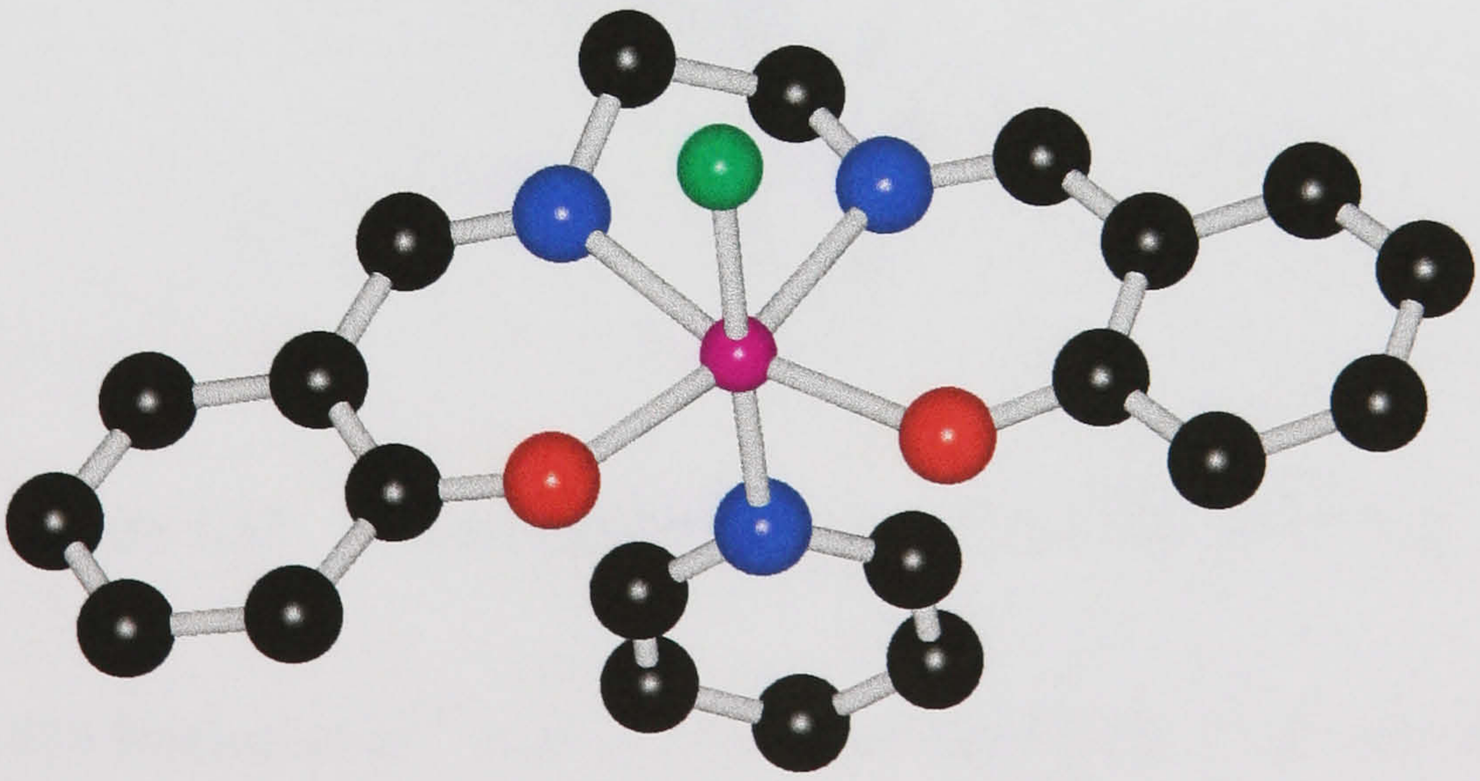

Figure 1.31 The molecular structure of [Ti(SALEN)Cl(py)]

The structure of [Ti(SALEN)Cl(py)] (Figure 1.31) showed that the titanium atom had a distorted octahedral stereochemistry. Again the SALEN ligand occupies the equatorial positions with the chlorine atom and the pyridine occupying the axial positions.

In 1979 Archer *et al*[110] synthesised the eight coordinate zirconium complex [Zr(SALOPHEN)$_2$] (Figure 1.32). The method of synthesis involved the condensation of tetrakis(salicylaldehydato)–zirconium(IV), [Zr(SAL)$_4$], and *o*–phenylenediamine. The [Zr(SALOPHEN)$_2$] unit possesses an eight coordinate metal atom with the ligand atoms in an almost perfect dodecahedral arrangement with the trapezoidal planes intersecting at 89.2°, even though the chelating ligands are puckered from these planes.

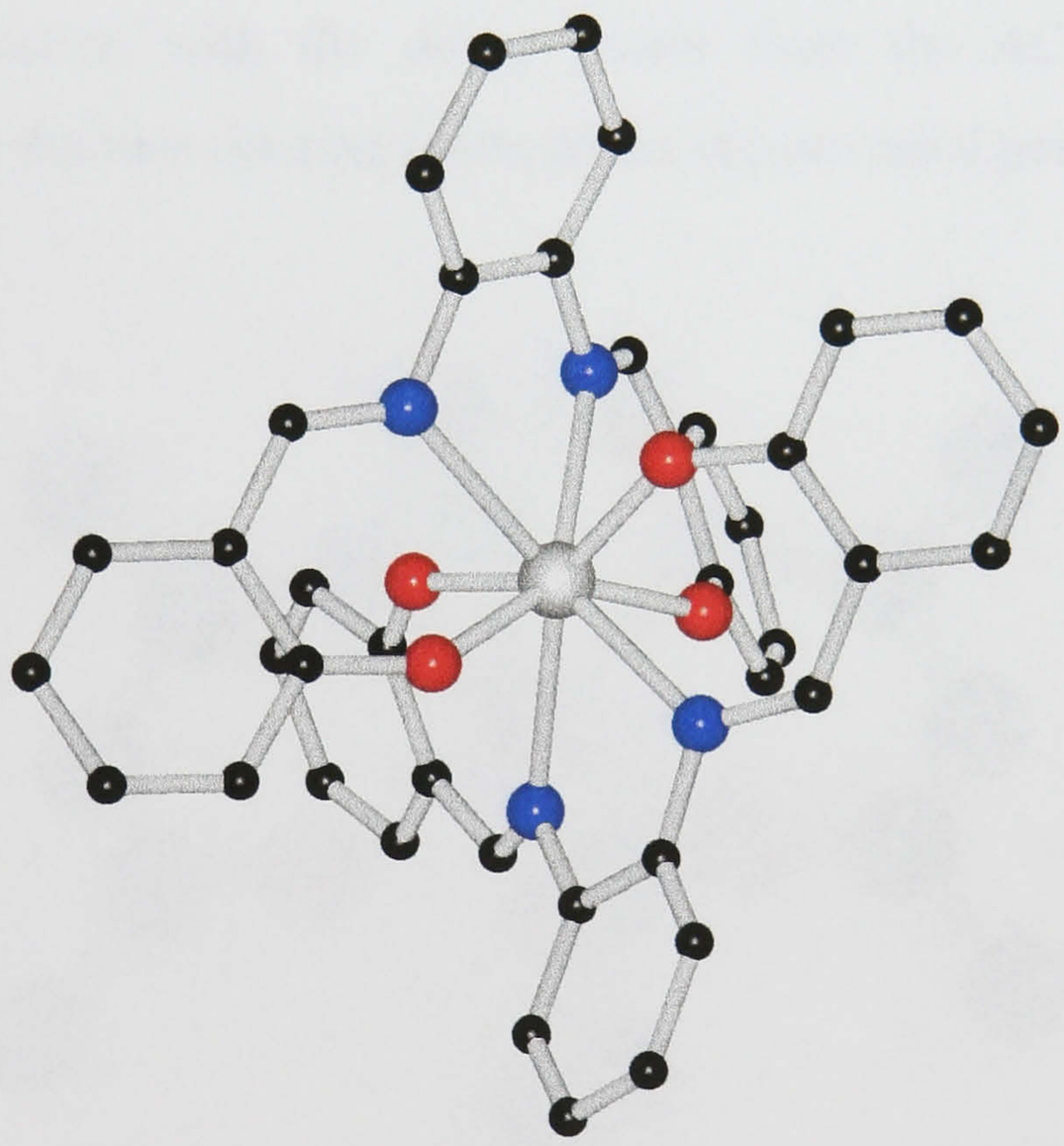

Figure 1.32 The molecular structure of [Zr(SALOPHEN)$_2$].

In 1989 Floriani *et al*[111] reported the reaction of $TiCl_4$.2THF and $TiCl_3$.3THF with Na_2ACEN [ACEN = N,N' ethylenebis(acetylacetoneiminate) dianion] giving the corresponding titanium(IV) [Ti(ACEN)Cl$_2$], and titanium(III) [Ti(ACEN)Cl(THF)] complexes in good yield.

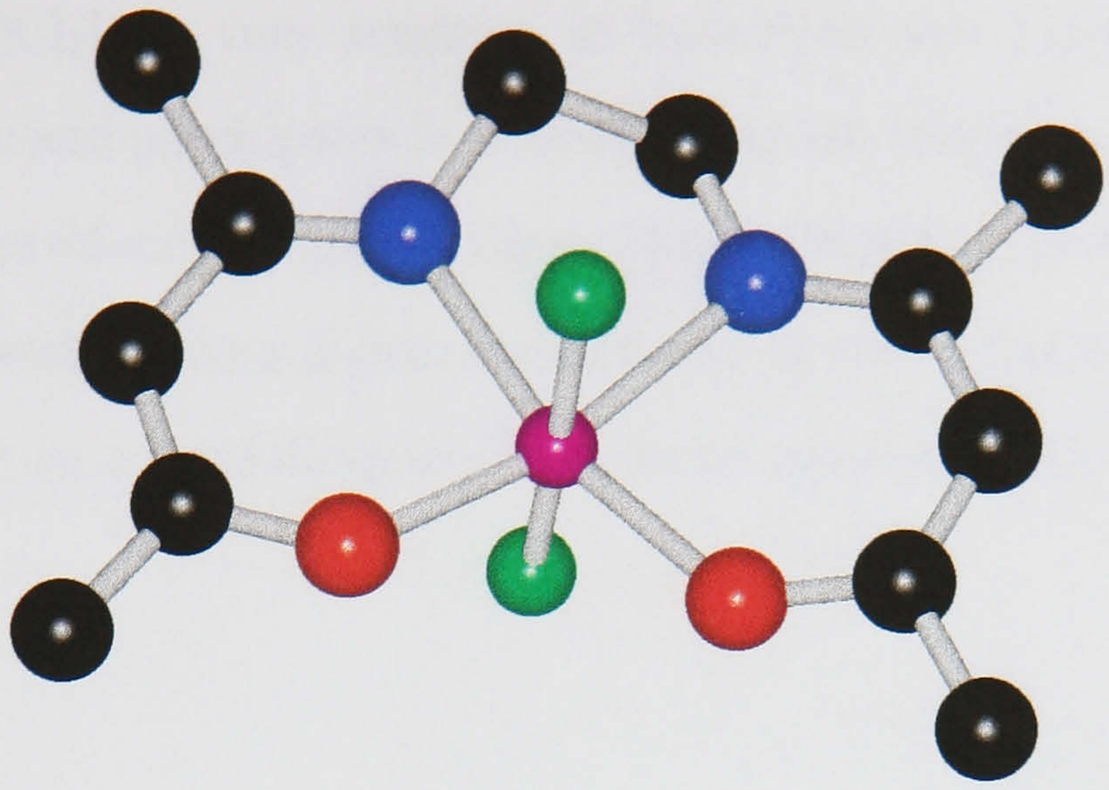

Figure 1.33 The molecular structure of [Ti(ACEN)Cl_2]

In the complex [Ti(ACEN)Cl_2] (Figure 1.33), the titanium atom exhibits a bipyramidal coordination with the donor atoms from the ACEN ligand in the equatorial plane and the two chlorine atoms again in *trans* axial positions.

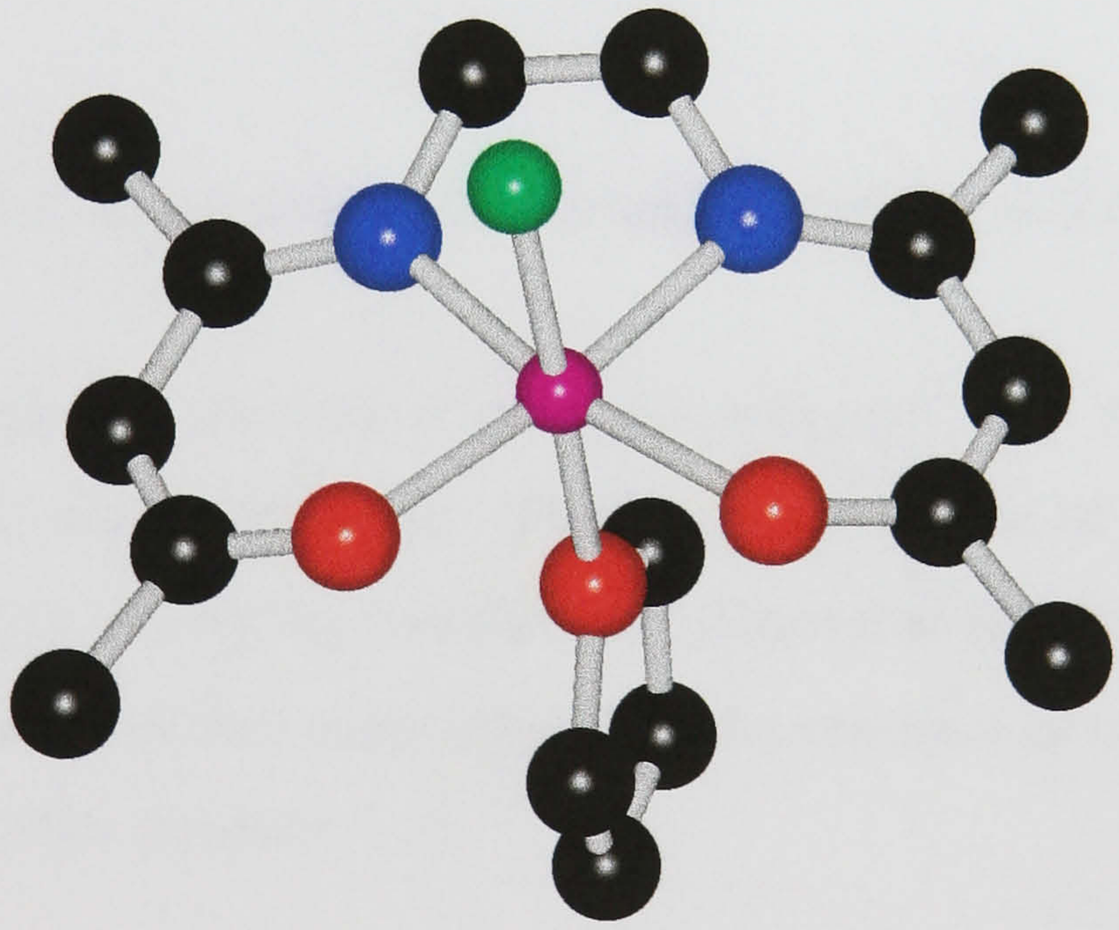

Figure 1.34 The molecular structure of [Ti(ACEN)Cl(THF)].

In the complex [Ti(ACEN)Cl(THF)] (Figure 1.34) an oxygen atom from a THF molecule replaces a chlorine atom of the [Ti(ACEN)Cl_2] complex. The coordination of ACEN is not strictly planar, the titanium atom is displaced by 0.166(1)Å from the N_2O_2 plane towards chlorine.

[Ti(ACEN)Cl_2] is very sensitive to hydrolysis and [Ti(ACEN)Cl(THF)] is sensitive to oxygen and participates in various oxidation reactions. The reaction with molecular oxygen produces the μ–oxo dimer [{Ti(ACEN)Cl}$_2$(μ–O)]. The molecular structure of this dimer shows a μ–oxo ligand bridging two Ti(ACEN)Cl units with the oxygen atom lying on a crystallographic centre of symmetry (Ti–O–Ti bond angle = 180°).

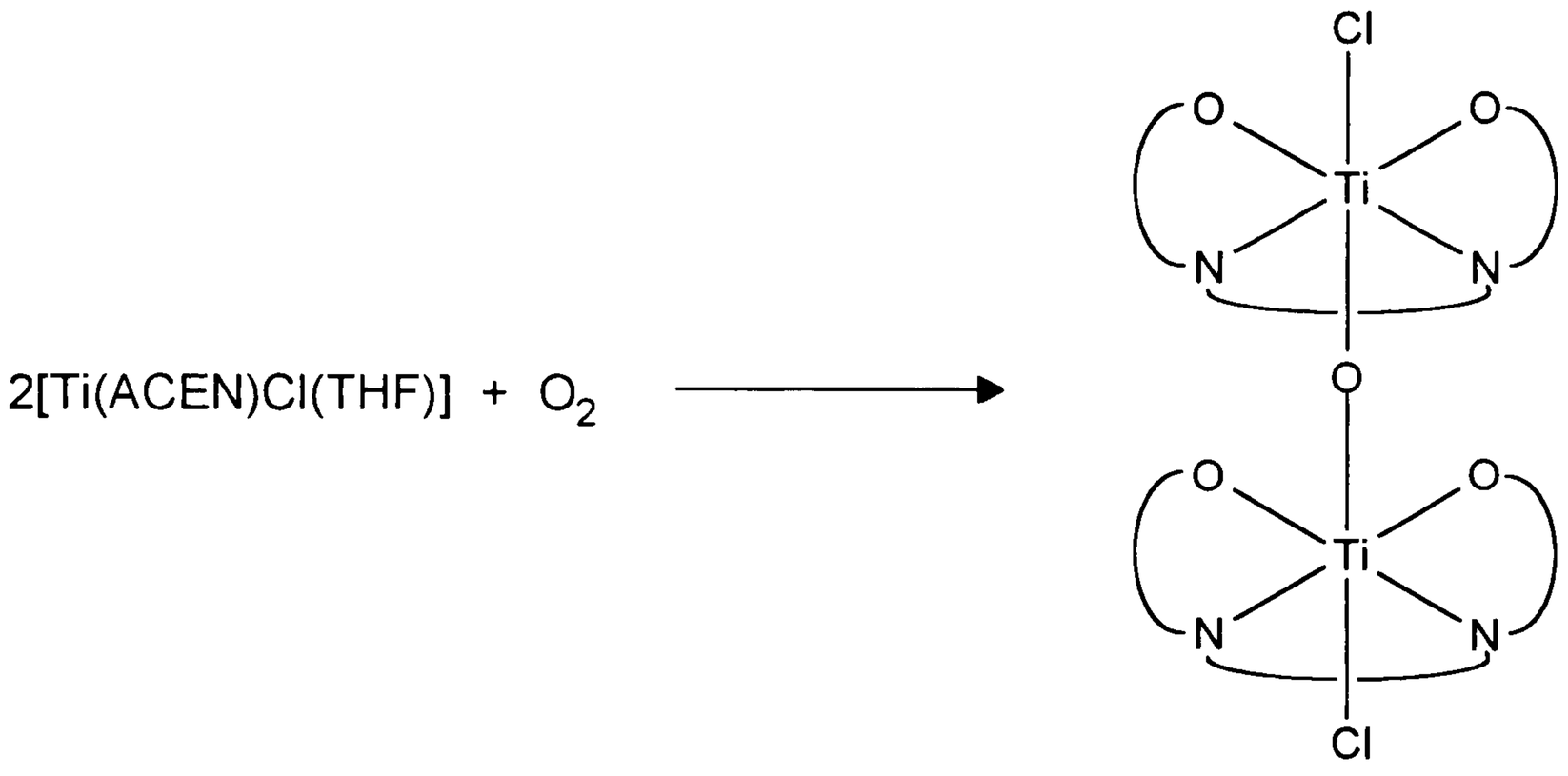

Equation 1.2 Reaction of molecular oxygen and [Ti(ACEN)Cl(THF)]

In this same year Floriani *et al*[112] also reported some of the reactions of titanium(IV) Schiff base compounds. They reported studies of the alkylation and arylation of the [Ti(SALEN)Cl_2] complex, and discovered that these reactions were much more complex than they expected due to the presence of electrophilic sites in the SALEN ligand (See Equation 1.3).

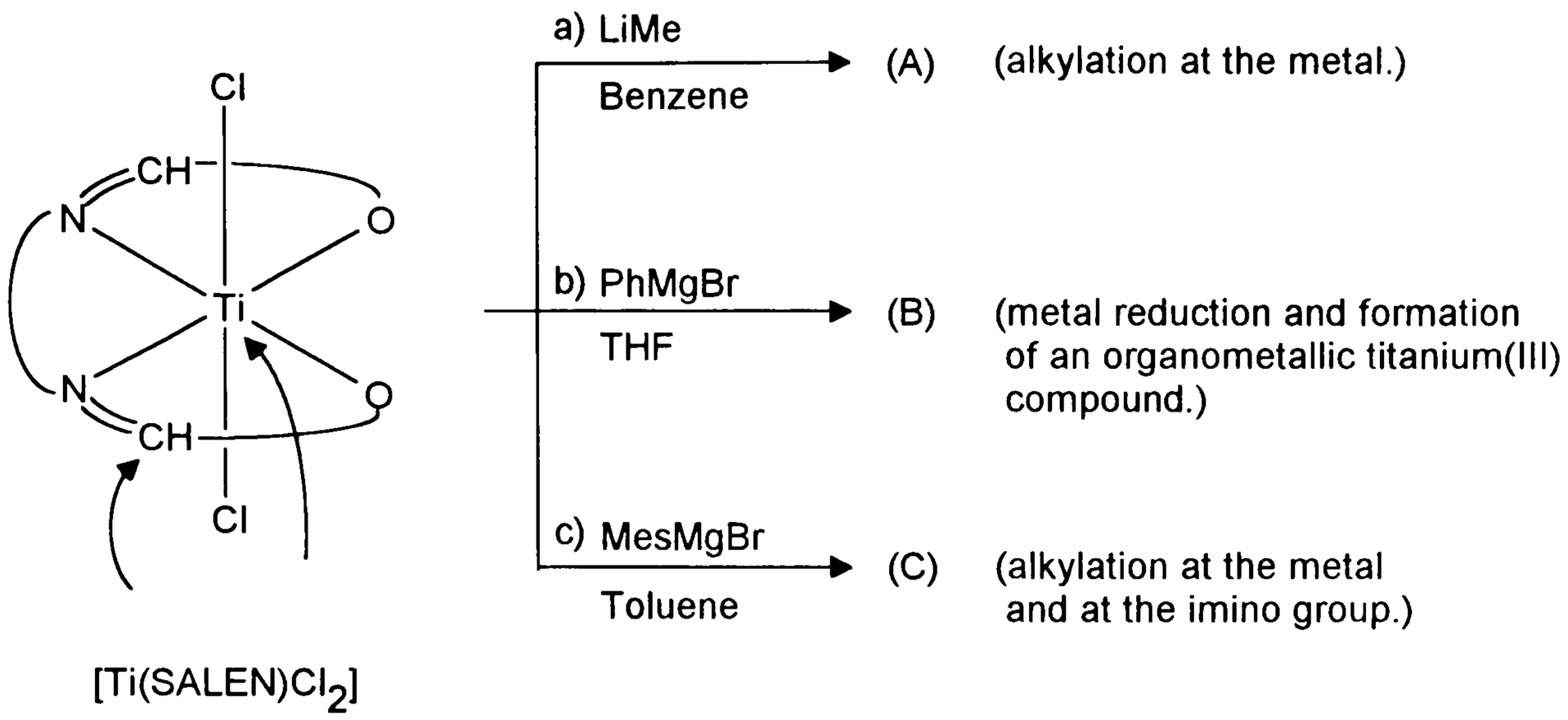

Equation 1.3 Reactions of [Ti(SALEN)Cl_2] (the arrows indicate the possible alkylation sites in the complex).

As can be seen these reactions can follow three different pathways depending upon the nucleophile and solvent. These reactions result in the complexes shown in Figure 1.35

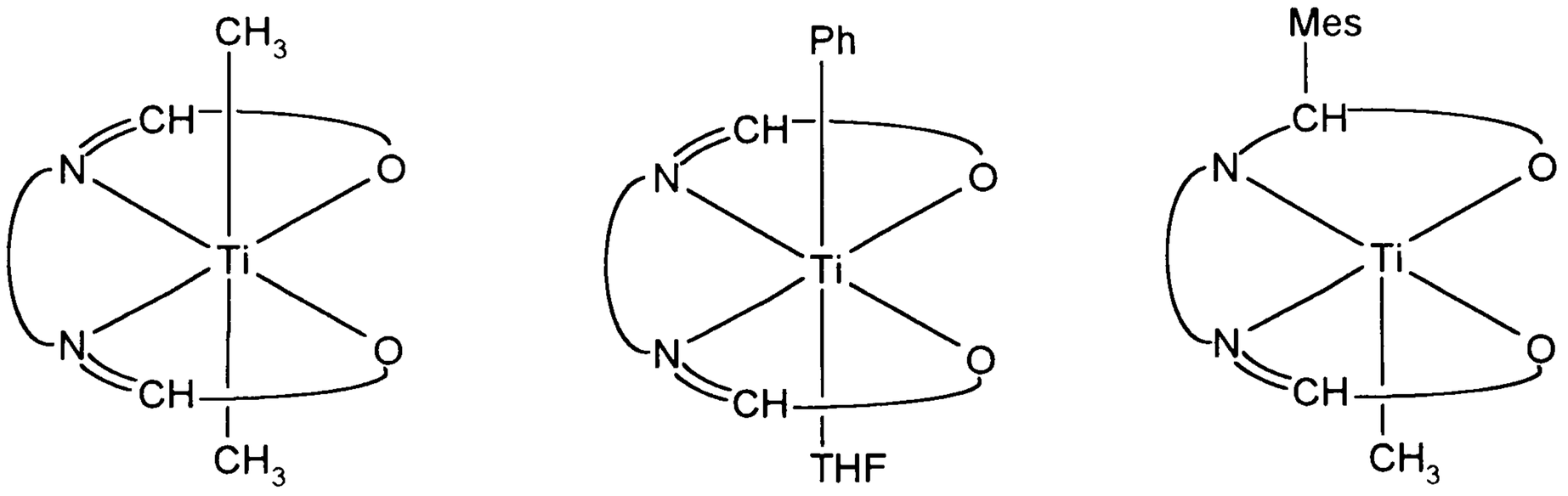

Figure 1.35 Possible reaction products from reactions with [Ti(SALEN)Cl_2]

Floriani *et al* concluded that the polarity of the solvent was probably the major factor in determining the reaction pathway. Alkylation using LiMe yielded the complex [Ti(SALEN)Me_2]; again the SALEN ligand occupies the equatorial plane and the two methyl groups occupy the *trans* axial positions.

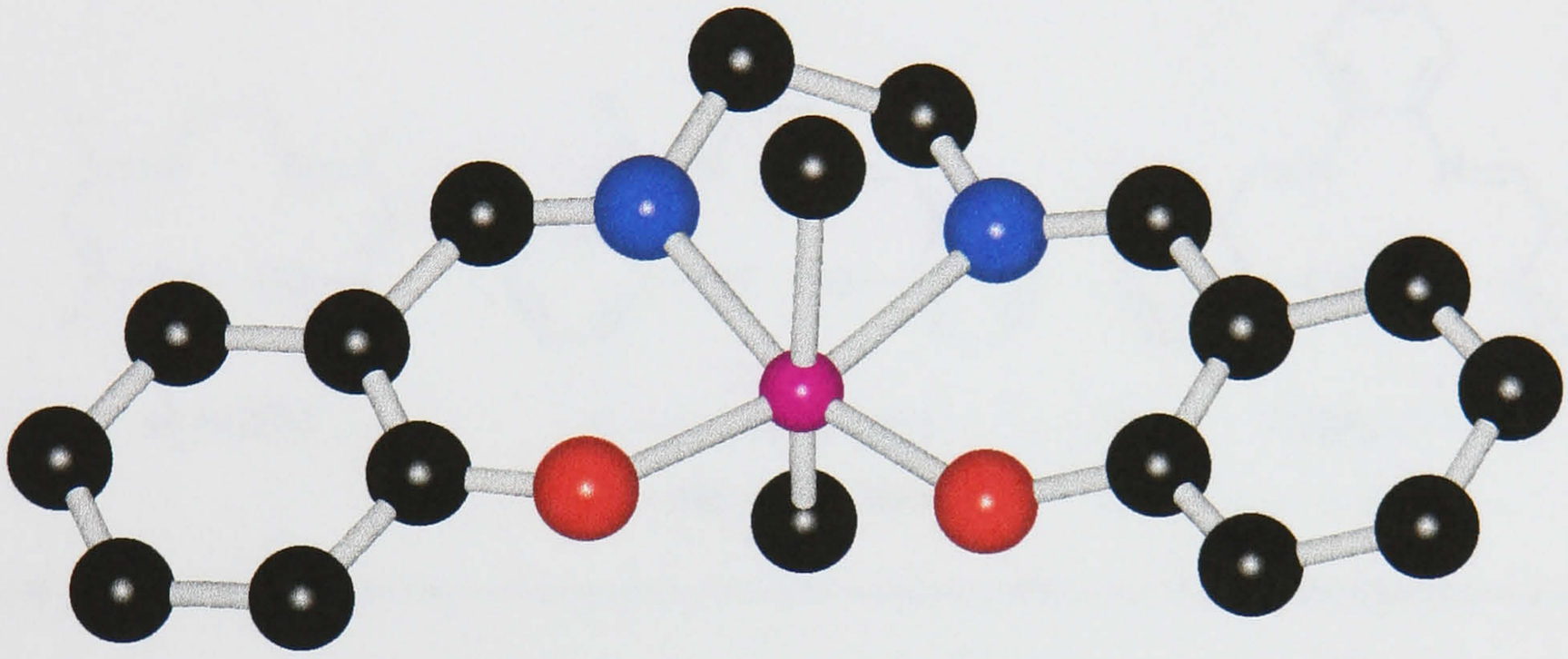

Figure 1.36 The molecular structure of [Ti(SALEN)Me_2].

Up until this time, all structural information on these Group 4 transition metal tetradentate Schiff base complexes had shown the Cl–M–Cl unit occurred in a *trans* configuration. However, in 1990 Floriani *et al*[113] reported the structures of both *cis* and *trans* dichloro derivatives of six and seven coordinate zirconium and hafnium bonded to tetradentate Schiff base ligands. These complexes had been prepared by the reaction of MCl_4.2THF (M = Zr, Hf) with the sodium salt of tetradentate Schiff bases H_2ACEN, H_2SALEN, H_2DMSALEN and H_2SALOPHEN.

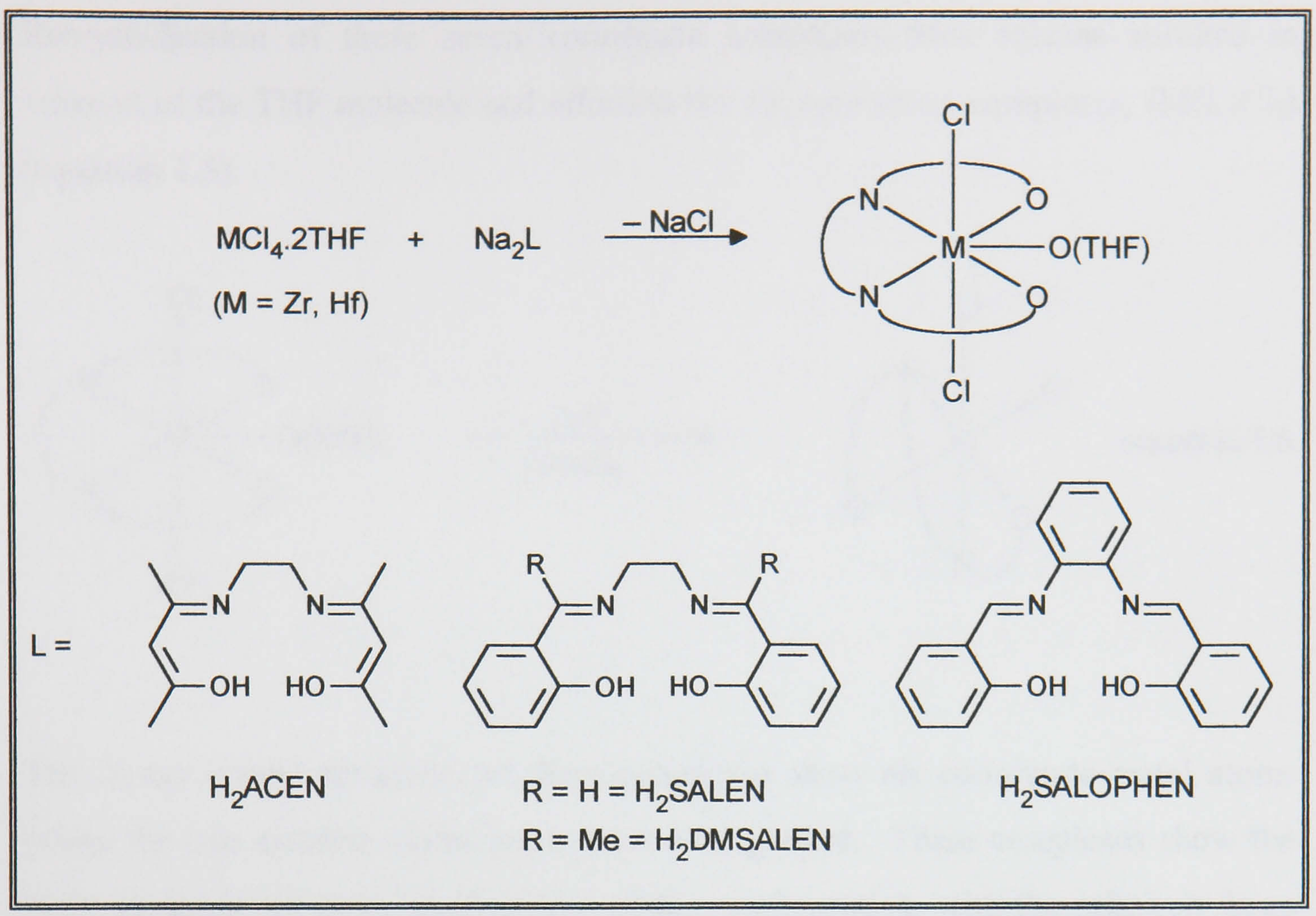

Equation 1.4 Showing the preparation of $[M(L)Cl_2(THF)]$ complexes

The X–ray crystallographic analyses of these complexes, $[M(L)Cl_2(THF)]$, showed the metal ion is seven coordinate with a pseudo–pentagonal bipyramidal geometry. The equatorial plane of the bipyramid is defined by the N_2O_2 donor atoms and by the oxygen atom of the THF molecule, while the apices are occupied by the two chlorine atoms in a significantly bent *trans* arrangement.

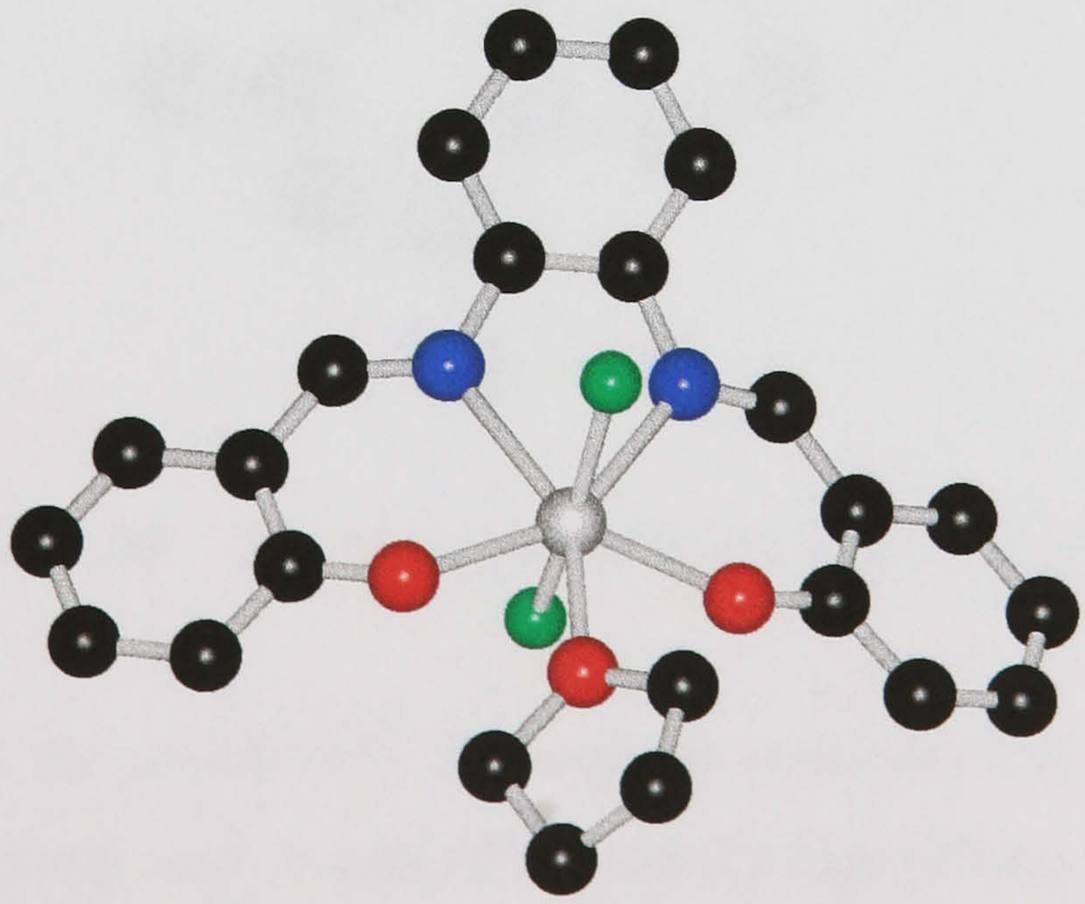

Figure 1.37 The molecular structure of $[Hf(SALOPHEN)Cl_2(THF)]$

Recrystallisation of these seven coordinate complexes from toluene resulted in removal of the THF molecule and afforded the six coordinate complexes, $[M(L)Cl_2]$ (equation 1.5).

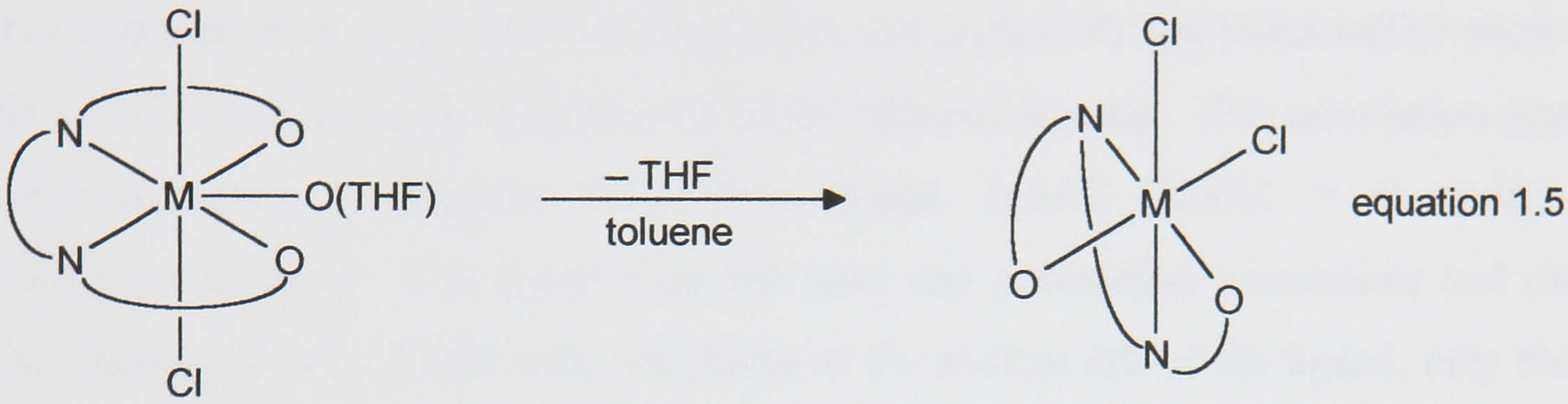

equation 1.5

The X–ray crystal structures of these complexes show six coordinate metal atoms where the two chlorine atoms are in a *cis* arrangement. These complexes show the N_2O_2 cavity is not in its usual square–planar configuration, with the relatively large zirconium and hafnium atoms forcing the ligand to bend and thus impose a *cis* arrangement of the chlorine atoms.

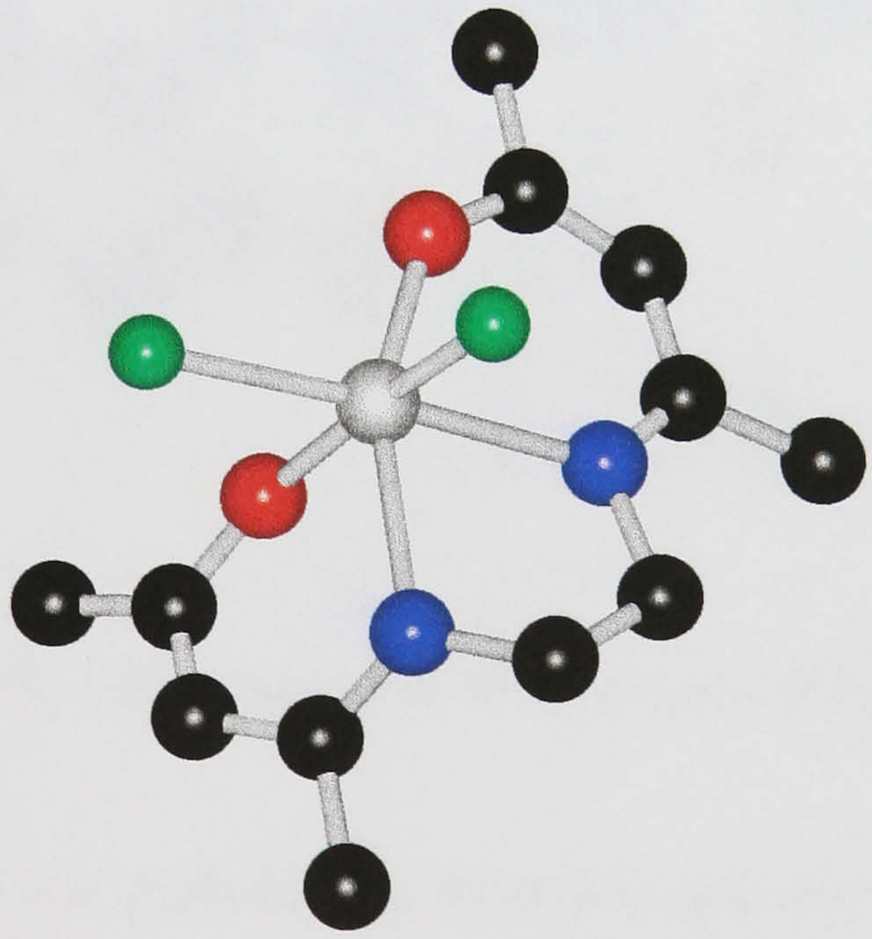

Figure 1.38 The molecular structure of $[Zr(ACEN)Cl_2]$

The loss of the coordinated THF solvent molecule from the complexes was reported to be relatively easy in spite of the metal's high affinity for oxygen. As can be seen in Figure 1.38 the loss of the solvent molecule results in a rearrangement of

the coordination geometry at the metal centre, with the chlorine ligands moving from a nearly *trans* to a *cis* arrangement.

It was also proved by ^{1}H N.M.R studies that in non–coordinating solvents, e.g. C_6H_6 or CH_2Cl_2, the *cis* and *trans* isomers do not interconvert. They concluded that in the absence of geometrical constraints, zirconium(IV) and hafnium(IV) prefer six coordination and a *cis* arrangement of the chlorine ligands. This conclusion was confirmed using a bidentate Schiff base ligand, MSAL (MSAL = N–methyl–salicylideneiminate). This ligand does not have any geometrical constraints and on the reaction of $ZrCl_4.2THF$ with two moles of the sodium salt of the ligand, only the *cis* isomer of the complex, $[Ti(MSAL)_2Cl_2]$ was obtained even in the presence of a coordinating solvent. The structure of this *cis* isomer has been confirmed by X–ray crystallography (Figure 1.39).

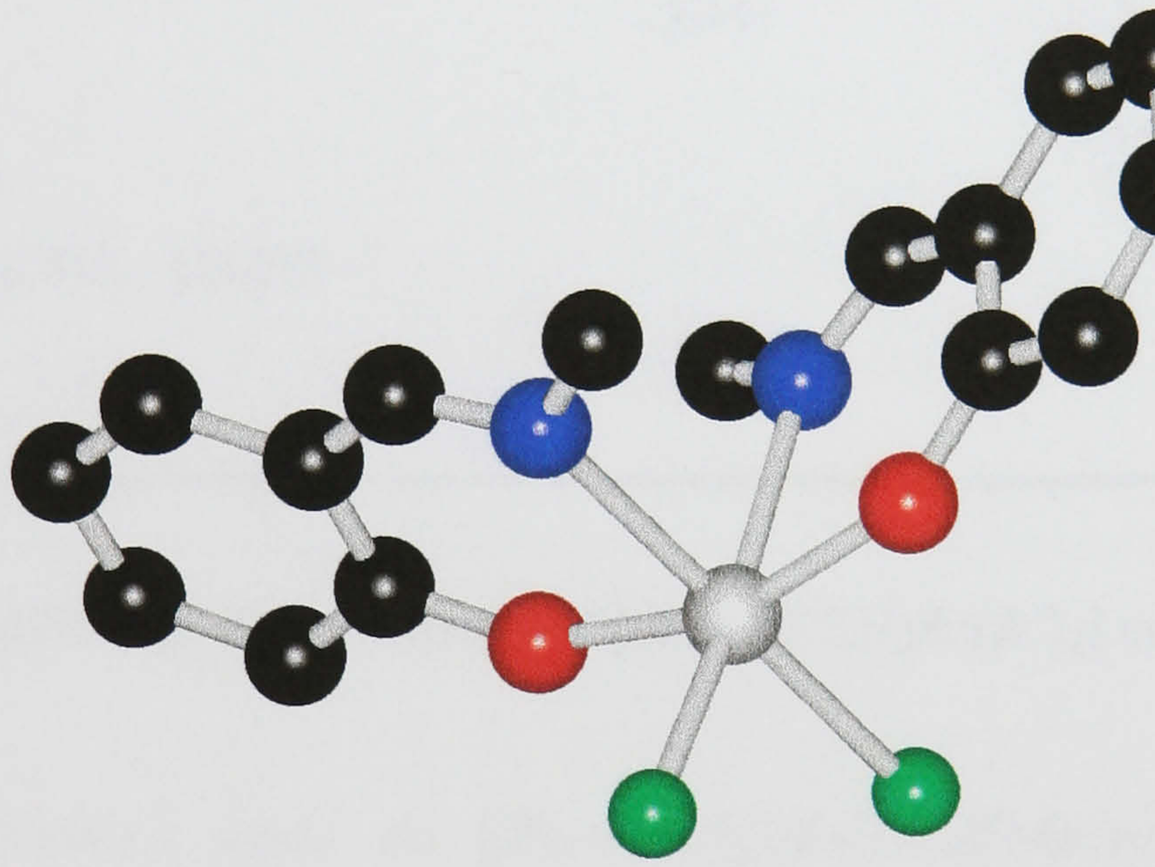

Figure 1.39 The molecular structure of $[Ti(MSAL)_2Cl_2]$

The most recent and probably the most relevant work to the research carried out in this thesis was published in 1995 by Jordan *et al.*[83] They reported the synthesis, structure and the reactivity of both neutral $[(R_6–ACEN)Zr(R')_2]$ and the cationic $[(R_6–ACEN)Zr(R')]^+$ alkyl complexes (where R = H, F; R' = CH_2CMe_3, CH_2Ph). Their objectives were to develop efficient syntheses of $[(N_2O_2–chelate)MR_2]$ and $[(N_2O_2–chelate)MR]^+$ complexes and to compare the reactivity of the $[(N_2O_2–chelate)MR]^+$ cations with that of $[Cp_2MR]^+$.

As Floriani[112,114] had shown, Jordan *et al* discovered that the generation of $[(R_6–ACEN)Zr(R')_2]$ complexes by the alkylation of the corresponding dichloride complex was not an efficient method. This method resulted in the generation of *cis* and *trans* isomers along with alkyl migration products which could not be separated. As a result they used the alkane elimination reaction between ZrR'_4 ($R' = CH_2CMe_3$, CH_2Ph) with the free ligand $H_2(R_6–ACEN)$ which yield the desired $[(R_6–ACEN)Zr(R')_2]$ complexes.

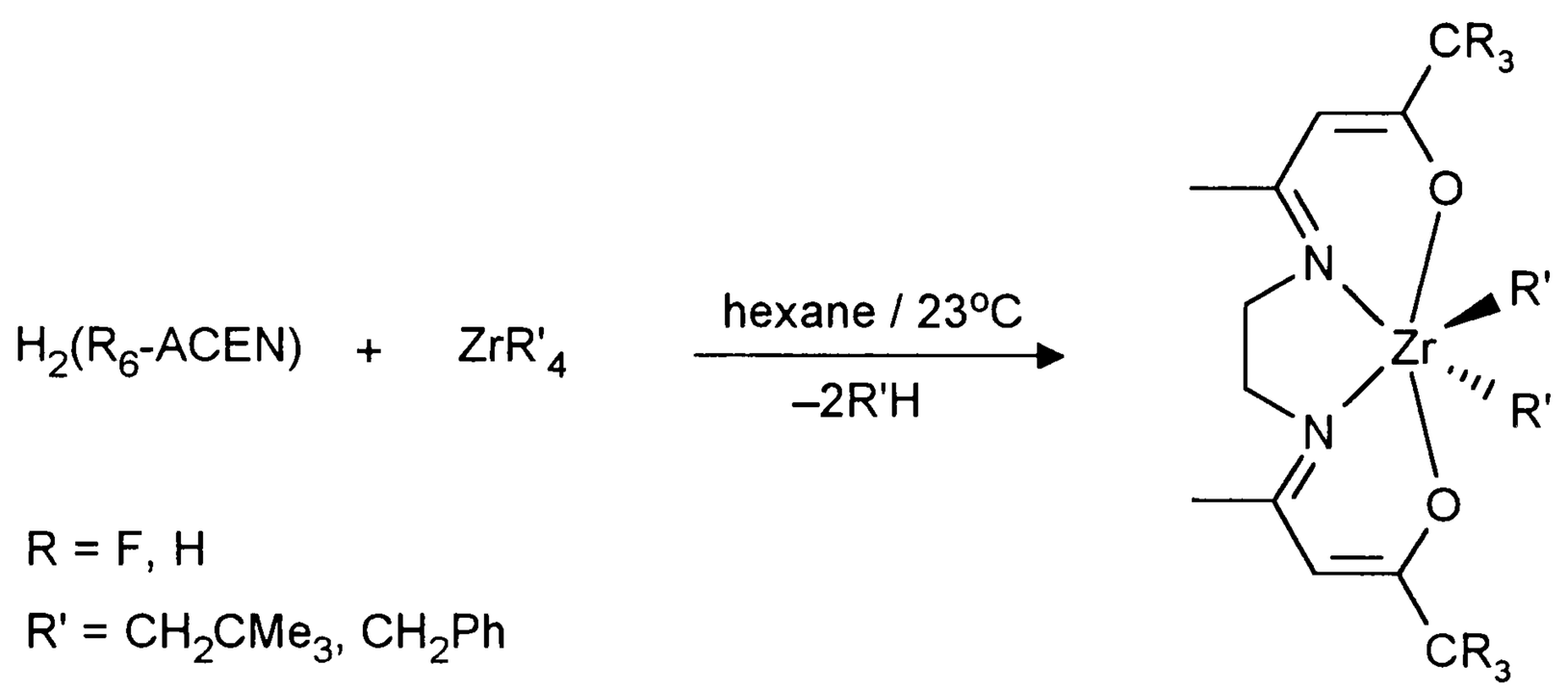

Equation 1.6 The synthesis of $[(R_6–ACEN)Zr(R')_2]$ complexes

The X–ray diffraction study on $[(F_6–ACEN))Zr(CH_2CMe_3)_2]$ showed that the complex adopts a monomeric elongated trigonal prismatic structure. The C–Zr–C bond angle (129.9(2)°) is much larger than the corresponding Cl–Zr–Cl (87.2(1)°) bond angle.

They then achieved the synthesis of cationic complexes by protonolysis with HNR_3^+ reagents, using $B(C_6F_5)_4$ as the counteranion. Protonolysis of $[(R_6–ACEN)Zr(CH_2CMe_3)_2]$ with $[HNMe_2Ph][B(C_6F_5)_4]$ in CH_2Cl_2 affords the salt $[(R_6–ACEN)Zr(CH_2CMe_3)(NMe_2Ph)][B(C_6F_5)_4]$ involving the released NMe_2Ph amine coordinated to the metal centre.

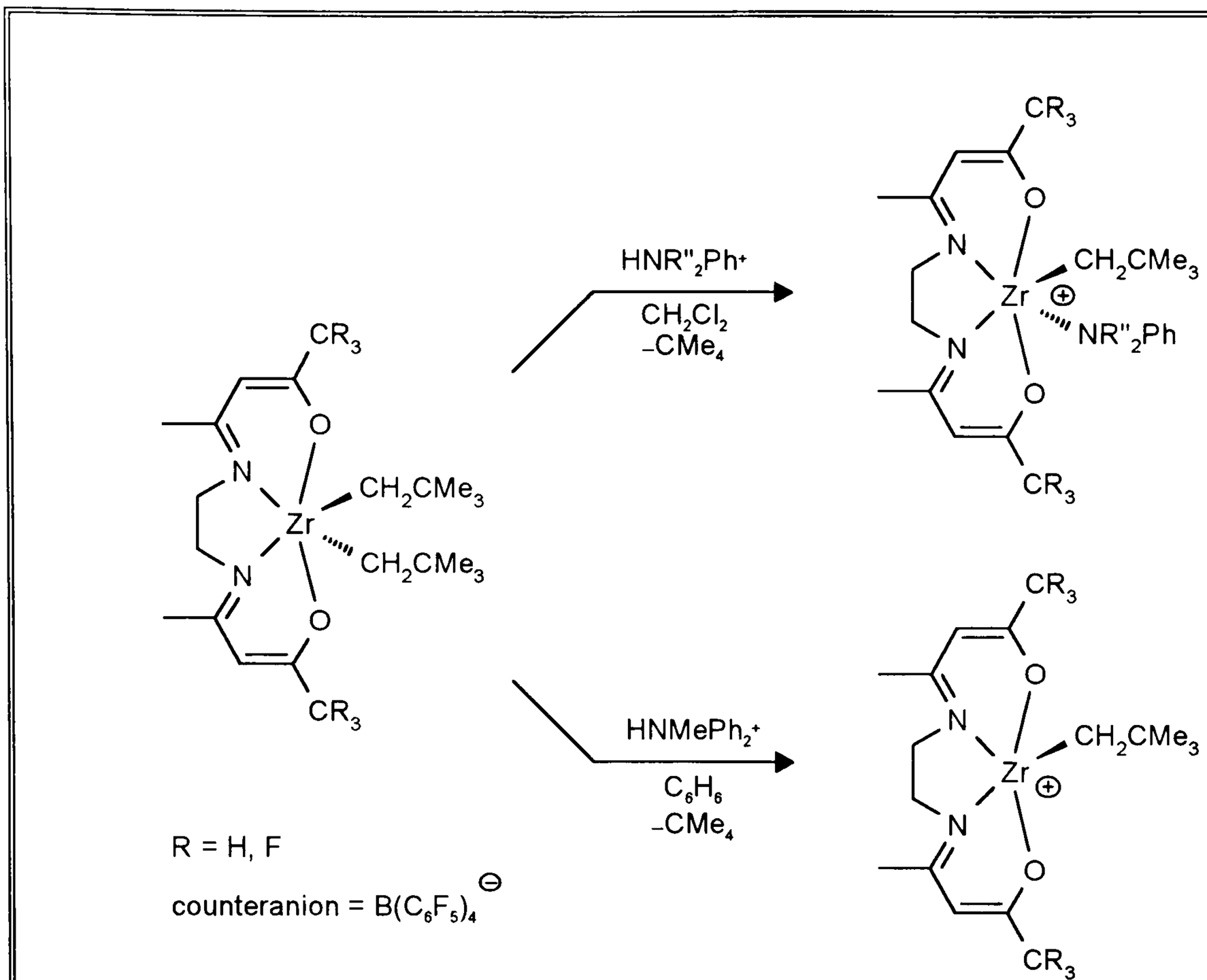

Scheme 1.2 The synthesis of cationic $[(R_6\text{–ACEN})Zr(R')]^+$ complexes

These cationic species were shown to react with CO and benzophenone to afford the expected insertion products, but did not insert ethylene or alkynes in the absence of aluminium alkyl cocatalysts. However, in the presence of small amounts of aluminium trialkyl cocatalyst these $[(R_6\text{–ACEN})Zr(R')]^+$ cationic species are moderately active ethylene polymerisation catalysts.

In all the previous research featured above it is noteworthy that the *cis* arrangement of the MCl_2 unit has only been achieved for zirconium and hafnium compounds. Furthermore such an arrangement was ascribed to be due to the larger size of the two heavier Group 4 metals, compared with that of titanium where quoted values for the covalent radius are about 0.416Å, the corresponding values for zirconium and hafnium being 0.517Å and 0.517Å respectively. It is therefore of interest to determine whether it is possible to achieve both the *cis* and *trans* geometries for complexes involving titanium, and to gain some understanding of the major factors involved in controlling the *cis–trans* stereochemistry.

CHAPTER 2

Tetradentate Schiff Base Ligands and their Group 4 Metal Complexes

CHAPTER 2 Tetradentate Schiff Base Ligands and their Group 4 Metal Complexes.

Introduction

The previous chapter provided a detailed overview of the previous reactions studied between tetradentate Schiff base ligands and Group 4 transition metals. My work within this chapter describes the synthesis of tetradentate Schiff base Group 4 metal complexes. These complexes have been synthesised so that a study could be made of their properties, including the factors which might influence the stereochemistry of the type of complex $[M(L)Cl_2]$ (L = Schiff base dianion). In addition their potential for use as Ziegler–Natta catalysts when combined with aluminium alkyl derivatives was of interest to the sponsors of the C.A.S.E. award.

The complexes which will be described below have been targeted as possible replacements for the *ansa*–metallocene homogeneous catalysts [Figure 2.1(a)]. The reasoning behind the choice of such complexes, is that there is a wide range of tetradentate Schiff base ligands available and these ligands are easily substituted at various sites within the ligand framework. Therefore if the ligand could be combined with molecules of the MCl_4 (M = Ti, Zr, etc.) type to yield a complex containing a *cis* or *trans* MCl_2 fragment [Figure 2.1 (b) and (c)], it would be of interest to compare the properties of such complexes with the *ansa*–type metallocenes.

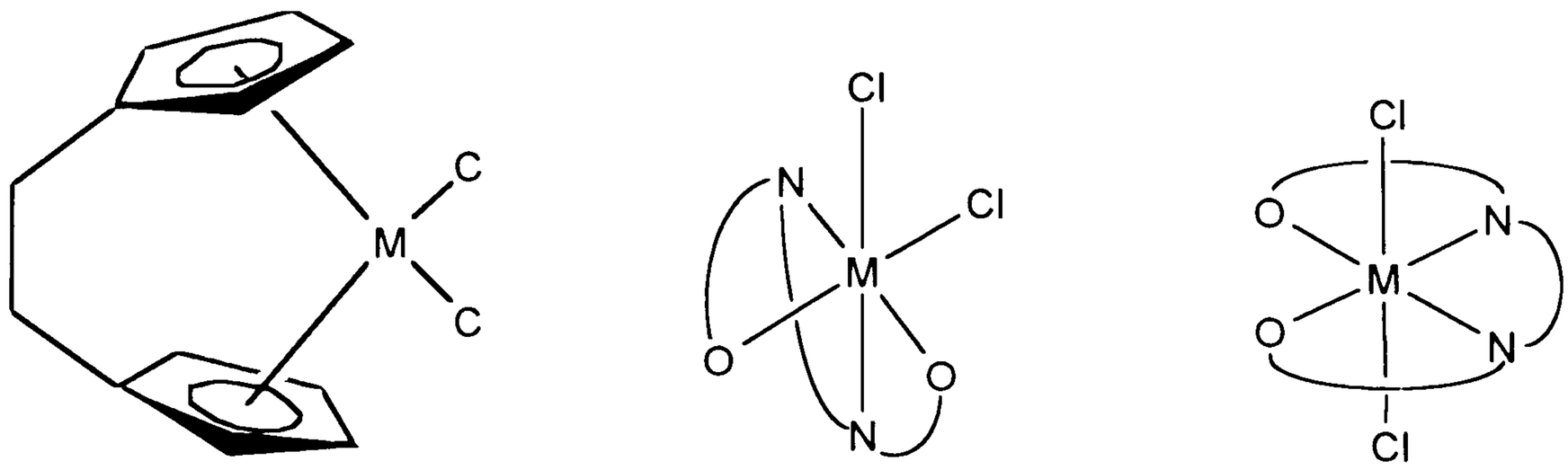

(a) (b) (c)

Figure 2.1 A diagrammatic representation of (a) an *ansa*–metallocene, (b) a *cis* Schiff base complex and (c) a *trans* Schiff base complex

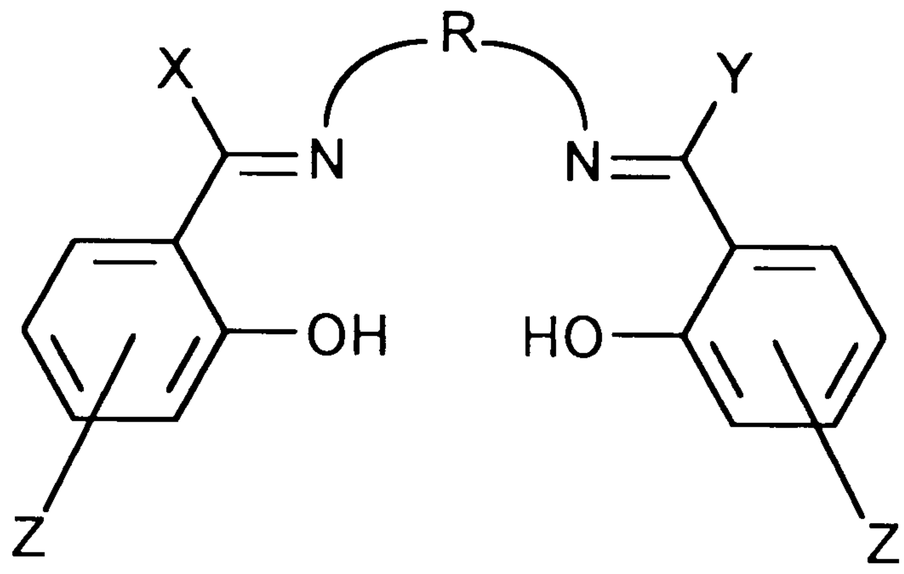

Figure 2.2 A diagrammatic representation of a tetradentate Schiff base ligand showing the sites available for ligand modification (R, X, Y, Z)

The diagram above (Figure 2.2) shows that these ligands possess a great deal of scope for the manipulation of the steric and/or the electronic properties of the ligand, by substitution at various positions within the ligand framework. If these complexes should show catalytic activity, further modifications could be made to the ligand structure to test whether steric or electronic factors have any effect on the activity of a catalyst, on the rate of polymerisation or the tacticity of the polymer produced.

The stereochemistry of the complexes

Previous research on Group 4 transition metal halide tetradentate Schiff base complexes has shown that all six coordinate complexes of titanium have a *trans*-MCl_2 stereochemistry, whereas six coordinate zirconium and hafnium complexes have been found with a *cis*-MCl_2 geometry at the metal centre, with no *trans*-MCl_2 structure known. This difference in geometry has been attributed to the size of the metal centres.[113] It is worth mentioning that in the case of zirconium and hafnium an initial seven coordinate complex can be formed with a coordinated solvent such as THF in the seventh coordination site (see introduction p.44–46). The removal of the THF molecule by recrystallisation from hot toluene yields the six coordinate complex.

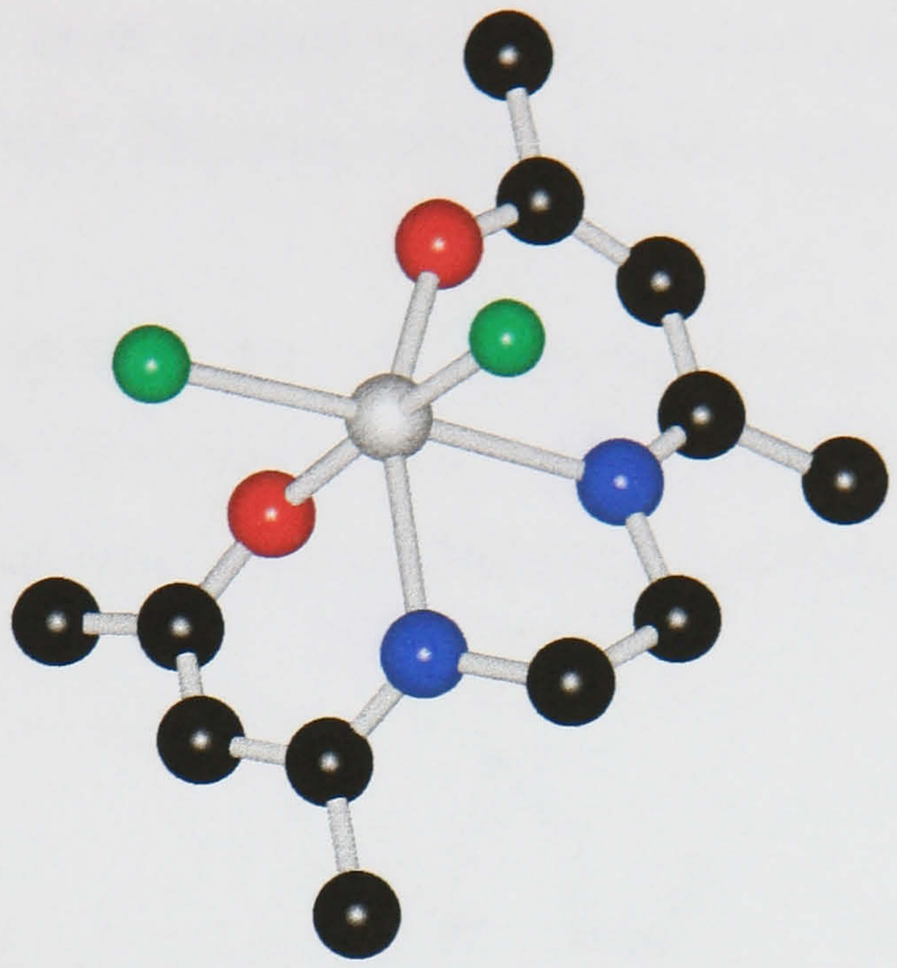

Figure 2.3 The molecular structure of $[Zr(ACEN)Cl_2]$

The aims of the research carried out within this chapter are:

(a) to synthesise both *cis*-MCl_2 and *trans*-MCl_2 complexes of Group 4 metals with tetradentate Schiff bases.

(b) to test and study the effect that the stereochemistry of these complexes has on the catalytic behaviour to assess the relative importance of a *cis*-MCl_2 or *trans*-MCl_2 geometry at the metal centre.

(c) As a consequence of this, if a *cis*-MCl_2 geometry is required for catalysis, to use ligand design to control the stereochemistry of the resultant complex by the introduction of steric restraints, within the ligand framework, to produce the desired *cis*-MCl_2 stereochemistry at the metal centre.

Ligand systems

Three types of tetradentate Schiff base ligand systems have been prepared and studied. These three different ligand systems have been chosen because of the varying degree of steric hindrance associated with the backbone of these ligands. This steric effect of the ligand backbone, coupled with substitution at the imine carbon atoms, should provide enough steric bulk to produce the desired *cis* stereochemistry at the metal centre with at least some of these ligands. Prior to synthetic work, the effect that these ligands might have on the final stereochemistry at

the metal centre has been studied by using a molecular modelling package, *HYPERCHEM* version 4.5. The results obtained from this study can be found later in this chapter p.103.

These ligand systems are all symmetrical Schiff bases derived from salicylaldehyde and its derivatives. The condensation reaction involved in the preparation of Schiff base ligands is described in the introduction, p.32–33.

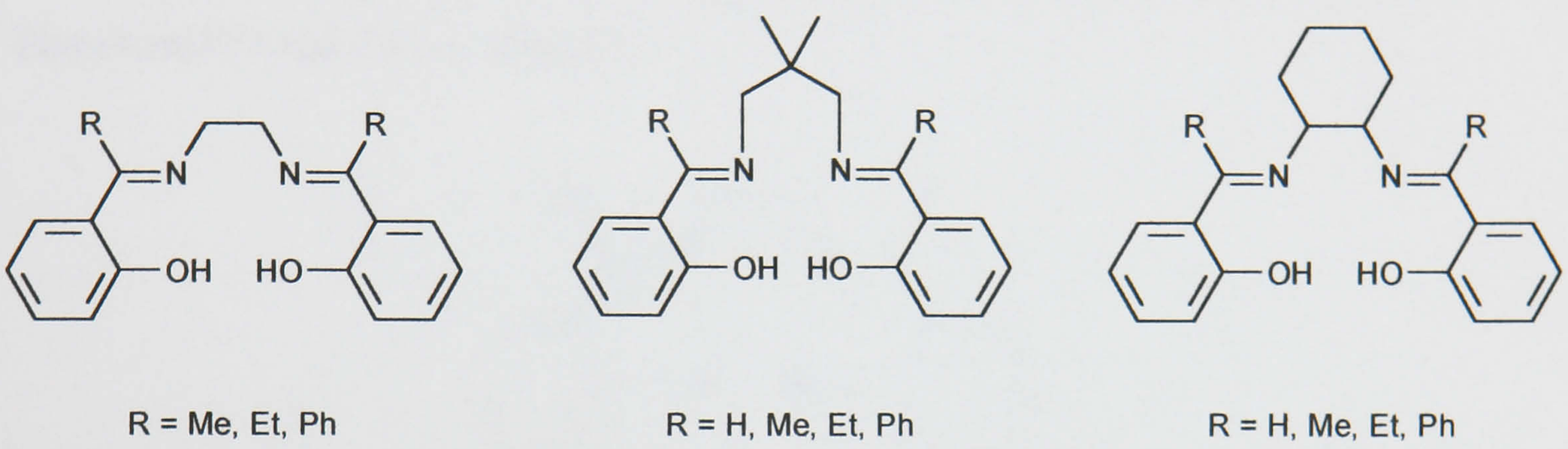

Figure 2.4 Diagrammatic representations of the three types of tetradentate Schiff base ligand studied

Although, when this research was started, the X–ray structures of several metal complexes with Schiff base ligands had been reported (ten Group 4 complexes), very few of the free ligands had been characterised.[115] For tetradentate ligands of the type above, the solid state structures of only five free ligands have been determined.[100,116–120]

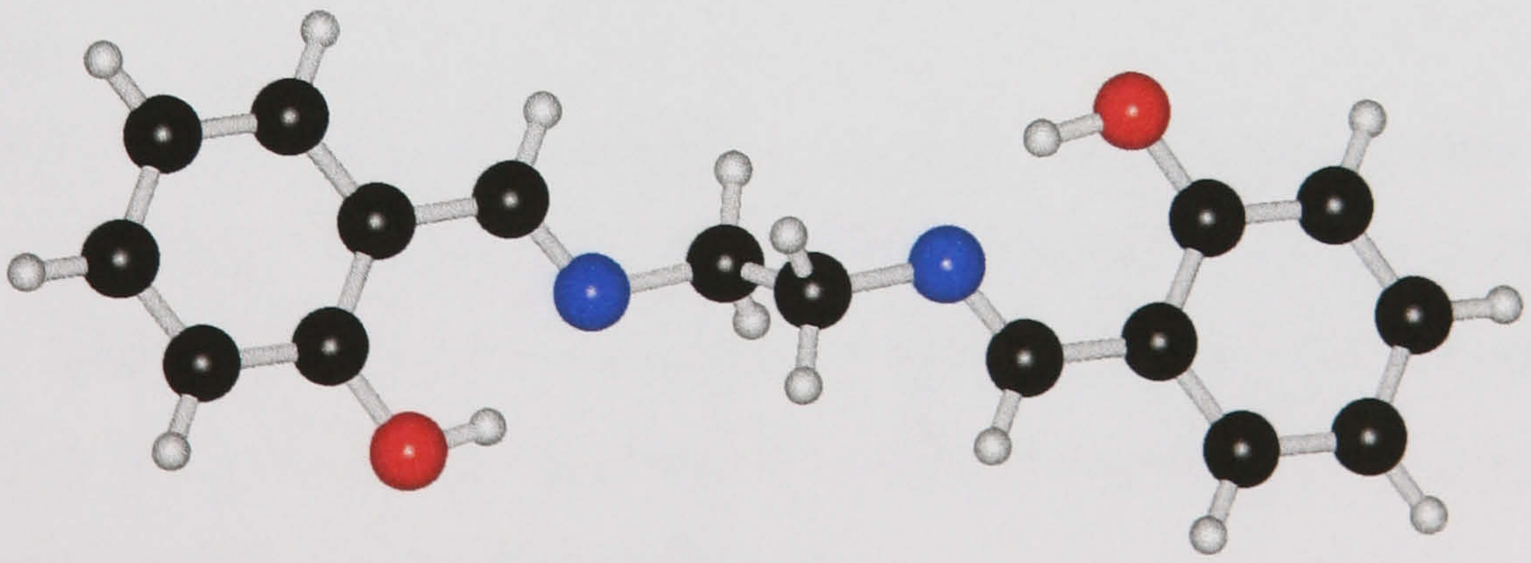

Figure 2.5 The molecular structure of the free ligand H_2SALEN

For this reason the structures of several of the free ligands synthesised for this study have been determined, so that any subsequent changes upon coordination to a metal may be investigated, and to see whether there are any significant changes in the Schiff base ligands themselves as the degree of substitution within these ligands is changed.

Preparation of the SALEN Type Schiff Base Ligands and their Complexes with Titanium(IV) and Zirconium(IV)

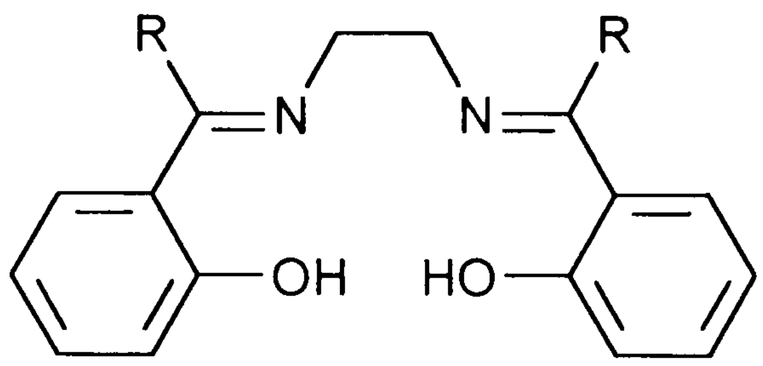

Figure 2.6 A representation of the SALEN type Schiff base ligands

The free ligands are readily synthesised by the condensation reaction between 1,2–diaminoethane (ethylenediamine) and the appropriate aldehyde or ketone. One mole of ethylenediamine is added to 2 moles of the appropriate aldehyde or ketone, using methanol as solvent, resulting in the loss of water and the precipitation of the desired free ligand. These reactions are very efficient and result in excellent yields of the desired ligand. The ligands are bright yellow solids which are air stable and readily soluble in almost all the common organic solvents, such as MeOH, hexane, toluene etc..

There have been two strategies adopted for the preparation of metal complexes of these ligands within this thesis, although other methods may be available. The first is the direct reaction of the free ligand with the metal halide (equation 1), the second is the synthesis of Schiff base complexes by using the alkali metal salt of the dianionic ligand (reaction 2).

$$H_2L + MCl_4 \longrightarrow [M(L)Cl_2] + 2\,HCl\,(g) \qquad (1)$$

This reaction (1) was initially used, however, difficulties were encountered with this method. Firstly, an initial problem is involved with the handling of MCl_4, especially, with titanium tetrachloride ($TiCl_4$) which is a liquid at room temperature and extremely reactive and therefore the precise stoichiometric amount was often difficult to measure accurately.

Another problem with this method also involves the extreme reactivity of the MCl_4 compounds. It was discovered at various temperatures (ranging from –78 to 25°C) that the reaction upon addition of either ligand to metal, or metal to ligand was extremely vigorous resulting in not only the desired $[M(L)Cl_2]$, but in unknown polymeric species and in certain instances resulted in the breakdown of the ligand itself by attack at the carbon atom of the imine bond. This method thus provided a poor yield of the desired $[M(L)Cl_2]$ complex which was often difficult to separate from undesired products from the reaction. This method, however, can and has been used to successfully isolate the desired $[M(L)Cl_2]$ complex.

$$Na_2L + MCl_4 \longrightarrow [M(L)Cl_2] + 2\,NaCl\,(s) \quad (2)$$

(L = Schiff base)

Floriani *et al*[113] reported that the use of the alkali metal salts had significant advantages over the other method, namely the complete and easy substitution of all protic hydrogens prior to reaction with the metal halide, and the control of the extent of substitution of the chloride ligands in MX_n halides. For this reason, the sodium salt of the ligand has been used in the preparation of almost all the complexes. The preparation of another alkali metal salt (e.g. the dilithio salt) has not been attempted due to the convenient preparation of the disodium salt.

The sodium salt is generally prepared and used in situ by the reaction of the free ligand with two moles of sodium hydride (NaH), under refluxing conditions for two hours in THF solvent.

$$H_2L + 2\,NaH \xrightarrow{THF} Na_2L + 2\,H_2$$

(L = Schiff base)

The reaction of equimolar quantities of the sodium salt of the Schiff base ligand and the THF adduct of the Group 4 metal tetrahalide ($MCl_4.2THF$; M = Ti, Zr) using THF as the solvent at low temperatures, followed by subsequent heating to 50 °C, results in the precipitation of two moles of sodium chloride (NaCl) and the formation of the desired complex, $[M(L)Cl_2]$.

$$Na_2L + [MCl_4.2THF] \xrightarrow{THF} [M(L)Cl_2] + 2\ NaCl$$

The pure complexes can be obtained by removing the NaCl by filtration. However, a greater yield can be achieved by extracting the filtered solid with THF. The 1:1 metal to ligand molar ratio must be strictly controlled with zirconium, since a slight excess of the Schiff base leads to the overall replacement of all of the chlorides, and the formation of complexes analogous to $[Zr(SALOPHEN)_2]$ (see introduction p.36).[110]

It is worth mentioning that in the reactions for the preparation of metal complexes, the THF adduct of the metal tetrahalide, $[MCl_4.2THF]$, is always used rather than the metal tetrahalide (MCl_4) itself. This is because $[MCl_4.2THF]$ are crystalline solids which are easier to handle than, with say, the highly reactive, liquid titanium tetrachloride. Another reason is that these adducts are much more readily soluble than the tetrahalides themselves, and this leads to a better reaction as both reactants can be dissolved prior to mixing. Finally, and perhaps most importantly, these $[MCl_4.2THF]$ adducts are less reactive than the metal tetrahalides, and as a result a slower, more controlled reaction occurs which results in the unique production of the required $[M(L)Cl_2]$ complex. We have shown that when the metal tetrahalides are used in the reaction, due to their greater reactivity, other products are formed in the reaction mixture e.g. polymeric complexes, and there is also evidence that the metal tetrahalide can also destroy the ligand by reaction at the imine bond. This results in the loss of yield, and also these other complexes are not readily separated from the required $[M(L)Cl_2]$ complex.

As mentioned in the introduction, the preparation of complexes with titanium differs from that with zirconium and hafnium. Due to their preference for high

coordination numbers, both zirconium and hafnium initially form a seven coordinate complex with a THF molecule in the seventh coordination site.

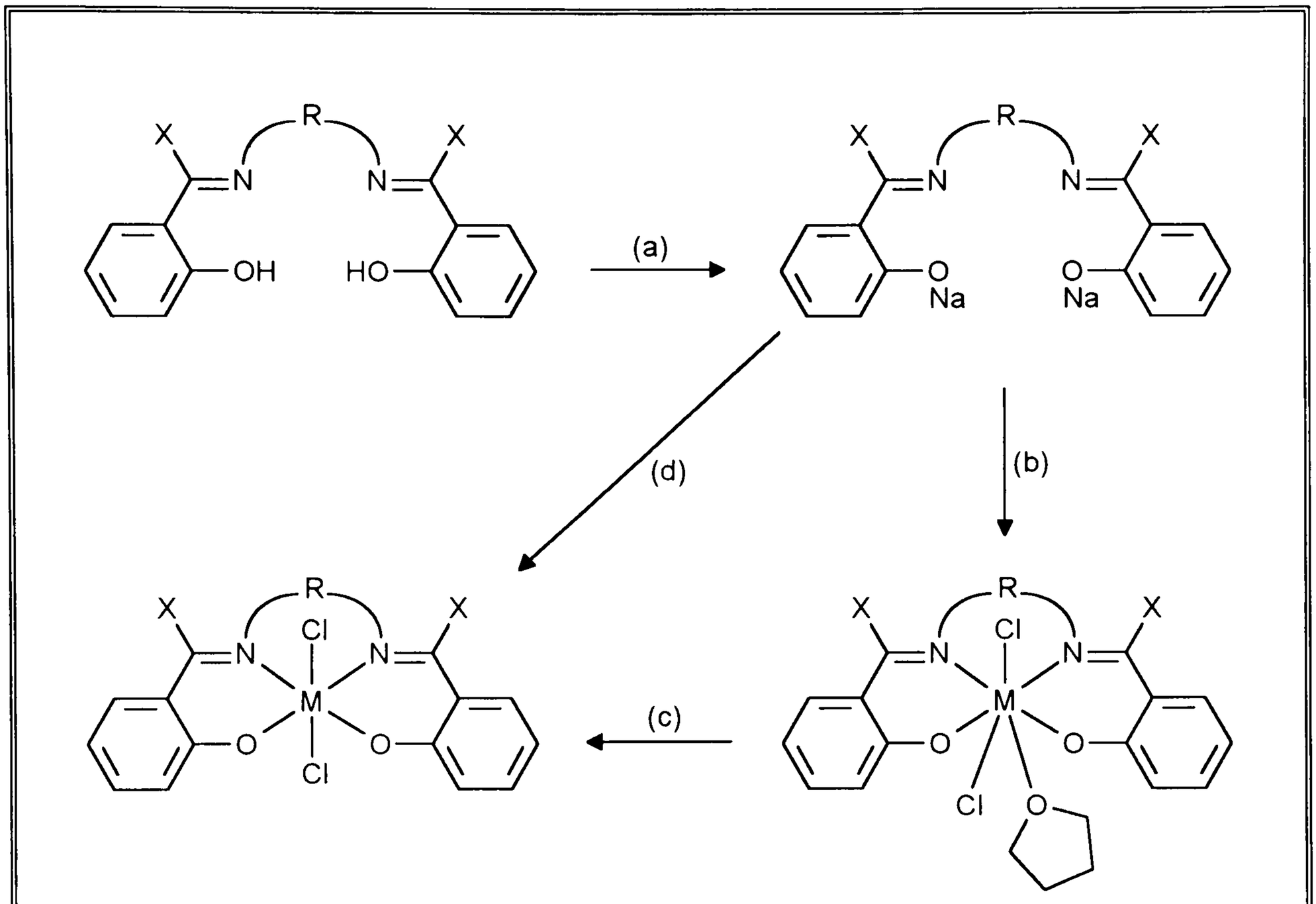

Reagents and conditions: (a) sodium hydride, (b) (MCl_4.2THF M = Zr, Hf),
(c) reflux in toluene, (d) ($TiCl_4$.2THF).

Scheme 2.1 Showing the pathways to $[M(L)Cl_2]$ complexes

The unsolvated six coordinate complexes of zirconium and hafnium can be achieved relatively easily by recrystallisation from hot toluene. The loss of the THF solvent molecule is facile in spite of the high affinity of zirconium for oxygen.

The desolvation of these zirconium complexes is assumed to be accompanied by a rearrangement of the coordination geometry around the metal. That is the metal becomes six coordinate, and the two chloride ligands move from a nearly *trans* to a *cis* arrangement. This preference for the *cis* arrangement has been proved by the synthesis of $[Zr(MSAL)_2Cl_2]$ (see introduction p.46) which, having no geometrical restraints, is six coordinate with a *cis* arrangement of chloride ligands. The titanium

complexes are rigorously octahedral and probably adopts a *trans* arrangement of chloride ligands. This difference in the coordination geometry is again attributed to the difference in the metal ion size.

The titanium and zirconium complexes are fairly soluble in moderately polar solvents such as dichloromethane, chloroform, toluene and tetrahydrofuran, allowing a spectroscopic characterisation by N.M.R spectroscopy, but are totally insoluble in non–polar solvents such as pentane and hexane. As solids they decompose in the air, and the seven coordinate zirconium complexes are very sensitive to moisture, and the formation of oxo compounds has been observed.[113] As solutions in organic solvents they are very sensitive to hydrolysis. However, these compounds can be conveniently handled in an inert atmosphere, and manipulations were therefore carried out in a nitrogen filled glove box or by using a Schlenk–line equipped with dry argon or nitrogen.

All the ligands used in this work were recrystallised and vacuum dried before use, and handled in the glove box to ensure the absence of impurities, such as water. The absence of water, is essential for the correct and clean preparation of the sodium salts of the ligands. The removal of impurities was also found to greatly enhance the potential for obtaining crystalline solids from the reaction mixture.

Spectroscopic Characterisation of the SALEN Type Schiff Base Ligands and their Complexes with Titanium and Zirconium.

Nuclear Magnetic Resonance Spectra

^{1}H N.M.R. spectra have been recorded routinely during the course of this work, and have proved useful in verifying both the stoichiometry and purity of the reaction products. Details of the ^{1}H N.M.R. data for individual compounds are given in the experimental section. All the spectra for the free Schiff base ligands were recorded in $CDCl_3$ solutions, whereas those for the metal complexes were recorded in $CDCl_3$, CD_2Cl_2 or d^6–DMSO solutions.

The ^{1}H N.M.R. spectra of the free SALEN type Schiff base ligands are relatively straightforward, showing that all the ligands are symmetrical. All the ligand

resonances are well defined and therefore provide a good handle for comparison with ^{1}H N.M.R. spectra obtained from the metal complexes.

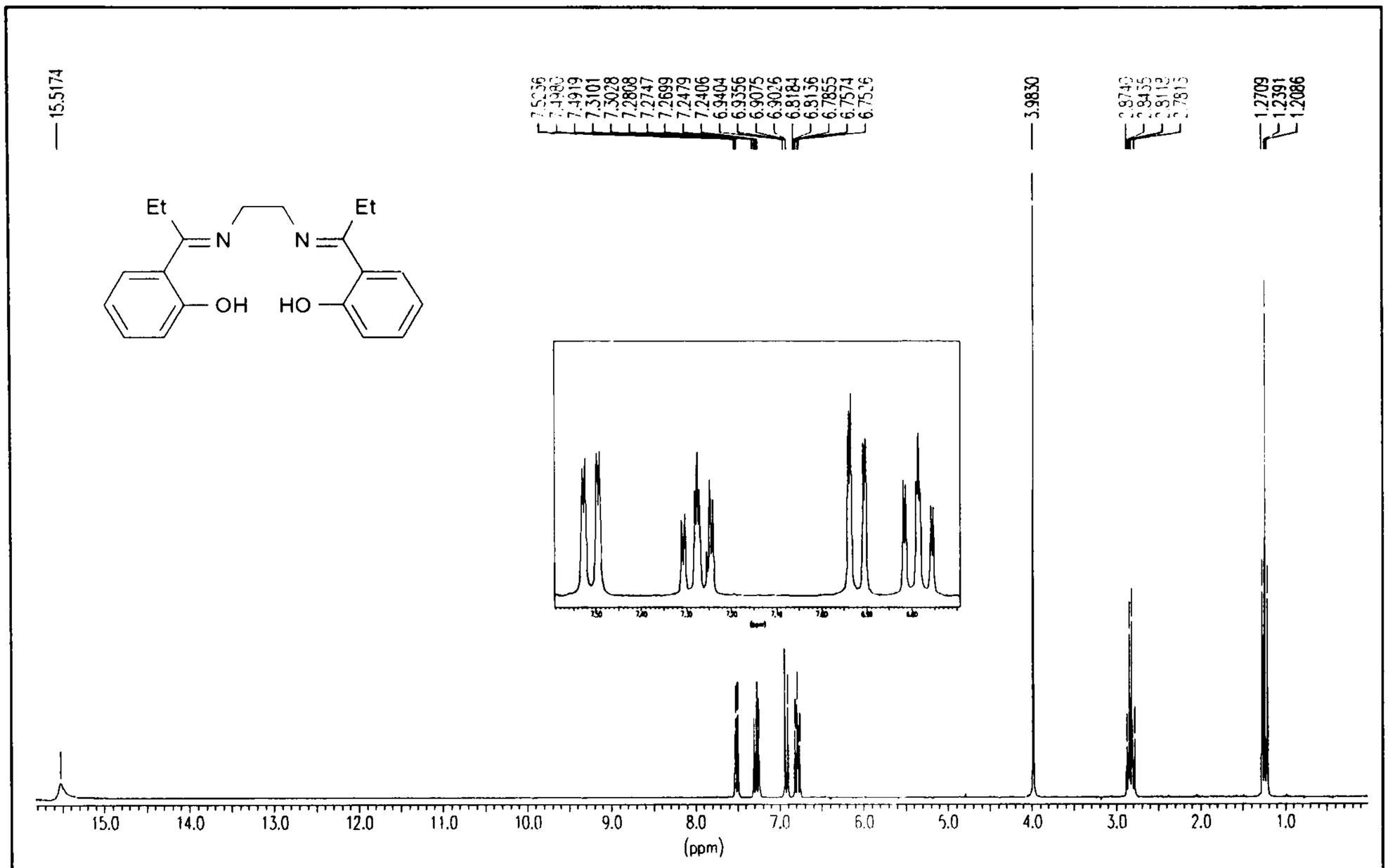

Figure 2.7 The ^{1}H N.M.R. spectrum of the free ligand H_2EtSALEN

Figure 2.7 shows a typical spectrum obtained from a free SALEN type Schiff base ligand, H_2EtSALEN. The OH resonances are seen as a slightly broad singlet integrating for two protons at δ 15.5 ppm. The aromatic resonances appear in the expected region between δ 6 and 8 ppm.. These aromatic resonances are split into two doublet of doublets and two doublet of triplets each integrating for two protons. The two backbone CH_2 groups are seen as an extremely sharp singlet at δ 4 ppm. integrating for four protons. Finally, the CH_2 protons of the ethyl group are seen as a quartet at δ 2.8 ppm. integrating for four protons, and the two methyls of the ethyl groups are seen as a triplet at δ 1.2 ppm. integrating for six protons.

The ^{1}H N.M.R. spectra of the titanium and zirconium complexes with the SALEN type ligands are also relatively simple. A typical spectrum of a complex, [Zr(DMSALEN)Cl_2].THF can be seen in Figure 2.9. There is no further splitting of

the resonances, or extra resonances indicating that the complex is also symmetrical in solution. The loss of the OH resonance at δ 12–16 ppm. is essential in the spectra of such complexes, and any resonance in this region means either the reaction did not proceed to completion or that hydrolysis of the complex has occurred. The CH_2 resonances from the backbone of the ligand are still seen as a singlet and the splitting of the aromatic peaks remains the same. However, there are some slight shifts in these resonances compared with those in the free ligand.

^{13}C N.M.R. spectra have also been recorded for all of the compounds prepared, and the data for both ^{1}H and ^{13}C N.M.R. is summarised and assigned in Tables 2.1 and 2.2.

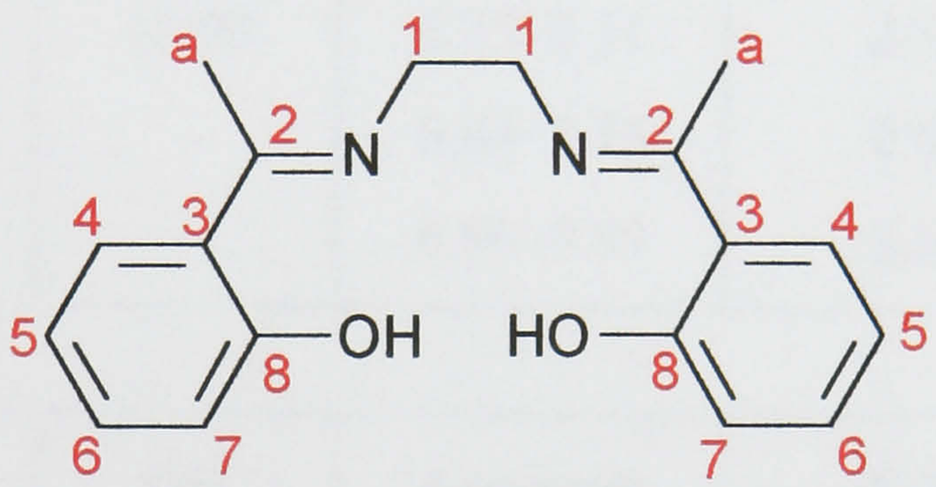

Figure 2.8 Showing the numbering of the carbons in the SALEN ligands

The resonances in the ^{13}C N.M.R. spectra of these compounds are as numbered in Figure 2.8, with the corresponding resonances for the group (a) on the imine carbon seen as expected. The C=N resonance is the most downfield resonance and can be seen between 165-180 ppm., the aromatic C–O resonance is also downfield at 160–165 ppm.. The remaining aromatic carbons are seen in the expected region of the spectrum between 100 and 140 ppm.. The aliphatic carbons are then seen at the upfield region between 60 and 0 ppm., with the CH_2 backbone carbons seen at 50–55 ppm and the methyl carbons around 20 ppm..

The N.M.R. spectra of the seven coordinate complexes, $[Zr(L)(Cl)_2(THF)]$ (L = DMSALEN, EtSALEN) are especially interesting. The ^{1}H N.M.R spectra of these complexes showed no further splitting of the ligand resonances indicating that the seven coordinate complexes are also symmetrical in solution. The only difference of

these spectra compared to those of six coordinate complexes is the presence of two multiplet resonances at approximately δ 3.4 and 1.6 ppm. which were attributed to the coordinated THF molecule (free uncoordinated THF resonances are at δ 3.75 and 1.75 ppm.). This was also found to be the case in the work performed by Floriani *et al*[113] on the complexes [Zr(SALEN)(THF)Cl_2] and [Hf(SALEN)(THF)Cl_2].

Table 2.1 Summary of ^{1}H N.M.R data (δ / ppm) of SALEN type Schiff base ligands and their Group 4 complexes

Compound	**OH**	**Aromatic**	**N=C–Me**	**CH_2–CH_2**
H_2DMSALEN	13.90	6.75–7.51	2.37	3.97
[Ti(DMSALEN)Cl_2]	–	6.84–7.75	2.66	4.26
[Zr(DMSALEN)Cl_2]	–	6.86–7.89	2.61	4.23

Compound	**OH**	**Aromatic**	**N=C–Et**	**CH_2–CH_2**
H_2EtSALEN	13.69	6.75–7.51	1.19–1.26 (6H) + 2.76–2.85 (4H)	3.96
[Ti(EtSALEN)Cl_2]	–	6.81–8.04	1.18–1.27 (6H) + 3.07–3.20 (4H)	4.20
[Zr(EtSALEN)Cl_2]	–	6.83–7.64	1.19–1.22 (6H) + 3.04–3.10 (4H)	4.27

Compound	**OH**	**Aromatic**	**N=C–Ph**	**CH_2–CH_2**
H_2PhSALEN	14.56	6.61–7.52	6.61–7.52	3.64
[Ti(PhSALEN)Cl_2]	–	6.91-7.36	7.55–7.61	3.72
[Zr(PhSALEN)Cl_2]	–	6.72–7.10	7.49–7.58	3.63

Table 2.2 Summary of Proton decoupled ^{13}C N.M.R data (δ / ppm) of SALEN type Schiff base ligands and their Group 4 complexes

Compound	R–C=N	C–O	Aromatic	R–C=N	CH_2–CH_2
H_2DMSALEN	172.60	163.05	132.35, 128.05, 119.36, 118.37, 117.27	14.66	50.06
[Ti(DMSALEN)Cl_2]	170.11	161.87	134.82, 131.26, 127.68, 122.69, 116.54	19.66	54.47
[Zr(DMSALEN)Cl_2]	171.02	162.09	133.99, 131.11, 126.95, 122.53, 116.96	18.95	54.04
H_2EtSALEN	177.46	164.00	132.40, 127.99, 118.71, 117.70, 117.23	21.16, 11.74	49.23
[Ti(EtSALEN)Cl_2]	173.66	161.82	134.79, 132.06, 125.84, 122.96, 116.37	23.11, 11.39	52.35
[Zr(EtSALEN)Cl_2]	174.29	162.11	134.21, 131.72, 124.97, 121.02, 116.89	22.91, 11.53	52.69
H_2PhSALEN	175.36	162.81	132.38, 127.16, 119.77, 117.80, 117.39	133.89, 131.55, 128.94, 128.75	52.27
[Ti(PhSALEN)Cl_2]	171.72	162.63	129.68, 127.32, 126.54, 122.45, 116.36	135.49, 129.38, 128.43, 127.62	54.81
[Zr(PhSALEN)Cl_2]	172.36	162.22	130.21, 127.22, 125.01, 121.17, 117.38	134.60, 130.83, 128.81, 128.09	54.38

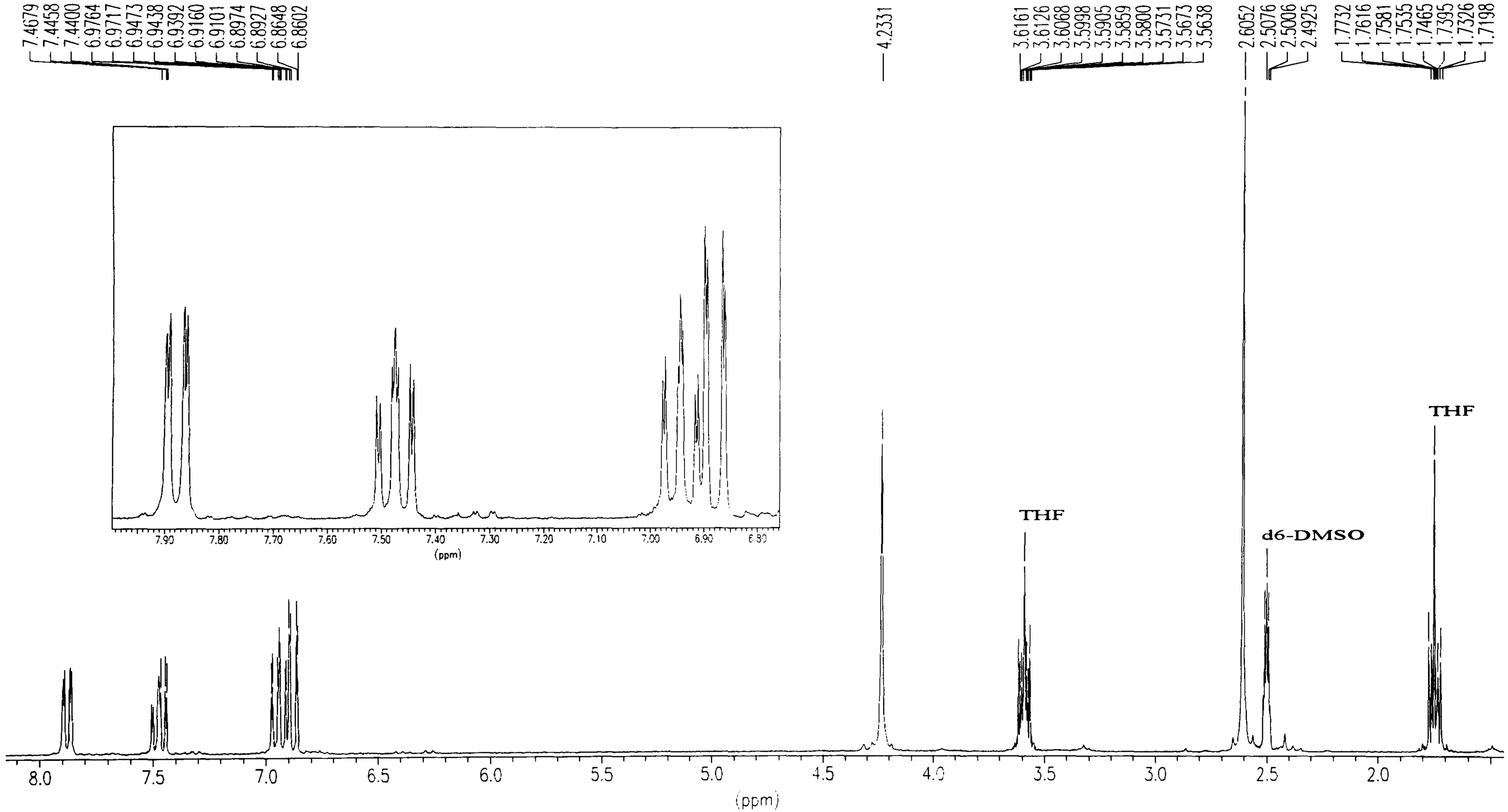

Figure 2.9 The ^{1}H N.M.R. spectrum of the complex $[Zr(DMSALEN)Cl_2].THF$

Mass Spectra

E.I. and C.I. mass spectra have been obtained for both the free Schiff base ligands and their corresponding titanium and zirconium complexes.

The E.I. spectra of the free ligands were obtained at source temperatures typically ranging from ca. 25–150 °C and showed strong peaks corresponding to the molecular ions. The fragmentation pattern is relatively straightforward, involving the breakage of the backbone bond and then subsequent fragmentation of the $[RC_8H_6NO]^+$ ion.

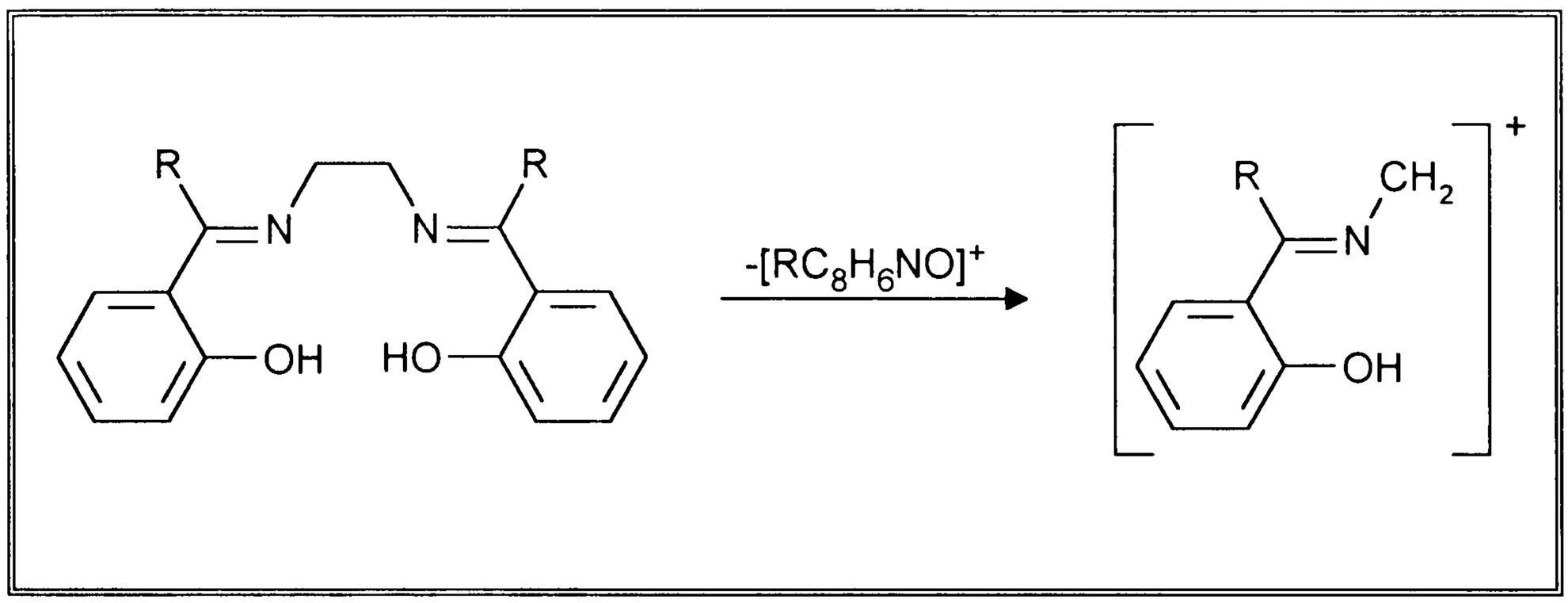

Figure 2.10 The fragmentation of SALEN type ligands.

The mass spectra of the complexes proved to be extremely difficult to obtain. Due to the moisture and oxygen sensitivity of the complexes, the handling of the compounds was important. Fast atom bombardment (F.A.B) was found to be an unsuccessful method because the nitrobenzylalcohol (NBA) matrix hydrolysed the complexes and another suitable matrix could not be found. Suitable E.I. and C.I. spectra were obtained using higher source temperatures (typically > 350 °C). These spectra occasionally gave the molecular ion (as an extremely weak peak), but mainly yielded the $[M–Cl]^+$ ion and the $[M–2Cl]^+$ ion again these peaks are weak. These spectra showed the typical isotope pattern associated with chlorine atoms. These complexes showed no significant fragmentation patterns, only the fragmentation associated with the free ligand.

Table 2.3 Summary of the E.I and C.I spectra for SALEN type ligands and complexes

Compound	m/z	Intensity (%)	Assignment
H_2DMSALEN	296	28.9	$[M]^+$
	297	30.2	$[M+1]^+$
H_2EtSALEN	324	32.7	$[M]^+$
	325	100	$[M+1]^+$
H_2PhSALEN	420	14.7	$[M]^+$
	421	19.5	$[M+1]^+$
[Ti(DMSALEN)Cl_2]	377	1.8	$[M–Cl]^+$
	378	1.1	$[(M–Cl)+1]^+$
[Zr(DMSALEN)Cl_2]	456	0.3	$[M]^+$
	420	1.5	$[M–Cl]^+$
	421	0.9	$[(M–Cl)+1]^+$
[Ti(EtSALEN)Cl_2]	441	0.1	$[M]^+$
	402	1.5	$[M–Cl]^+$
	375	3.3	$[M–2Cl]^+$
[Zr(EtSALEN)Cl_2]	446	1.3	$[M–Cl]^+$
	485	0.6	$[M+1]^+$
	447	1.4	$[(M–Cl)+1]^+$
[Ti(PhSALEN)Cl_2]	537	0.3	$[M]^+$
	501	1.5	$[M–Cl]^+$
[Zr(PhSALEN)Cl_2]	580	1.2	$[M]^+$
	543	6.1	$[M–Cl]^+$
	506	0.4	$[M–2Cl]^+$
	581	0.1	$[M+1]^+$
	544	0.7	$[(M–Cl)+1]^+$

X–Ray Crystallographic Studies

The molecular structures of the free ligands H_2DMSALEN, H_2EtSALEN and H_2PhSALEN were determined by X–ray diffraction techniques and are shown in Figure 2.11.

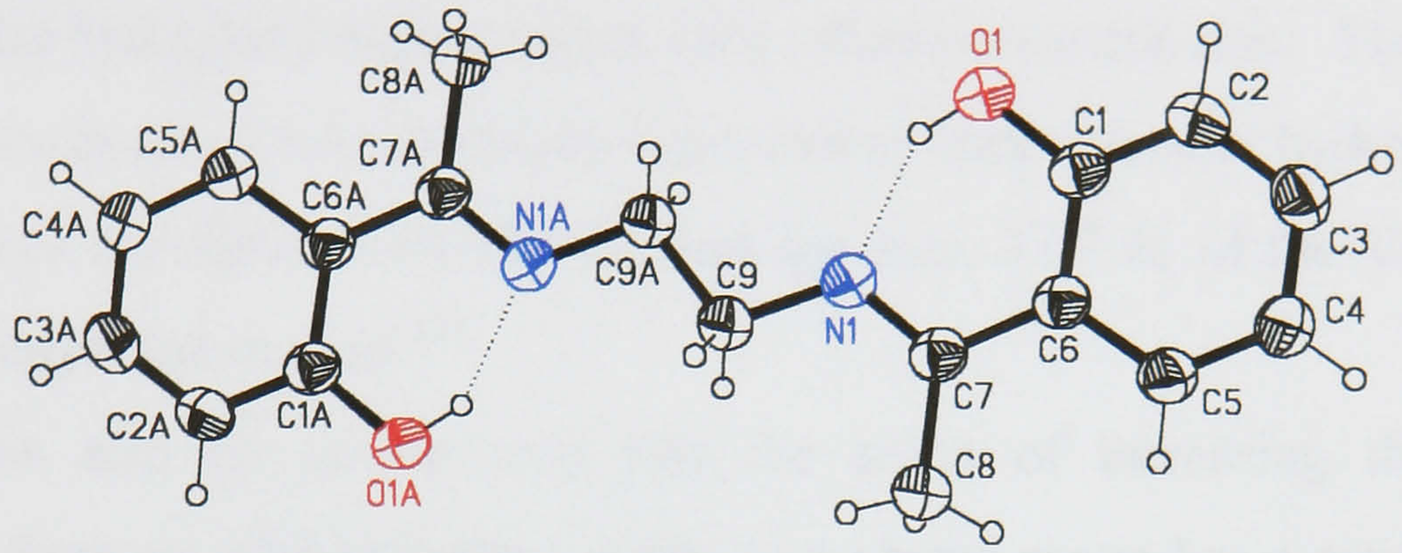

(a)

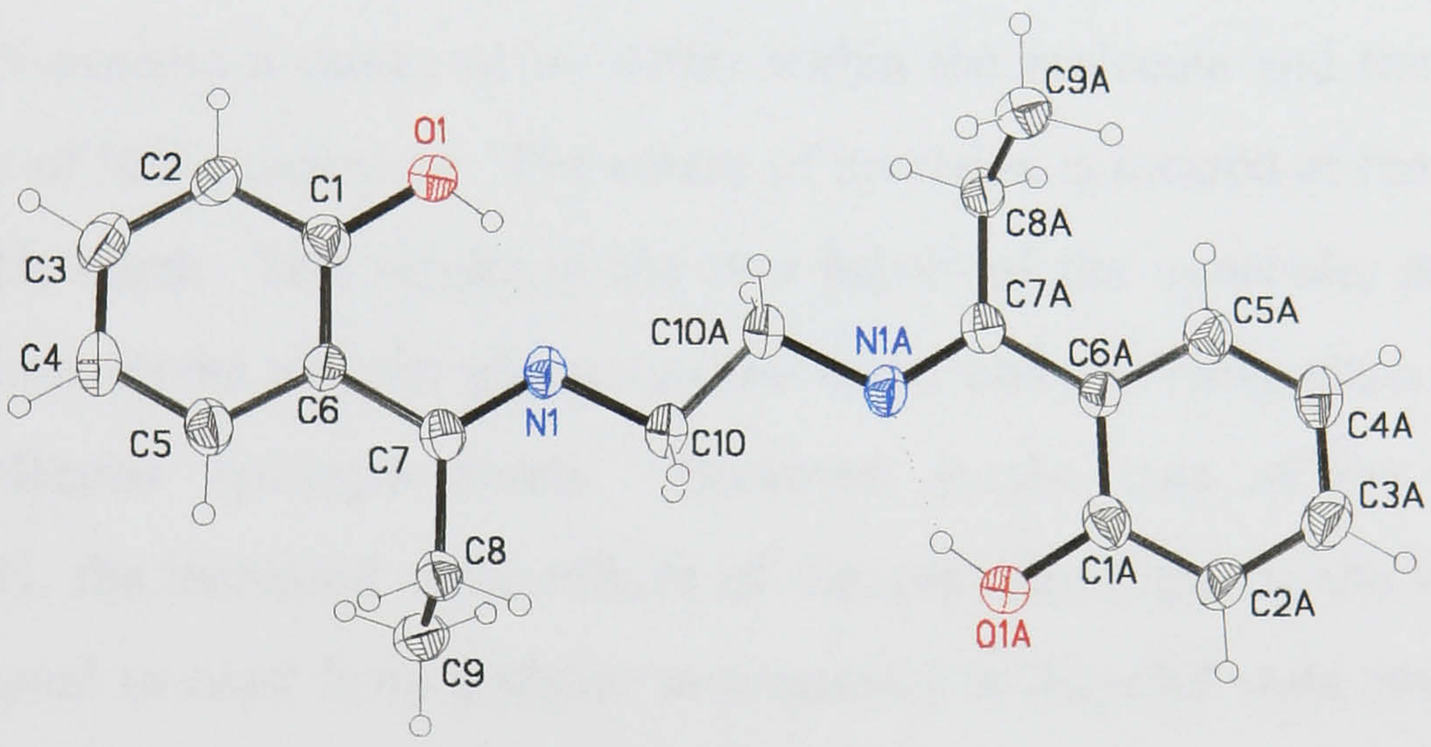

(b)

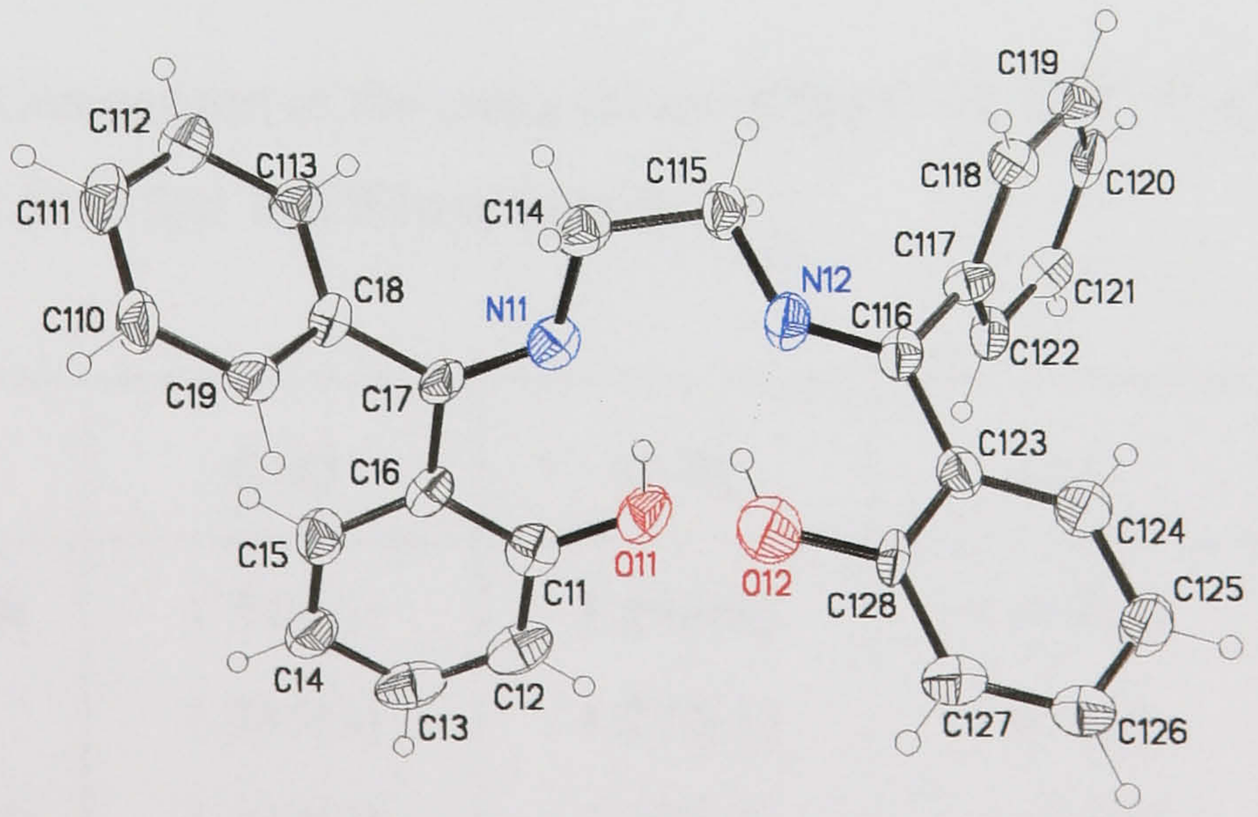

(c)

Figure 2.11 The molecular structures of (a) H_2DMSALEN, (b) H_2EtSALEN and (c) H_2PhSALEN

It is clear that the enolimine tautomer is favoured over the ketamine form in all the molecular structures (see introduction p.34). This is evident from the O–C and N–C bond lengths within the ligands (see Table 2.4) being consistent with O–C single bond and N=C double bond lengths respectively. There is also evidence for intramolecular hydrogen bonding within each salicylideneimine unit. The N1–O1 and N2–O2 distances of ~2.5 Å are clearly indicative of intramolecular hydrogen bonding; these distances are significantly shorter than the sum, 3.07 Å, of the Van der Waals radii for nitrogen and oxygen.[121]

It can also be clearly seen that the affect of increasing the degree of substitution from an ethyl or methyl group to a phenyl group has a marked effect on the solid state structure of the ligand. Both the ligands H_2DMSALEN and H_2EtSALEN possess a centre of inversion within the molecule and the asymmetric unit consists of half a molecule. The centre of inversion is located at the midpoint of the CH_2–CH_2 bond. This results in the two halves of the molecule, excluding the ethylene bridge atoms and the groups on the imine carbon, being planar because of the intramolecular hydrogen bonds. However, in the case of the free ligand, H_2PhSALEN, the increased steric effects of the aromatic rings on the imine carbon force the ligand to twist from a planar arrangement in its solid state structure. The angle between the two phenol rings is 71.24(10)°.

Table 2.4 Comparison of the mean values of the C–O, N–C, C–C bond lengths (Å) in free Schiff base ligands

Compound	C–O	C–N	C–C	Reference
H_2SALOPHEN	1.345(6)	1.288(6)	1.448(7)	116
H_2SALEN	1.345(3)	1.270(3)	1.456(4)	97
H_2DMSALEN	1.340(2)	1.287(2)	1.424(3)	This work
H_2EtSALEN	1.351(3)	1.295(3)	1.434(5)	This work
H_2PhSALEN	1.346(6)	1.302(6)	1.419(9)	This work

The conformation of these free ligands in the solid state is also of interest in relation to that required in a metal complex. It is clear from the above molecular structures that the conformation of these ligands is inappropriate for direct coordination to a metal ion, and therefore considerable rearrangement of the ligand is required for metal ion coordination to occur.

The molecular structures of the six coordinate [Ti(DMSALEN)Cl_2] and [Ti(PhSALEN)Cl_2] have been determined by X–ray crystallography.

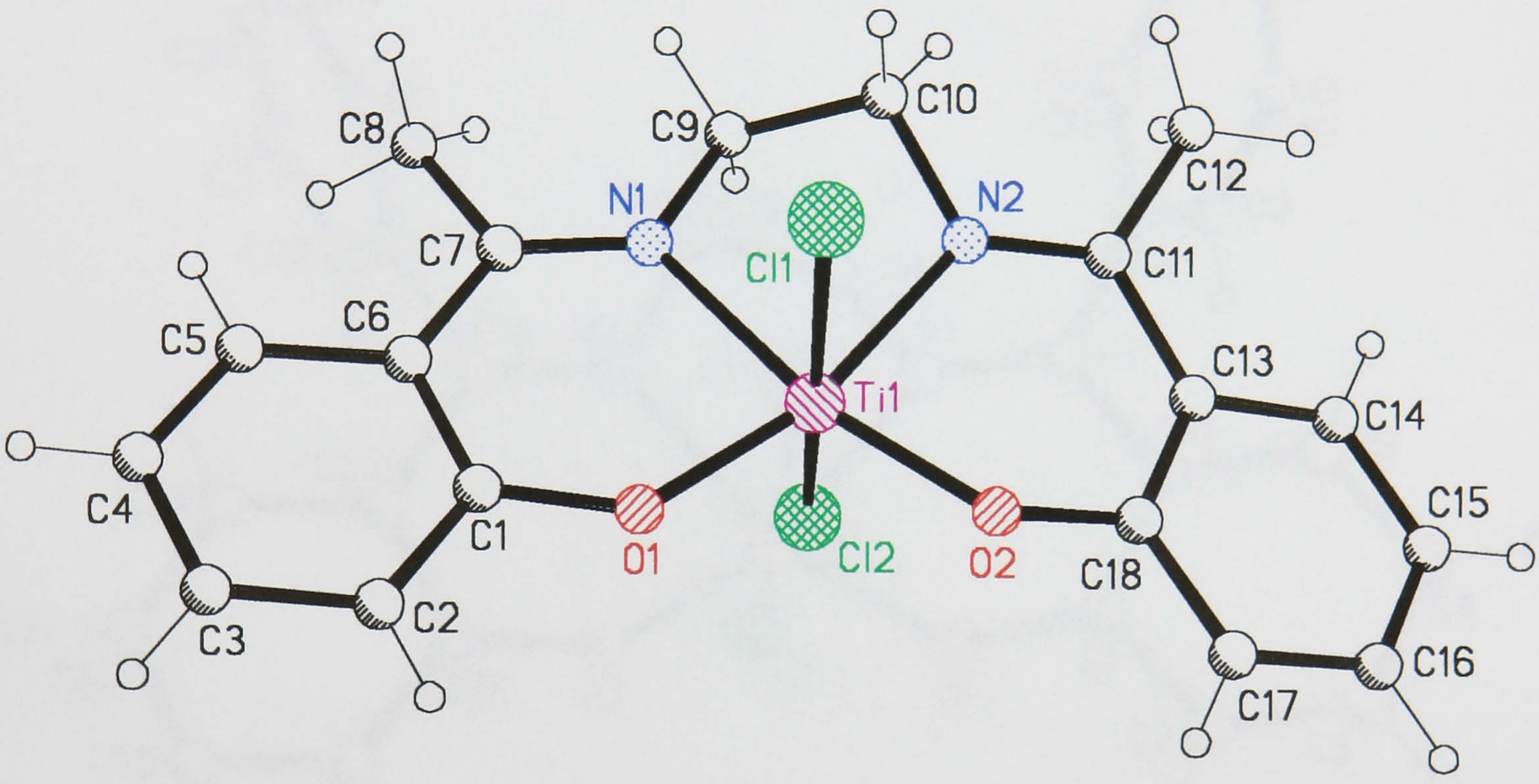

Figure 2.12 The molecular structure of [Ti(DMSALEN)Cl_2]

The molecule [Ti(DMSALEN)Cl_2] is shown in Figure 2.12 and the bond lengths and angles, with standard deviations, are reported in the appendix. The coordination around the titanium atom is approximately octahedral but there is considerable distortion with bond angles around titanium varying from 79.27(9) to 109.67(9)°. The donor atoms from the DMSALEN ligand occupy the equatorial plane and the two chlorine atoms are in the *trans* axial positions. The O1 and O2 atoms of the ligand are slightly above and below the plane described by the Ti1, N1 and N2 atoms, the distances from it being 0.025(1) and 0.029(1) Å respectively. The chlorine atoms are not on the normal to the equatorial plane but are symmetrically bent towards the N atoms with a Cl1–Ti1–Cl2 bond angle of 168.36(3)°. The ligand

around the metal is not planar, but has the phenol rings inclined at an angle of 13.57(13)° to each other. The bond lengths within the complex are comparable with other related hexacoordinate titanium complexes (Table 2.6)

The molecular structure of the six coordinate titanium complex [Ti(PhSALEN)Cl_2] is shown below (Figure 2.13)

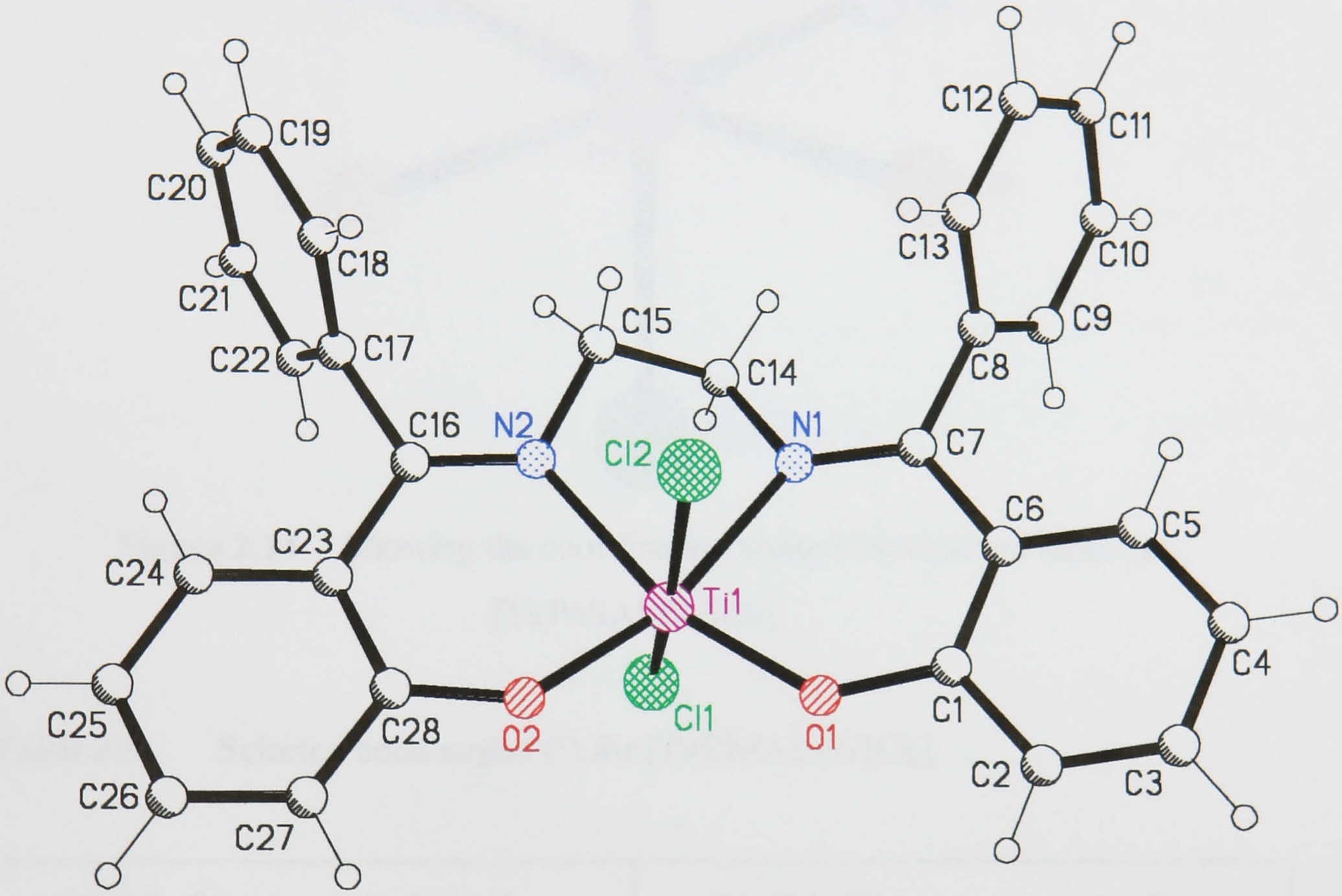

Figure 2.13 The molecular structure of [Ti(PhSALEN)Cl_2]

The complex consists of discrete [Ti(PhSALEN)Cl_2] molecules and disordered THF solvent molecules of crystallisation in a complex/solvent molar ratio of 1:0.5. The coordination around the titanium atom is pseudo–octahedral with bond angles around titanium varying from 78.3(2) to 110.1(2)°. The donor atoms from the ligand occupy the equatorial plane and the two chlorine atoms are in *trans* axial positions. These chlorine atoms are not on the normal to the equatorial plane but are symmetrically bent towards the N atoms with a Cl1–Ti1–Cl2 bond angle of 167.00(7)°.

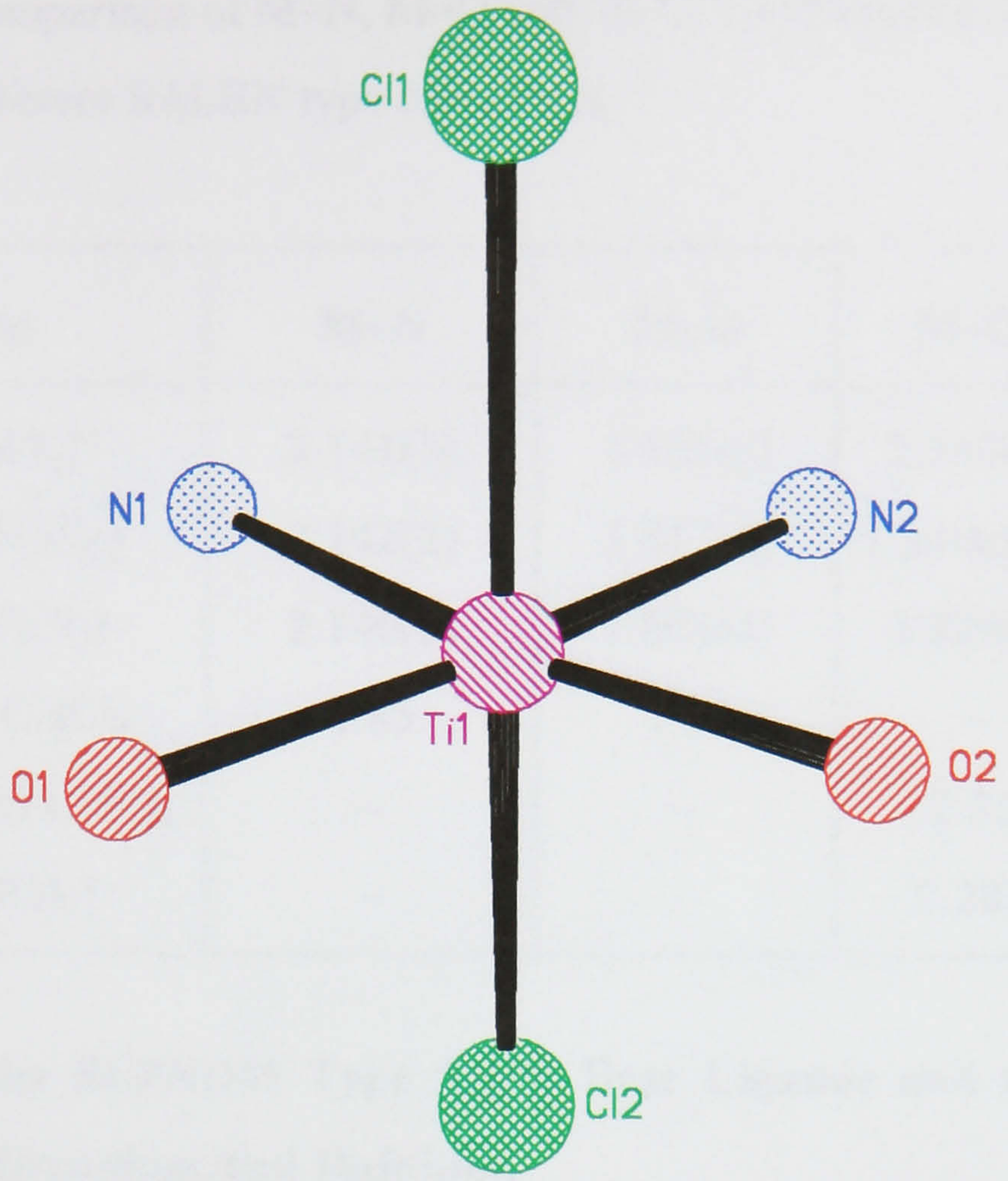

Figure 2.14 Showing the coordination around the titanium atom in [Ti(PhSALEN)Cl_2]

Table 2.5 Selected bond angles (°) for [Ti(PhSALEN)Cl_2]

O1–Ti1–O2	110.1(2)	O1–Ti1–N1	85.4(2)
O2–Ti1–Cl2	93.4(2)	O2–Ti1–N2	85.9(2)
O1–Ti1–Cl1	97.5(2)	O2–Ti1–Cl1	94.3(2)
N2–Ti1–Cl1	87.0(1)	O1–Ti1–Cl2	89.8(2)
N1–Ti1–N2	78.3(2)	Cl1–Ti1–Cl2	167.00(7)
N1–Ti1–Cl2	83.1(2)	N2–Ti1–Cl2	83.0(2)

The ligand around the metal is not planar with an angle of 7.79(17)° between the two phenol rings. The bond lengths within the complex are comparable with other six coordinate titanium complexes (Table 2.6).

Table 2.6 Comparison of M–N, M–O and M–Cl bond lengths (Å) in different SALEN type complexes

Compound	M–N	M–O	M–Cl	Reference
$[Ti(SALEN)Cl_2]$	2.141(5)	1.835(5)	2.346(2)	108
$[Ti(DMSALEN)Cl_2]$	2.142(2)	1.817(2)	2.3406(10)	This work
$[Ti(PhSALEN)Cl_2]$	2.140(5)	1.805(4)	2.329(8)	This work
$[Co(SALEN)].CHCl_3$	1.85	1.85	–	122
$[TiCl(C_5H_7O_2)_2]_2O.CHCl_3$	–	–	2.31	123
$[TiCl_2(C_9H_6NO)_2]$	–	–	2.283	124

Preparation of the SLPNDM Type Schiff Base Ligands and their Complexes with Titanium, Zirconium and Hafnium.

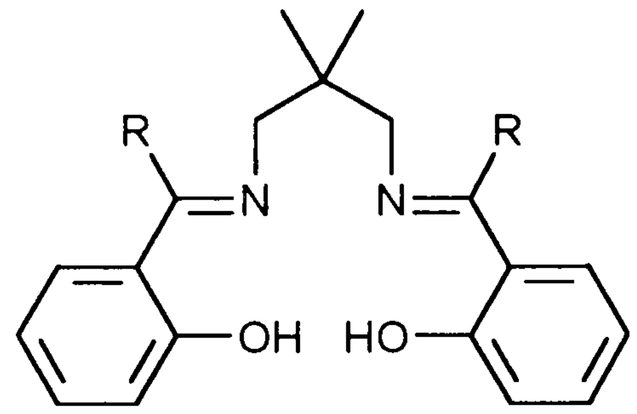

R = H, Me, Et, Ph

Figure 2.15 A representation of the SLPNDM type Schiff base ligands

These free Schiff base ligands are again readily prepared by the condensation reaction between the appropriate aldehyde or ketone and 2,2–dimethyl–1,3–propanediamine. These ligands are bright yellow, air stable, crystalline solids at room temperature, and can be prepared in excellent yields. These ligand are also readily soluble in most solvents.

These ligands differ from the (SALEN) type ligand in the backbone of the ligand, since the simple ethylene bridge has been replaced with a substituted propylene bridge. It was believed that these ligands would have greater potential for synthesis of metal complexes with the desired *cis* configuration at the metal centre.

The reason for this is the greater steric influence the ligand has because of the substituted propylene bridge rather than the relatively sterically unhindered ethylene bridge. Further evidence that the *cis* geometry may be the preferred stereochemistry with these ligands came from the [VO(OMe)(SLPNDM)] complex synthesised by Leigh *et al.*[125]

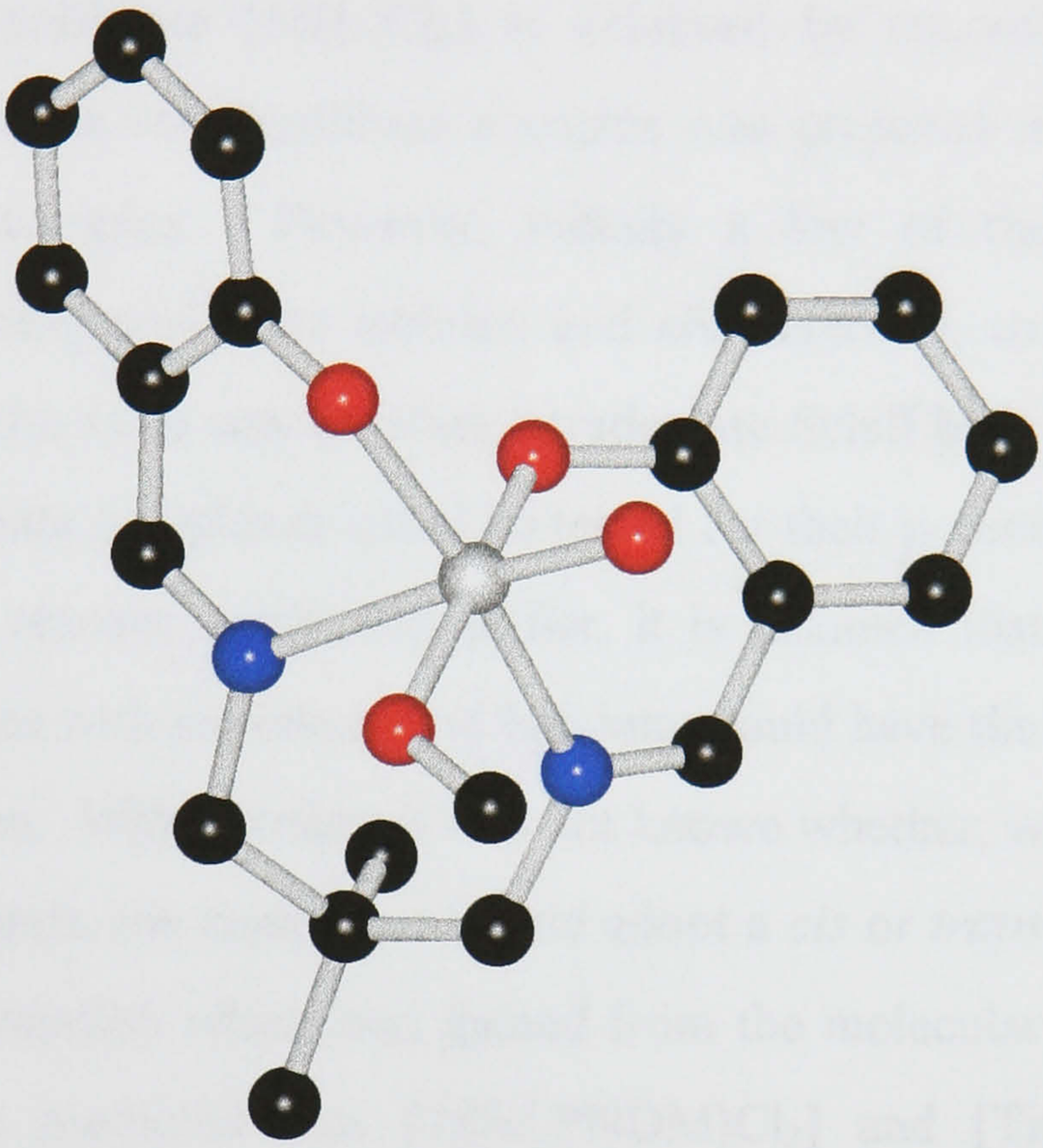

Figure 2.16 The molecular structure of [VO(OMe)(SLPNDM)] showing its cis stereochemistry at the metal centre

Whilst studying the structure of [VO(SLPNDM)], which is a 'polymer' with chains of [VO(SLPNDM)] molecules arranged along a two–fold axis, Leigh *et al* isolated [VO(OMe)(SLPNDM)] from a solution of oxidised [VO(SLPNDM)] in methanol. They then synthesised [VO(OMe)(SLPNDM)] starting from [VO(SLPNDM)][BF_4].MeCN and reacting it with LiOMe in methanol. When single crystals were eventually isolated, and the molecular structure determined, they discovered that V=O and V–OMe are unequivocally in *cis* positions rather than the expected *trans* configuration. This coordination of the tetradentate dianionic Schiff base derivative is unusual. One explanation for this coordination may be the extra Me_2–carbon atom in the backbone of H_2SLPNDM as compared to H_2SALEN. Because such a *cis* structure had been isolated and characterised by X–ray crystallography it was hoped that, especially with titanium, complexes prepared with

such ligand types would also exhibit this coordination forming complexes with the desirable *cis* conformation.

Again in the synthesis of $[M(L)Cl_2]$ complexes, the preparation with titanium differs from that of zirconium and hafnium; with the latter metals an initial seven coordinate complex is formed, with a THF molecule in the seventh coordination site. The desired six coordinate $[M(L)Cl_2]$ is achieved by recrystallisation from hot toluene. In general the six coordinate complex was prepared without isolating the seven coordinate complex. However, initially a few of the seven coordinate $[M(L)Cl_2(THF)]$ complexes were isolated and characterised, to confirm that these ligands behaved in the same way as other tetradentate Schiff base ligands, and so that these seven coordinate complexes could be tested for their potential as Ziegler–Natta catalysts. For the reasons mentioned earlier, it is assumed that the six coordinate $[M(L)Cl_2]$ complexes with zirconium and hafnium would have the two chlorine atoms in a *cis* configuration. With titanium it was not known whether, with this added steric influence of the ligands, the complexes would adopt a *cis* or *trans* arrangement at the metal centre. Information which was gained from the molecular modelling of these complexes (p.103) predicted that $[Ti(SLPNDM)Cl_2]$ and $[Ti(DMSLPNDM)Cl_2]$ would be *trans* and that $[Ti(EtSLPNDM)Cl_2]$ and $[Ti(EtSLPNDM)Cl_2]$ would have *cis* stereochemistries.

These complexes are slightly soluble in moderately polar solvents such as dichloromethane, and totally insoluble in non–polar solvents such as hexane. As solids they decompose in the air, with the seven coordinate zirconium and hafnium complexes being extremely sensitive to moisture. As solutions in organic solvents they are very sensitive to hydrolysis. However, these compounds can be conveniently handled in an inert atmosphere and manipulations were therefore carried out in a nitrogen filled glove box or by using a Schlenk–line equipped with dry argon or nitrogen.

As with the preparation of $[M(SALEN)Cl_2]$ complexes, all the free ligands were recrystallised and dried in vacuo before use to eliminate impurities, and the THF adduct of the metal tetrachloride $[MCl_4.2THF]$ was used in the complexation reaction.

Spectroscopic Characterisation of the SLPNDM Type Schiff Base Ligands and their Complexes with Titanium, Zirconium and Hafnium.

Nuclear Magnetic Resonance Spectra

Details of the ^{1}H N.M.R. and ^{13}C N.M.R. data for individual compounds are given in the experimental section. The ^{1}H N.M.R. spectra of the compounds has proved to be extremely useful in verifying both the stoichiometry and the purity of the reaction products. The ^{1}H N.M.R. spectra of the free ligands were routinely recorded in $CDCl_3$ and they showed that these ligands are symmetrical in solution. The most significant peak in the spectrum is the OH resonance at around δ 12–14 ppm. The absence of this resonance in the spectra of the complexes is essential in order for the desired product to have been formed.

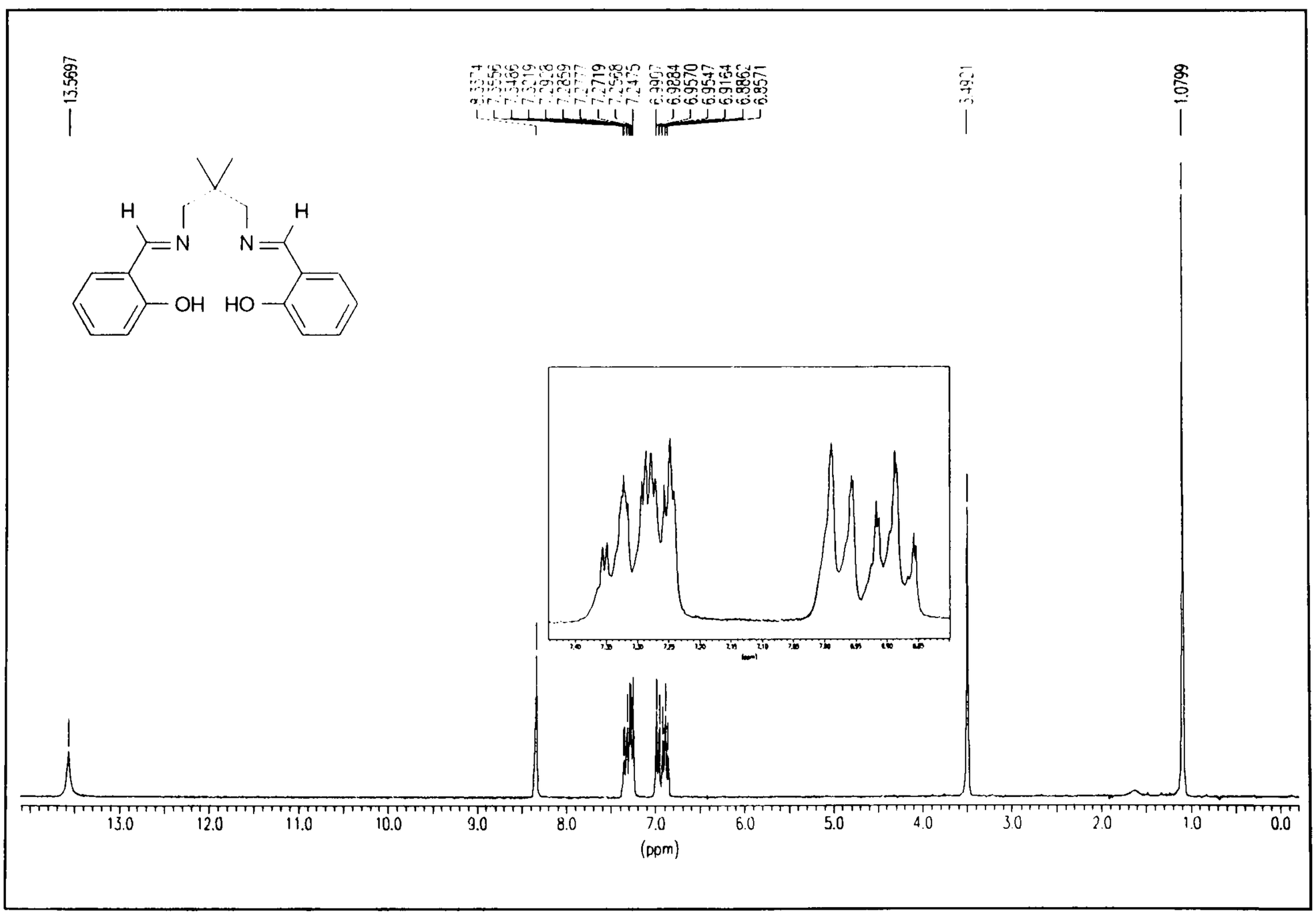

Figure 2.17 The ^{1}H N.M.R spectrum of $H_2SLPNDM$

The ^{1}H N.M.R spectrum of $H_2SLPNDM$ is shown in Figure 2.17 as a typical representative of this type of Schiff base ligand. These spectra are similar to the

spectra obtained with the SALEN type ligands. The OH resonance is again seen as a slightly broad singlet at δ 13.5 ppm. and the aromatic resonances are seen at δ 6–8 ppm.. The differences in the spectra arise from the different backbone of the SLPNDM type ligands. A sharp singlet resonance is seen at δ 3.5 ppm., which integrates for four protons, and is due to the two CH_2 groups in the ligand backbone. The two methyl resonances are seen as a sharp singlet at δ 1.0 ppm. which integrates for six protons. The substituted group on the imine carbon is seen in the expected region of the spectrum as a singlet at δ 8.3 ppm. which integrates for two protons.

A major problem with obtaining ^{1}H N.M.R. and ^{13}C N.M.R. spectra of the complexes was their poor solubility. Due to this solubility problem, the most convenient solvent for obtaining the ^{1}H N.M.R. and ^{13}C N.M.R. spectra of the complexes was d^{6}–DMSO. The solution was prepared and the spectra recorded immediately to avoid degradation of the complex by the DMSO. The spectra of the complexes showed that in solution they are also symmetrical because there is no further splitting of the ligand resonances. The ^{1}H N.M.R. spectrum of [Zr(PhSLPNDM)Cl_2] is given in Figure 2.18 as a typical example for the series. In these spectra there are slight differences in the chemical shifts of the resonances from the complexes compared to those of the free ligands.

The ^{1}H and ^{13}C chemical shift data and assignments for the free ligands and their hafnium complexes are listed in tables 2.7 and 2.8.

Table 2.7 Summary of ^{1}H N.M.R data (δ / ppm) of SLPNDM type Schiff base ligands and their hafnium complexes

Compound	OH	Aromatic	R–C=N	N–CH$_2$–C(CH$_3$)$_2$	CH$_2$–C(CH$_3$)$_2$
H_2SLPNDM	13.62	6.85–7.35	8.31	3.46	1.07
H_2DMSLPNDM	13.16	6.76–7.51	2.15–2.31	3.51	1.21
H_2EtSLPNDM	12.95	6.72–7.49	1.14–1.20 + 2.72–2.88	3.55	1.23
H_2PhSLPNDM	14.11	6.60–7.45	6.60–7.45	3.22	1.03
[Hf(SLPNDM)Cl$_2$	–	6.36–6.42	8.09	3.76	0.94
[Hf(DMSLPNDM)Cl$_2$	–	6.77–7.67	2.42	3.58	1.10
[Hf(EtSLPNDM)Cl$_2$	–	6.76–7.65	1.06–1.12 + 2.81–2.90	3.65	1.12
[Hf(PhSLPNDM)Cl$_2$	–	6.66–7.49	6.66–7.49	3.14	0.96

Table 2.8 Summary of Proton decoupled ^{13}C N.M.R data (δ / ppm) of SLPNDM type Schiff base ligands and their hafnium complexes

Compound	R–<u>C</u>=N	<u>C</u>–O	Aromatic	<u>R</u>–C=N	CH_2–<u>C</u>$(CH_3)_2$	N–<u>C</u>H_2–C$(CH_3)_2$	CH_2–C$(\underline{C}H_3)_2$
H_2SLPNDM	166.71	161.15	132.28, 131.34, 118.64, 118.58, 116.89	–	67.98	36.13	24.27
H_2DMSLPNDM	172.34	164.00	132.48, 128.00, 119.08, 118.55, 116.95	14.51	57.50	35.79	24.55
H_2EtSLPNDM	177.20	165.00	132.50, 127.80, 118.90, 117.00, 116.80	20.90 + 11.50	56.32	35.60	24.50
H_2PhSLPNDM	174.71	163.27	132.34, 127.08, 119.66, 117.16, 117.79	133.78, 131.37, 128.84, 128.63	59.94	36.15	24.42
[Hf(SLPNDM)Cl_2	168.36	160.76	135.78, 132.73, 122.19, 119.20, 117.28	–	72.39	36.71	22.70
[Hf(DMSLPNDM)Cl_2	174.62	162.66	133.05, 128.99, 125.40, 119.60, 117.39	15.51	56.85	36.09	23.66
[Hf(EtSLPNDM)Cl_2	188.19	163.60	132.91, 128.86, 125.43, 118.26, 117.34	21.23 + 11.61	56.87	35.69	23.67
[Hf(PhSLPNDM)Cl_2	174.73	162.43	132.76, 127.15, 125.39, 119.39, 117.67	133.21, 131.24, 129.31, 128.89	35.99	24.03	21.14

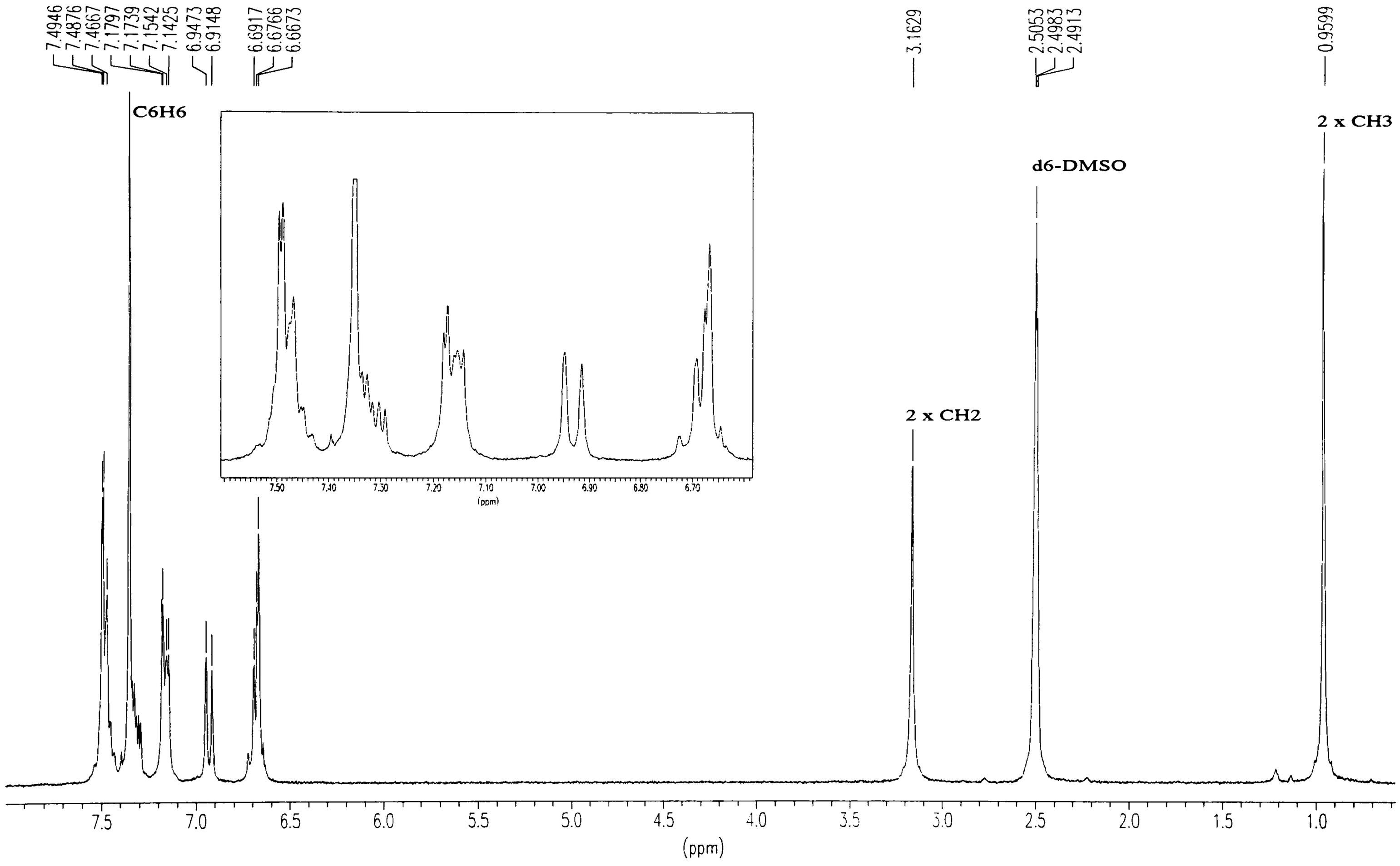

Figure 2.18 The ^{1}H N.M.R spectrum of the complex $[Zr(PhSLPNDM)Cl_2]$

Mass Spectra

The E.I. and C.I. of the free ligands, and their Group 4 metal complexes have been obtained. The free ligand spectra were typically obtained at source temperatures ca. 25–100 °C. The fragmentation of the ligands is unspectacular and involves the breakage of the ligand in two places within the backbone (Figure 2.19) followed by further fragmentation of these ions.

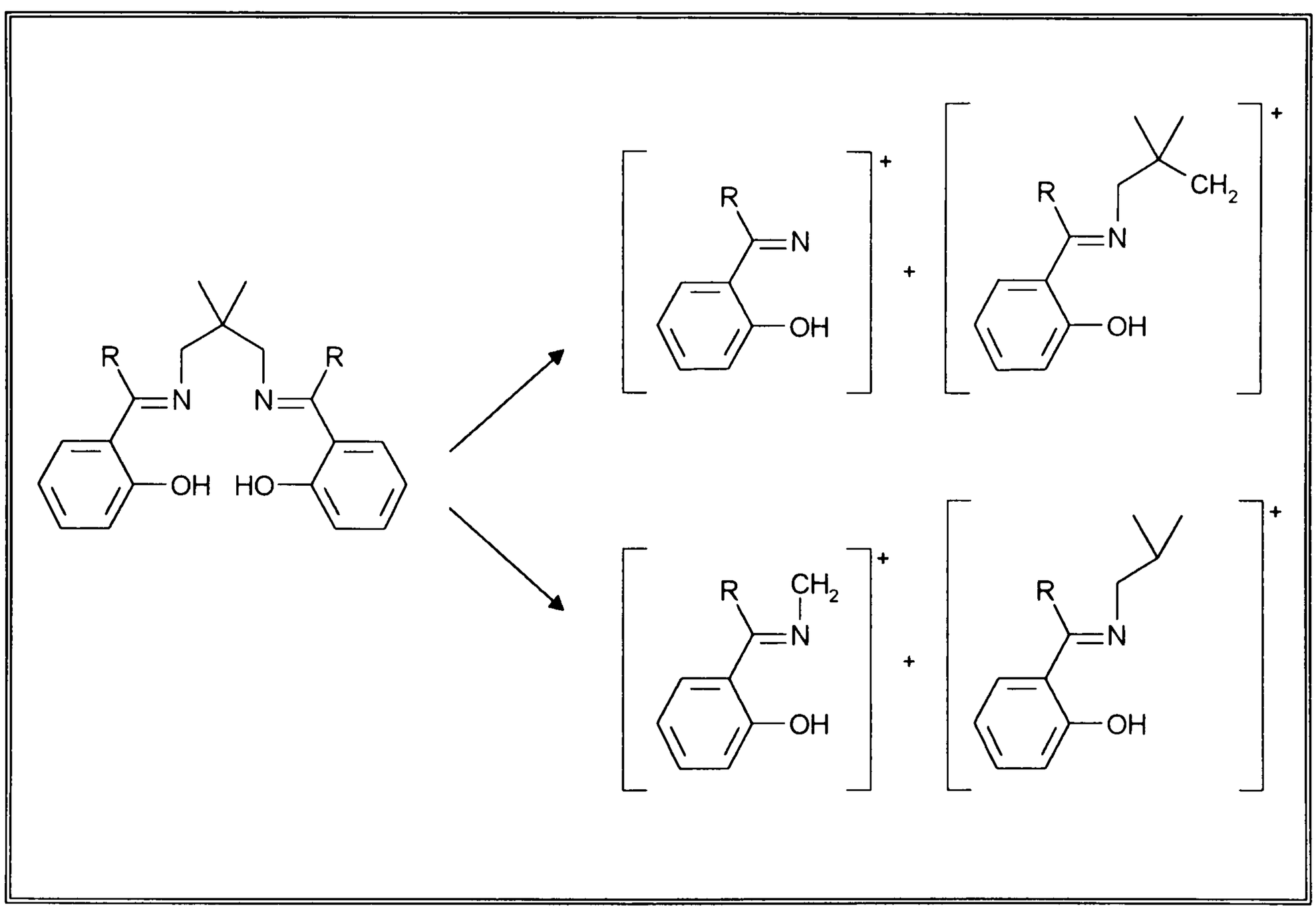

Figure 2.19 The fragmentation of SLPNDM type ligands.

As before the spectra of the complexes proved to be difficult to obtain due to the air sensitivity of the complexes. The use of F.A.B. mass spectrometry was again unsuccessful due to the hydrolysis of the complexes by the matrix, NBA, and the inability to find another suitable matrix. The spectra were eventually obtained by using a source temperature typically > 350 °C. The spectra show very weak intensity peaks due to the molecular ions, and to the ions corresponding to the loss of chlorine atoms. These spectra all possess the expected isotope pattern associated with the

presence of chlorine atoms. The major ion peaks within the spectra correspond to ions associated to the ligand.

Table 2.9 Summary of the E.I and C.I spectra for SLPNDM type free ligands and their hafnium complexes

Compound	m/z	Intensity (%)	Assignment
H_2SLPNDM	310	28.4	$[M]^+$
	311	30.6	$[M+1]^+$
H_2DMSLPNDM	338	28.5	$[M]^+$
	339	25.7	$[M+1]^+$
H_2EtSLPNDM	366	48.0	$[M]^+$
	367	36.4	$[M+1]^+$
H_2PhSLPNDM	412	69.8	$[M]^+$
	413	100	$[M+1]^+$
[Hf(SLPNDM)Cl_2]	557	2.2	$[M]^+$
	522	16.2	$[M–Cl]^+$
	523	0.9	$[(M–Cl)+1]^+$
[Hf(DMSLPNDM)Cl_2]	586	0.5	$[M]^+$
	551	1.7	$[M–Cl]^+$
	552	0.2	$[(M–Cl)+1]^+$
[Hf(EtSLPNDM)Cl_2]	613	0.5	$[M]^+$
	577	0.9	$[M–Cl]^+$
[Hf(PhSLPNDM)Cl_2]	710	0.2	$[M]^+$
	673	0.6	$[M–Cl]^+$

X–Ray Crystallographic Studies

The molecular structure of the free ligand H_2SLPNDM[126] was determined and can be seen in Figure 2.20 It is clear that the enolimine tautomer is favoured over the ketamine form. This is evident from the observed O1–C1 and O2–C19 bond distances of 1.356(4) and 1.352(4) Å respectively which are consistent with O–C single bonds ; similarly the N1–C7 and N2–C13 distances of 1.284(4) and 1.263(4) Å are consistent with N=C double bonding. There is also evidence for intramolecular hydrogen bonding within each salicylideneimine unit. The N1–O1 and N2–O2 distances of 2.593(4) and 2.566(4) Å are clearly indicative of intramolecular hydrogen bonding; these distances are significantly shorter than the sum, 3.07 Å, of the van der Waals radii for nitrogen and oxygen.[121]

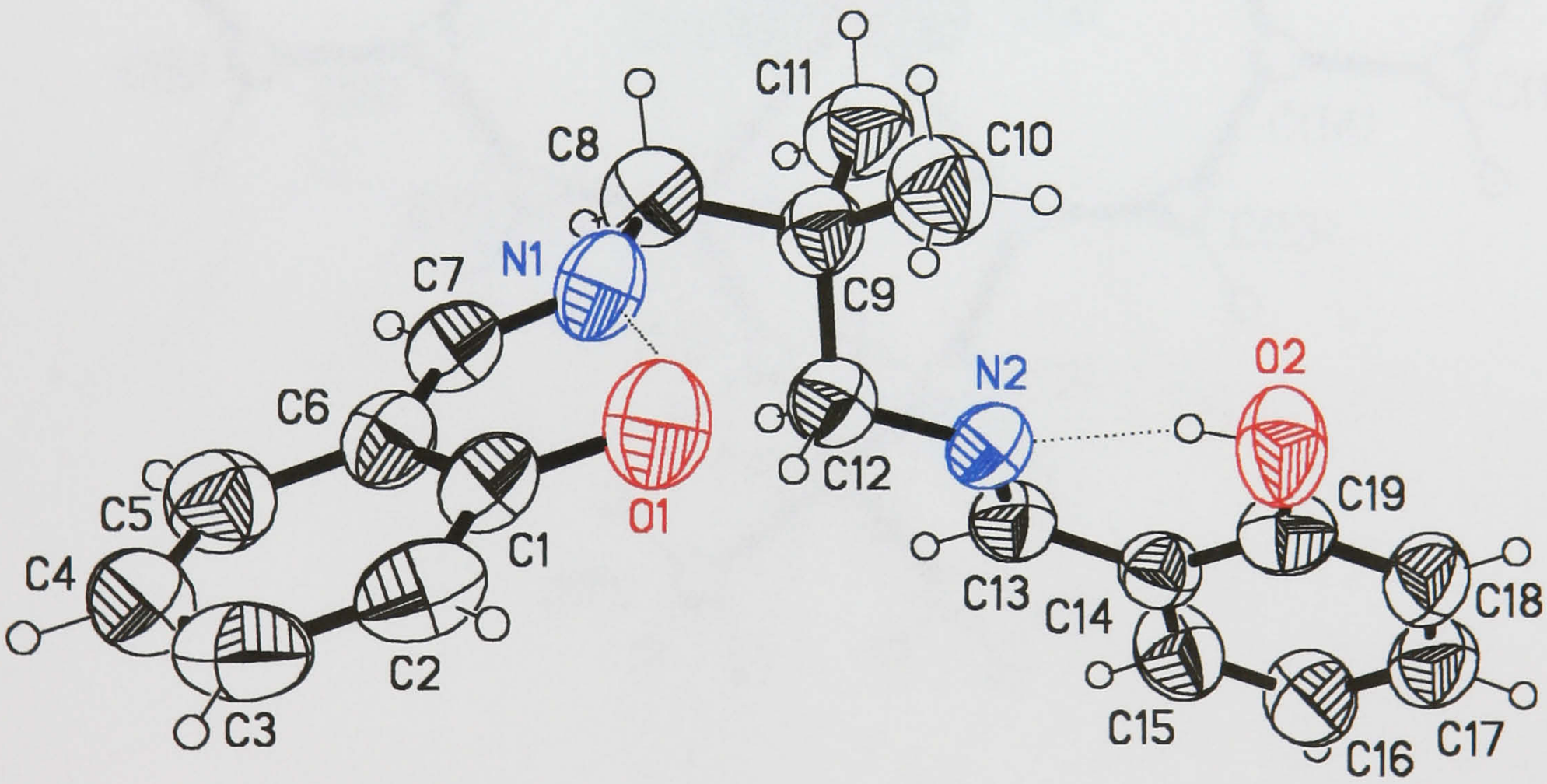

Figure 2.20 The molecular structure of the free ligand H_2SLPNDM

The conformation of the free ligand in the solid state is of particular interest in relation to that required in a metal complex. The torsion angle N2–C12–C9–C8 is 174.0(3)°, but the corresponding value for N1–C8–C9–C12 is 62.9(4)°. The overall effect is that the least–squares–planes through the two aromatic rings are inclined at an angle of 68.66(11)°. Clearly this conformation is inappropriate for direct coordination to a metal ion. This is further emphasised by the large O1–O2

separation of 6.621(4) Å, and therefore rearrangement of the ligand is required for coordination to occur, although of course the structure of the ligand in solution may differ slightly from that observed here in the solid state.

The molecular structures of both the six coordinate [Ti(SLPNDM)Cl_2] and the seven coordinate [Zr(SLPNDM)Cl_2(THF)] were also determined. The bond lengths and angles of all the compounds are presented in the Appendix. The titanium complex is shown in Figure 2.21.

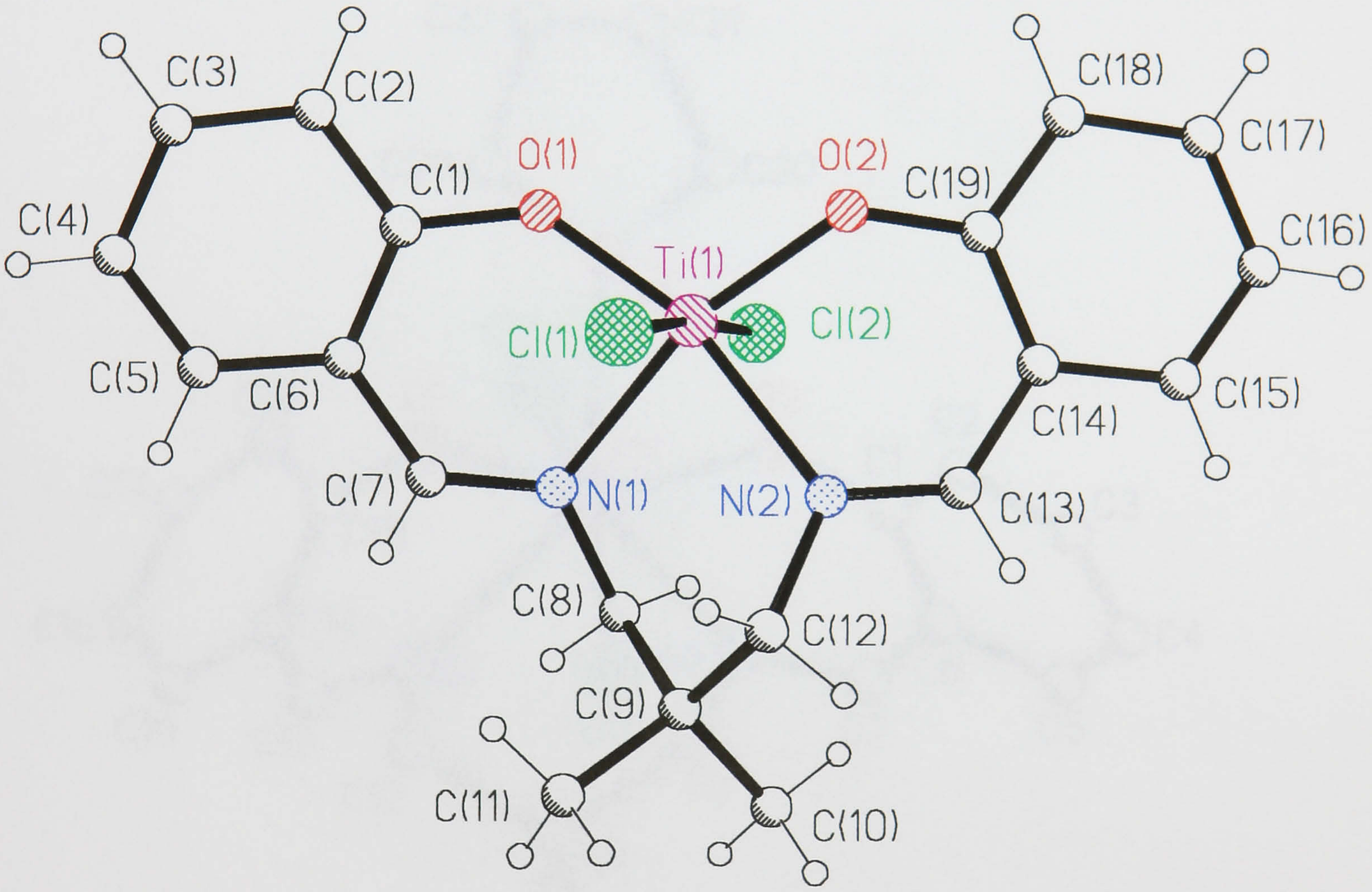

Figure 2.21 The molecular structure of [Ti(SLPNDM)Cl_2]

The complex consists of discrete [Ti(SLPNDM)Cl_2] molecules and disordered THF solvent molecules of crystallisation in a complex/solvent molar ratio of 1:1. The coordination around the titanium is pseudo–octahedral with the donor atoms from the ligand in the equatorial plane and the two chlorine atoms in *trans* axial positions. The (Cl–Ti–Cl) bond angle is actually 174.16(5)° and not 180°. The Ti–Cl (2.361 Å), Ti–O (1.835 Å) and Ti–N (2.168 Å) distances are in good agreement with previously

observed values in other titanium Schiff base derivatives.[105,124] In this complex, even with the substituted propylene backbone, the ligand is not sterically demanding enough on its own to force folding and produce a complex with the two chlorine atoms in a *cis* arrangement.

The molecular structure of the seven coordinate [Zr(SLPNDM)Cl_2(THF)] complex can be seen in Figure 2.22. The complex consists of discrete [Zr(SLPNDM)Cl_2(THF)] molecules where the zirconium metal is seven coordinate with a pseudo–pentagonal bipyramidal geometry.

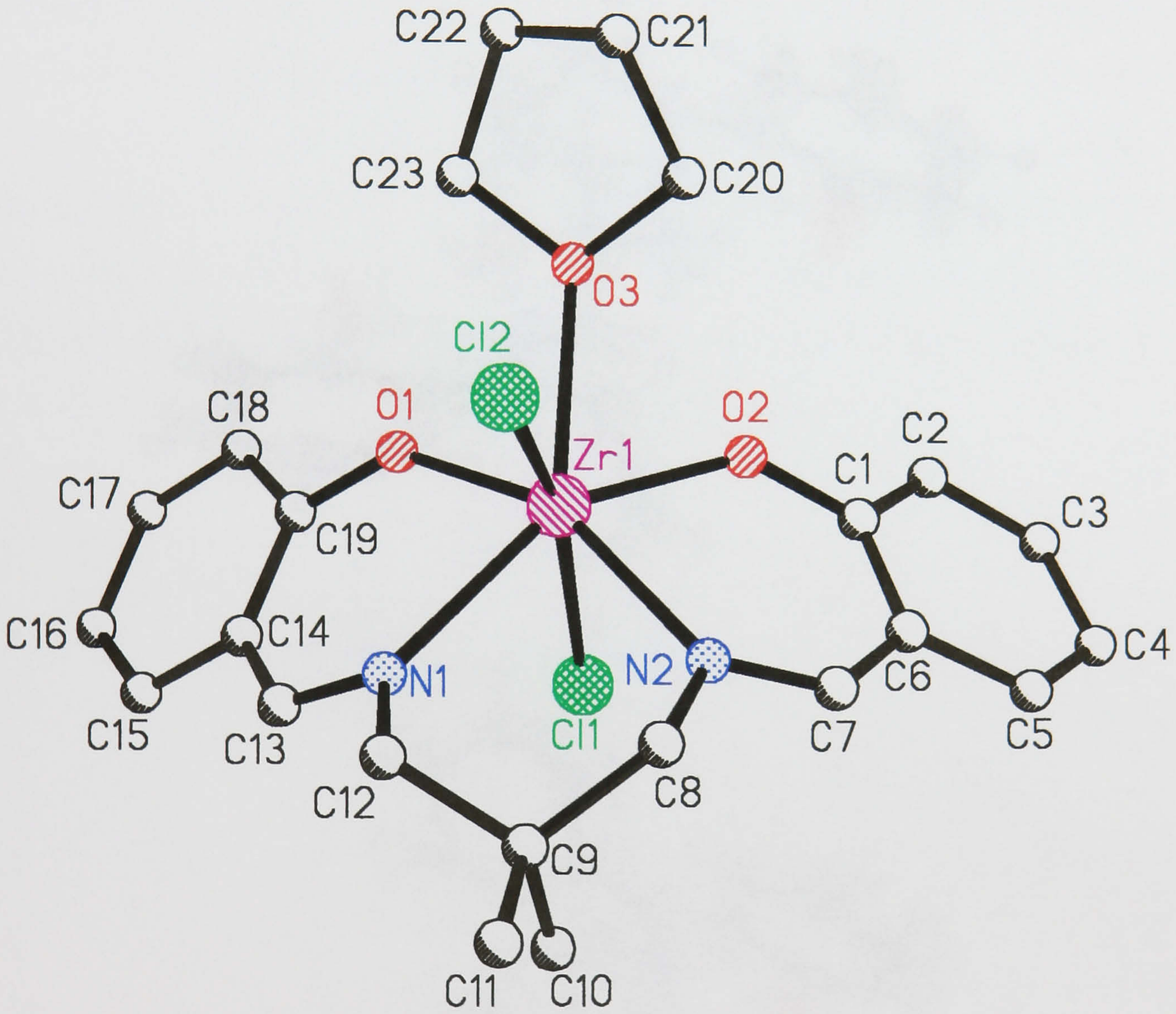

Figure 2.22 The molecular structure of [Zr(SLPNDM)Cl_2(THF)]

The equatorial plane is roughly defined by the donor atoms of the SLPNDM ligand and by the oxygen atom of the THF molecule. The apices are occupied by two chlorine atoms in a significantly bent *trans* arrangement [Cl(1)–Zr(1)–Cl(2) 156.67(8)°]. The SLPNDM ligand assumes an umbrella conformation[115,128,129] with the two salicylaldimine groups approximately planar and at an angle of 68.10(46)° to

each other. The *trans* arrangement of the chlorine atoms causes an enlargement of the N_2O_2 cavity to allow formation of the seven coordinate metal.

Because the effect of the backbone of the ligand alone had not caused the required steric restraints to force the formation of a folded–*cis* complex with titanium (the six coordinate zirconium and hafnium complexes were assumed to be folded–*cis* complexes), the effect of added steric hindrance by substitution at the imine carbon was also studied. The molecular structures of the two ligands H_2EtSLPNDM and H_2PhSLPNDM were determined and can be seen in Figure 2.23.

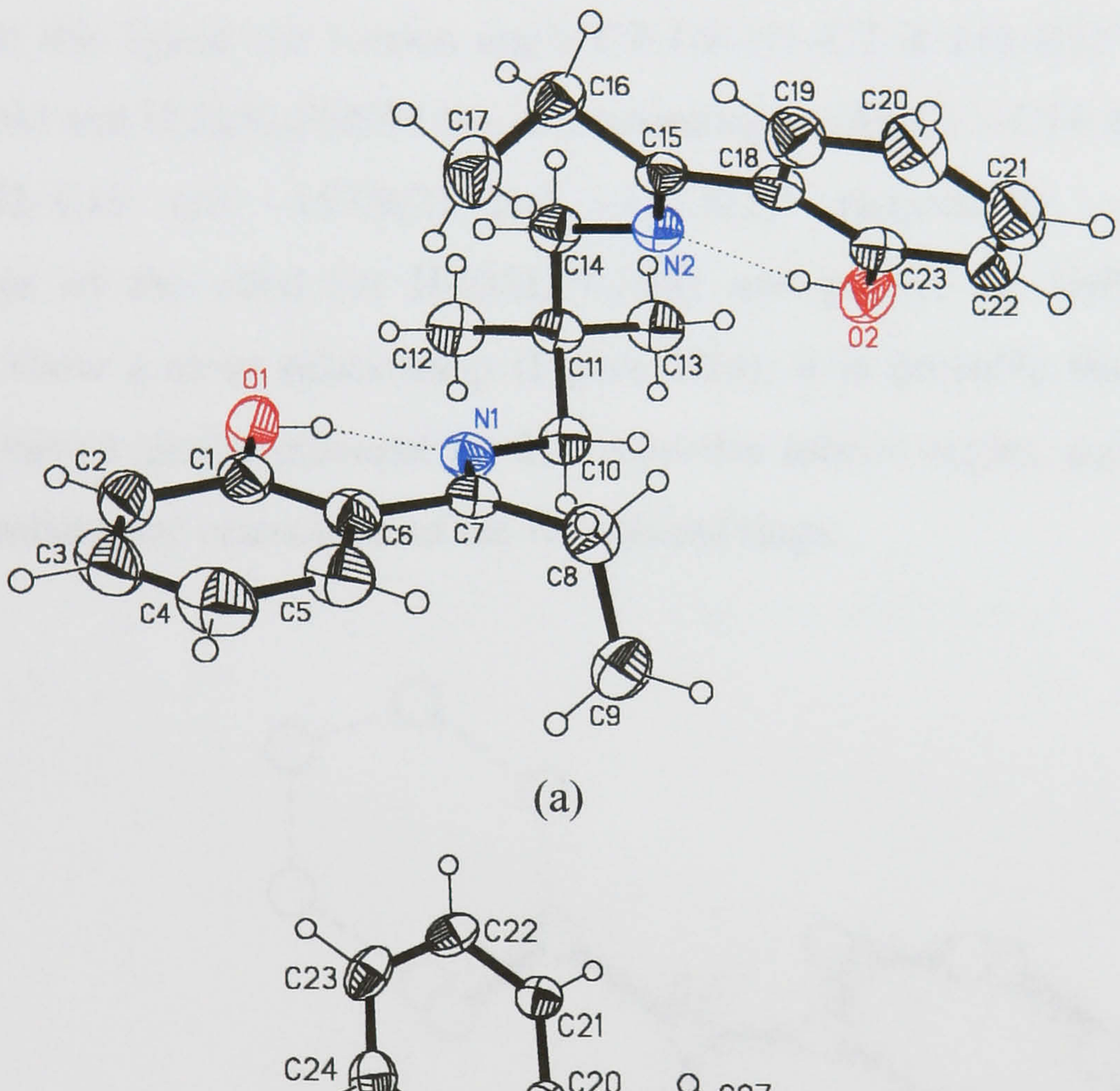

Figure 2.23 The molecular structure of the free ligands (a) H_2EtSLPNDM and (b) H_2PhSLPNDM

The bond lengths and angles for the above structures are again unexceptional, but confirm that the enolimine tautomers are favoured. Furthermore, the shortest N...O distances [2.476(2) and 2.502(2) Å for H_2EtSLPNDM and 2.518(3) and 2,528(2) Å for H_2PhSLPNDM] are indicative of intramolecular hydrogen bonding. There is a striking similarity in the angles between the planes of the two phenol rings in H_2EtSLPNDM and H_2PhSLPNDM of 45.37(9) and 44.50(9)° respectively. These values are noticeably smaller than the corresponding angle of 68.66(11)° in the ligand H_2SLPNDM, where the imine carbon atom carries an H–atom substituent. Moreover, in this ligand the torsion angle C9–C8–N1–C7 is 141.3(3)° whereas in H_2EtSLPNDM and H_2PhSLPNDM the corresponding angles C11–C14–N2–C15 and C15–C18–N2–C19 are –153.9(2) and –151.8(2)° respectively. Since the conformations of the ethyl (in H_2EtSLPNDM) and phenyl (in H_2PhSLPNDM) substituents show a close relationship (Figure 2.24), it is probable that these two substituents have a similar influence on the respective torsion angles, and thus play a role in determining the orientation of the two phenyl rings.

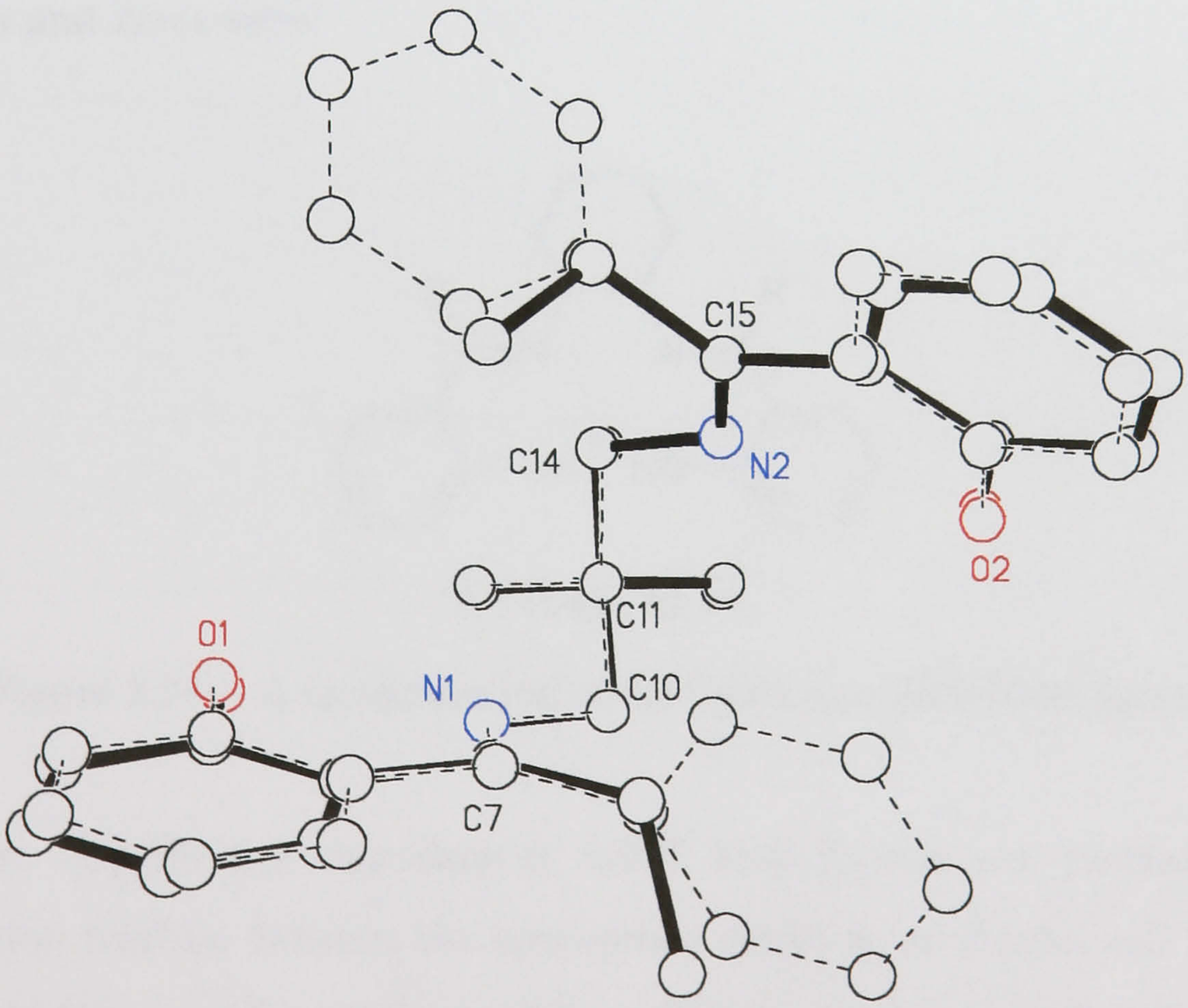

Figure 2.24 The superposition of the two molecules H_2EtSLPNDM and H_2PhSLPNDM

The conformation of the free ligand in the solid state is of interest with respect to that required in the metal complex. For such species to act in the usual way found for tetradentate ligands, significant rearrangements from the solid state structure must occur as is emphasised by the large O1...O2 separations of 7.181(5) and 7.166(6) Å for H_2EtSLPNDM and H_2PhSLPNDM, respectively. This distance is reduced to 3.006(3) Å when the H–substituted ligand, (H_2SLPNDM), is coordinated to a Ti(IV) centre through the four N and O atoms.

These more imposing steric effects which are obtained with both H_2EtSLPNDM and H_2PhSLPNDM are believed to produce complexes with all three Group 4 metals which have the desired *cis* conformation. These beliefs are backed up by the information obtained from the molecular modelling of these complexes (see molecular modelling section p.103). Unfortunately single crystals, suitable for X–ray crystallography, of any of these complexes were not obtained to assign definitively the stereochemistry.

Preparation of the CycH Type Schiff Base Ligands and their Complexes with Titanium and Zirconium

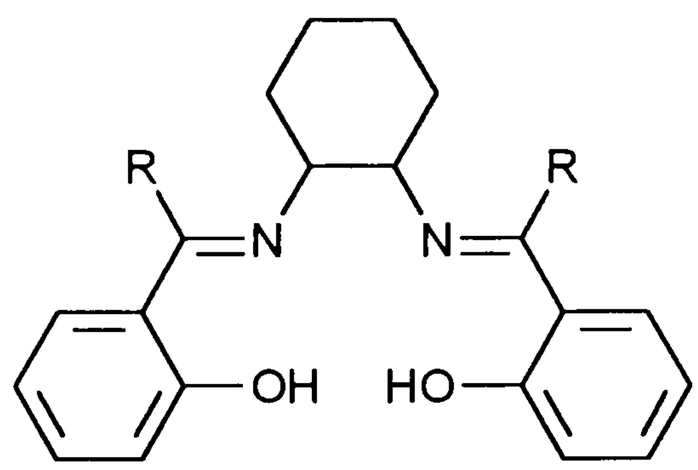

R = H, Me, Et, Ph

Figure 2.25 A representation of the CycH type Schiff base ligands

The (CycH) type tetradentate Schiff base ligands are prepared by the condensation reaction between the appropriate aldehyde or ketone and *trans*–1,2–diaminocyclohexane. The synthesis of these ligands requires refluxing conditions to ensure complete reaction and high yields. These ligands are bright yellow, air stable

solids which are less soluble in most solvents than the SALEN and SLPNDM type ligands.

These ligands have the sterically demanding cyclohexyl ring as the backbone. This ring imposes rigidity in the backbone, as well as providing the desired steric bulk, and so imposing restraints so that a *cis* stereochemistry could result upon complexation. These ligands are also chiral, the chirality being introduced with the *trans*–1,2–diaminocyclohexane. This introduction of chirality may be of significance in determining both the desired catalyst stereochemistry, and in the potential of these complexes for stereoregular Ziegler–Natta polymerisation.

Again in the synthesis of $[M(L)Cl_2]$ complexes, the preparation with titanium differs from that of zirconium and hafnium; with these latter metals an initial seven coordinate complex is formed, with a THF molecule in the seventh coordination site. The desired six coordinate $[M(L)Cl_2]$ is achieved by recrystallisation from hot toluene.

A major problem with these complexes is that they are poorly soluble in polar solvents such as dichloromethane, and totally insoluble in non–polar solvents such as hexane. This poor solubility proved to be a problem in obtaining good characterisation by N.M.R spectroscopy. As solids they decompose in the air, with the seven coordinate zirconium complexes being extremely sensitive to moisture. As solutions in organic solvents they are also very sensitive to hydrolysis. However, these compounds can be conveniently handled in an inert atmosphere, and manipulations were therefore carried out in a nitrogen filled glove box or by using a standard Schlenk–line.

As with the preparation of $[M(SALEN)Cl_2]$ complexes, all the free ligands were recrystallised and dried in vacuo before use to eliminate impurities and the THF adduct of the metal tetrachloride $[MCl_4.2THF]$ was used in the complexation reaction.

The molecular modelling of these complexes (p.103) indicated that as expected all six coordinate zirconium complexes would have a *cis* geometry. The titanium complexes were predicted to be as follows, $[Ti(CycH)Cl_2]$ and $[Ti(DMCycH)Cl_2]$ to have a *trans* geometry at the metal centre and $[Ti(EtCycH)Cl_2]$ and $[Ti(PhCycH)Cl_2]$ to have the two chlorine atoms in the desired *cis* configuration.

Spectroscopic Characterisation of the CycH Type Schiff Base Ligands and their Complexes with Titanium and Zirconium.

Nuclear Magnetic Resonance Spectra

Details of the ^{1}H N.M.R. and ^{13}C N.M.R. data for individual compounds are given in the experimental section. The ^{1}H N.M.R. spectra of these compounds proved to be useful in verifying both the correct stoichiometry and purity of the reaction products. The ^{1}H N.M.R. spectra of the ligands were routinely recorded in $CDCl_3$. However, due to the extremely poor solubility of the complexes their ^{1}H N.M.R. spectra had to be recorded in d^6–DMSO because a strong enough spectrum could not be obtained from an alternative solvent. Because of this the solution had to be prepared and recorded instantly to avoid any degradation of the complex by the DMSO. It was for the above reason that suitable ^{13}C N.M.R. spectra of the complexes have not been obtained, although the ^{13}C N.M.R. spectra of the ligands have been obtained in $CDCl_3$.

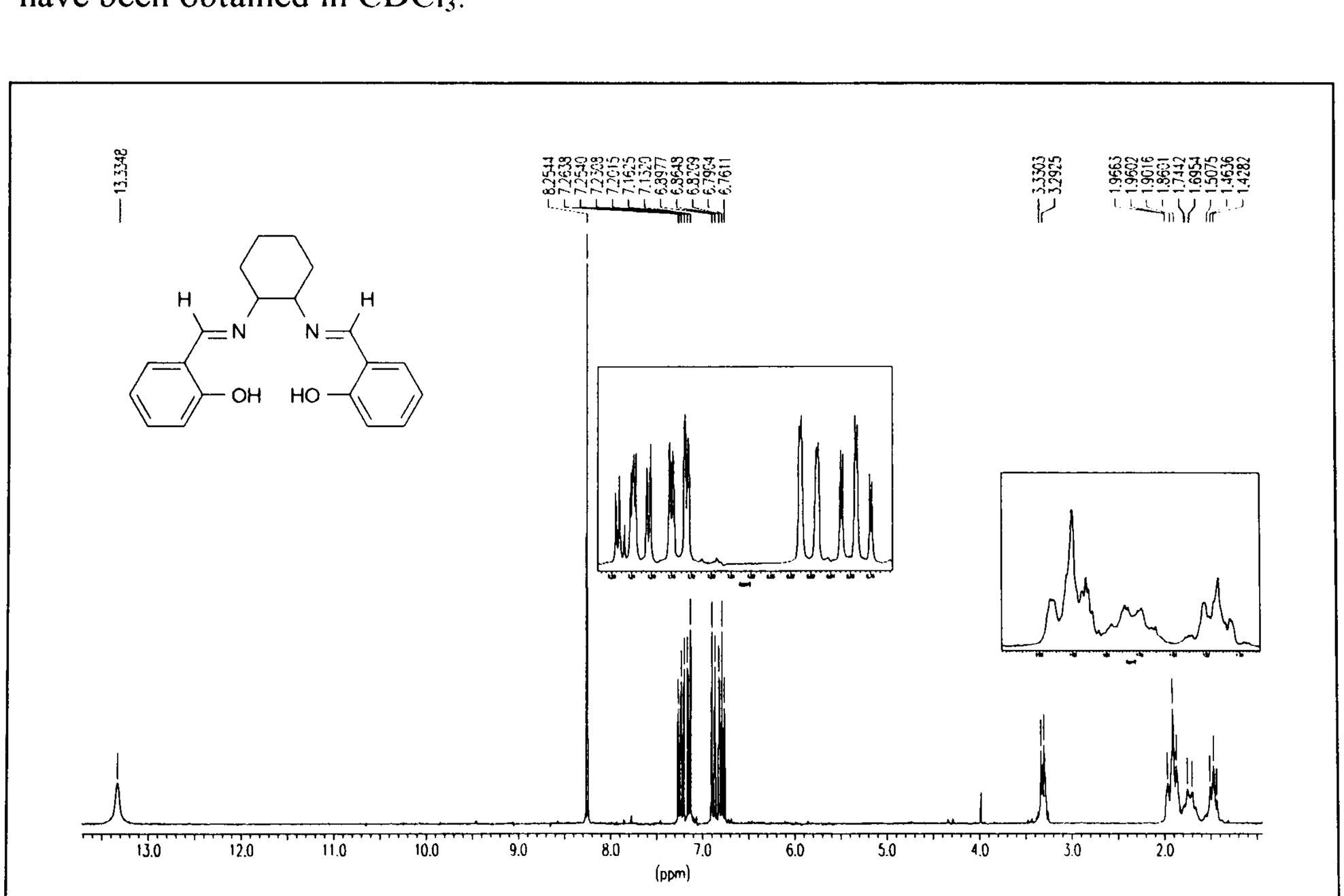

Figure 2.26 The ^{1}H N.M.R spectrum of the free ligand H_2CycH

Due to the cyclohexyl ring, the ^1H N.M.R. spectra of the ligands and their corresponding complexes have proved interesting. One major problem with these compounds is that the resonances associated with the cyclohexyl ring are rather broad, and this broadness proves to be more complex in the spectra of the complexes.

The spectrum of H_2CycH is shown in Figure 2.26. The OH δ 13 ppm and aromatic resonances δ 6–7.7 ppm are found in the same regions as those in the spectra of the SALEN and SLPNDM type ligands. The resonances associated with the substituted group on the imine carbon are again seen as expected, and in the spectrum of H_2CycH, the imine proton resonance is seen at δ 8.25 ppm. integrating for two protons.

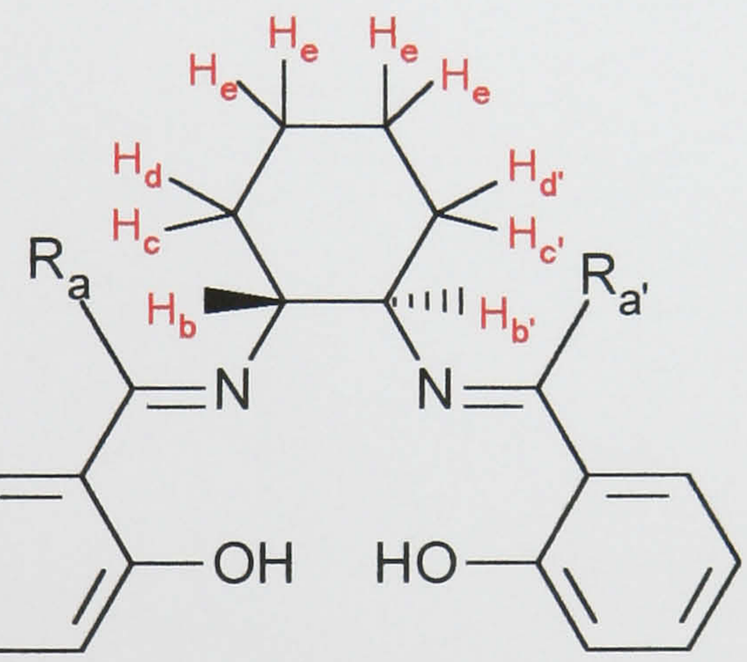

Figure 2.27 Representation of the protons in CycH type ligands and their complexes

The resonances associated with the cyclohexyl backbone are of interest and are described in more detail below. If these compounds are represented as in Figure 2.27 then the spectra can be interpreted as follows. The protons H_c–H_e and $H_{c'}$–$H_{d'}$ are seen as rather broad resonances at around δ 1.4–2.0 ppm, they overlap and are not easily distinguishable, especially in the spectra of the Group 4 complexes. The protons that are of most interest and provide the most information in these spectra are the protons H_b and $H_{b'}$ which are adjacent to the imine. In the spectra of the free ligands these protons appear as a sharp doublet at δ 3.30 and 3.29 ppm. However in the majority of complexes of these ligands, the two protons, H_b and $H_{b'}$, are seen as

two broad singlets as far apart as 0.5-1.0 ppm and are clearly inequivalent. There are two exceptions viz., [Ti(PhCycH)Cl_2] and [Zr(PhCycH)Cl_2] where H_b and $H_{b'}$ appear as a sharp doublet c.a., uncomplexed ligand.

With the ligand H_2CycH and its corresponding Group 4 complexes (i.e. R = H) another difference is seen between their spectra. In the ligand the protons R and R' are seen as a singlet at δ 8.5 ppm; however, in the complexes of this ligand these protons appear inequivalent and can be seen as two singlets at approximately δ 8.6 and 9.0 ppm.

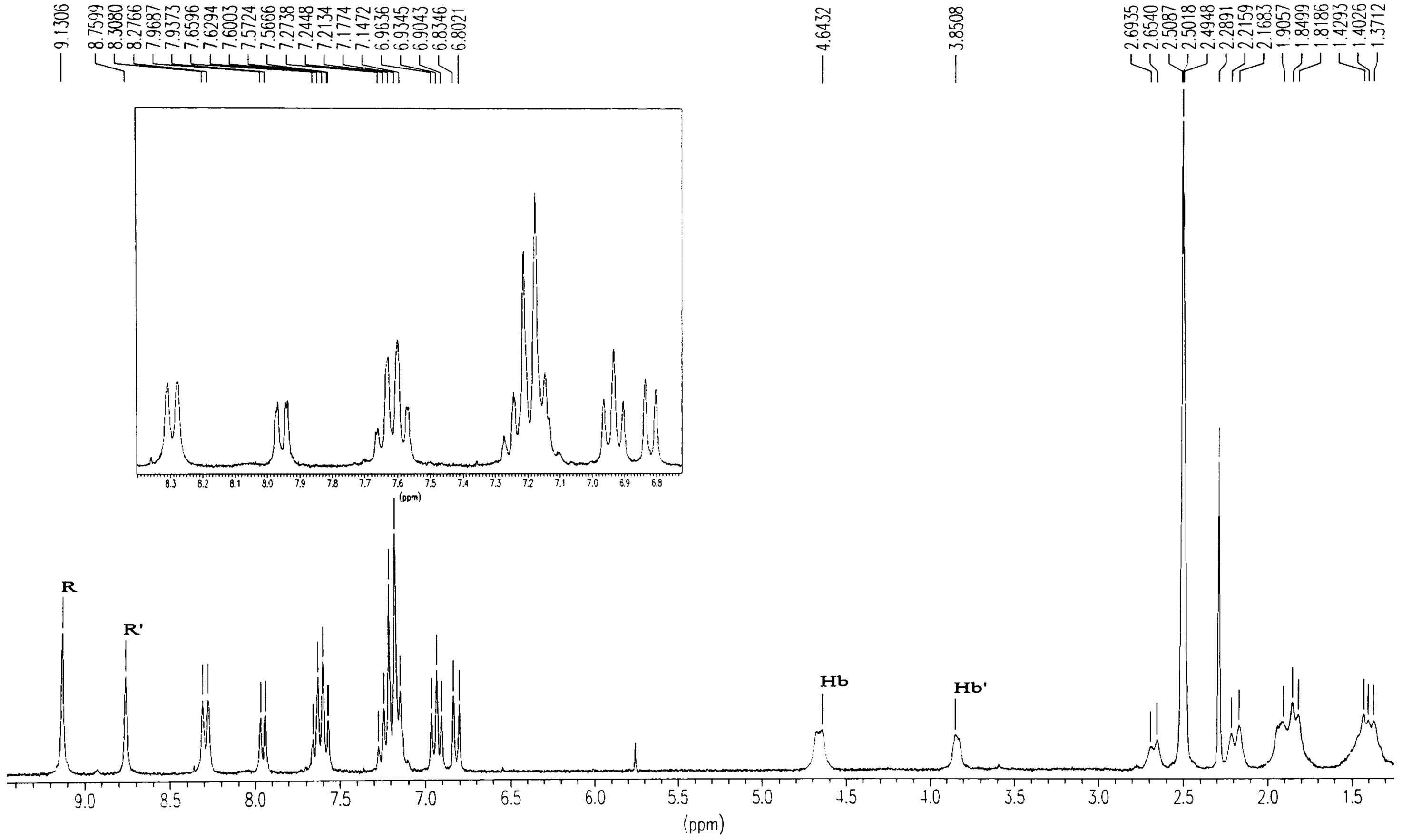

Figure 2.28 The ^{1}H N.M.R spectrum of the complex $[Ti(CycH)Cl_2]$

Mass Spectra

The E.I. and C.I. mass spectra of both the free ligands, and their Group 4 metal complexes have been obtained. The spectra of the free ligands were obtained at source temperatures typically ca. 25–100 °C. The fragmentation of the ligands is not unusual and involves the breakage of the ligand in one place within the backbone (Figure 2.29) followed by further fragmentation of these ions.

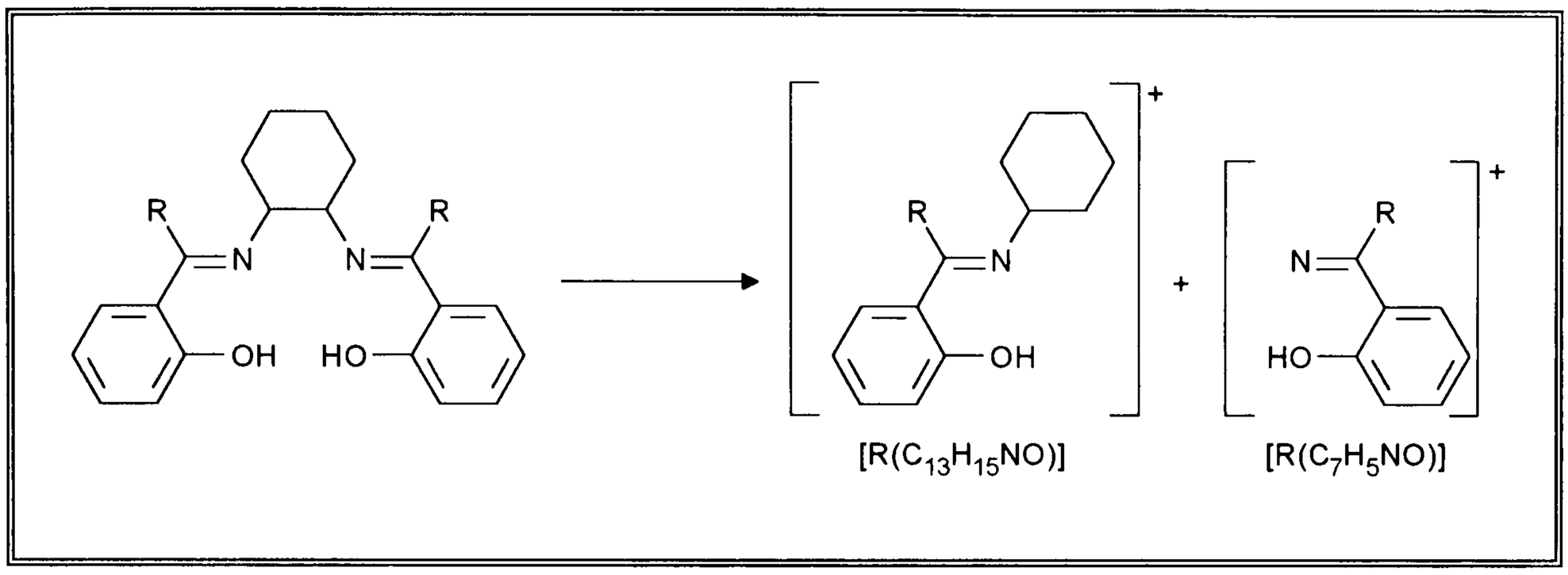

Figure 2.29 The fragmentation of CycH type ligands

The spectra of the complexes proved to be difficult to obtain due to the sensitivity of the complexes. The use of F.A.B. mass spectrometry was not possible due to both the insolubility of the complexes and the hydrolysis of the complexes by the matrix, NBA, and the lack of any other inert matrix. The E.I. and C.I. spectra were eventually obtained by using source temperature typically > 350 °C. The spectra show very weak intensity peaks due to the molecular ions, and to the ions corresponding to the loss of chlorine atoms. These spectra all possess the expected isotope pattern associated with the presence of chlorine atoms.

Table 2.10 Summary of the E.I spectra for CycH type free ligands

Ligand	m/z	Intensity	Assignment
H_2CycH	322	33.8	$[M]^+$
	203	83.6	$[R(C_{13}H_{15}NO)]^+$
	121	50.2	$[R(C_7H_5NO)]^+$
$H_2DMCycH$	350	29.7	$[M]^+$
	215	71.4	$[R(C_{13}H_{15}NO)]^+$
	136	49.4	$[R(C_7H_5NO)]^+$
$H_2EtCycH$	413	37.2	$[M]^+$
	229	67.1	$[R(C_{13}H_{15}NO)]^+$
	147	43.6	$[R(C_7H_5NO)]^+$
$H_2PhCycH$	474	52.7	$[M]^+$
	355	85.8	$[R(C_{13}H_{15}NO)]^+$
	273	40.9	$[R(C_7H_5NO)]^+$

Table 2.11 Summary of the E.I and C.I spectra for the titanium and zirconium complexes of the CycH type ligands

Compound	m/z	Intensity	Assignment
$[Ti(CycH)Cl_2]$	433	0.5	$[(M–Cl)+1]^+$
	432	2.1	$[M–Cl]^+$
	395	0.4	$[M–2Cl]^+$
$[Zr(CycH)Cl_2]$	447	0.2	$[(M–Cl)+1]^+$
	446	0.8	$[M–Cl]^+$
$[Ti(DMCycH)Cl_2]$	432	0.7	$[(M–Cl)+1]^+$
	431	1.1	$[M–Cl]^+$
	394	0.3	$[M–2Cl]^+$
$[Zr(DMCycH)Cl_2]$	511	0.6	$[M]^+$
	475	0.4	$[(M–Cl)+1]^+$
	474	3.8	$[M–Cl]^+$
$[Ti(EtCycH)Cl_2]$	495	0.5	$[M]^+$
	459	30.9	$[(M–Cl)+1]^+$
	458	29.5	$[M–Cl]^+$
	422	19.7	$[(M–2Cl)+1]^+$
$[Zr(EtCycH)Cl_2]$	538	0.5	$[M+1]^+$
	537	8.0	$[M]^+$
	501	4.6	$[(M–Cl)+1]^+$
	500	26.6	$[M–Cl]^+$
$[Ti(PhCycH)Cl_2]$	609	0.4	$[(M+NH_3)+1]^+$
	557	1.4	$[(M–Cl)+1]^+$
	555	11.2	$[M–Cl]^+$
	520	0.2	$[(M–2Cl)+1]^+$
	520	5.8	$[M–2Cl]^+$
$[Zr(PhCycH)Cl_2]$	481	0.3	$[M–2Ph]^+$

X–Ray Crystallographic Studies

The molecular structure of the free ligand H_2DMCycH was determined and is shown in Figure 2.30.

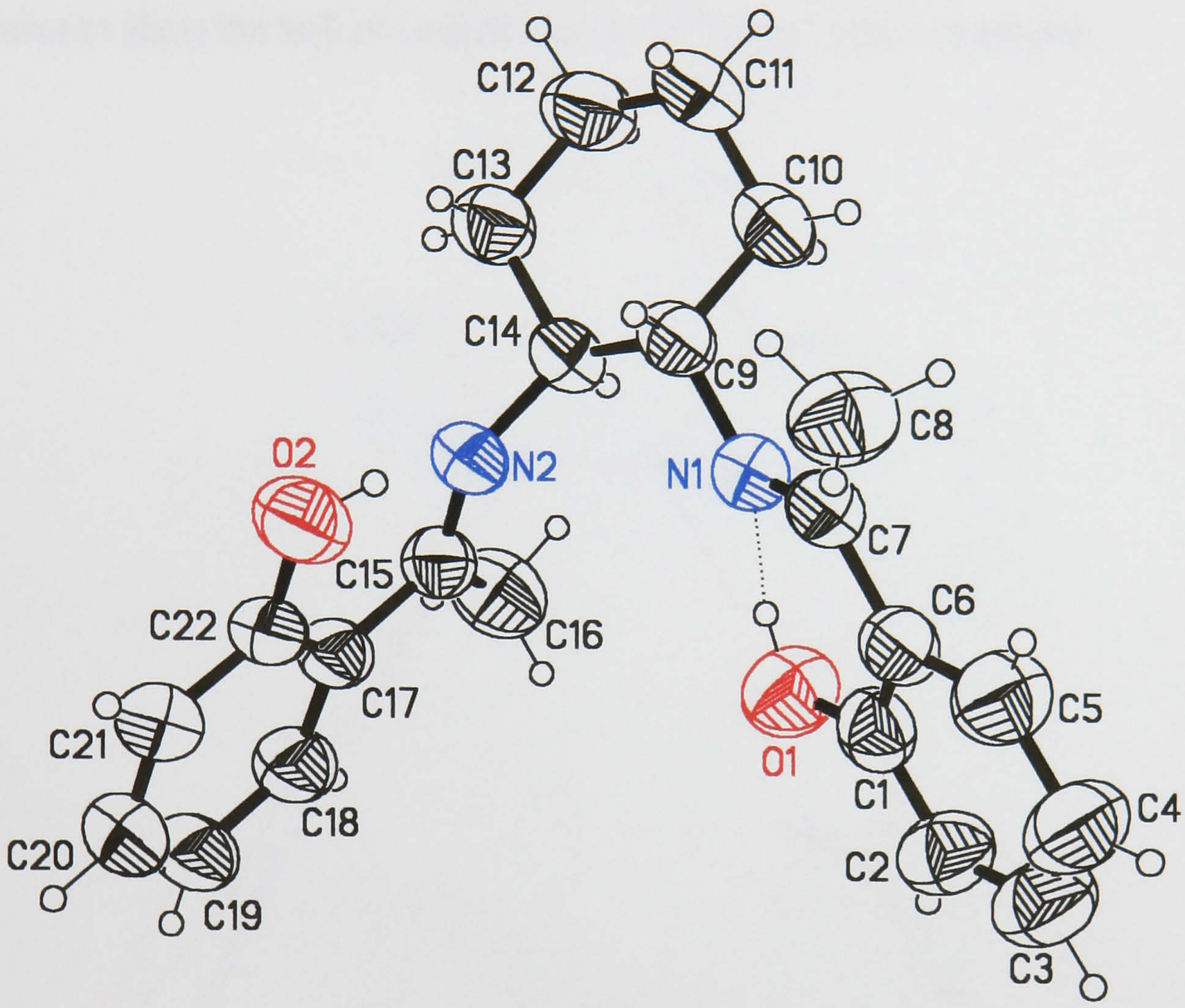

Figure 2.30 The molecular structure of the free ligand H_2DMCycH

When a comparison is made between the molecular structures of H_2DMCycH and H_2CycH[130] it is evident that the methyl groups have a significant effect upon the overall conformation. The bond lengths and angles for these two ligands, while unexceptional, clearly indicate as with the other ligands that the enolimine tautomer is favoured. The N–O distances [average 2.604(3) Å for H_2CycH; average 2.515(3) Å for H_2DMCycH] are again indicative of intramolecular hydrogen bonding.

The most interesting comparative aspect of these two structures involves the influence of the methyl groups upon the molecular conformation. While several of the corresponding torsion angles are very similar, a large difference is noted between C7–N1–C9–C14 and C7–N1–C8–C13. The effect of this difference is that the

orientation of the two aromatic rings is 56.5(1)° in H_2CycH, but 83.15(8)° in H_2DMCycH. An alternative way of expressing these differences between the conformation of the two molecules is to note that the O atoms are 6.082(3) Å apart in H_2CycH, but only 5.544(5) Å apart in H_2DMCycH. The overall situation can be seen in Figure 2.31 in which the cyclohexane rings have been superimposed for the two molecules to show the lack of coincidence in the 'wings' of the molecules.

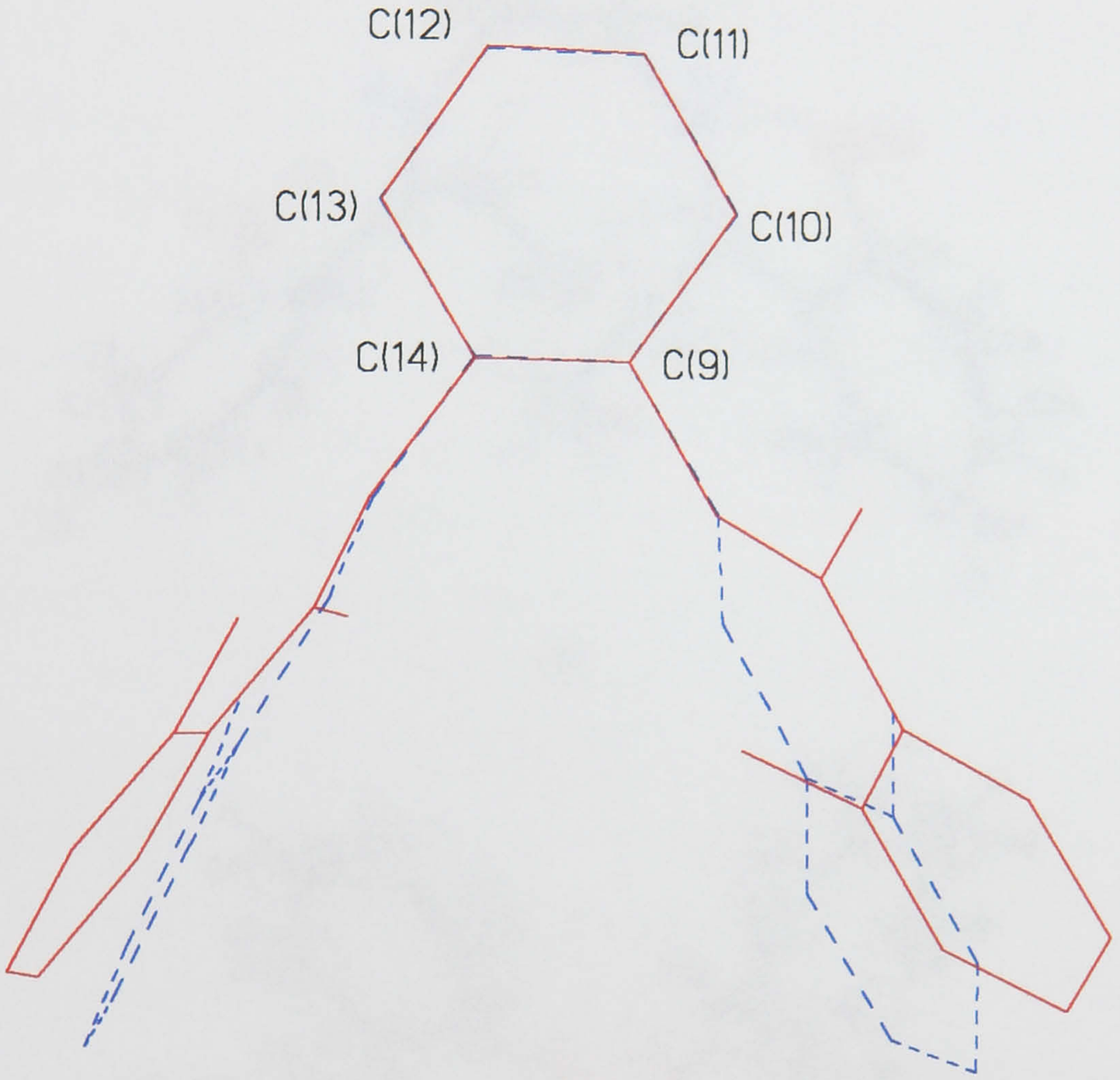

Figure 2.31 The superposition of H_2CycH and H_2DMCycH with respect to the cyclohexane rings

The molecular structure of the free ligands H_2EtCycH and H_2PhCycH have also been determined and can be seen in Figure 2.32.

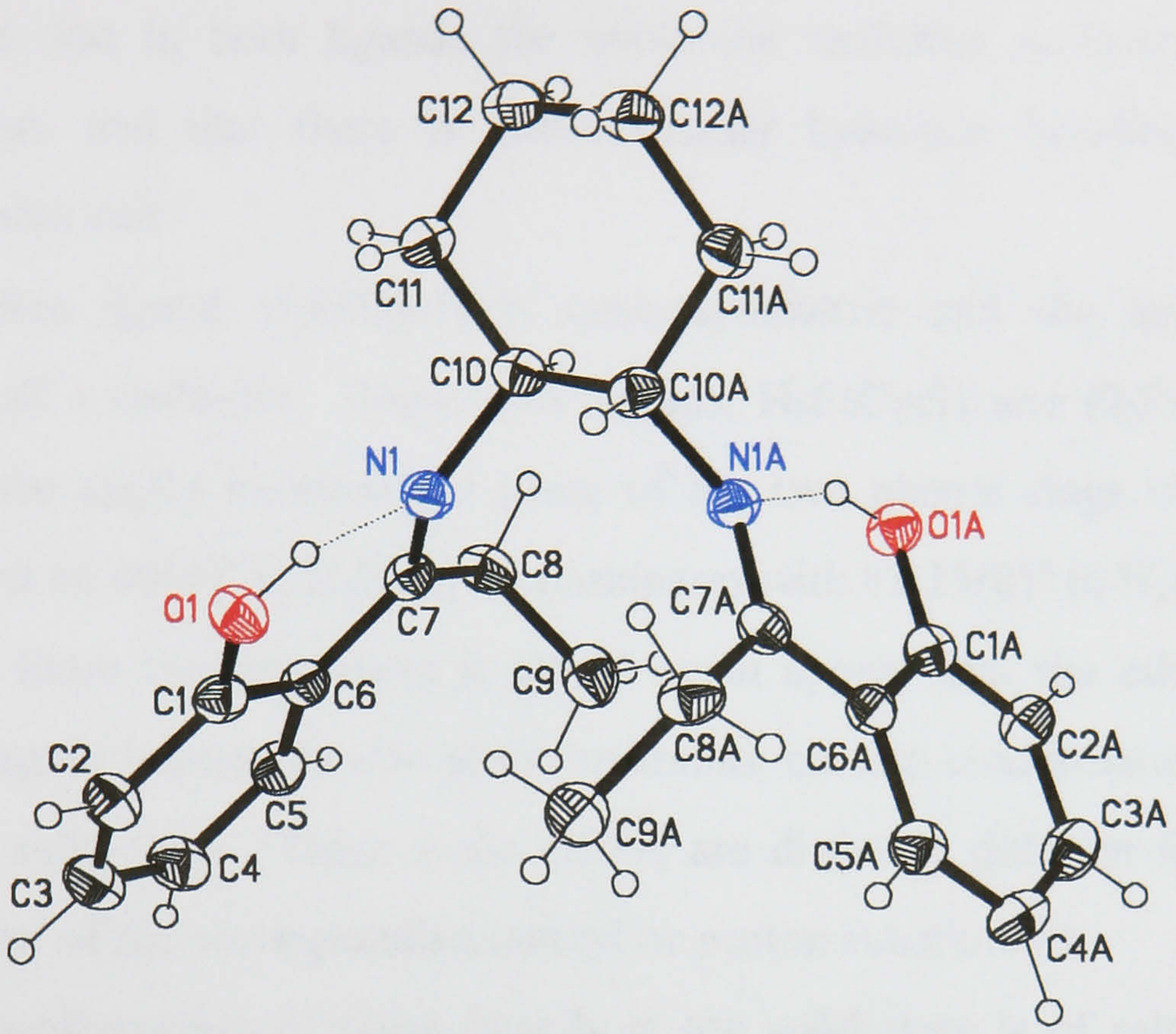

(a)

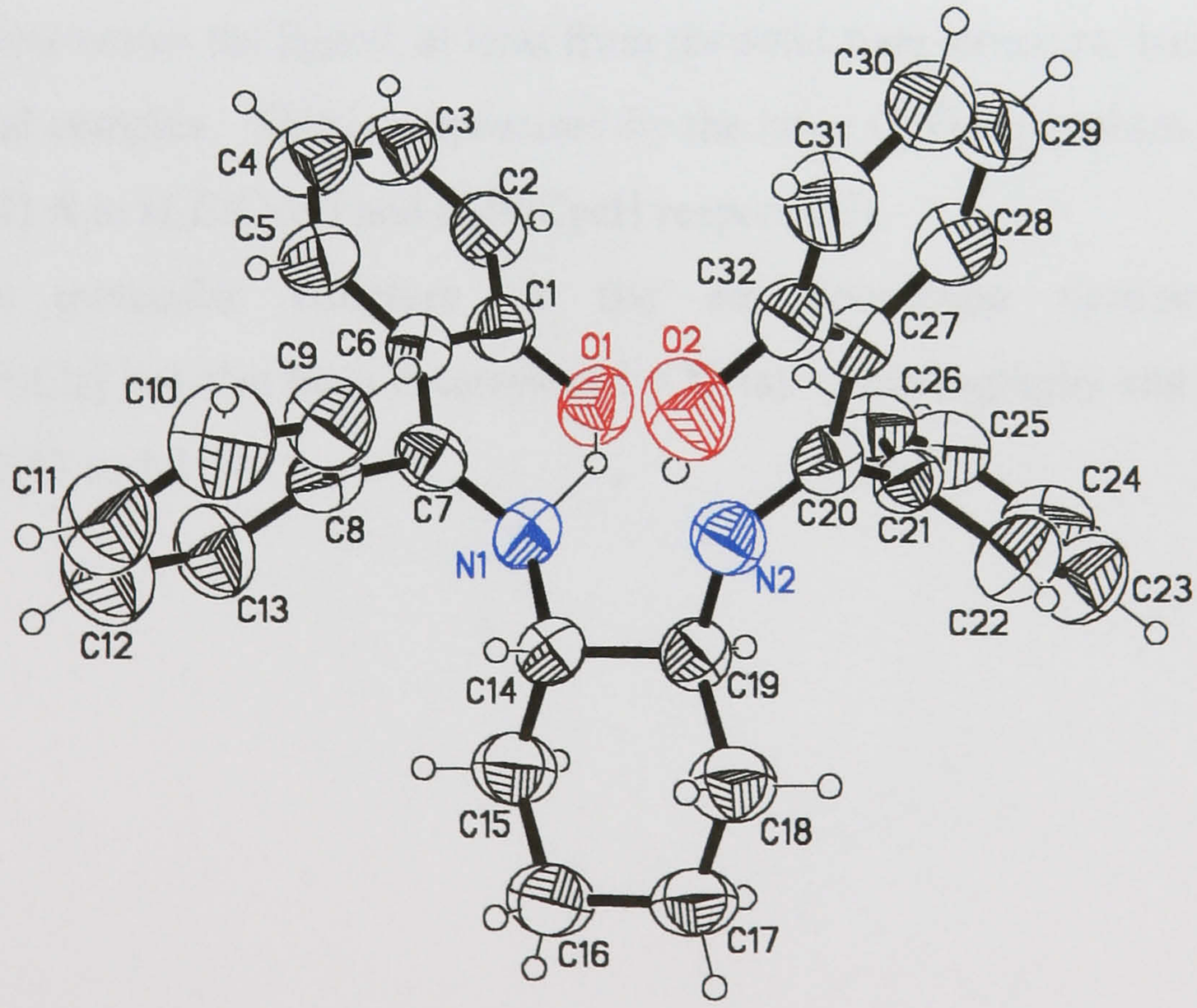

(b)

Figure 2.32 The molecular structures of the free ligands (a)H_2EtCycH and (b)H_2PhCycH

The molecular structures show bond lengths which are unexceptional and a full listing of all bond lengths and angles for these molecules can be found in the Appendix. It is again evident that in both ligands the enolimine tautomer is favoured over the ketamine form, and that there is intramolecular hydrogen bonding within each salicylideneimine unit.

The free ligand H_2EtCycH is centrosymmetric and the asymmetric unit consists of half a molecule. These two ligands, H_2EtCycH and H_2PhCycH have a similarity in the angles between the plane of the two phenol rings of 68.48(8)° in H_2EtCycH and 66.40(4)° in H_2PhCycH (compares with 83.15(8)° in H_2DMCycH).

From these two structures it would again appear that the ethyl and phenyl substituents again impose similar steric restraints on the conformation of the free ligand in the solid state. These steric effects are distinctly different from the steric effects of either of the corresponding methyl or proton substituents.

The conformation of these ligands in the solid state is of relevance to that required in a metal complex. These molecular structures show that a significant rearrangement within the ligand, at least from the solid state structure, has to occur to form a metal complex. This is emphasised by the large O..O separations of 6.861(4) and 6.298(4) Å in H_2EtCycH and H_2PhCycH respectively.

The molecular structure of the six coordinate titanium complex [Ti(EtCycH)Cl_2] has also been determined by X–ray crystallography and can be seen in Figures 2.33 and 2.34.

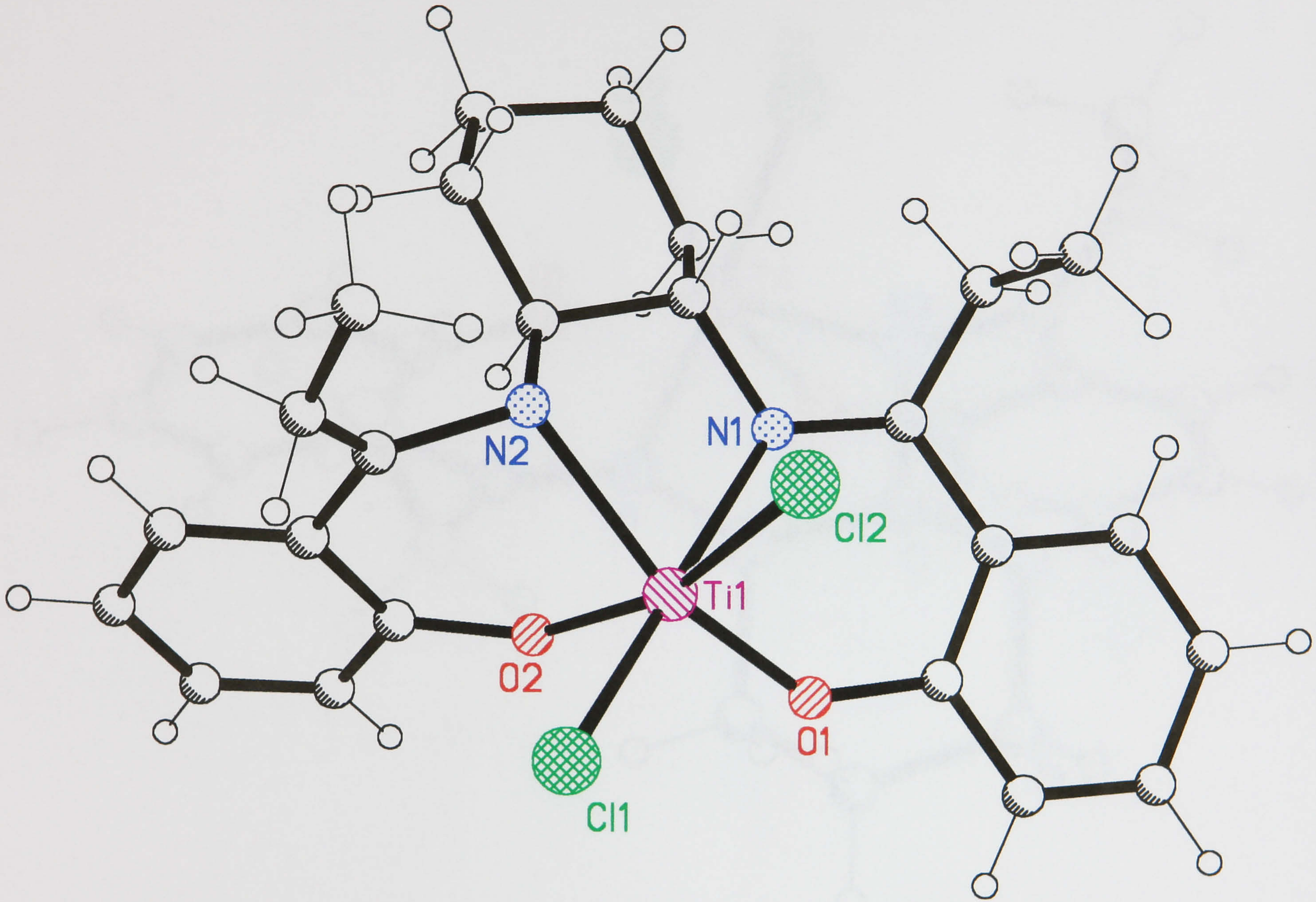

Figure 2.33 The molecular structure of ***cis***–[Ti(EtCycH)Cl_2]

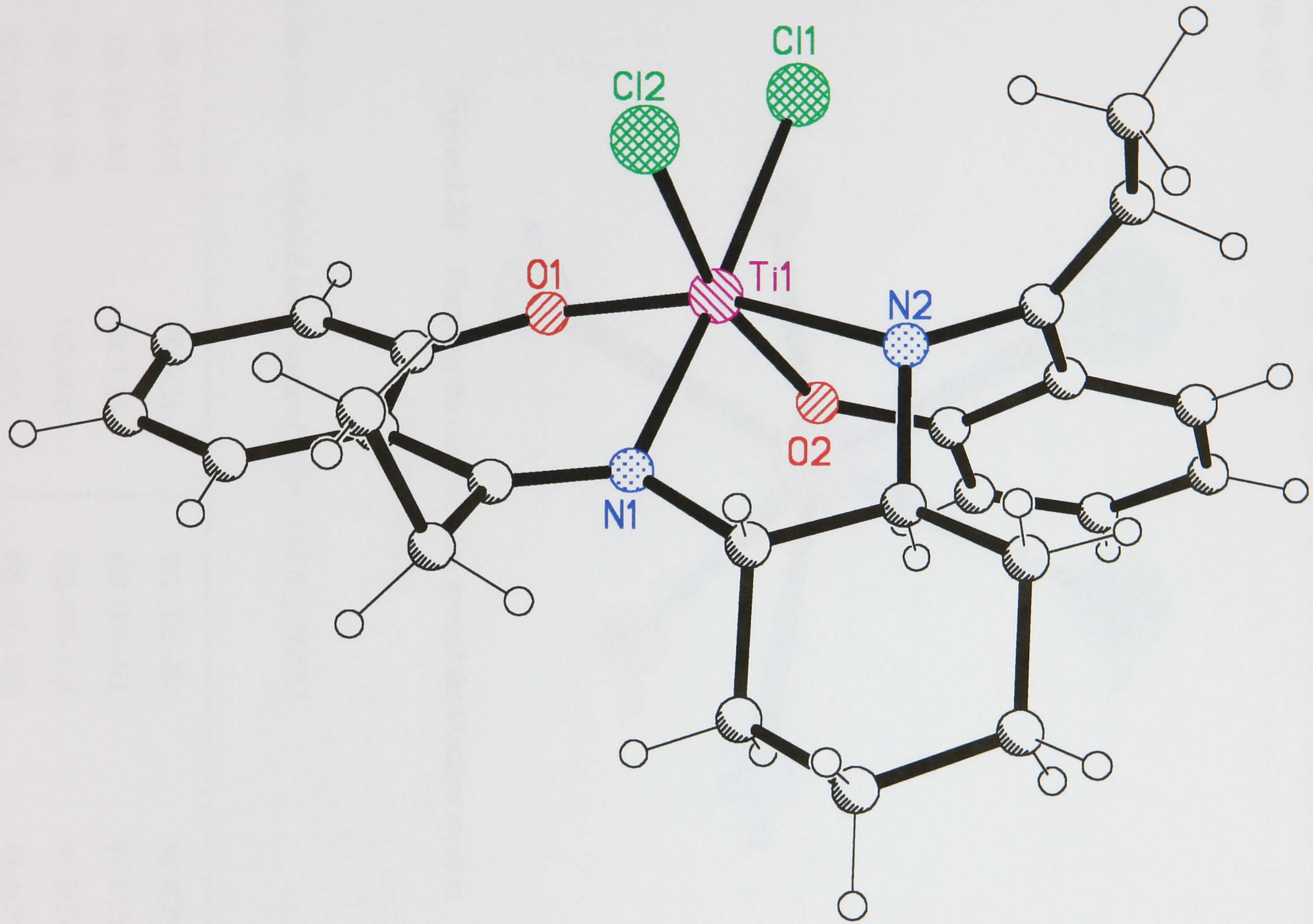

Figure 2.34 Another view of the molecular structure of ***cis***–[Ti(EtCycH)Cl_2]

The complex consists of discrete [Ti(EtCycH)Cl_2] molecules and $CHCl_3$ solvent molecules of crystallisation in a complex/solvent molar ratio of 1:1. The coordination around the titanium atom is approximately octahedral but there is considerable distortion with bond angles around titanium varying from 76.5(2) to 101.4(2)°.

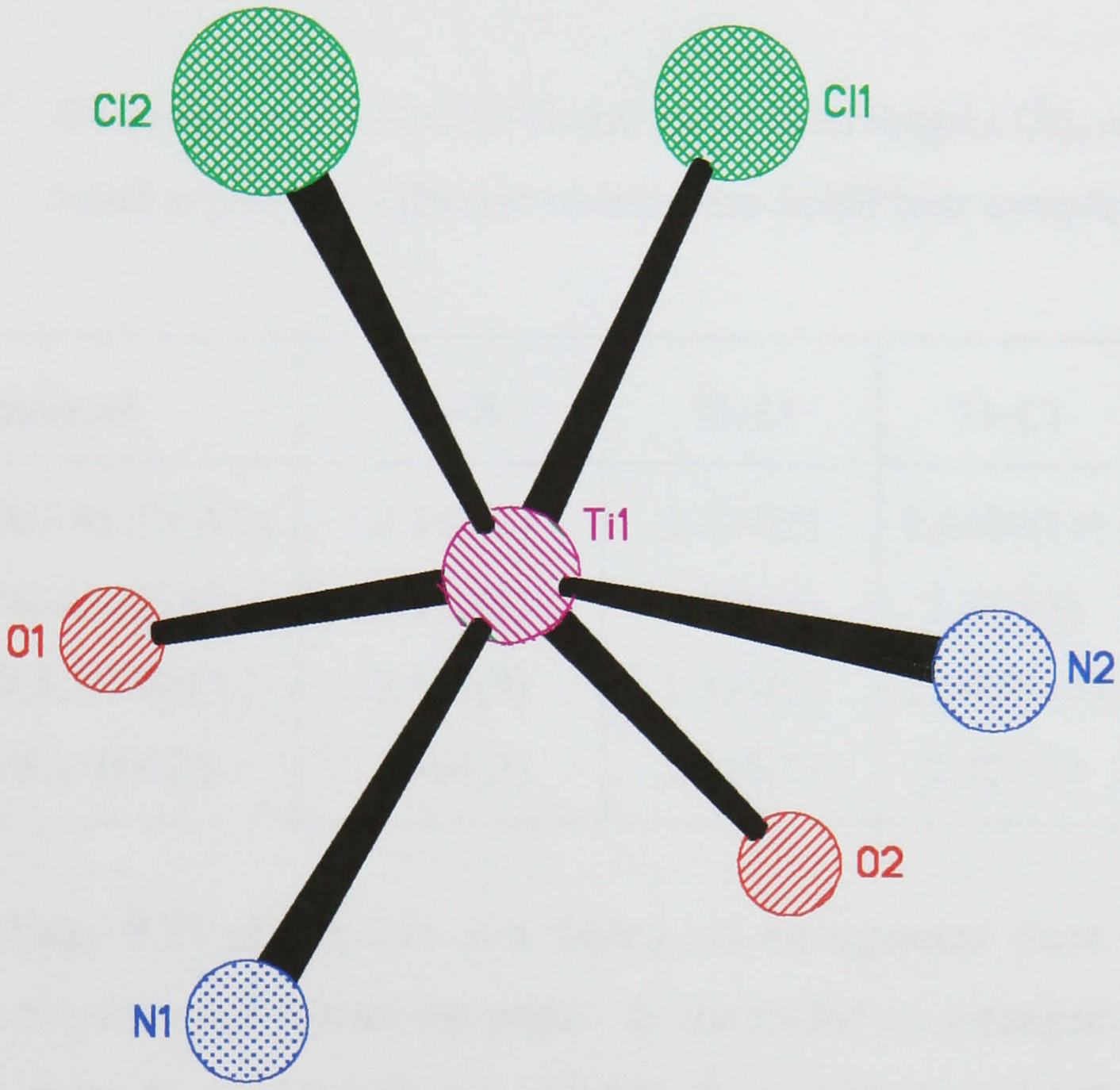

Figure 2.35 Showing the coordination around the titanium atom in [Ti(EtCycH)Cl_2]

Table 2.12 Selected bond angles (°) for [Ti(EtCycH)Cl_2]

O1–Ti1–O2	99.5(2)	O1–Ti1–N1	82.6(2)
O2–Ti1–N1	98.7(2)	O2–Ti1–N2	81.1(2)
O1–Ti1–Cl1	101.4(2)	O2–Ti1–Cl1	91.0(2)
N2–Ti1–Cl1	99.7(2)	O1–Ti1–Cl2	98.4(2)
N1–Ti1–N2	76.5(2)	Cl1–Ti1–Cl2	86.90(9)
N1–Ti1–Cl2	82.2(2)	N2–Ti1–Cl2	81.7(2)

However, the coordination around the titanium is such that the two chlorine atoms are in *cis*–positions to each other with a Cl1–Ti1–Cl2 bond angle of 86.90(9)°. **This is the first known tetradentate Schiff base titanium complex with such a *cis* arrangement at the metal centre**; all complexes reported to date show a *trans* conformation at the titanium atom. The ligand around the metal has folded such that the angle between the two phenol rings is 58.54(10)°.

Table 2.13 Comparison of Ti–N, Ti–O and Ti–Cl bond lengths (Å), and Cl–Ti–Cl bond angle (°) in different tetradentate Schiff base complexes

Compound	Ti–N	Ti–O	Ti–Cl	Cl–Ti–Cl
trans-[Ti(DMSALEN)Cl_2]	2.142(2)	1.817(2)	2.3406(10)	168.36(3)
trans-[Ti(PhSALEN)Cl_2]	2.140(5)	1.805(4)	2.329(8)	167.00(7)
trans-[Ti(SLPNDM)Cl_2]	2.168(3)	1.835(2)	2.3607(13)	174.16(5)
cis-[Ti(EtCycH)Cl_2]	1.794(5)	2.182(6)	2.323(2)	86.90(9)

The above Table 2.13 shows that in a folded *cis* arrangement there is a marked difference in bond lengths around the metal. In the folded *cis* arrangement the Ti–N bond length shortens considerably to 1.794(5) Å compared to 2.142(2) Å in the *trans*-dichloro [Ti(DMSALEN)Cl_2] complex. The Ti–O bond length on the other hand increases by around 0.35 Å to 2.182 Å in the *cis*-dichloro [Ti(EtCycH)Cl_2] compared to 1.835(2) Å in the *trans*-dichloro [Ti(SLPNDM)Cl_2] complex.

It is believed from the modelling studies (p.103) that the titanium complex [Ti(PhCycH)Cl_2] will also have a folded *cis* arrangement similar to [Ti(EtCycH)Cl_2].

Modelling studies

In addition to the synthesis and characterisation of these metal complexes, the complexes have been modelled using *HYPERCHEM* version 4.5. The zirconium(IV) and hafnium(IV) tetradentate Schiff base complexes have not been studied because it is assumed that these six coordinate complexes possess the desired *cis* arrangement as found by Floriani *et al.*[113] It was envisaged that these studies would give an insight into the likely stereochemistry at the metal centre in these tetradentate Schiff base titanium(IV) complexes. Help in performing these studies was provided by Dr. S. Smith.[131]

The use of molecular mechanics for structural analysis. Investigation of the complexes between Ti(IV) and a range of tetradentate Schiff base ligands

Titanium(IV) complexes possessing two labile *cis* sites are of great interest as potential alkene polymerisation catalysts. Since NMR, IR, UV–Visible spectroscopy, and mass spectrometry could not determine conclusively whether the two remaining chlorine atoms were arranged in either a *cis* or *trans* geometry, the two possible geometries were examined by molecular mechanics analysis.

It is necessary to provide the molecular mechanics model with equilibrium bond lengths and force constants for all the titanium–ligand bonds. The values used were taken from published structures of related systems and are as follows; Ti–N(imine), 2.137 Å; Ti–O(phenolic), 1.873 Å; and Ti–Cl, 2.305 Å; all with a force constant of 2.250 mdyne $Å^{-1}$.[132,133] The minimum energy conformations for both the *cis* and *trans* geometries were then determined and a comparison of the calculated energies undertaken (Table 2.14).

Table 2.14 Comparison of the calculated minimum energies for the *cis* and *trans* isomers of titanium(IV) Schiff base complexes

	Calculated minimum energy (kJ mol^{-1})	
Complex	***cis* chlorines**	***trans* chlorines**
[Ti(DMSALEN)Cl_2]	174.2	156.8
[Ti(EtSALEN)Cl_2]	189.1	172.9
[Ti(PhSALEN)Cl_2]	209.4	196.6
[Ti(SLPNDM)Cl_2]	81.9	75.1
[Ti(DMSLPNDM)Cl_2]	199.5	186.7
[Ti(EtSLPNDM)Cl_2]	195.4	208.7
[Ti(PhSLPNDM)Cl_2]	354.1	426.3
[Ti(CycH)Cl_2]	124.3	102.1
[Ti(DMCycH)Cl_2]	268.3	233.3
[Ti(EtCycH)Cl_2]	257.5	262.7
[Ti(PhCycH)Cl_2]	259.8	266.7

The results of the calculations clearly show that the *trans* orientation is the more energetically favoured structure in most cases. However, the *cis* orientation is found to be favoured from four of the calculations, namely [Ti(EtSLPNDM)Cl_2], [Ti(PhSLPNDM)Cl_2], [Ti(EtCycH)Cl_2] and [Ti(PhCycH)Cl_2]. The results from the molecular modelling can be confirmed by comparison with crystal structures which have been obtained.

The titanium complexes of the two Schiff base ligands H_2DMSALEN and H_2SLPNDM (Figure 2.36) have been considered in detail and the predicted model compared with the actual X–ray structure of the titanium complexes. These X–ray structures also allow a comparison of experimentally determined and calculated geometries (Tables 2.14 and 2.15).

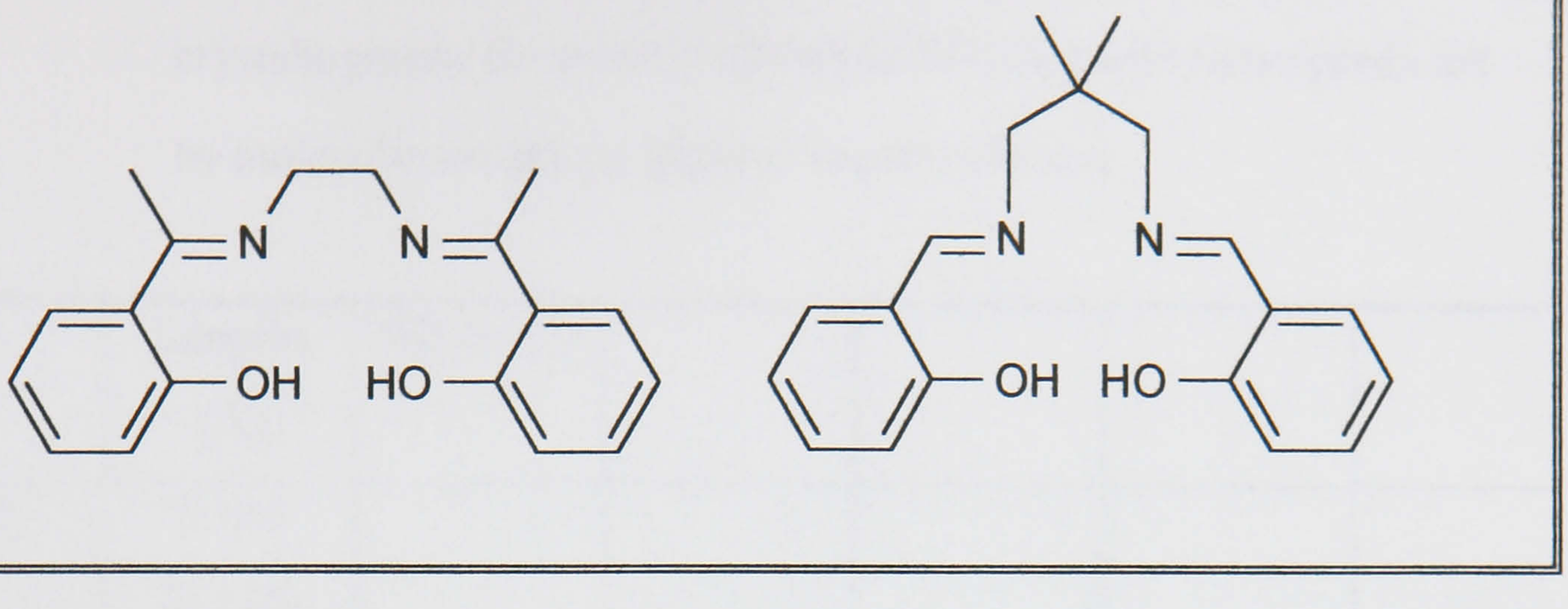

Figure 2.36 Diagram illustrating the structures of the ligands H_2DMSALEN (left)and H_2SLPNDM (right)

A superimposition of the calculated minimum energy conformation of [Ti(DMSALEN)Cl_2] and that obtained from an x–ray structural analysis is shown in Figure 2.37.

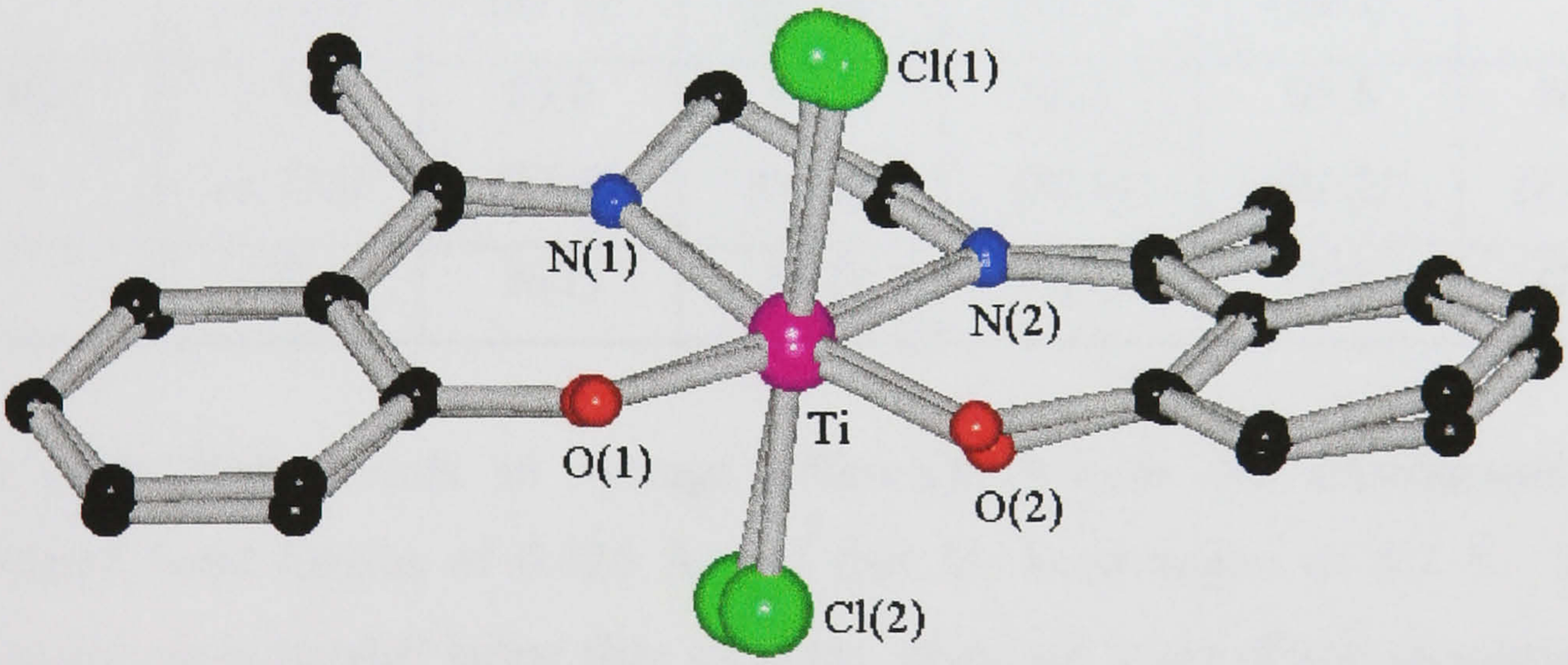

Figure 2.37 Overlay of the calculated minimum energy structure of *trans* [Ti(DMSALEN)Cl_2] with the structure determined by X–ray crystallography showing the atomic numbering system.

Table 2.15 Comparison of selected bond lengths and angles determined by X–ray crystallography for *trans* [Ti(DMSALEN)Cl_2] with those predicted by molecular modelling (*figures in parentheses*)

Ti–	Lengths (Å)	Angles (°)				
N(1)	2.166 *(2.138)*					
N(2)	2.141 *(2.138)*	79.1 *(80.8)*				
O(1)	1.824 *(1.857)*	85.6 *(91.1)*	164.2 *(171.1)*			
O(2)	1.820 *(1.857)*	164.6 *(171.0)*	85.6 *(91.0)*	109.9 *(97.3)*		
Cl(1)	2.350 *(2.323)*	85.6 *(87.1)*	87.1 *(92.0)*	95.3 *(91.2)*	91.9 *(89.5)*	
Cl(2)	2.352 *(2.323)*	85.0 *(92.1)*	85.1 *(87.2)*	90.1 *(89.4)*	95.5 *(91.2)*	168.8 *(179.0)*
	Ti	N(1)	N(2)	O(1)	O(2)	Cl(1)

This comparison reveals an average difference between the experimental and calculated bond lengths of 0.026 Å, and that for bond angles of 5.1 °. These deviations are somewhat larger than expected, given the limits of accuracy expected for molecular mechanics calculations, with bond lengths predicted to within 0.01 Å and bond angles within 2°.[134] However, any differences can be explained by the absence in molecular mechanics calculations of the effects of any solvent incorporated on crystallisation and crystal packing forces, which will all influence the observed structure to varying degrees.

Furthermore, it may have been possible to improve upon these fits by adjustment of the supplied bond lengths and force constants, although for octahedrally coordinated metal ions, repulsive Van der Waal's forces, or steric

crowding, tends to dominate the calculation below a metal–ligand bond length of *ca.* 2.00 Å. In such cases, the calculated bond lengths will always be much longer than the given equilibrium or strain free bond lengths. In general, the ability of a given potential energy term to dominate the calculation in such cases of steric crowding are, repulsive van der Waal's forces > bond length deformation forces > bond angle deformation forces ≥ torsional forces > attractive van der Waal's forces.[134] Therefore, without the use of unrealistically high force constants, > 100 mdyne $Å^{-1}$, it would be impossible to effect a significant improvement on the calculated geometry.

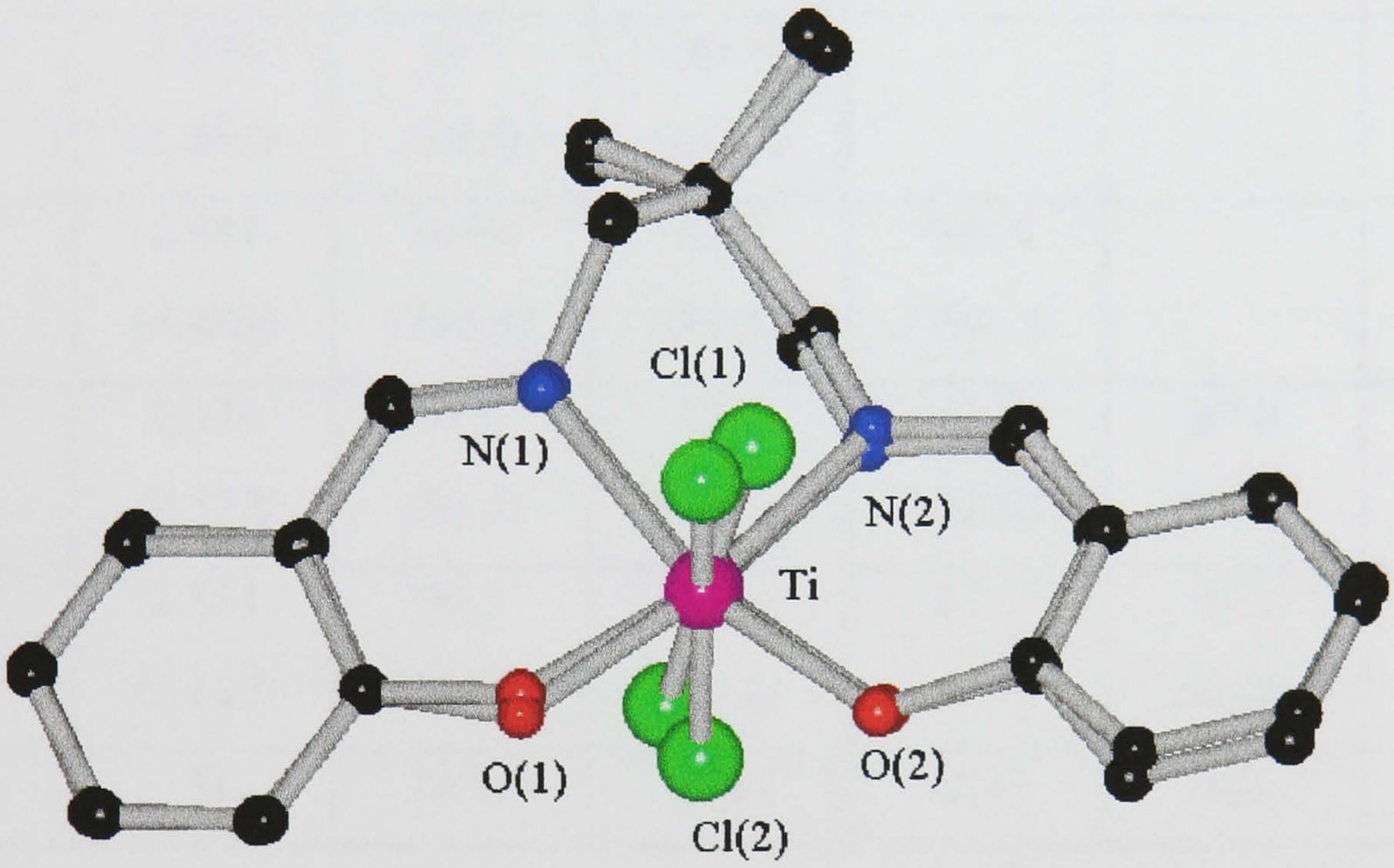

Figure 2.38 Overlay of the calculated minimum energy structure of *trans* [Ti(SLPNDM)Cl_2] with the structure determined by X–ray crystallography showing the atomic numbering system

Table 2.16 Comparison of selected bond lengths and angles determined by X–ray crystallography for *trans* [Ti(SLPNDM)Cl_2] with those predicted by molecular modelling (*figures in parentheses*)

Ti–	Lengths (Å)	Angles (°)				
N(1)	2.166 *(2.146)*					
N(2)	2.170 *(2.146)*	80.7 *(81.6)*				
O(1)	1.840 *(1.883)*	85.5 *(89.5)*	163.6 *(161.7)*			
O(2)	1.831 *(1.883)*	163.0 *(161.8)*	85.0 *(89.5)*	109.9 *(103.2)*		
Cl(1)	2.370 *(2.327)*	84.5 *(84.3)*	92.0 *(106.8)*	95.5 *(88.0)*	87.0 *(83.1)*	
Cl(2)	2.351 *(2.327)*	90.5 *(106.7)*	84.3 *(84.2)*	87.1 *(83.1)*	97.1 *(88.0)*	174.2 *(165.8)*
	Ti	N(1)	N(2)	O(1)	O(2)	Cl(1)

For *trans* [Ti(SLPNDM)Cl_2] an analogous comparison reveals a comparable degree of accuracy for the calculation, with an average difference between the experimental and calculated bond lengths of 0.034 Å, and that for bond angles of 5.6°.

Experimental.

All compounds were handled using a conventional Schlenk or high–vacuum line, and in a dry nitrogen–filled Miller–Howe glove box fitted with a circulating system. Glassware was oven dried or heated under vacuum before use.

Solvents were dried and distilled under dry nitrogen prior to use. Tetrahydrofuran, toluene, benzene and diethyl ether were dried using potassium or sodium, and hexane, dichloromethane and chloroform were dried using calcium hydride. Most solvents were pre–dried using sodium wire. N.M.R solvents were dried over 4 Å molecular sieves before use.

Routine ^{1}H and ^{13}C N.M.R spectra were run using a Bruker Associates ACF250 (250MHz) instrument connected to a personal computer running WIN–NMR. Additional ^{1}H and ^{13}C N.M.R spectra were recorded using a Bruker Associates ACP400 (400MHz) spectrometer. ^{1}H and ^{13}C N.M.R shifts are quoted relative to tetramethylsilane, with downfield shifts being assigned positive values.

Infra–red spectra were recorded from Nujol mulls using either a Perkin Elmer 580B (4000–200 cm^{-1}), or Perkin Elmer 1720X (4000–400 cm^{-1}) spectrophotometer, using caesium iodide plates. Nujol was dried over sodium wire and stored in a glove box.

Elemental analyses were obtained by the Analytical Department at Warwick University. Carbon, hydrogen and nitrogen analyses were determined on a Leeman Labs CE440 elemental analyser.

Preparation of tetrachlorobis(tetrahydrofuran)titanium(IV), **$[TiCl_4(THF)_2]$**

Into a dry Schlenk tube was placed 5.0 g (26 mmol) of titanium tetrachloride dissolved in 50 cm^3 of dichloromethane. Anhydrous tetrahydrofuran (7.62 g, 0.10 mole) was added dropwise (slowly), and the solution stirred at room temperature under nitrogen for 15 min. Dry pentane (50 cm^3) was added and the solution was chilled to –25°C for 1 h. The resultant bright yellow solid was collected on a filter stick and washed with 25 cm^3 dry pentane.

Yield = 80 %, mp = 126–128 °C, IR: strong sharp peak 990 cm^{-1}, strong broad peak 825–845 cm^{-1}

Preparation of tetrachlorobis(tetrahydrofuran)zirconium(IV), **[$ZrCl_4(THF)_2$]**

Into a dry Schlenk tube, equipped with a magnetic stirrer bar, was placed zirconium tetrachloride (23.3 g, 100 mmol) in 300 cm^3 of dichloromethane at room temperature. Anhydrous tetrahydrofuran (14.42 g, 200 mmol) was added dropwise to the suspension causing an exothermic reaction strong enough to reflux the dichloromethane. As the tetrahydrofuran was added, the zirconium tetrachloride dissolved giving a slightly turbid, colourless solution at the end of the addition. The solution was filtered and to the filtrate was added 250 cm^3 of dry hexane. The solution was chilled to –25°C for 2 h. The product was collected on a medium fritted filter stick, washed with 50 cm^3 of dry hexane and dried *in vacuo*. The product was a white crystalline solid.

Yield = 89 %; mp = 170–172°C; IR: strong sharp peak 990 cm^{-1}, strong sharp peak 820–840 cm^{-1}.

General preparation of Tetradentate Schiff base ligands:

The preparation of **H_2SALEN**

Salicylaldehyde (18.30 g, 150 mmol) was dissolved in methanol (75 cm^3) to give a pale yellow solution. 1,2–diaminoethane (4.55 g, 75.8 mmol) was dissolved in methanol (30 cm^3) by warming gently. This solution was slowly run into the solution of the aldehyde, with stirring, to form a yellow solution. This resulting solution was then stirred at 40 °C for 30 min and then placed in the freezer for 1 h. after this time a bright yellow solid had precipitated which was collected by filtration, washed with dry diethyl ether (2 x 25 cm^3) and dried *in vacuo*. Yield = 19.0 g (95 %)

^{1}H N.M.R ($CDCl_3$) δ/ppm: 3.91, s, 4H; 6.83–7.33, m, 8H; 8.34, s, 2H; 13.24, s, 2H.

^{13}C N.M.R ($CDCl_3$) δ/ppm: 166.40, 160.89, 132.30, 131.40, 118.58, 118.54, 116.85, 59.63. Analysis, calculated for $C_{16}H_{16}N_2O_2$ (M.W. 268.3): C, 71.62; H, 6.01: N, 10.44%. Found: C, 71.59; H, 6.05; N, 10.36%.

***Preparation of* H_2DMSALEN**

Procedure as for H_2SALEN, by condensing 2–hydroxyacetophenone with 1,2–diaminoethane.

^{1}H N.M.R ($CDCl_3$) δ/ppm: 2.37, s, 6H; 3.97, s, 4H; 6.75–7.53, m, 8H; 13.90, s, 2H

^{13}C N.M.R ($CDCl_3$) δ/ppm: 172.6, 163.05, 132.35, 128.05, 119.36, 118.37, 117.27, 50.06, 14.66. Analysis, calculated for $C_{18}H_{20}N_2O_2$ (M.W. 296.37): C, 72.95; H, 6.80: N, 9.45%. Found: C, 72.81; H, 6.69; N, 9.52%.

***Preparation of* H_2EtSALEN**

Procedure as for H_2SALEN, by condensing 2–hydroxypropiophenone with 1,2–diaminoethane.

^{1}H N.M.R ($CDCl_3$) δ/ppm: 1.19–1.26, t, 6H; 2.76–2.85, q, 4H; 3.96, s, 4H; 6.75–7.51, m, 8H; 13,69, s, 2H. ^{13}C N.M.R ($CDCl_3$) δ/ppm: 177.46, 164.00, 132.40, 127.99, 118.71, 117.70, 117.23, 49.23, 21.16, 11.74. Analysis, calculated for $C_{20}H_{24}N_2O_2$ (M.W. 324.42): C, 74.05; H, 7.45: N, 8.63%. Found: C, 73.85; H, 7.50; N, 8.69%.

***Preparation of* H_2PhSALEN**

Procedure as for H_2SALEN, by condensing 2–hydroxybenzophenone with 1,2–diaminoethane.

^{1}H N.M.R ($CDCl_3$) δ/ppm: 3.64, s, 4H; 6.61–7.52, m, 18H; 14.56, s, 2H. ^{13}C N.M.R ($CDCl_3$) δ/ppm: 175.36, 162.81, 133.89, 132.38, 131.55, 128.94, 128.75, 127.16, 119.77, 117.80, 117.39, 52.27. Analysis, calculated for $C_{28}H_{24}N_2O_2$ (M.W. 420.51): C, 79.98; H, 5.75: N, 6.66%. Found: C, 79.88; H, 5.72; N, 6.66%.

***Preparation of* H_2SLPNDM**

Procedure as for H_2SALEN, by condensing salicylaldehyde with 2,2–dimethyl–1,3–propanediamine.

^{1}H N.M.R ($CDCl_3$) δ/ppm: 1.07, s, 6H; 3.46, d, 4H; 6.85–7.35, m, 8H; 8.31, s, 2H;13.62, s, 2H. ^{13}C N.M.R ($CDCl_3$) δ/ppm: 166.71, 161.15, 132.28, 131.34,

118.64, 118.58, 116.89, 67.98, 36.13, 24.27. Analysis, calculated for $C_{19}H_{22}N_2O_2$ (M.W. 310.4): C, 73.52; H, 7.14: N, 9.03%. Found: C, 73.48; H, 7.02; N, 9.11%.

***Preparation of* H_2DMSLPNDM**

Procedure as for H_2SALEN, by condensing 2–hydroxyacetophenone with 2,2–dimethyl–1,3–propanediamine.

^{1}H N.M.R ($CDCl_3$) δ/ppm: 1.21, s, 6H; 2.15–2.31, d, 6H; 3.51, s, 4H; 6.76–7.51, m, 8H; 13.16, s, 2H. ^{13}C N.M.R ($CDCl_3$) δ/ppm: 172.34, 164.00, 132.48, 128.00, 119.08, 118.55, 116.95, 57.50, 35.79, 24.55, 14.51. Analysis, calculated for $C_{21}H_{26}N_2O_2$ (M.W. 338.45): C, 74.53; H, 7.74: N, 8.28%. Found: C, 74.49; H, 7.76; N, 8.35%.

***Preparation of* H_2EtSLPNDM**

Procedure as for H_2SALEN, by condensing 2–hydroxypropiophenone with 2,2–dimethyl–1,3–propanediamine.

^{1}H N.M.R ($CDCl_3$) δ/ppm: 1.14–1.20, t, 6H; 1.23, s, 6H; 2.72–2.88, q, 4H; 3.55, s, 4H; 6.72–7.49, m, 8H; 12.95, s, 2H. ^{13}C N.M.R ($CDCl_3$) δ/ppm: 177.20, 165.00, 132.50, 127.80, 118.90, 117.00, 116.80, 56.32, 35.60, 24.50, 20.90, 11.50. Analysis, calculated for $C_{23}H_{30}N_2O_2$ (M.W. 366.5): C, 75.38; H, 8.25: N, 7.64%. Found: C, 75.32; H, 8.24; N, 7.73%.

***Preparation of* H_2PhSLPNDM**

Procedure as for H_2SALEN, by condensing 2–hydroxybenzophenone with 2,2–dimethyl–1,3–propanediamine.

^{1}H N.M.R ($CDCl_3$) δ/ppm: 1.03, s, 6H; 3.22, s, 4H; 6.60–7.45, m, 18H; 14.11, s, 2H.

^{13}C N.M.R ($CDCl_3$) δ/ppm: 174.71, 163.27, 133.78, 132.34, 131.37, 128.84, 128.63, 127.08, 119.66, 117.79, 117.16, 59.94, 36.15, 24.42. Analysis, calculated for $C_{31}H_{30}N_2O_2$ (M.W. 462.59): C, 80.49; H, 6.54: N, 6.06%. Found: C, 79.97; H, 6.49; N, 6.03%.

***Preparation of* H_2CycH**

Procedure as for H_2SALEN, by condensing salicylaldehyde with *trans*–1,2–diaminocyclohexane.

^{1}H N.M.R ($CDCl_3$) δ/ppm: 1.46–1.97, m, 8H; 3.29–3.33, m, 2H; 6.79–7.26, m, 8H; 8.26, s, 2H; 13.34, s, 2H. ^{13}C N.M.R ($CDCl_3$) δ/ppm: 164.51, 160.77, 131.97, 118.40, 116.57, 72.41, 32.89, 23.98. Analysis, calculated for $C_{20}H_{22}N_2O_2$ (M.W. 322.41): C, 74.51; H, 6.88: N, 8.69%. Found: C, 74.65; H, 6.88; N, 8.70%.

***Preparation of* H_2DMCycH**

Procedure as for H_2SALEN, by condensing 2–hydroxyacetophenone with *trans*–1,2–diaminocyclohexane.

^{1}H N.M.R ($CDCl_3$) δ/ppm: 1.45–1.99, m, 8H; 2.29, s, 6H; 3.90, m, 2H; 6.68–7.41, m, 8H; 13.40, s, 2H. ^{13}C N.M.R ($CDCl_3$) δ/ppm: 170.75, 163.58, 132.29, 128.30, 117.04, 62.85, 32.27, 24.10, 14.30. Analysis, calculated for $C_{22}H_{26}N_2O_2$ (M.W. 350.46): C, 75.40; H, 7.48: N, 7.99%. Found: C, 75.19; H, 7.53; N, 8.03%.

***Preparation of* H_2EtCycH**

Procedure as for H_2SALEN, by condensing 2–hydroxypropiophenone with *trans*–1,2–diaminocyclohexane.

^{1}H N.M.R ($CDCl_3$) δ/ppm: 1.16–1.22, t, 6H; 1.46–1.95, m, 8H; 2.70–2.81, q, 4H; 3.86–3.90, m, 2H; 6.68, m, 8H; 13.24, s, 2H. ^{13}C N.M.R ($CDCl_3$) δ/ppm: 175.74, 164.53, 132.26, 128.21, 118.77, 117.41, 116.92, 62.29, 32.77, 24.11, 20.67, 12.64. Analysis, calculated for $C_{24}H_{30}N_2O_2$ (M.W. 378.51): C, 76.16; H, 7.99: N, 7.40%. Found: C, 75.14; H, 7.90; N, 7.46%.

***Preparation of* H_2PhCycH**

Procedure as for H_2SALEN, by condensing 2–hydroxybenzophenone with *trans*–1,2–diaminocyclohexane.

^{1}H N.M.R ($CDCl_3$) δ/ppm: 1.09–1.79, m, 8H; 3.44–3.57, m, 2H; 6.61–7.53, m, 18H; 14.50, s, 2H. ^{13}C N.M.R ($CDCl_3$) δ/ppm: 173.59, 162.75, 133.79, 132.13, 131.73,

129.02, 128.75, 128.22, 128.08, 126.67, 119.89, 117.63, 117.28, 64.66, 32.36, 23.71. Analysis, calculated for $C_{32}H_{30}N_2O_2$ (M.W. 474.6): C, 80.98; H, 6.37: N, 5.90%. Found: C, 80.76; H, 6.38; N, 5.92%.

General Method for the Preparation of* [M(L)Cl$_2$(THF)] *and* [M(L)Cl$_2$] *Complexes (H_2L = tetradentate Schiff base ligand)

$$H_2L + 2\,NaH \longrightarrow Na_2L + 2\,H_2$$

$$Na_2L + MCl_4(THF)_2 \longrightarrow [M(L)Cl_2] + 2\,NaCl$$

To a solution of the ligand (0.5 g, 1 eq) in tetrahydrofuran (THF, 50 cm^3) was added slowly sodium hydride (2 eq). The suspension was stirred until the evolution of H_2 was complete, then refluxed for 2 h. The solution/suspension was allowed to cool to room temperature, cooled to –78 °C, then a solution of [$MCl_4(THF)_2$] (M = Ti, Zr, Hf 1 eq) in THF (50 cm^3) was added. The resultant suspension was stirred at 50 °C for 5 h, then filtered hot through a fine filter stick. The filtrate was evaporated to dryness, the solid was washed with hot toluene to remove any THF (Yield = 40%). A greater yield can be obtained by extracting the solid containing NaCl.

***Preparation of* [Ti(DMSALEN)Cl$_2$]**

^{1}H N.M.R (CD_2Cl_2) δ/ppm: 2.66, s, 6H; 4.26, s, 4H; 6.84–6.87, dd, 2H; 7.04–7.08, dt, 2H; 7.46–7.52, dt, 2H; 7.72–7.75, dd, 2H. ^{13}C N.M.R (CD_2Cl_2) δ/ppm: 170.11, 161.87, 134.82, 131.26, 127.68, 122.69, 116.54, 54.47, 19.66 Analysis, calculated for $C_{18}H_{18}N_2O_2TiCl_2$ (M.W. 413.14): C, 52.33; H, 4.39; N, 6.78%. Found: C, 52.69; H, 4.42; N, 6.81%.

***Preparation of* [Ti(DMSALEN)Cl$_2$].THF**

^{1}H N.M.R ($CDCl_3$) δ/ppm: 1.85, THF, 4H; 2.63, s, 6H; 3.74, THF, 4H; 4.21, s, 4H; 6.84–6.8, dd, 2H; 7.01–7.08, dt, 2H; 7.46–7.51, dt, 2H; 7.72–7.76, dd, 2H.

^{13}C N.M.R ($CDCl_3$) δ/ppm: 170.14, 161.82, 134.80, 131.22, 127.69, 122.71, 116.54, 54.46, 19.66 Analysis, calculated for $C_{22}H_{26}N_2O_3TiCl_2$ (M.W. 485.25): C, 54.46; H, 5.40; N, 5.77%. Found: C, 54.92; H, 5.60; N, 5.60%.

***Preparation of* [Zr(DMSALEN)Cl_2(THF)]**

^{1}H N.M.R (d^6–DMSO) δ/ppm: 1.62, THF, 4H; 2.66, s, 6H; 3.41, THF, 4H; 4.55, s, 4H, 6.99–7.79, m, 8H. Analysis, calculated for $C_{22}H_{26}N_2O_3ZrCl_2$ (M.W. 528.59): C, 49.99; H, 4.96: N, 5.30%. Found: C, 50.16; H, 4.89; N, 5.42%.

***Preparation of* [Zr(DMSALEN)Cl_2]**

^{1}H N.M.R (d^6–DMSO) δ/ppm: 2.61, s, 6H; 4.23, s, 4H; 6.86–6.90, dd, 2H; 6.91–6.97, dt, 2H; 7.44–7.51, dt, 2H; 7.85–7.89, dd, 2H. Analysis, calculated for $C_{18}H_{18}N_2O_2ZrCl_2$ (M.W. 456.48): C, 47.36; H, 3.97: N, 6.14%. Found: C, 47.42; H, 4.08; N, 6.20%.

***Preparation of* [Ti(EtSALEN)Cl_2]**

^{1}H N.M.R (d^6–DMSO) δ/ppm: 1.18–1.27, t, 6H; 3.07–3.20, q, 4H; 4.20, s, 4H; 6.81–6.83, dd, 2H; 7.12–7.19, dt, 2H; 7.55–7.57, dt, 2H; 8.01–8.04, dd, 2H.

^{13}C N.M.R (d^6–DMSO) δ/ppm: 173.66, 161.82, 134.79, 132.06, 125.84, 122.96, 116.37, 52.35, 23.11, 11.39. ^{13}C N.M.R (CD_2Cl_2) δ/ppm: 173.66, 161.82, 134.79, 132.06, 125.84, 122.96, 116.37, 52.35, 23.11, 11.39. Analysis, calculated for $C_{20}H_{22}N_2O_2TiCl_2$ (M.W. 441.19): C, 54.45; H, 5.03; N, 6.35%. Found: C, 54.52; H, 4.99; N, 6.41%.

***Preparation of* [Zr (EtSALEN)Cl_2]**

^{1}H N.M.R (d^6–DMSO) δ/ppm: 1.19–1.22, t, 6H; 3.04–3.10, q, 4H; 4.27, s, 4H; 6.83–6.94, m, 4H; 7.38–7.47, t, 2H; 7.61–7.64, d, 2H. ^{13}C N.M.R (CD_2Cl_2) δ/ppm: 174.29, 162.11, 134.21, 131.72, 124.97, 121.02, 116.89, 52.69, 22.91, 11.53. Analysis, calculated for $C_{20}H_{22}N_2O_2ZrCl_2$ (M.W. 484.53): C, 49.58; H, 4.58; N, 5.78%. Found: C, 49.65; H, 4.49; N, 5.84%.

***Preparation of* [Ti(PhSALEN)Cl_2]**

^{1}H N.M.R (CD_2Cl_2) δ/ppm: 3.72, s, 4H; 6.91–7.05, m, 4H; 7.28–7.36, m, 4H; 7.55–7.61, m, 10H. ^{13}C N.M.R (CD_2Cl_2) δ/ppm: 171.72, 162.63, 135.49, 129.68, 129.38, 128.43, 127.62, 127.32, 126.54, 122.45, 116.36, 54.81. Analysis, calculated for $C_{28}H_{22}N_2O_2TiCl_2$ (M.W. 537.28): C, 62.59; H, 4.13; N, 5.21%. Found: C, 63.02; H, 4.19; N, 5.30%.

***Preparation of* [Zr (PhSALEN)Cl_2]**

^{1}H N.M.R (d^6–DMSO) δ/ppm: 3.63, s, 2H; 3.74, s, 2H; 6.72–6.77, m, 4H; 6.96–7.10, m, 4H; 7.49–7.58, m, 10H. ^{13}C N.M.R (d^6–DMSO) δ/ppm: 172.36, 162.22, 134.60, 130.83, 130.21, 128.81, 128.09, 127.22, 125.01, 121.17, 117.38, 54.38. Analysis, calculated for $C_{28}H_{22}N_2O_2ZrCl_2$ (M.W. 580.62): C, 57.92; H, 3.82; N, 4.82%. Found: C, 57.99; H, 3.79; N, 4.88%.

***Preparation of* [Ti(SLPNDM)Cl_2]**

^{1}H N.M.R ($CDCl_3$) δ/ppm: 1.20, s, 6H; 3.99, d, 4H; 6.83–6.87, dd, 2H; 7.01, 7.08, dt, 2H; 7.48–7.56, m, 4H; 8.26, s, 2H. ^{13}C N.M.R (d^6–DMSO) δ/ppm: 165.23, 160.94, 132.61, 131.33, 119.94, 118.21, 116.35, 68.41, 35.92, 22.36. Analysis, calculated for $C_{19}H_{20}N_2O_2TiCl_2$ (M.W. 427.17): C, 53.42; H, 4.72; N, 6.56%. Found: C, 53.55; H, 4.68; N, 6.62%.

***Preparation of* [Zr(SLPNDM)Cl_2(THF)]**

^{1}H N.M.R ($CDCl_3$) δ/ppm: 1.27, s, 6H; 1.61, THF, 4H; 3.00–3.04, d, 2H; 3.40, THF, 4H; 5.20–5.24, d, 2H; 6.10–6.14, dd, 2H; 6.36–6.42, dt, 2H; 6.78–6.85, dt, 2H; 7.00–7.04, dd, 2H; 8.08, s, 2H. Analysis, calculated for $C_{23}H_{28}N_2O_3ZrCl_2$ (M.W. 542.61): C, 50.91; H, 5.20; N, 5.16%. Found: C, 51.00; H, 5.12; N, 5.21%.

***Preparation of* [Zr(SLPNDM)Cl_2]**

^{1}H N.M.R ($CDCl_3$) δ/ppm: 1.28, s, 6H; 3.00–3.05, d, 2H; 5.20–5.24, d, 2H; 6.11–6.14, dd, 2H; 6.36–6.42, dt, 2H; 6.78–6.85, dt, 2H; 7.00–7.04, dd, 2H; 8.09, s, 2H.

^{13}C N.M.R (d^6–DMSO) δ/ppm: 166.74, 162.13, 132.94, 132.00, 118.72, 118.36, 116.54, 66.02, 34.99, 21.22. Analysis, calculated for $C_{19}H_{20}N_2O_2ZrCl_2$ (M.W. 470.51): C, 48.50; H, 4.28; N, 5.95%. Found: C, 48.59; H, 4.21; N, 6.02%.

Preparation of **[Hf(SLPNDM)Cl_2]**

^{1}H N.M.R (d^6–DMSO) δ/ppm: 0.94, s, 6H; 3.76, s, 4H; 6.73–6.76, d, 2H; 6.96–7.02, t, 2H; 7.56–7.61, t, 2H; 7.96–7.99, d, 2H; 8.55, s, 2H. ^{13}C N.M.R (d^6–DMSO) δ/ppm: 168.36, 160.76, 135.78, 132.73, 122.19, 119.20, 117.28, 72.39, 36.71, 22.70. Analysis, calculated for $C_{19}H_{20}N_2O_2HfCl_2$ (M.W. 557.78): C, 40.91; H, 3.61; N, 5.02%. Found: C, 40.95; H, 3.53; N, 5.11%.

Preparation of **[Ti(DMSLPNDM)Cl_2]**

^{1}H N.M.R ($CDCl_3$) δ/ppm: 1.14, s, 6H; 2.62, s, 6H; 4.28, s, 4H; 6.85–6.86, dd, 2H; 7.03–7.09, dt, 2H; 7.47–7.51, dt, 2H; 7.70–7.71, dd, 2H. ^{13}C N.M.R (d^6–DMSO) δ/ppm: 172.06, 163.54, 132.38, 129.10, 118.98, 118.43, 116.82, 56.50, 3459, 23.45, 12.98. Analysis, calculated for $C_{21}H_{24}N_2O_2TiCl_2$ (M.W. 455.22): C, 55.41; H, 5.31; N, 6.15%. Found: C, 55.44; H, 5.23; N, 6.24%.

Preparation of **[Zr(DMSLPNDM)Cl_2]**

^{1}H N.M.R (d^6–DMSO) δ/ppm: 1.11, s, 6H; 2.44, s, 6H; 3.60, s, 4H; 6.77–6.83, t, 2H; 6.88–6.91, d, 2H; 7.32–7.40, t, 2H; 7.63–7.66, d, 2H. ^{13}C N.M.R (d^6–DMSO) δ/ppm: 173.62, 162.02, 132.95, 128.66, 123.40, 119.21, 116.99, 55.95, 36.49, 23.27, 14.81. Analysis, calculated for $C_{21}H_{24}N_2O_2ZrCl_2$ (M.W. 498.56): C, 50.59; H, 4.85; N, 5.62%. Found: C, 50.62; H, 4.78; N, 5.64%.

Preparation of **[Hf(DMSLPNDM)Cl_2]**

^{1}H N.M.R (d^6–DMSO) δ/ppm: 1.10, s, 6H; 2.42, s, 6H; 3.58, s, 4H6.77–6.83, t, 2H; 6.86–6.89, d, 2H; 7.28–7.34, t, 2H; 7.65–7.67, d, 2H. ^{13}C N.M.R (d^6–DMSO) δ/ppm: 174.62, 162.66, 133.05, 128.99, 125.40, 119.60, 117.39, 56.85, 36.09, 23.66, 15.51. Analysis, calculated for $C_{21}H_{24}N_2O_2HfCl_2$ (M.W. 585.83): C, 43.06; H, 4.13; N, 4.78%. Found: C, 43.10; H, 4.15; N, 4.86%.

***Preparation of* [Ti(EtSLPNDM)Cl_2]**

^{1}H N.M.R ($CDCl_3$) δ/ppm: 1.14, s, 6H; 1.15–1.19, t, 6H; 3.02–3.06, q, 4H; 4.25, s, 4H; 6.84–6.88, dd, 2H; 7.03–7.09, dt, 2H; 7.46–7.53, dt, 2H; 7.72–7.76, dd, 2H. Analysis, calculated for $C_{23}H_{28}N_2O_2TiCl_2$ (M.W. 483.27): C, 57.16; H, 5.84; N, 5.80%. Found: C, 57.24; H, 5.76; N, 5.91%.

***Preparation of* [Zr(EtSLPNDM)Cl_2]**

^{1}H N.M.R (d^6–DMSO) δ/ppm: 1.00, s, 6H; 1.08–1.13, t, 6H; 2.85–2.91, q, 4H; 3.65, s, 4H; 6.78–6.85, t, 2H; 6.89–6.93, d, 2H; 7.30–7.36, t, 2H; 7.62–7.65, d, 2H. Analysis, calculated for $C_{23}H_{28}N_2O_2ZrCl_2$ (M.W. 526.61): C, 52.46; H, 5.36; N, 5.32%. Found: C, 52.55; H, 5.34; N, 5.39%.

***Preparation of* [Hf(EtSLPNDM)Cl_2]**

^{1}H N.M.R (d^6–DMSO) δ/ppm: 1.06–1.12, t, 6H; 1.12, s, 6H; 2.81–2.90, q, 4H; 3.60, s, 4H; 6.76–6.82, dt, 2H; 6.83–6.86, dd, 2H; 7.27–7.34, dt, 2H; 7.61–7.65, dd, 2H. ^{13}C N.M.R (d^6–DMSO) δ/ppm: 188.19, 163.60, 132.91, 128.86, 118.26, 117.34, 56.87, 35.69, 23.67, 21.23, 11.61. Analysis, calculated for $C_{23}H_{28}N_2O_2HfCl_2$ (M.W. 613.88): C, 45.00; H, 4.60; N, 4.56%. Found: C, 45.09; H, 4.54; N, 4.64%.

***Preparation of* [Ti(PhSLPNDM)Cl_2]**

^{1}H N.M.R (d^6–DMSO) δ/ppm: 0.98, s, 6H; 3.27, s, 4H; 6.70–6.75, m, 4H; 7.05–7.53, m, 14H. ^{13}C N.M.R (d^6–DMSO) δ/ppm: 174.24, 164.27, 134.18, 132.34, 131.37, 128.84, 128.63, 127.08, 119.66, 117.79, 117.16, 59.94, 35.14, 22.41. Analysis, calculated for $C_{31}H_{28}N_2O_2TiCl_2$ (M.W. 579.36): C, 64.27; H, 4.87; N, 4.84%. Found: C, 64.83; H, 4.78; N, 4.99%.

***Preparation of* [Zr(PhSLPNDM)Cl_2]**

^{1}H N.M.R (d^6–DMSO) δ/ppm: 0.95, s, 6H; 3.16, s, 4H; 6.66–6.69, m, 4H; 6.91–6.94, d, 2H; 7.14–7.18, m, 4H; 7.28–7.34, m, 2H; 7.45–7.49, 6H. ^{13}C N.M.R (d^6–DMSO) δ/ppm: 173.27, 160.18, 133.21, 132.65, 131.14, 128.73, 128.59, 128.00,

126.89, 125.39, 119.39, 117.67, 35.99, 23.83, 20.96. Analysis, calculated for $C_{31}H_{28}N_2O_2ZrCl_2$ (M.W. 622.70): C, 59.79; H, 4.53; N, 4.50%. Found: C, 58.78; H, 4.84; N, 4.96%.

***Preparation of* [Hf(PhSLPNDM)Cl_2]**

^{1}H N.M.R (d^6–DMSO) δ/ppm: 0.96, s, 6H; 3.14, s, 4H; 6.66–6.68, m, 4H; 6.89–7.49, m, 14H. ^{13}C N.M.R (d^6–DMSO) δ/ppm: 174.73, 162.43, 133.21, 132.76, 131.24, 129.31, 128.89, 128.28, 127.15, 125.39, 119.39, 117.67, 35.99, 24.03, 21.14. Analysis, calculated for $C_{31}H_{28}N_2O_2HfCl_2$ (M.W. 709.97): C, 52.44; H, 3.98; N, 3.95%. Found: C, 52.51; H, 3.96; N, 4.08%.

***Preparation of* [Ti(CycH)Cl_2]**

^{1}H N.M.R (d^6–DMSO) δ/ppm: 1.37–1.90, m, 6H; 2.16–2.29, m, 2H; 3.85, s, 1H; 4.64, s, 1H; 6.80–6.83, d, 2H; 6.90–6.96, t, 2H; 7.56–7.96, m, 4H; 8.75, s, 1H; 9.13, s, 1H. Analysis, calculated for $C_{20}H_{20}N_2O_2TiCl_2$ (M.W. 439.18): C, 54.70; H, 4.59; N, 6.38%. Found: C, 54.91; H, 4.52; N, 6.44%.

***Preparation of* [Zr(CycH)Cl_2]**

^{1}H N.M.R (d^6–DMSO) δ/ppm: 1.33–1.91, m, 6H; 2.10–2.15, d, 1H; 2.38–2.43, d, 1H; 3.95, s, 1H; 4.55, s, 1H; 6.84–6.87, dd, 2H; 6.89–6.96, dt, 2H; 7.48–7.55, m, 4H; 8.66, s, 1H; 9.05, s, 1H. Analysis, calculated for $C_{20}H_{20}N_2O_2ZrCl_2$ (M.W. 482.52): C, 49.78; H, 4.18; N, 5.81%. Found: C, 49.90; H, 4.11; N, 5.88%.

***Preparation of* [Ti(DMCycH)Cl_2]**

^{1}H N.M.R (d^6–DMSO) δ/ppm: 1.30–2.31, broad m, 8H; 2.77–3.15, m, 6H; 4.50–4.90, broad, 2H; 6.85–7.95, m, 8H. Analysis, calculated for $C_{22}H_{24}N_2O_2TiCl_2$ (M.W. 467.23): C, 56.55; H, 5.18; N, 6.00%. Found: C, 65.58; H, 5.23; N, 5.95%.

***Preparation of* [Zr(DMCycH)Cl_2]**

^{1}H N.M.R (d^6–DMSO) δ/ppm: 1.04–2.28, m, 8H; 2.77–3.02, m, 6H; 3.97–5.08, broad q, 2H; 6.81–7.96, m, 8H. Analysis, calculated for $C_{22}H_{24}N_2O_2ZrCl_2$ (M.W. 510.57): C, 51.75; H, 4.74; N, 5.49%. Found: C, 51.88; H, 4.69; N, 5.57%.

***Preparation of* [Ti(EtCycH)Cl_2]**

^{1}H N.M.R (d^6–DMSO) δ/ppm: 0.82–1.05, broad m, 6H; 1.22–2.16, broad m, 8H; 2.91–3.07, broad m, 4H; 4.22–4.79, broad m, 2H; 6.93–7.50, m, 8H. Analysis, calculated for $C_{24}H_{28}N_2O_2TiCl_2$ (M.W. 495.28): C, 58.20; H, 5.70; N, 5.66%. Found: C, 58.18; H, 5.66; N, 5.73%.

***Preparation of* [Zr(EtCycH)Cl_2]**

^{1}H N.M.R (d^6–DMSO) δ/ppm: 0.86–1.07, m, 6H; 1.34–2.27, m, 8H; 2.93–3.45, broad m, 4H; 4.24, broad s, 1H; 4.71, broad s, 1H; 6.75–7.84, m, 8H. Analysis, calculated for $C_{24}H_{28}N_2O_2ZrCl_2$(M.W. 538.62): C, 53.52; H, 5.24; N, 5.20%. Found: C, 53.48; H, 5.30; N, 5.26%.

***Preparation of* [Ti(PhCycH)Cl_2]**

^{1}H N.M.R (d^6–DMSO) δ/ppm: 1.03–1.73, broad m, 8H; 3.51, broad d, 2H; 6.60–6.71, d+t, 4H; 6.98–7.01, d, 2H; 7.30–7.35, m, 6H; 7.60–7.63, m, 6H. Analysis, calculated for $C_{32}H_{28}N_2O_2TiCl_2$ (M.W. 591.37): C, 64.99; H, 4.77; N, 4.74%. Found: C, 65.07; H, 4.68; N, 4.81%.

***Preparation of* [Zr(PhCycH)Cl_2]**

^{1}H N.M.R (d^6–DMSO) δ/ppm: 0.89–1.76, broad m, 8H; 3.38–3.41, broad d, 2H; 6.56–6.60, dd, 2H; 6.63–6.68, dt, 2H; 7.24–7.30, m, 6H; 7.58–7.61, m, 6H. Analysis, calculated for $C_{32}H_{28}N_2O_2ZrCl_2$ (M.W. 634.71): C, 60.56; H, 4.45; N, 4.41%. Found: C, 60.62; H, 4.41; N, 4.46%.

Table 2.17 Summary of infra–red band frequencies of selected Group 4 tetradentate Schiff base complexes

Compound	Infra–red bands (cm^{-1})
$[Ti(EtSALEN)Cl_2]$	1622, 1505, 1417, 1377, 1339, 1317, 1209, 1160, 1098, 1039, 933, 862, 763, 719, 671, 608, 521, 441, 310–340.
$[Zr(EtSALEN)Cl_2]$	1602, 1554, 1509, 1456, 1416, 1377, 1341, 1322, 1254, 1209, 1161, 1142, 1097, 1039, 933, 860, 764, 718, 674, 637, 595, 524, 436, 402, 280–310.
$[Ti(PhSALEN)Cl_2]$	1593, 1546, 1504, 1466, 1412, 1377, 1328, 1242, 1222, 1155, 1122, 1077, 1024, 1000, 920, 855, 762, 703, 667, 637, 604, 502, 465, 419, 320–340.
$[Zr(PhSALEN)Cl_2]$	1597, 1546, 1506, 1461, 1416, 1377, 1244, 1222, 1156, 1077, 1023, 851, 763, 721, 702, 635, 596, 497, 418, 280–305.
$[Hf(SLPNDM)Cl_2]$	1589, 1542, 1505, 1465, 1417, 1377, 1331, 1316, 1259, 1123, 1077, 1039, 1026, 1000, 951, 901, 881, 848, 774, 717, 703, 685, 634, 295.
$[Hf(DMSLPNDM)Cl_2]$	1595, 1541, 1504, 1464, 1412, 1377, 1331, 1316, 1259, 1225, 1158, 1123, 1077, 1039, 1026, 1000, 951, 901, 881, 774, 717, 703, 685, 300.
$[Ti(EtSLPNDM)Cl_2]$	1598, 1551, 1505, 1496, 1418, 1377, 1337, 1304, 1249, 1217, 1162, 1139, 1097, 1058, 1040, 935, 865, 764, 720, 685, 597, 522, 416, 320, 340.
$[Zr(EtSLPNDM)Cl_2]$	1602, 1554, 1509, 1456, 1419, 1377, 1338, 1312, 1250, 1216, 1163, 1142, 1097, 1059, 1041, 935, 855, 765, 721, 686, 593, 521, 452, 417, 300.
$[Ti(PhSLPNDM)Cl_2]$	1589, 1545, 1504, 1464, 1412, 1377, 1331, 1316, 1259, 1225, 1158, 1123, 1077, 1039, 1026, 1000, 951, 901, 881, 848, 774, 717, 703, 685, 634, 340.
$[Zr(PhSLPNDM)Cl_2]$	1592, 1548, 1507, 1480, 1416, 1377, 1319, 1280, 1261,

	1224, 1159, 1123, 1077, 1065, 1040, 951, 900, 885, 772, 751, 690, 595, 526, 502, 491, 464, 335, 300.
$[Ti(CycH)Cl_2]$	1646, 1599, 1550, 1466, 1377, 1277, 1217, 1156, 1123, 1080, 1032, 958, 907, 871, 833, 807, 759, 733, 664, 649, 605, 571, 470, 432, 330–350.
$[Zr(CycH)Cl_2]$	1641, 1605, 1549, 1475, 1413, 1377, 1352, 1280, 1216, 1157, 1126, 1078, 1031, 958, 930, 907, 871, 805, 758, 734, 697, 648, 596, 568, 548, 465, 431, 419, 320.
$[Ti(DMCycH)Cl_2]$	1598, 1550, 1504, 1463, 1417, 1377, 1317, 1246, 1220, 1162, 1089, 1072, 1034, 960, 870, 753, 686, 598, 553, 517, 486, 435, 330.
$[Zr(DMCycH)Cl_2]$	1601, 1551, 1505, 1462, 1418, 1377, 1318, 1247, 1220, 1163, 1072, 1034, 976, 868, 752, 593, 551, 462, 431, 305.
$[Ti(EtCycH)Cl_2]$	1597, 1548, 1505, 1462, 1417, 1377, 1310, 1246, 1208, 1162, 1093, 1061, 1041, 851, 762, 724, 683, 596, 529, 424, 380.
$[Zr(EtCycH)Cl_2]$	1602, 1552, 1511, 1461, 1419, 1377, 1338, 1318, 1247, 1209, 1163, 1083, 1061, 1042, 911, 850, 761, 724, 681, 591, 551, 529, 512, 425, 320, 310.
$[Ti(PhCycH)Cl_2]$	1593, 1543, 1506, 1462, 1416, 1377, 1337, 1317, 1248, 1219, 1154, 1120, 1075, 1040, 1001, 953, 900, 845, 765, 725, 702, 633, 595, 510, 451, 425, 404, 345.
$[Zr(PhCycH)Cl_2]$	1595, 1544, 1510, 1479, 1461, 1417, 1377, 1338, 1320, 1250, 1219, 1156, 1122, 1066, 1040, 1001, 952, 900, 843, 764, 724, 702, 682, 632, 589, 507, 405, 315, 305.

Molecular modelling studies

Setup procedure.

All the molecular mechanics and dynamics calculations described throughout this work were performed using the commercially available package *HYPERCHEM* (version 4.5).[135] The systems studied were initially entered into the program as 2-dimensional representations, which were then converted into 3-dimentional models suitable for molecular mechanics calculations using the program's model generator. In creating this 3D model the program seeks to produce a structure in which all the bond lengths and bond angles are at their equilibrium positions as specified in the forcefield chosen. This is achieved by first assigning each atom within the molecule a label, known as an *atom type*, which defines both the constituent element and the nature of the bonding to it. These atom types correspond to the descriptions of bonds, angles and interactions contained within the forcefield. For example, if the carbon atoms of a benzene ring are assigned the label "**ca**", to signify an aromatic carbon atom, then the corresponding forcefield entry referring to a carbon-carbon bond in benzene would be, "ca-ca, 8.065, 1.392, 0.000" describing the bond type, force constant (mdyne $Å^{-1}$), equilibrium bond length (Å), and bond dipole (Debyes) respectively.

For this study the MM+ forcefield was chosen as it was developed to accurately reproduce the interactions within small organic molecules such as the ligands discussed in this study. However, MM+ does not contain any parameters for the bonding of transition metal ions, and so before beginning the molecular mechanics calculations the forcefield supplied was modified using the parameters listed in Table 2.17, to take account of the desired metal-ligand bonding interactions.

Table 2.18 List of the parameters used when customising the MM+ forcefield contained within HYPERCHEM to incorporate the desired transition metal ion-ligand interactions

Atom type 1	Atom type 2	Bond-stretch force constant (mdyne Å^{-1})	Strain free bond length (Å)	Bond dipole (Debyes)
ti4	n3	2.250	2.296	0.000
ti4	na	2.250	2.137	0.000
ti4	o2	2.250	1.873	0.000
ti4	cl	2.250	2.305	0.000

The customisation of the existing MM+ forcefield first required entering the new atom types **ti4** (for Ti^{4+}) into the list of recognised MM+ atom types contained within the file **mmptyp.txt**. This achieved, it was then possible to add the list of bond stretch parameters in **Table 2.19** to the file **mmpstr.txt**, before recompiling the binary forcefield utilised by the program using the respective command in the *HYPERCHEM* setup menu.

Molecular Mechanics calculations.

Despite the fact that when building the 3-dimensional model all the bond lengths and angles are set to their equilibrium positions, the exclusion of any steric or electrostatic interactions in this process means that the structure generated is not that with overall minimum energy. Structural refinement utilises a procedure known as geometry optimisation, which seeks to find the geometry where the total energy of the system is at a minimum. These geometry optimisations utilised the Polak–Ribiere conjugate gradient algorithm, a first order minimiser. The advantage of a conjugate gradient method is that since both the current potential energy gradient and the previous search direction are used, it ensures the future search direction moves directly towards the minimum energy point, as opposed to cycling around the top of the

potential energy well. It also contains a scaling factor to determine the step size which is important in ensuring that the calculation does not pass continually over the minimum energy conformation without ever reaching it.[135] The geometry optimisation procedure was stopped when the calculated potential energy surface had a gradient of < 0.01 kcal $Å^{-1}$ mol^{-1}

Molecular Dynamics calculations.

Molecular dynamics simulations usually begin with a molecular structure refined by geometry optimisation, but without atomic velocities. Therefore, before starting a molecular dynamics simulation from this static structure, the program assigns atomic velocities which are realistic for the molecular system at the designated starting temperature. For these simulations this was set to 0 K. The calculation then proceeds to adjust the velocities as it elevates the temperature from the initial value (0K) to the preset simulation temperature (T_o, 4 000 K). Heating could take place in a single temperature step (τ), but it is better to heat in small increments since the system will then require less time at the simulation temperature to reach equilibrium. In all cases discussed here, 2000 temperature steps were allowed for the heating process (*i.e.* 2 K per step).

After the heating and equilibration processes it is necessary to cool the system back to 0 K. Cooling, called simulated annealing, serves to direct the newly determined high energy state towards a more stable conformation. Furthermore, since this high energy system can overcome all potential energy barriers, it is able to move the molecule into a lower energy conformation than the one obtained initially by geometry optimisation. As in the initial heating process, 2000 temperature steps were allowed for cooling. In essence, molecular dynamics simulations should provide the system with sufficient kinetic energy to raise it above all potential energy barriers and allow, on cooling, the system to adopt the global minimum energy conformation.[120] However, in reality the structure produced following a molecular dynamics simulation is, like that following the initial model build, not at a true minimum energy conformation and requires subsequent geometry optimisation. For all systems, this

cycle of molecular mechanics and dynamics simulations was performed three times on the lowest energy structure determined to ensure that the global minimum had indeed been attained.[136]

CHAPTER 3

Reactions of Group 4 Tetradentate Schiff Base Complexes

CHAPTER 3 Reactions of Group 4 Tetradentate Schiff Base Complexes

Introduction

A brief outline of Ziegler-Natta catalysis together with the possible reaction pathway for polymerisation of alkenes was given in Chapter 1. The use of MAO, formulated as $[MeAlO]_x$ as the initiator in such catalytic processes is very common, although the precise mechanism by which the MAO functions is not understood.

Another important factor associated with the potential activity of a catalyst is the reactivity of, and the stereochemical arrangement around, the metal centre. The reactivity is believed to be enhanced as the metal atom becomes more electrophilic in character, and cationic metal complexes are especially reactive. The more reactive the metal centre the better the potential for catalysis, because it is believed that at some stage the MAO has to alkylate at the metal centre for polymerisation to occur.

This chapter gives information on how Group 4 tetradentate Schiff base complexes will possibly behave in a polymerisation reaction. The aims of this part of the work are (a) to provide information on the reactivity of the metal centre within these complexes, and (b) if it is reactive, to clarify the type of reaction occurring at the metal centre. It will be of interest to discover if the Group 4 metals all behave in the same manner, as well as discovering whether the ligand is stable under the various reaction conditions. (c) it is hoped that an insight may be gained into the function of MAO in the polymerisation reaction. This will be achieved by observing how these complexes react with trimethyl aluminium, if at all, since free $AlMe_3$ is always present in the commercial MAO, and both $AlMe_3$ and MAO contain the reactive Al–Me bond. Here the aluminium alkyl is represented as $AlMe_3$ for simplicity rather than the actual dimeric form Al_2Me_6. It is believed that by characterising the products of these reactions an indication of how Group 4 tetradentate Schiff base complexes interact with MAO during a polymerisation reaction will be attained.

Reactions of $[M(L)Cl_2]$ (M = Ti, Zr; L = DMSALEN, EtSALEN, PhSALEN) complexes with trimethyl aluminium

It is known that MAO contains a small percentage of free trimethyl aluminium, but since up to 1000 molar excesses of MAO are used in a polymerisation reaction this could amount to a significant amount of $AlMe_3$. With this in mind, it was decided to react the Group 4 tetradentate Schiff base complexes with an aluminium alkyl in order to gain an insight into the reactions, if any, that may be occurring with the Schiff base catalysts in the polymerisation reaction process.

Initial studies were concentrated on the reaction of $[M(L)Cl_2]$ species with trimethylaluminium using a 1:1 molar ratio. The chosen solvent for these reactions was toluene because this is the solvent which we have used in the polymerisation studies. Due to the extreme reactivity of both compounds, precautions were taken to ensure that the solvent was dry, and that the reactions were performed under an inert, dry argon atmosphere. The Group 4 tetradentate Schiff base complexes initially chosen for these studies were based on the SALEN type. The reason for this choice was that SALEN type ligands are relatively simple ligands with the least complicated N.M.R spectra, and this should allow easier assignments of the spectra of the complexes produced from these reactions. It was believed that the most probable reaction would be alkylation of the metal with the loss of one or two chlorine atoms (Scheme 3.1), and also a possible interaction of the metal alkyl with the imine bonds in the ligand.

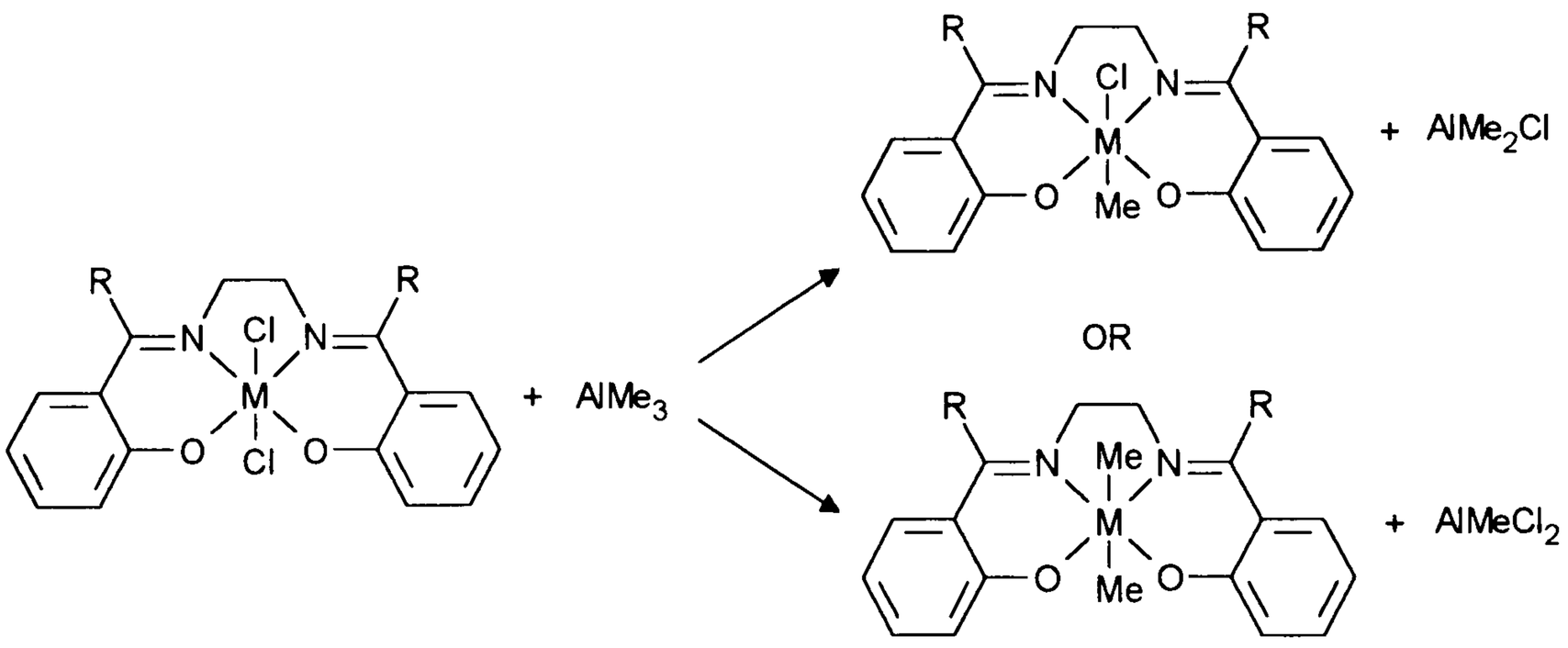

Scheme 3.1 The postulated possible reaction scheme for the action of $AlMe_3$ on Schiff base complexes. (M = Group 4 element; R = Me = DMSALEN, R = Et = EtSALEN, R = Ph = PhSALEN)

However, in these 1:1 reaction studies no alkylation was seen, and in each instance all that was recovered was the starting dihalide complex, $[M(L)Cl_2]$. No reaction was seen under a variety of reaction temperatures ranging from 0 °C to 120 °C. It was believed that the major factor in preventing such a reaction from occurring was the almost complete insolubility of the dihalide complex. This insolubility of the dihalide complex is also seen with other solvents, and therefore it was decided to persevere with toluene since it is an inert solvent and is essentially non–polar.

From these studies it was hoped that an excess of metal alkyl might assist in the solubility of the metal complex since we had observed in some earlier experiments that the addition of a slight excess of $AlMe_3$ over the 1:1 ratio did seem to cause some complex to dissolve. Therefore, it was decided to repeat the reactions using a 1:2 molar ratio of complex:$AlMe_3$. Again it was envisaged that these reactions would produce alkylation at the metal, M. The reactions were again carried out with toluene as the reaction solvent to mimic the reaction conditions in the polymerisation reaction. The two mole equivalents of $AlMe_3$ were slowly added to a suspension of $[M(L)Cl_2]$ (M = Ti or Zr) at 0 °C. On completion of the addition of 2 moles of $AlMe_3$ the complex had completely dissolved to produce a deep red (titanium) or orange (zirconium) solution. After a further 1 h at 0 °C the solution was filtered to remove any impurities, and the filtrate was evaporated to dryness to yield a orange/brown solid. Analyses (^1H and ^{13}C N.M.R., IR spectroscopy) of these solids revealed that the same type of reaction product, independent of which ligand or which metal is used in the reaction, is recovered indicating that the same type of reaction is proceeding in all cases. However, from the spectroscopic analyses, discussed in detail below, it is not believed that alkylation of the metal, M, occurs but instead the complex remains intact and the aluminium trimethyl adds in a different way to the complex. This is not the expected reaction pathway, but it does suggest that these complexes will not be destroyed by the harsh conditions of the polymerisation reaction. From the spectroscopic analyses of the products, it was concluded that there are three possible structures formed (Figure 3.1).

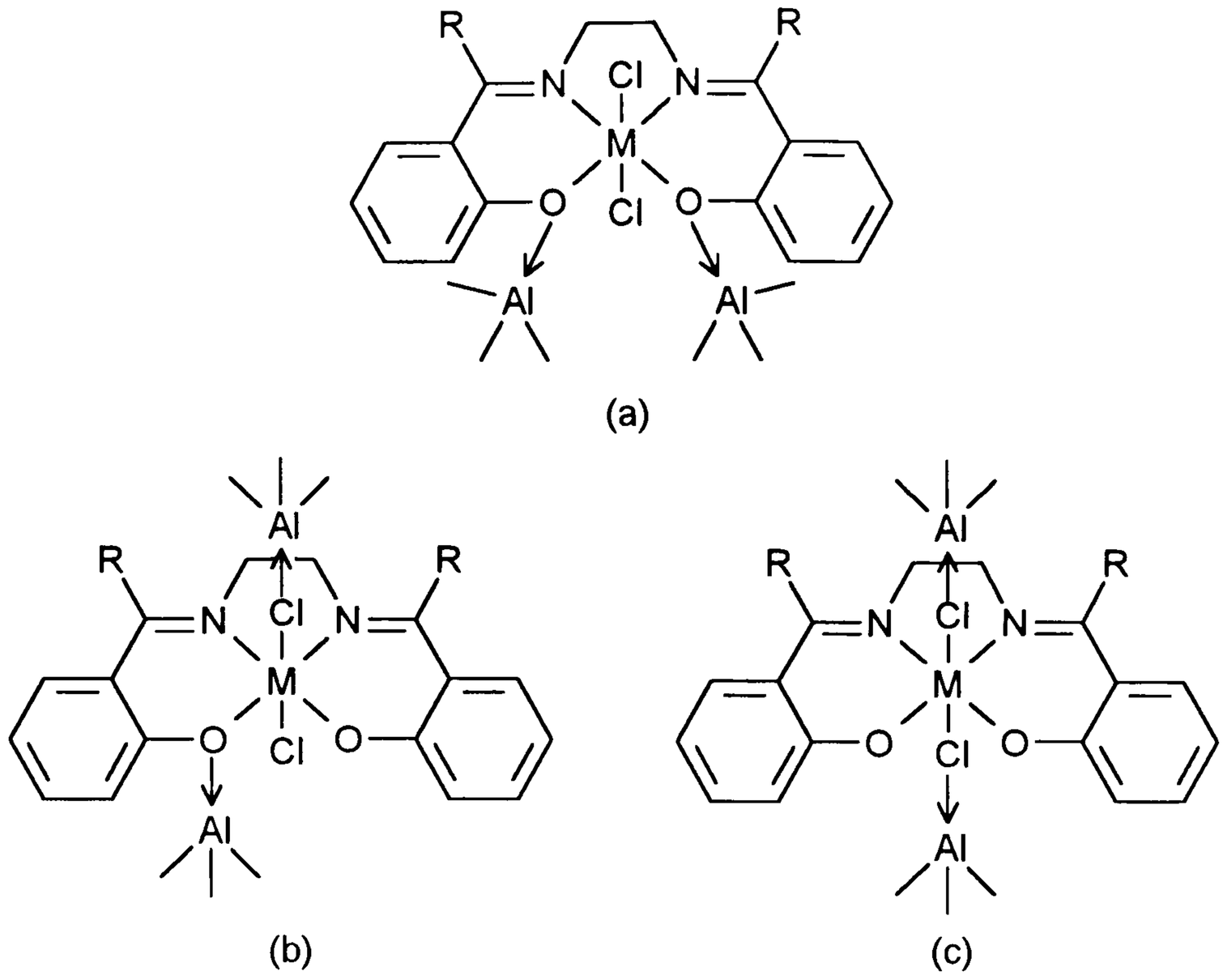

Figure 3.1 Showing the possible reaction products from the reaction of $[M(L)Cl_2]$ (M = Ti, Zr; L = DMSALEN, EtSALEN) with $2AlMe_3$

The ^1H N.M.R evidence suggests that the complex shown in Figure 3.1(b) is the most probable structure because two distinct Al–Me resonances are seen in their spectra. In the complexes (a) and (c) only one aluminium–methyl resonance would be expected due to the symmetry of these compounds.

The products are very air–sensitive, fuming in the air, and as a result the handling of these compounds is extremely difficult. They have been found to be soluble in most solvents, which enables a good characterisation of the complexes by N.M.R. spectroscopy.

The findings described above contrast with recent work published by Walker *et al*[137] in which they describe the reaction of $[Ti(SALEN)Cl_2]$ and $AlMe_3$ in toluene/hexane (1:1 ratio) affording the Ti(III) hetero–bimetallic $[Ti\{(\mu–Cl)(AlMe_2)\}\{(\mu–Cl)(AlMe_2X)\}(SALEN)]$ (X = Me or Cl) and the Ti(IV) $[TiMe\{(\mu–Cl)(AlCl_2Me)\}(SALEN)]$ species (Scheme 3.2).

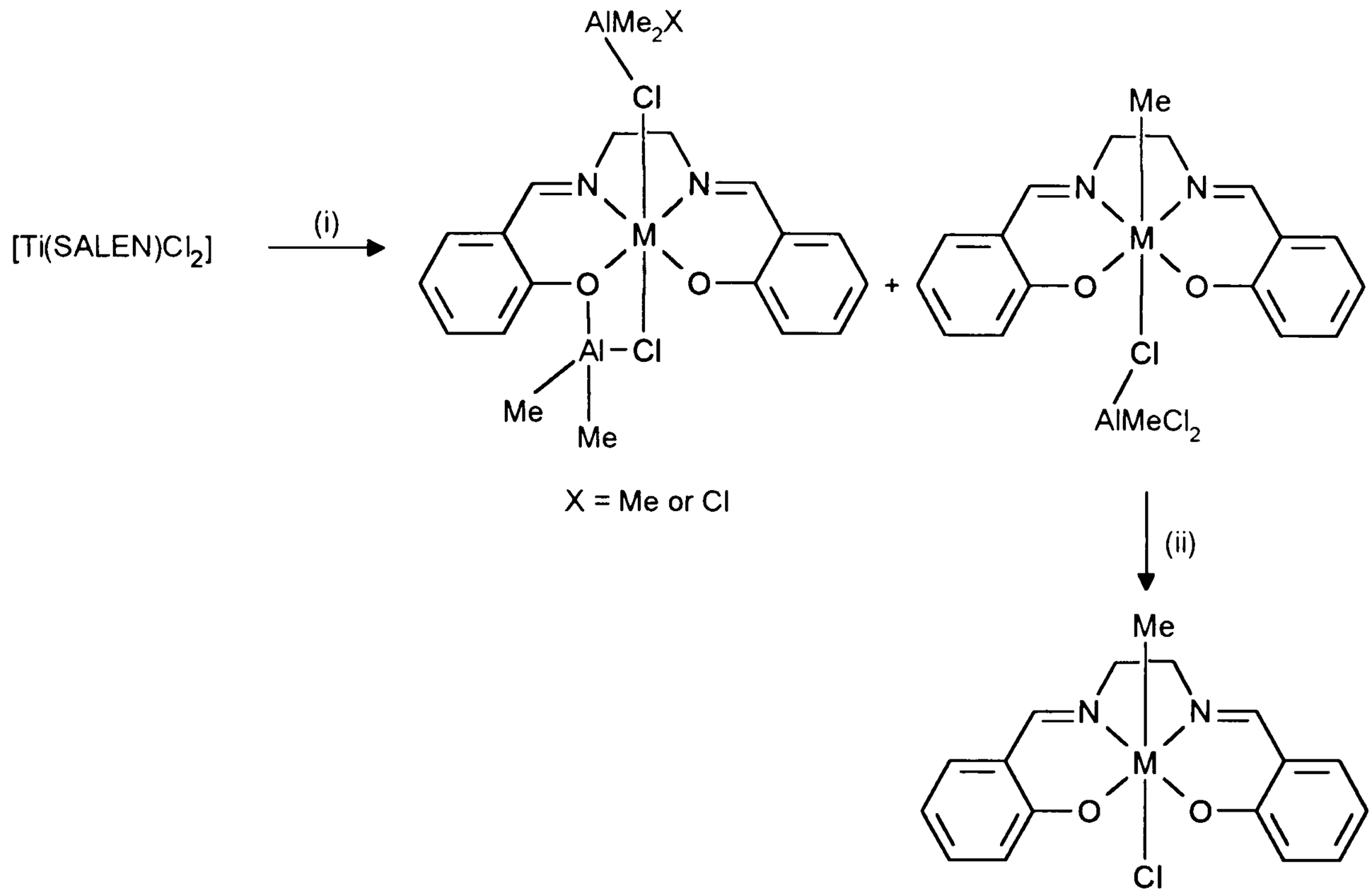

(i) 2 mol $AlMe_3$, toluene/hexane 1:1, RT, 0.5 h. (ii)THF, RT, 0.1 h.

Scheme 3.2 The reported products of the reaction of $[Ti(SALEN)Cl_2]$ with $AlMe_3$

This reduction of the complex seen by Walker *et al* has not been seen in any of the reactions studied in our laboratory, even if extreme conditions (e.g. high temperature) are used. The only explanation for these findings is that the complex with the SALEN ligand behaves in a different manner to those with the substituted SALEN ligands. It should also be noted that, in our work, when the reaction conditions were altered to a 1:4 molar ratio of complex:$AlMe_3$ the reaction products obtained were identical to those obtained for the analogous 1:2 molar ratio reactions.

In the present work we have also observed some interesting side reactions when solutions of these complexes have been left in an attempt to grow crystals suitable for X–ray crystallographic studies. These side reactions have occurred when a toluene/hexane solution of the $[M(L)Cl_2(AlMe_3)_2]$ complex has been cooled to –35°C under an inert argon atmosphere and left for five days.

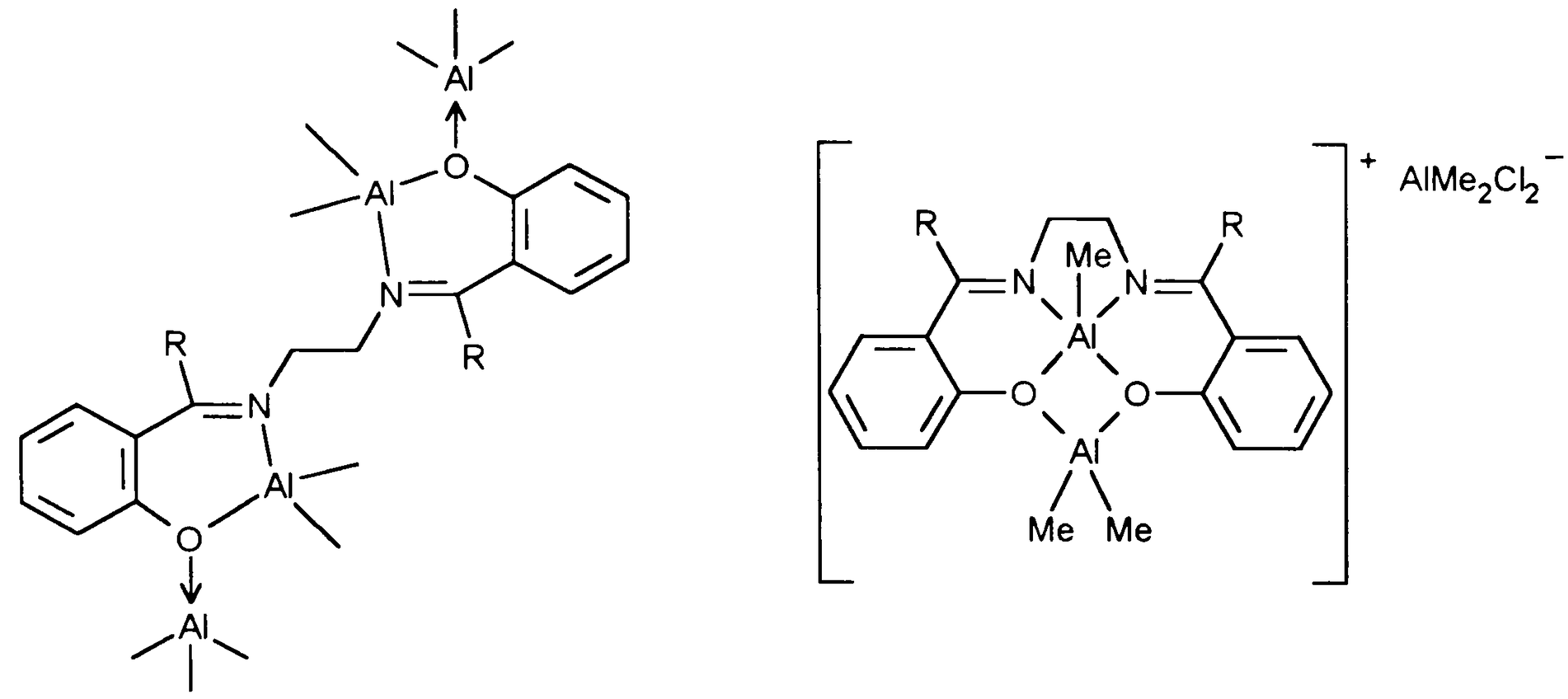

(a) (b)

Figure 3.2 Showing the side reaction products obtained from toluene solutions of $[Zr(DMSALEN)Cl_2(AlMe_3)_2]$ (a) and $[Ti(EtSALEN)Cl_2(AlMe_3)_2]$ (b)

Two different side reaction products have been observed which have been characterised by X–ray crystallography. Unfortunately, due to the extreme reactivity of these complexes and also the small amounts obtained, no further analytical data was obtained. However, complex (a) (Figure 3.2) has been synthesised by another reaction pathway and a more detailed analysis of the complex has been undertaken (see p.152). In both instances transmetallation has occurred with the Group 4 transition metal atom replaced by main group aluminium atoms. In both instances these complexes were colourless crystals, whereas the $[M(L)Cl_2(AlMe_3)_2]$ complexes are brown/orange crystalline solids.

Spectroscopic Properties

N.M.R. Spectra

The ^{1}H and ^{13}C N.M.R. spectra of the $[M(L)Cl_2(AlMe_3)_2]$ complexes resulting from the above reactions provided valuable information in verifying the stoichiometry of the reaction products, as well as information on the purity and the symmetry of the complexes. These N.M.R. spectra were recorded in C_6D_6 solvent to avoid any

possible further reaction of the complex with the N.M.R. solvent. Typical ^{1}H and ^{13}C N.M.R. spectra obtained from these reactions can be seen in Figure 3.5 (p.138)and Figure 3.6 (p.139).

As well as there being no colour change in these reactions, in the case of titanium, the ability to produce ^{1}H N.M.R. spectra of the products is proof that no reduction of the metal has occurred because the species is diamagnetic and not paramagnetic since there are no large shifts or broadening of the resonances. The ^{1}H N.M.R. spectra also confirm that a M–Me bond has not been formed by the alkylation of the metal, M, with trimethyl aluminium, because there is no resonance for the methyl protons in the expected region (approximately δ 0 ppm.) for an M–Me group. The ^{1}H N.M.R. spectra of these complexes provide good evidence that the complexes formed from these reactions are as postulated in Figure 3.1. From the ^{1}H N.M.R. of these complexes the most likely structure of the complexes formed is as shown below in Figure 3.3.

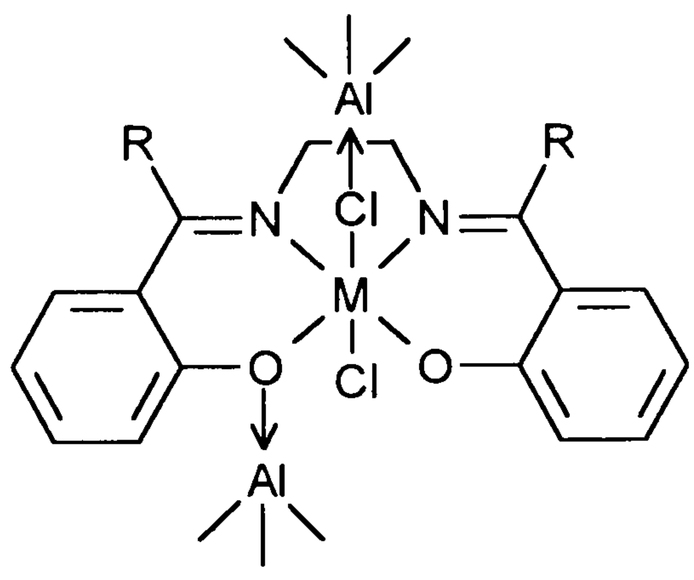

Figure 3.3 Showing the postulated structure of the reaction products.

This structure is consistent with the presence of two aluminium alkyl ^{1}H N.M.R. resonances in the extremely upfield region (δ <0 ppm). The presence of these two resonances, seen in all complexes, indicates that two different aluminium methyl groups are present within the complexes. These Al–Me resonances both integrate for 9 protons relative to the ligand resonance integration. For the complex $[Zr(EtSALEN)Cl_2(AlMe_3)_2]$ these aluminium methyl resonances are seen at δ –0.67 and δ –0.78 ppm. (Figure 3.5). One possible explanation for the coordination of one aluminium trialkyl to oxygen and the other to chlorine is that steric factors within the

complex prevent the addition of both aluminium atoms to both oxygen atoms within the complex. Therefore, the second aluminium trialkyl probably coordinates to a chlorine atom where the steric constraints are at a minimum.

The ^{1}H N.M.R. spectra also confirm that high symmetry associated with the ligands is retained within these complexes. In the ^{1}H N.M.R. spectra there is found to be no further splitting of any of the resonances associated with the coordinated aluminium trialkyl molecules, and these resonances associated with the ligand are all found in the same regions as the starting dihalide complexes. In the case of $[Zr(EtSALEN)Cl_2(AlMe_3)_2]$ the backbone CH_2 protons are seen as a singlet at δ 4.15 ppm which is slightly upfield from the dihalide complex at δ 4.27 ppm. The ethyl group protons are seen as a quartet and triplet at δ 3.1 and δ 1.2 ppm respectively, and the aromatic protons are found in the region at δ 6–8 ppm.

The ^{13}C N.M.R. spectra of these complexes also confirm that the high symmetry of the ligand is retained. The symmetry of these complexes can be explained with reference to either of the two structures shown in Figure 3.4 for the complex $[Zr(EtSALEN)Cl_2(AlMe_3)_2]$.

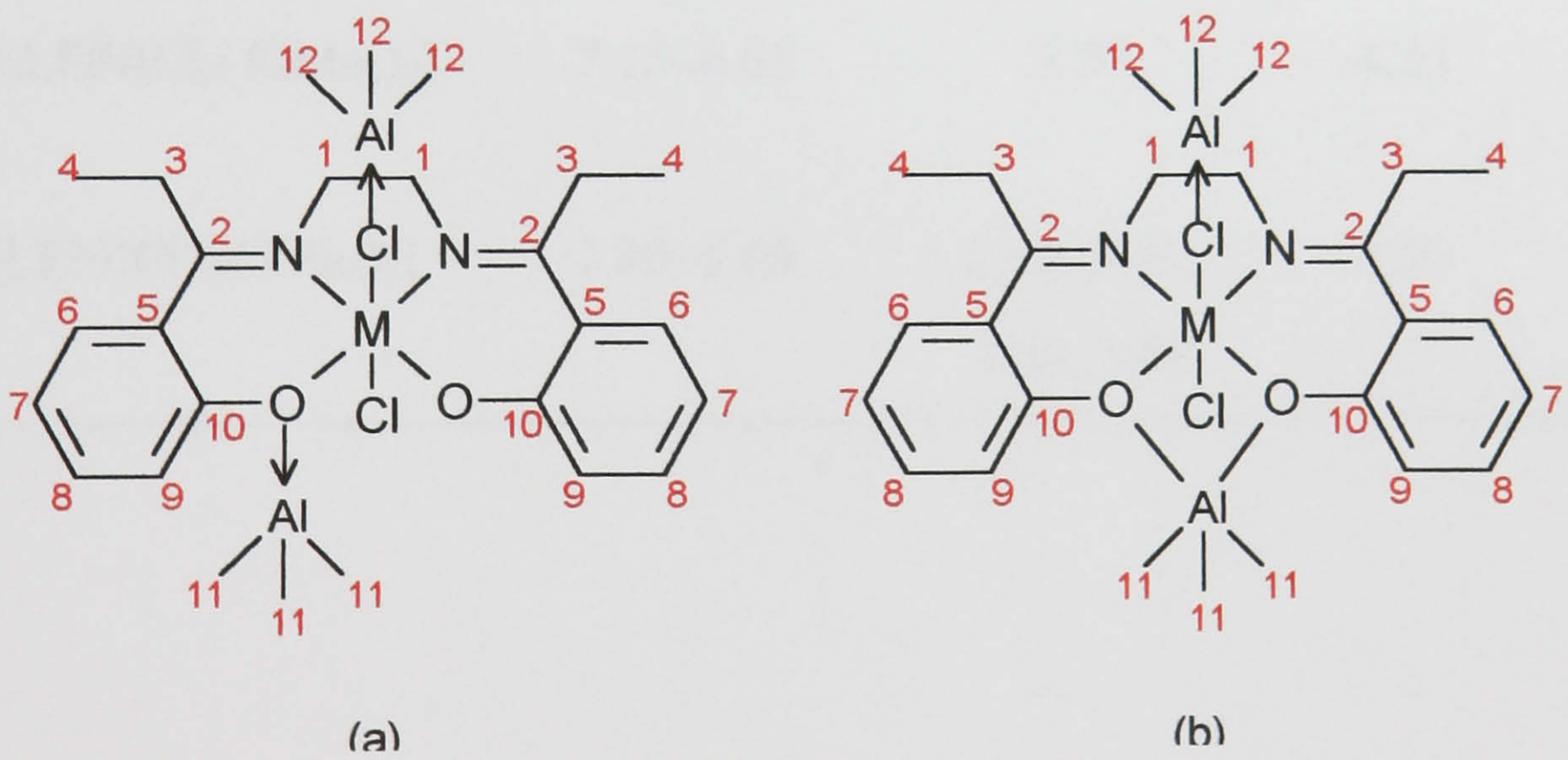

Figure 3.4 Possible structures for $[Zr(EtSALEN)Cl_2(AlMe_3)_2]$.

If the structure is as represented in (a) then the O–bonded $AlMe_3$ group must be fluxional between the two oxygen atoms. Alternatively the structure of these complexes is as represented in (b) where the $AlMe_3$ group is bridging across the two oxygen atoms therefore maintaining the symmetry of the ligand within the complexes.

There are twelve resonances seen in the ^{13}C N.M.R. of $[Zr(EtSALEN)Cl_2(AlMe_3)_2]$ which is as predicted for a symmetric complex. These resonances are observed in the same regions as for the dihalide complex, with in some case a considerable shift seen in these resonances. The Al–Me resonances are seen in the upfield region at approximately δ –10 ppm. These two resonances are almost coincident and are seen at δ –10.52 and δ –10.63 ppm. The resonances for the ^{1}H and ^{13}C chemical shifts are listed and assigned in Table 3.1 and 3.2.

Table 3.1 Summary of ^{1}H N.M.R data (δ / ppm) for $[M(L)Cl_2(AlMe_3)_2]$ complexes

Compound	Aromatic	R–C=N	CH_2–CH_2	Al–R
$[Zr(DMSALEN)Cl_2(AlMe_3)_2]$	7.37–7.21	2.82	4.13	–0.68, –0.77
$[Zr(EtSALEN)Cl_2(AlMe_3)_2]$	7.71–7.19	3.19–3.10, 1.35–1.29	4.15	–0.67, –0.78
$[Ti(DMSALEN)Cl_2(AlMe_3)_2]$	7.15–6.62	2.54	4.11	–0.34, –0.53
$[Ti(EtSALEN)Cl_2(AlMe_3)_2]$	7.20–6.65	2.55–2.46, 1.00–0.92	4.05	–0.21, –0.41

Table 3.2 Summary of Proton decoupled ^{13}C N.M.R data (δ / ppm) of $[M(L)Cl_2(AlMe_3)_2]$ complexes

Compound	R–C=N	C–O	Aromatic	R–C=N	CH_2–CH_2	Al–R
$[Zr(DMSALEN)Cl_2(AlMe_3)_2]$	181.42	135.10	129.81, 129.09, 128.29, 125.37, 125.22	21.29	48.75	–6.87, –10.66
$[Zr(EtSALEN)Cl_2(AlMe_3)_2]$	186.05	135.13	129.53, 129.10, 128.29, 125.36, 125.30	25.62, 12.18	48.84	–10.52, –10.63
$[Ti(DMSALEN)Cl_2(AlMe_3)_2]$	180.29	134.90	129.33, 128.64, 125.83, 124.32, 124.04	20.96	48.41	–6.94, –10.03
$[Ti(EtSALEN)Cl_2(AlMe_3)_2]$	185.97	134.51	128.77,128.07, 125.03, 124.81, 124.32	24.99, 11.74	48.56	–6.33, –10.43

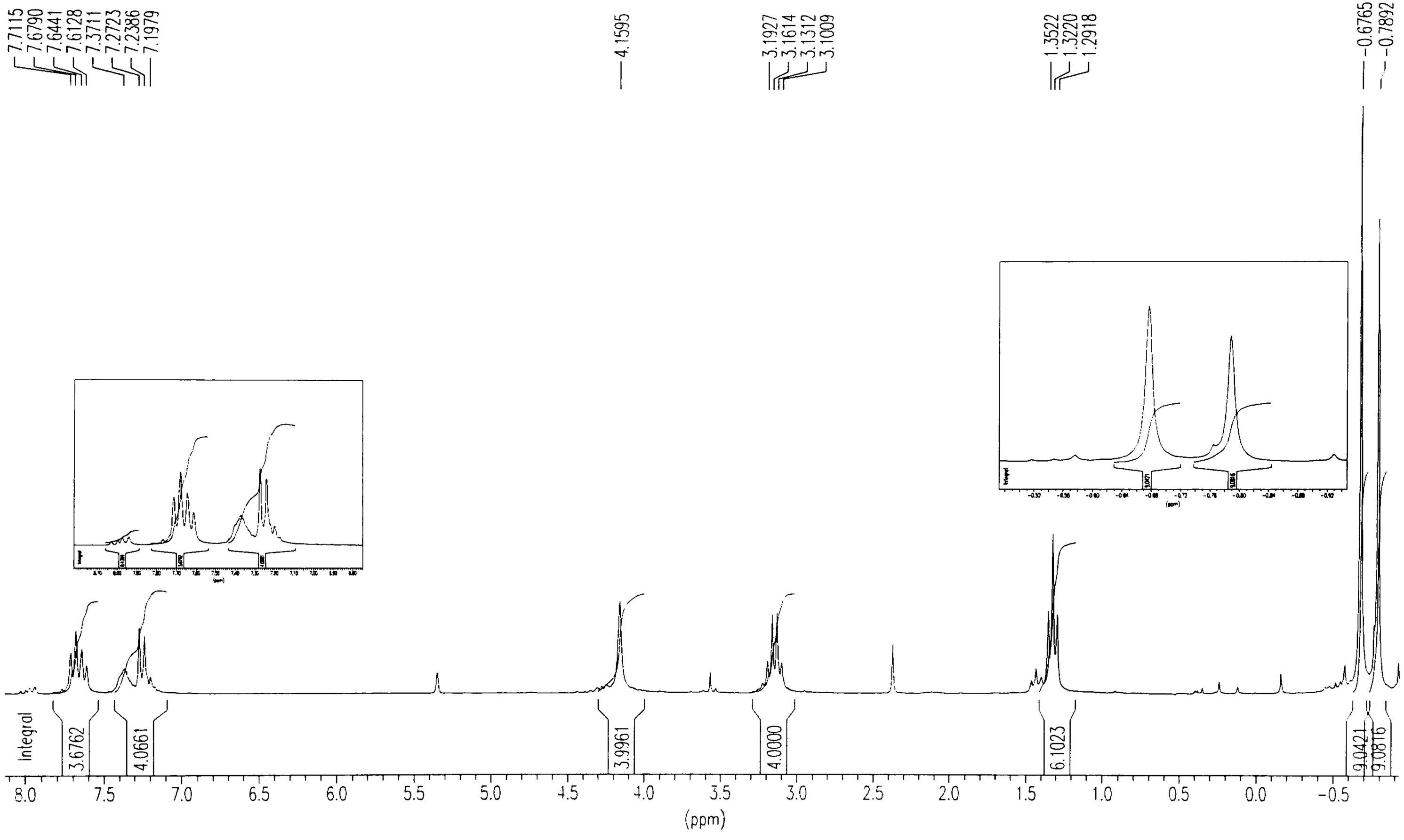

Figure 3.5 The ^{1}H N.M.R spectrum of $[Zr(EtSALEN)Cl_2(AlMe_3)_2]$

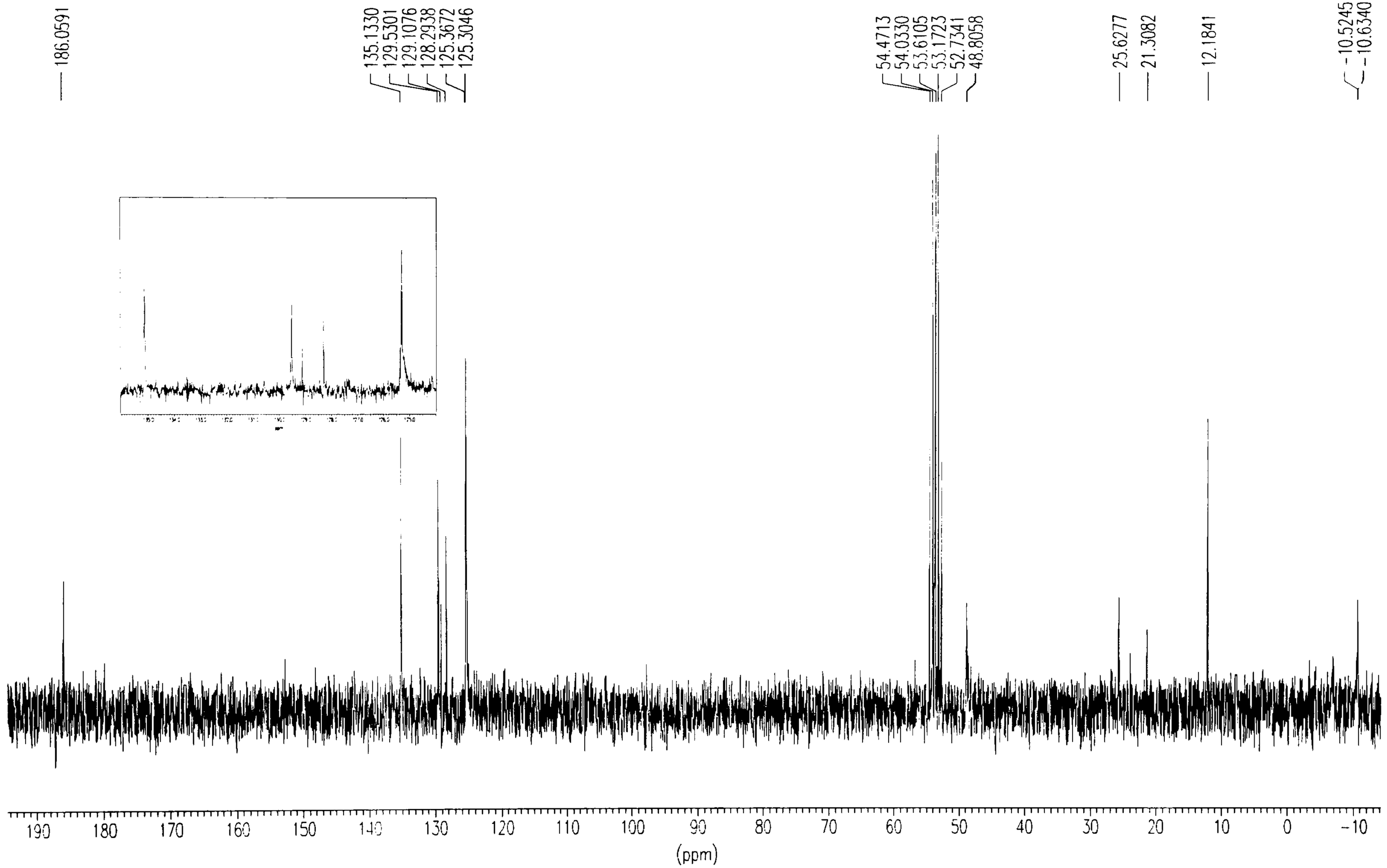

Figure 3.6 The proton decoupled ^{13}C N.M.R spectrum of $[Zr(EtSALEN)Cl_2(AlMe_3)_2]$

Mass Spectra

Great difficulty was experienced in obtaining mass spectra of these complexes. The main reason for this is their extreme reactivity. Most attempts to obtain a mass spectrum of one of these complexes proved to be unsuccessful no matter what conditions or technique was employed i.e. source temperature, EI, CI, F.A.B. However, in the case of $[Zr(DMSALEN)Cl_2(AlMe_3)_2]$ the EI mass spectrum was obtained providing evidence to support the structure predicted by the N.M.R and IR spectroscopic methods.

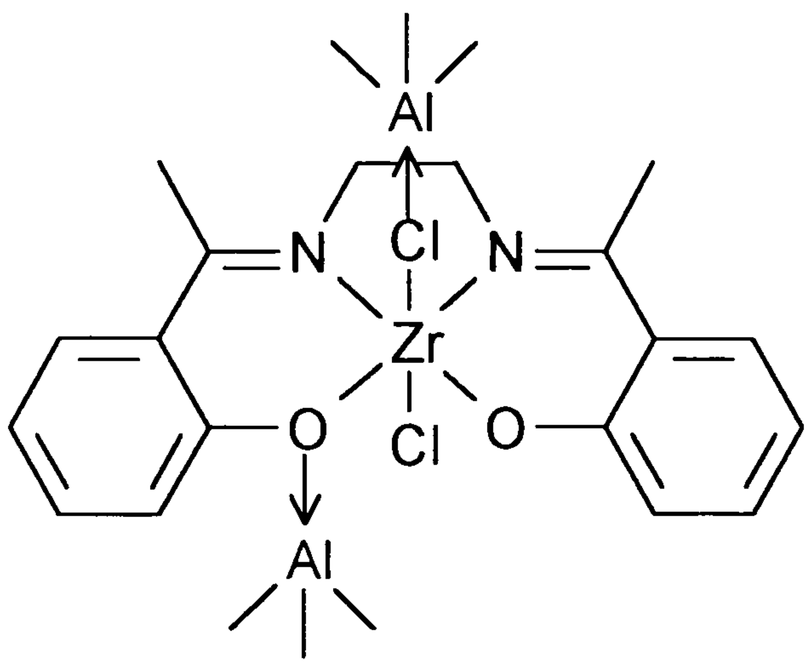

Although the molecular ion was not seen, fragment ions associated with the loss of a chlorine and/or the loss of methyl groups could be seen. Fragmentation of the complex involves both the loss of a chlorine atom followed by the loss of methyl groups, as well as the loss of $AlMe_3$ groups followed by further fragmentation (Figure 3.7).

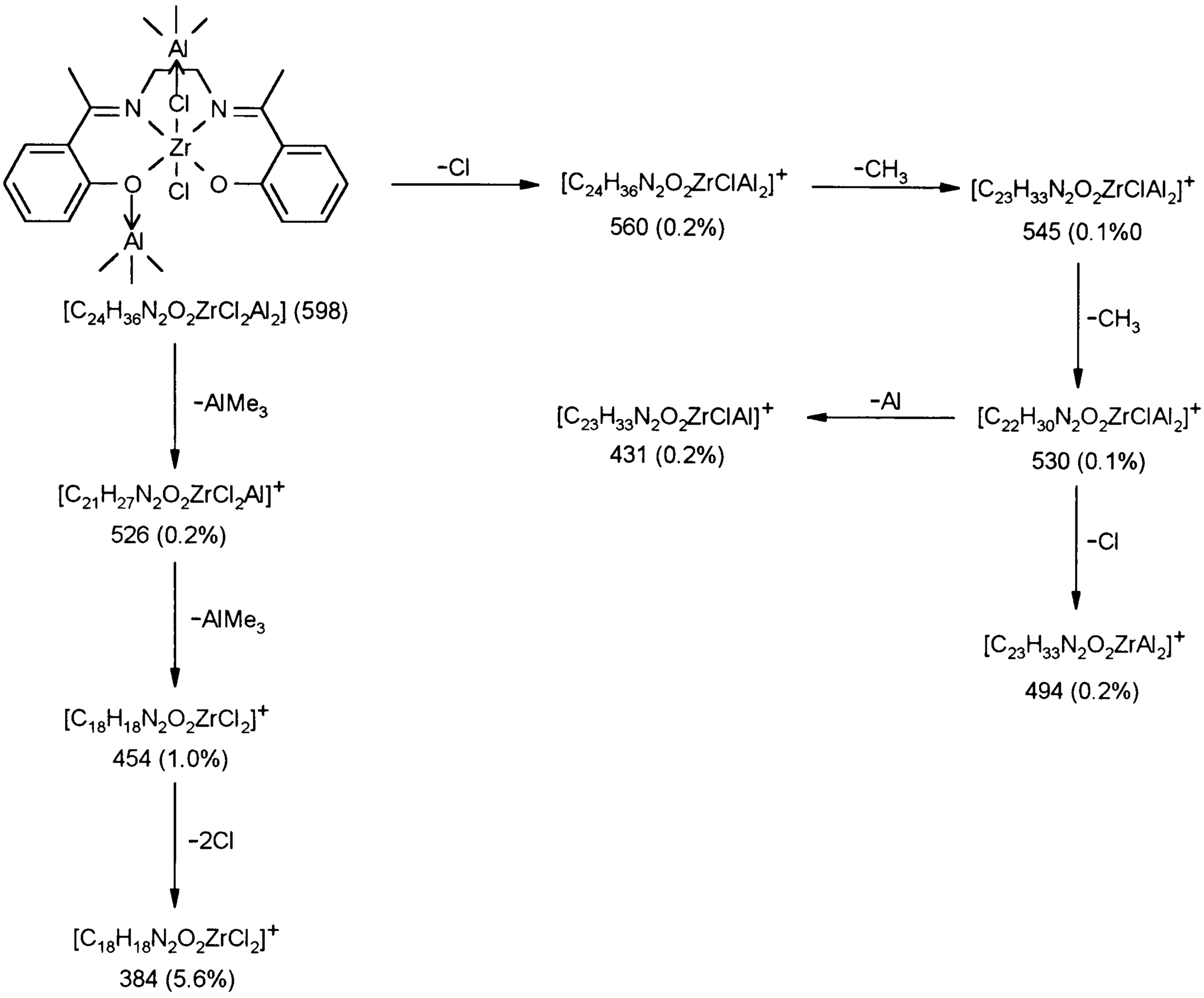

Figure 3.7 [Zr(DMSALEN)$Cl_2(AlMe_3)_2$] fragmentation pattern

X–ray Crystallographic Studies

To confirm the postulated structures assigned from all the analytical and spectroscopic data, a great deal of effort was put into the growth of suitable crystals for an X–ray crystallographic analysis. However, this proved to be extremely difficult due to the high reactivity of the complexes. All solvents had to be scrupulously dry and oxygen free, and all operations were carried out under an inert atmosphere. Although suitable crystals were eventually obtained, their analysis was unsuccessful due to the decay of the crystal before any useful data could be successfully obtained. As a result no structural data was gained from this technique. However, in the attempts to grow these crystals, other crystals were obtained from the side reactions

involved during crystal growth. These side reaction products were isolated and successfully studied by X–ray crystallography.

The molecular structure of $[AlMe(EtSALEN)Al(Me)_2]^+[AlMeCl_3]^-$ is shown in Figure 3.8. These crystals were grown from a toluene/hexane solution of $[Ti(EtSALEN)Cl_2(AlMe_3)_2]$ at –35 °C. The complex consists of discrete $[AlMe(EtSALEN)(AlMe_2)]^+$ and$[AlMeCl_3]^-$ ions.

The $[AlMeCl_3]^-$ anion has a distorted tetrahedral geometry around the aluminium atom. The $[AlMe(EtSALEN)(AlMe_2)]^+$ cation has bond lengths and angles which are very similar to those found in both the free ligand and other aluminium(III) SALEN type Schiff base complexes.[138,139] The coordination around Al2 (Figure 3.9) is that of a distorted square based pyramid. The bond lengths of Al2–N (1.962 Å, av.) and Al2–O (1.876 Å, av.) are consistent with those found in complexes of the type [(L)AlR] where L = tetradentate Schiff base ligand and R = Cl, methyl or ethyl.[139] The aluminium is displaced 0.54 Å out of the N_2O_2 plane in the direction of Al2–C24 which is also consistent with distances found in other [(L)AlR] complexes.[127] The Al2–C24 bond distance of 1.925(11) Å is similar to the terminal Al–C distance of 1.970 Å seen in Al_2Me_6,[140] and that of 1.976(3) Å seen for the 5–coordinate macrocyclic complex [AlEt(tmtaa)][141] (Table 3.4). This short Al–C bond distance indicates a strong metal–carbon bond.

The coordination around Al1 (Figure 3.10) is that of a distorted tetrahedral geometry. The Al–O (1.846(7) Å) and Al–C (1.936(11) Å) are closely related to values observed for other related structures containing tetrahedral aluminium.[142,143]

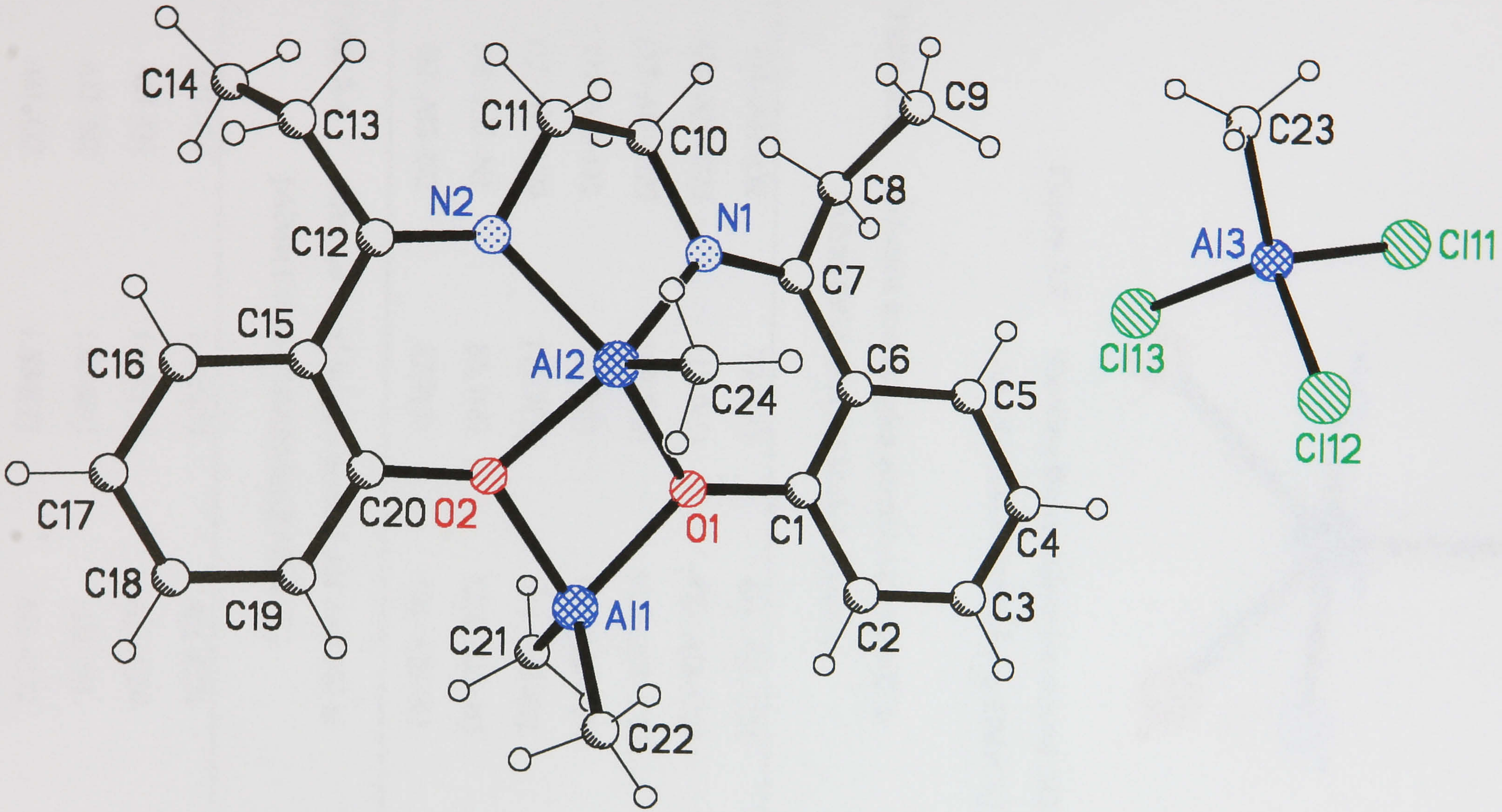

Figure 3.8 The molecular structure of $[AlMe(EtSALEN)Al(Me)_2][AlMeCl_3]$

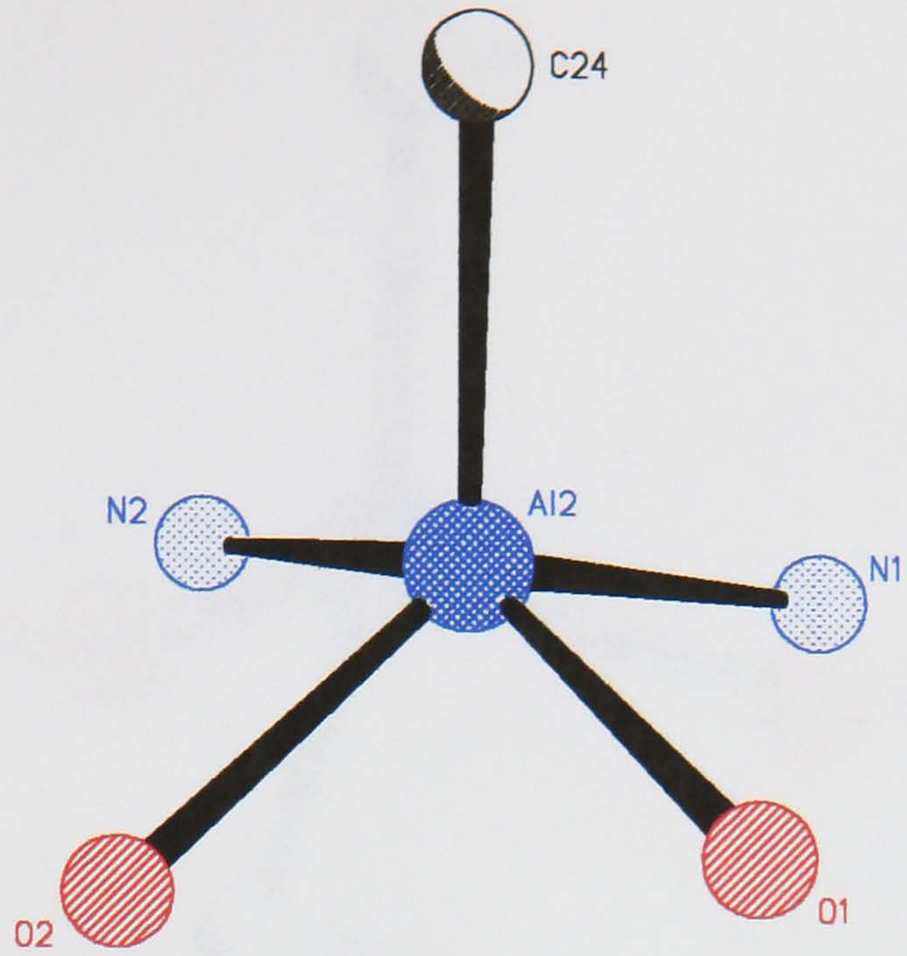

Figure 3.9 Showing the coordination around Al2 in $[AlMe(EtSALEN)Al(Me)_2][AlMeCl_3]$

Table 3.3 Selected bond angles around Al1 and Al2 in $[AlMe(EtSALEN)Al(Me)_2][AlMeCl_3]$

O1–Al1–O2	77.5(3)	O1–Al1–C21	112.0(5)
O2–Al1–C21	115.0(5)	O1–Al1–C22	113.6(5)
O2–Al1–C22	109.8(5)	C21–Al1–C22	121.0(6)
O1–Al2–O2	76.7(3)	O1–Al2–C24	104.7(4)
O2–Al2–C24	115.7(5)	O1–Al2–N2	149.7(4)
N2–Al2–N1	85.1(4)	C24–Al2–N1	107.8(3)
O2–Al2–N2	87.8(3)	O1–Al2–N1	88.2(3)

Table 3.4 Selected bond lengths around Al1 and Al2 in $[AlMe(EtSALEN)Al(Me)_2][AlMeCl_3]$

Al1–O1	1.846(7)	Al1–C21	1.908(12)
Al2–O1	1.870(1)	Al2–C24	1.925(11)
Al2–N2	1.954(9)	Al2–N1	1.970(10)
Al2–O2	1.884(7)	Al1–C22	1.936(11)
Al1–O2	1.875(7)	Al1–Al2	2.899(4)

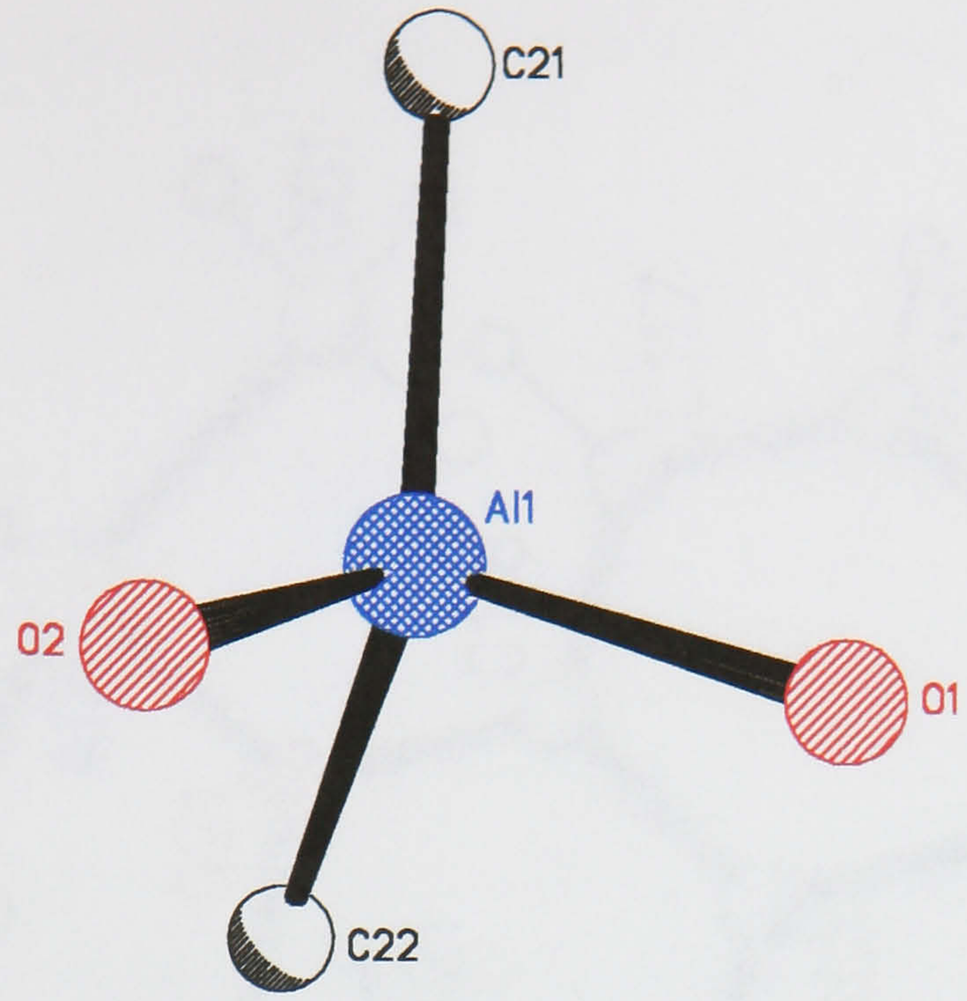

Figure 3.10 Showing the coordination around Al1 in $[AlMe(EtSALEN)Al(Me)_2][AlMeCl_3]$

The molecular structure of $[Al_2(Me_2)_2(DMSALEN)Al_2(Me_3)_2]$ shown in Figure 3.11 was also determined. These crystals were grown from a toluene/hexane solution of $[Zr(EtSALEN)Cl_2(AlMe_3)_2]$ at –35 °C. The crystals are extremely reactive and could be seen to react even under the inert perfluoropolyether oil when viewed under a microscope. Although the data from these crystals were poor, they were good enough to chemically identify the complex.

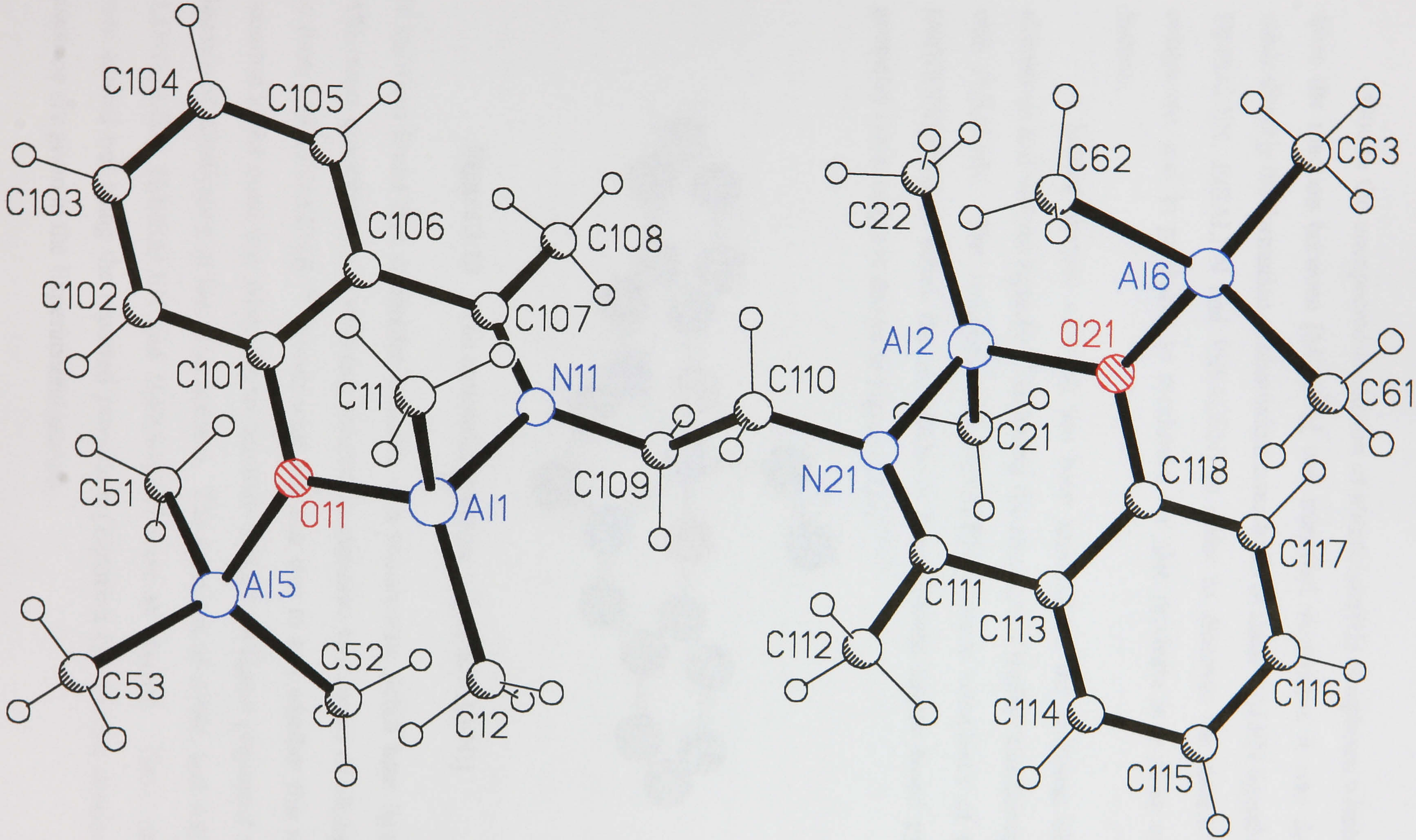

Figure 3.11 The molecular structure of $[Al_2(Me_2)_2(DMSALEN)Al_2(Me_3)_2]$

Preparation of tetradentate Schiff base metal alkyl complexes of Al(III)

Due to the unexpected formation of aluminium(III) complexes which resulted from the reaction between $[M(L)Cl_2]$ and trimethyl aluminium, it was decided to study directly the formation of aluminium complexes of these SALEN ligands (namely DMSALEN, EtSALEN and PhSALEN) in order to discover the nature of these complexes, and in particular to synthesise the side products in a more controlled fashion.

A limited amount of work has been reported on the reactions of triethyl aluminium and various ligands,[139] including the reaction of trialkyl aluminium species with H_2SALEN. The reactions with H_2SALEN produce complexes of the type [Al(R)(SALEN)] in which the aluminium is 5–coordinate square–based pyramidal geometry (an example is shown in Figure 3.12).[138,139]

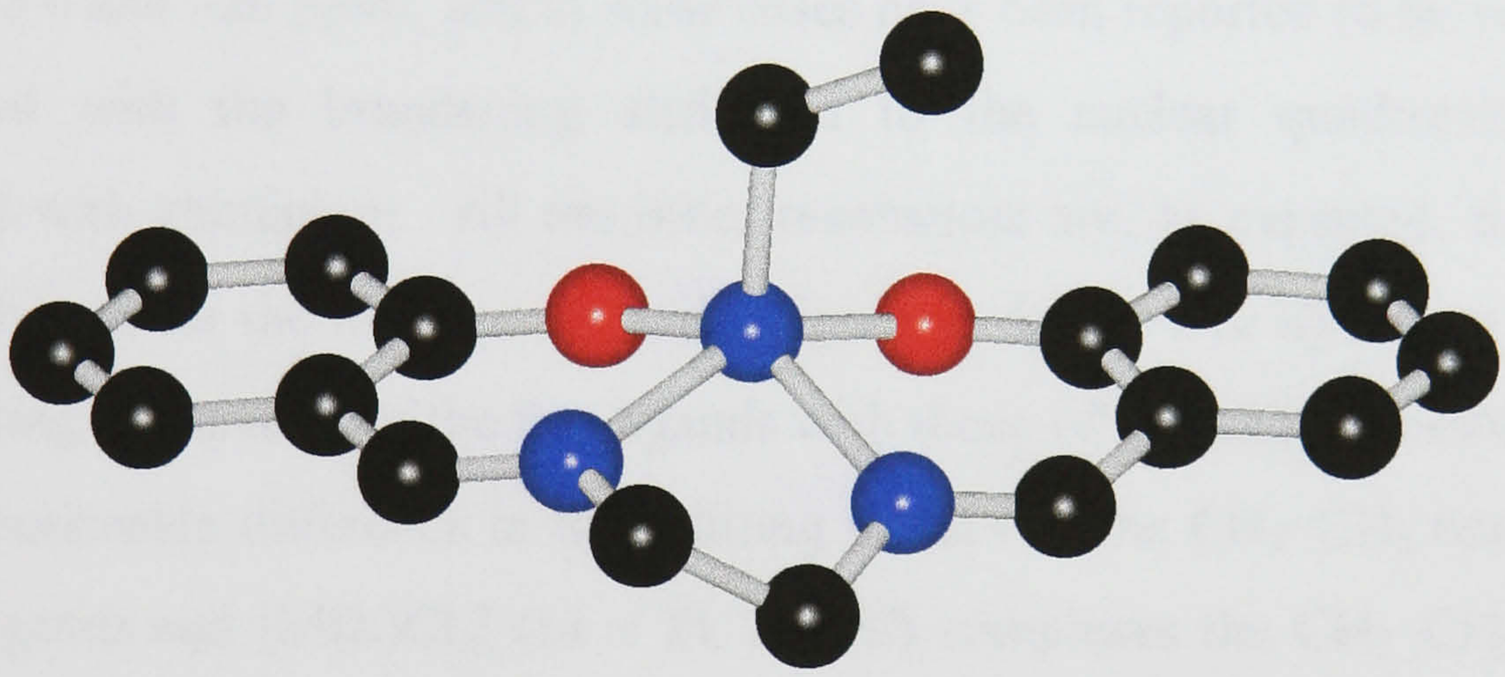

Figure 3.12 The molecular structure of [AlEt(SALEN)]

It has been found that equimolar amounts of a tetradentate Schiff base ligand and AlR_3 react quantitatively in refluxing toluene to eliminate two moles of alkane (RH) to form [Al(R)(SALEN)].[144] In our work the aim was to test whether this reaction occurred in the same way when the tetradentate Schiff base ligand possessed varying degrees of substitution at the imine carbon. The reactions of $AlMe_3$ and $AlEt_3$ with H_2DMSALEN, H_2EtSALEN and H_2PhSALEN were all studied. These reactions were carried out using the reported procedure (Equation 1). Precise details of the reactions are given in the Experimental section.

$$H_2L + AlR_3 \longrightarrow [AlR(L)] + 2\,RH \qquad (1)$$

The resultant complexes were characterised by ^{1}H and ^{13}C N.M.R., mass spectrometry, elemental analyses and infra–red spectroscopy. These analyses confirmed the formation of complexes of the type [AlR(L)].

Spectroscopic properties

N.M.R. Spectra

The ^{1}H and ^{13}C N.M.R. spectra of all the [AlR(L)] complexes obtained were recorded in $CDCl_3$, and are consistent with the results of related X–ray crystallographic studies.[136] The resonances for the ^{1}H and ^{13}C N.M.R. chemical shifts are listed and assigned in Table 3.5 and Table 3.6. The ^{1}H N.M.R. spectrum of a typical complex, [AlMe(EtSALEN)], is illustrated in Figure 3.14.

The aluminium alkyl resonances are often seen as broad upfield resonances (between δ 0 and –20 ppm), and in some cases have been reported to be very difficult to observe with the broadening attributed to the nuclear quadropole splitting associated with aluminium. All the other resonances are, as expected, found in the same regions as for the free ligands, and assigned as for the free ligands in Chapter 2.

In comparing the spectra of the free ligands with those of the Al(III) complexes, there was one noticeable difference in the splitting pattern of the CH_2–CH_2 backbone. In the free ligands and $[M(L)Cl_2]$ (M = Ti, Zr, Hf) complexes the CH_2–CH_2 backbone resonance is seen as a singlet, whereas in these Al(III) complexes of the substituted SALEN type Schiff bases the CH_2–CH_2 backbone resonance is split into a multiptlet (Figure 3.13).

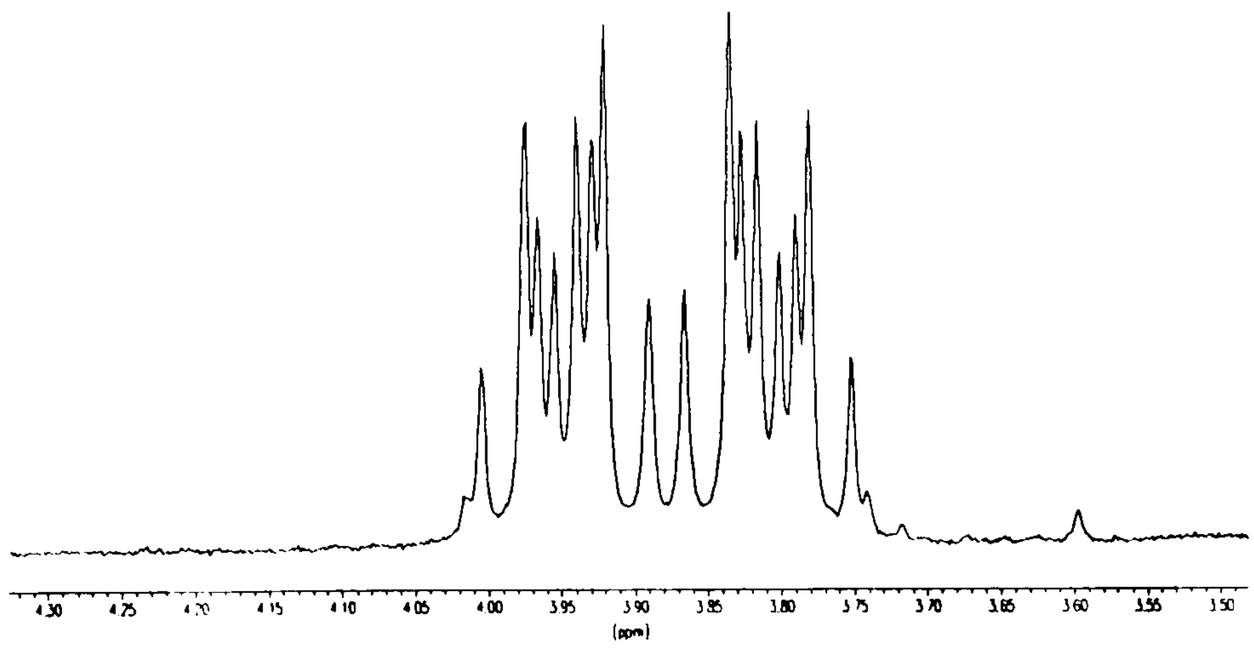

Figure 3.13 Showing the splitting of the CH_2–CH_2 backbone resonance in Al(III) complexes of the substituted SALEN type Schiff bases

The ^{13}C N.M.R. spectra of these complexes also showed the ligand resonances in the expected regions. The symmetry within these Al(III) complexes was also found to be the same as that found in the spectra of the free ligands and of the $[M(L)Cl_2]$ (M = Ti, Zr, Hf) complexes. The Al–R resonances in the ^{13}C N.M.R. spectra of these complexes are found upfield in the region between δ 20 and 0 ppm.

These ^{1}H and ^{13}C N.M.R. spectra along with the elemental analyses and infra–red spectroscopy studies confirm the synthesis of complexes of the type [Al(R)(L)], and these complexes are assumed to adopt the square–based pyramidal geometry.[135,136] All the substituted ligands were found to react in the same way as H_2SALEN with trialkyl aluminium(III).

Table 3.5 ^{1}H N.M.R. of SALEN type Schiff base aluminium(III) alkyl complexes in $CDCl_3$

Compound	**Aromatic**	**CH_2–CH_2**	**N=C<u>R</u>**	**Al–<u>R</u>**
[AlMe(DMSALEN)]	7.53–6.65	3.94–3.75	2.51	–1.15
[AlEt(DMSALEN)]	7.49–6.62	3.89–3.72	2.31	0.63–0.58, –0.41–(–0.48)
[AlMe(EtSALEN)]	7.29–6.65	4.00–3.74	2.99–2.84, 1.32–1.25	–1.10
[AlEt(EtSALEN)]	7.23–6.58	3.97–3.75	3.00–2.84, 1.33–1.27	0.71–0.65, –0.34–(–0.44)
[AlMe(PhSALEN)]	7.34–6.48	3.60–3.46, 3.25–3.11	7.49–7.14	–0.83
[AlEt(PhSALEN)]	7.32–6.46	3.56–3.42, 3.25–3.11	7.48–7.06	0.94–0.88, –0.08–(–0.17)

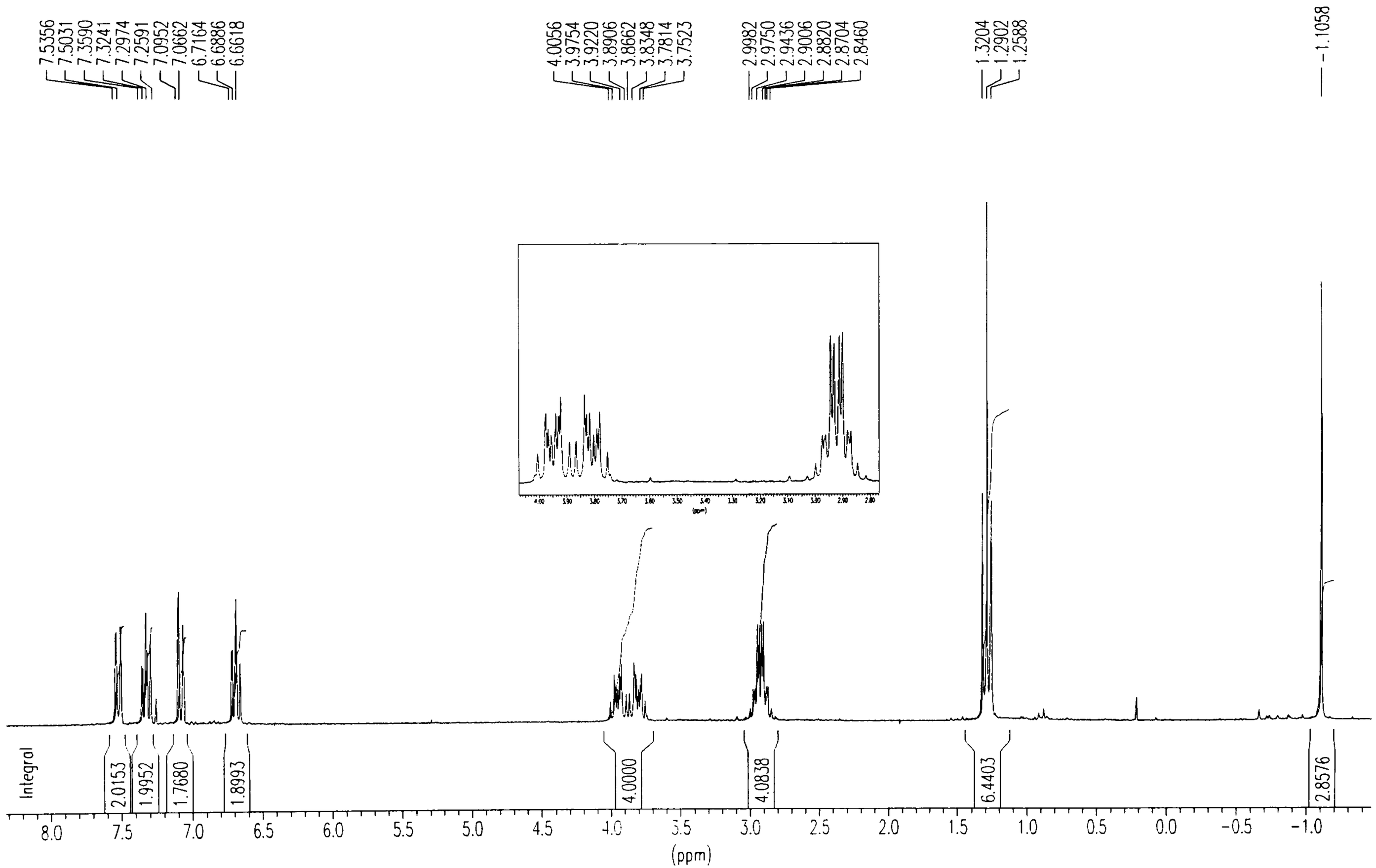

Figure 3.14 The ^{1}H N.M.R spectrum of [AlMe(EtSALEN)] in $CDCl_3$

Table 3.6 Summary of proton decoupled ^{13}C N.M.R shifts (δ/ppm.) for SALEN type Schiff base aluminium(III) alkyl complexes

Compound	C=N	C–O	Aromatic	CH_2–CH_2	R–C=N	Al–R
[AlMe(DMSALEN)]	175.02	164.94	134.28, 129.11, 123.73, 120.47, 115.81	48.29	18.29	3.24
[AlEt(DMSALEN)]	175.76	164.86	134.08, 129.23, 123.54, 120.34, 116.02	47.99	18.40	10.41, 9.92
[AlMe(EtSALEN)]	179.18	165.66	134.31, 128.97, 124.03, 118.83, 115.94	47.62	23.97, 11.95	7.09
[AlEt(EtSALEN)]	179.38	165.95	134.28, 128.93, 123.96 118.96, 115.86	47.72	24.01	12.00, 10.19
[AlMe(PhSALEN)]	177.25	166.13	135.67, 129.05, 123.29, 120.10, 115.65	50.45	135.67, 133.18, 128.94, 126.44	21.38
[AlEt(PhSALEN)]	177.47	166.41	134.87, 133.15, 123.21, 120.19, 115.56	50.56	135.72, 129.05, 128.94, 126.44	10.42, 9.85

Once it was established that all these ligands reacted in the same way with trialkyl aluminium(III), the preparation of complexes of the type $[(AlMe_2)_2(AlMe_3)_2(L)]$ was attempted. The only reported similar reaction to these involved the work of Storr *et al*[145] who reacted H_2SALEN with trimethyl gallium. When an excess of Me_3Ga was used in the reaction (an excess greater than 2:1 of Me_3Ga:ligand) they obtained the reaction product $[(GaMe_2)_2(SALEN)]$ (Figure 3.15).

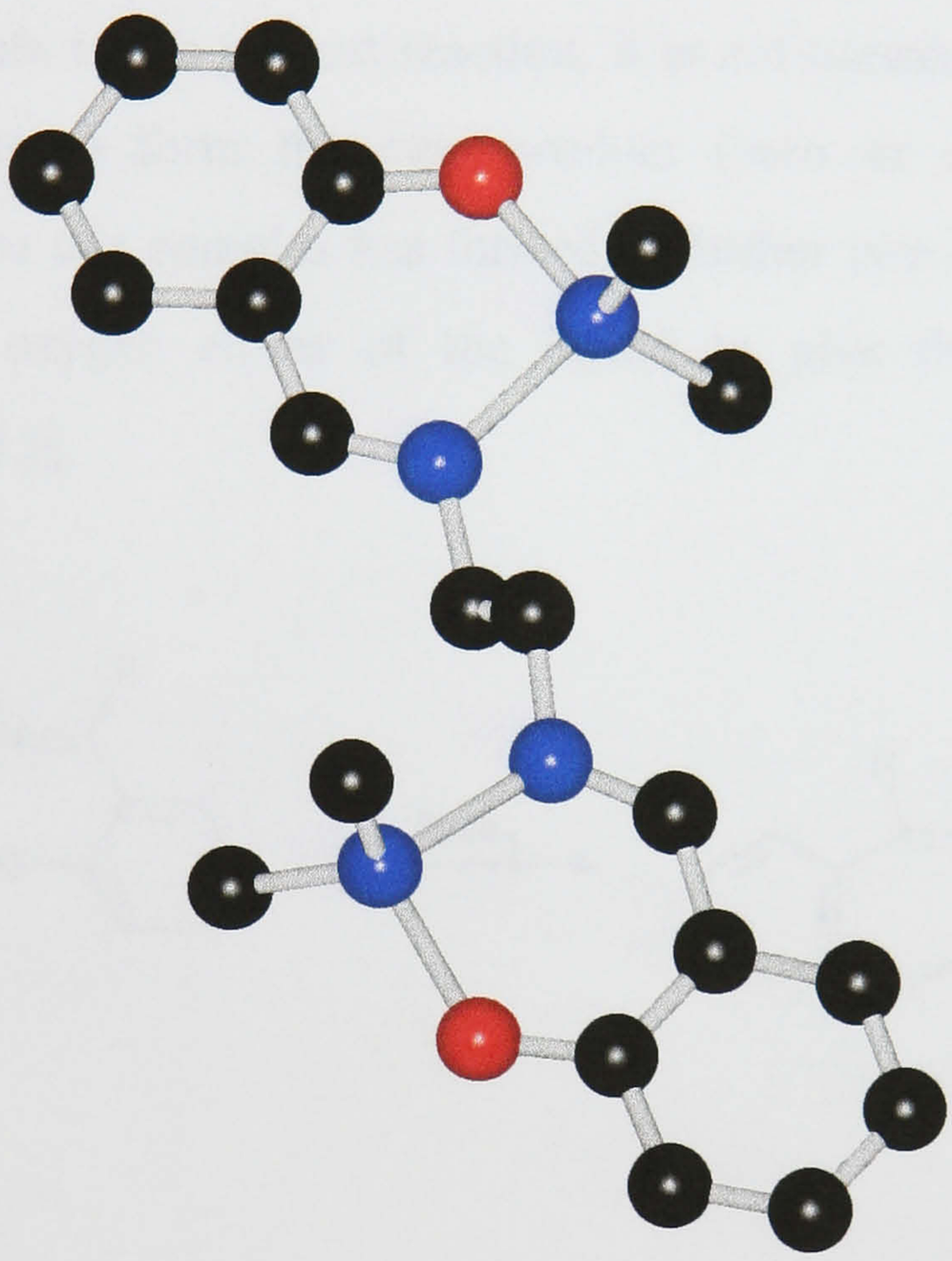

Figure 3.15 The molecular structure of $[(GaMe_2)_2(SALEN)]$

The reaction with $GaMe_3$ was carried out using xylene as solvent, and at a constant temperature of 110 °C for 48 h. These are very forcing conditions which were found to be necessary for the reaction to proceed. In our work similar forcing conditions were subsequently used in the reactions of excess trimethyl aluminium with each of the SALEN type ligands to obtain complexes of the type $[(AlMe_2)_2(AlMe_3)_2(L)]$.

In our studies these reactions were carried out in dry toluene, and with the two ligands H_2DMSALEN and H_2EtSALEN.

$$H_2L + 4\,AlMe_3 \xrightarrow[80\ ^oC]{\text{toluene}} [(AlMe_2)_2(AlMe_3)_2(L)] + 2\,CH_4 \qquad (2)$$

The ligand was dissolved in toluene and the solution cooled to –78 °C, before the slow addition of 4 equivalents of a 2 molar hexane solution of $AlMe_3$. An initial white solid is formed on warming, and this suspension is heated to 80 °C for 50 h yielding a clear yellow solution. The solid obtained by evaporation of this solution was then analysed by the usual spectroscopic techniques.

The proposed reaction pathway is shown in Scheme 3.3. The initial white solid is reported by Storr,[145] and Cannadine[144] to be $[(HL)AlMe_2]$, and considering this is an intermediate in the present reaction, it is not unreasonable to suggest that this then rearranges to form the next product (seen as a yellow suspension), $[(L)(AlMe_2)_2]$. Once this complex has formed, a further two moles of $AlMe_3$ could coordinate to the oxygen atoms of the ligand to give the observed complex, $[(AlMe_2)_2(AlMe_3)_2(L)]$.

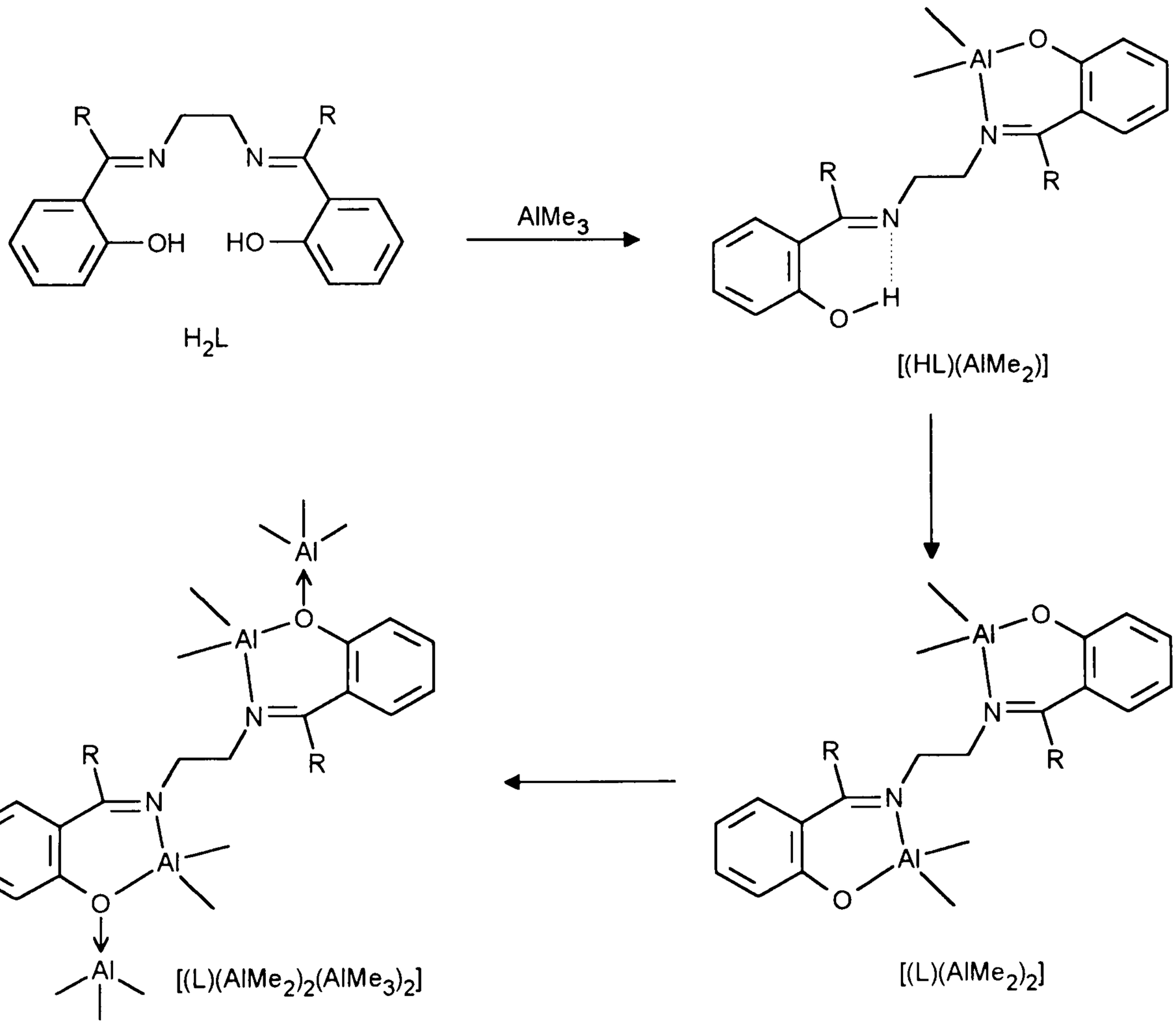

Scheme 3.3 Showing the postulated reaction pathway for the formation of complexes, $[(AlMe_2)_2(AlMe_3)_2(L)]$

Spectroscopic properties of the products from the reaction of tetradentate Schiff base ligands and excess $AlMe_3$

N.M.R. Spectra

The ^{1}H and ^{13}C N.M.R. spectra of all these complexes were recorded in C_6D_6 to avoid any further possible reaction with the N.M.R. solvent. The ^{1}H N.M.R. spectrum of the complex $[(AlMe_2)_2(AlMe_3)_2(EtSALEN)]$ can be seen in Figure 3.18. The ^{1}H and ^{13}C N.M.R. spectra are consistent with the formation of a highly symmetric complex, which was confirmed by the X–ray molecular structure of the related compound $[Al_2(Me_2)_2(DMSALEN)Al_2(Me_3)_2]$ (Figure 3.16)

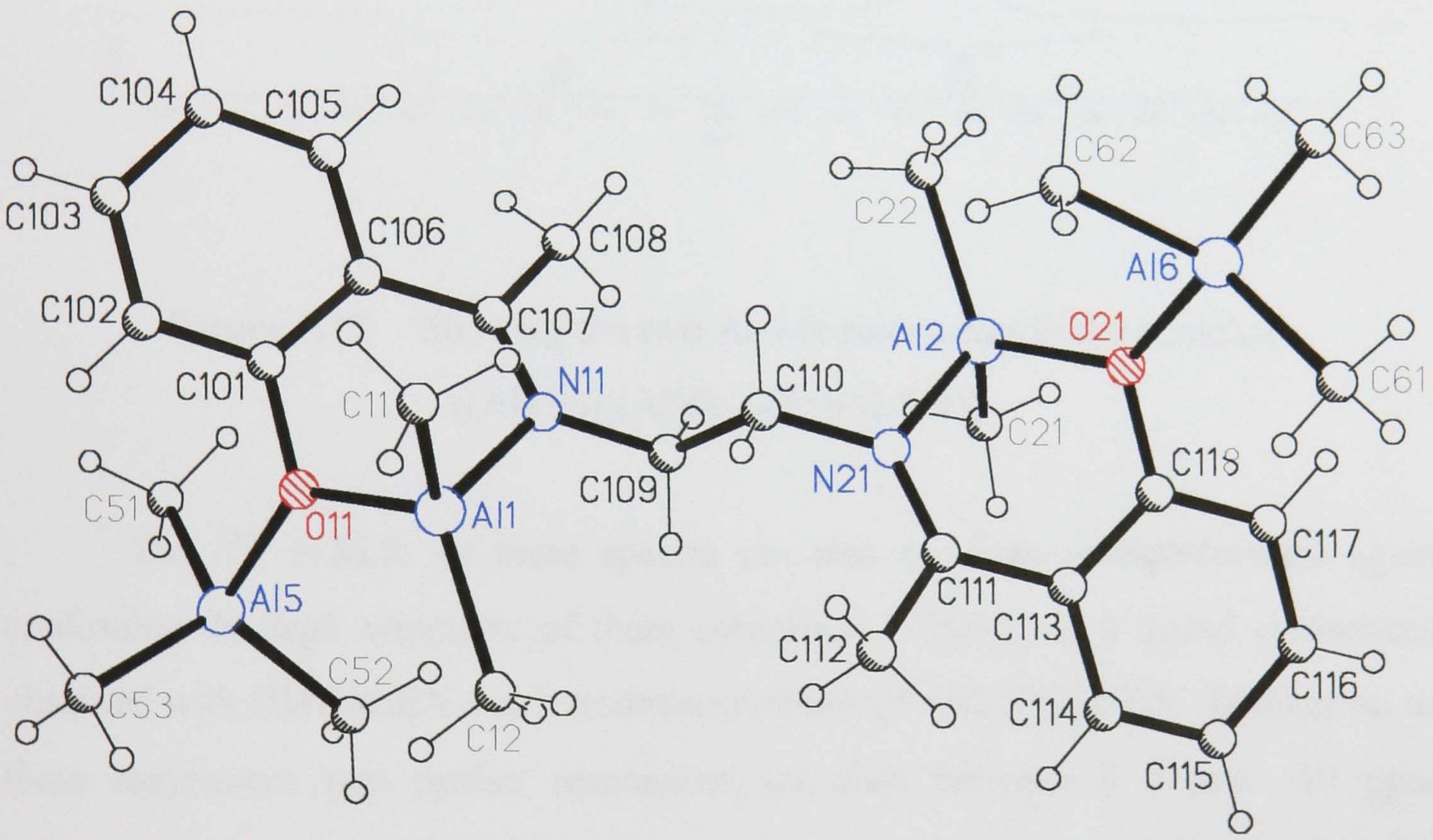

Figure 3.16 The molecular structure of $[Al_2(Me_2)_2(DMSALEN)Al_2(Me_3)_2]$

In the ^{1}H N.M.R. spectra the resonances associated with the ligand appear in the same region as for the free ligands, and there is no splitting of these resonances. There is no splitting of the CH_2–CH_2 backbone resonance in these complexes which is an interesting difference from the splitting observed of this resonance in complexes of the type [AlR(L)], described above.

Two Al–Me resonances are seen of relative integrals 18:12, again consistent with the structure in Figure 3.16. The presence of two Al–Me resonances confirms

the presence of two different aluminium environments and the relative integrals are as expected for the presence of $AlMe_3$ and $AlMe_2$ groups.

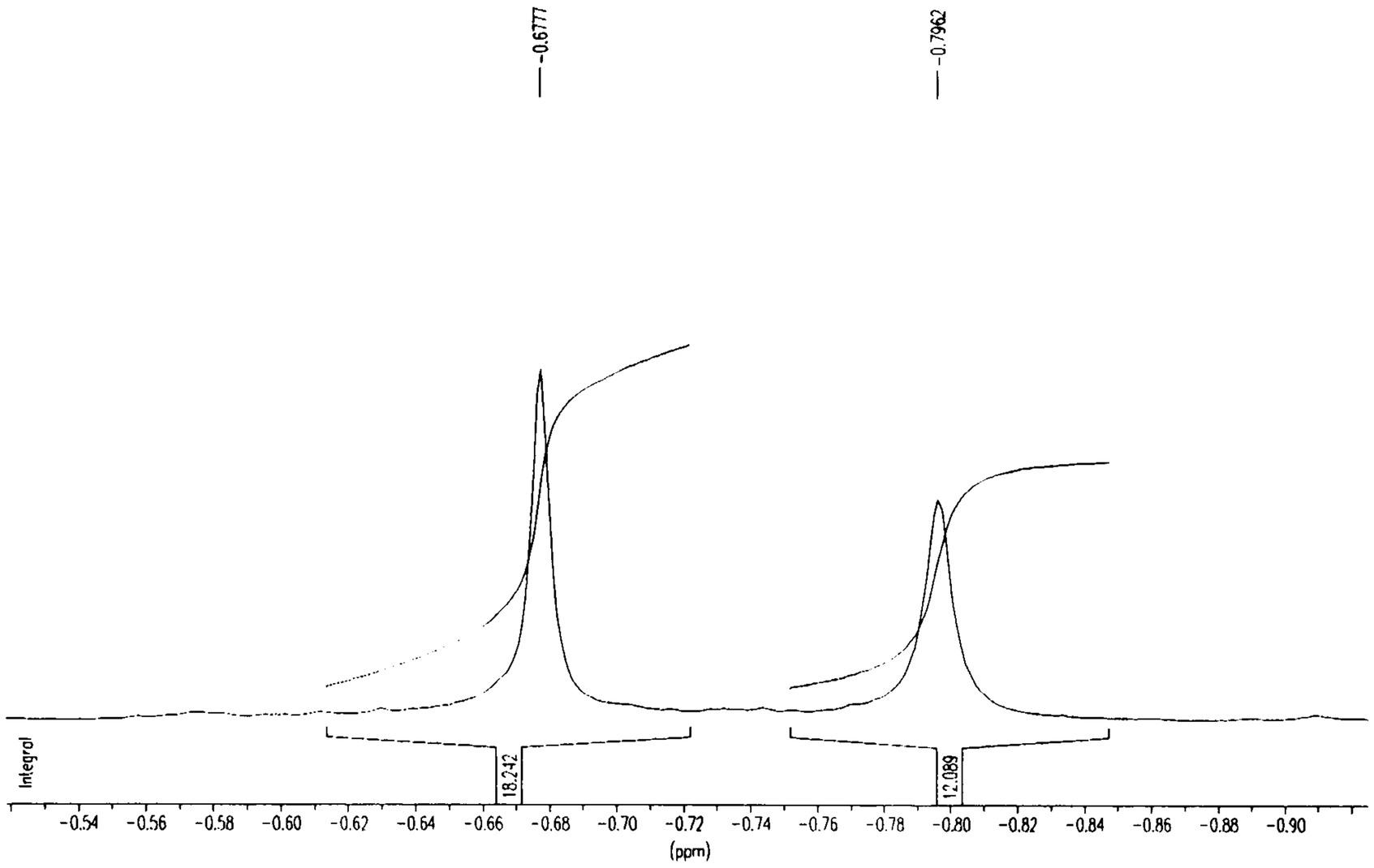

Figure 3.17 Showing the two Al–Me resonances in the complex $[(AlMe_2)_2(AlMe_3)_2(EtSALEN)]$.

The ^{13}C N.M.R. of these spectra are also relatively straightforward again confirming the high symmetry of these complexes. There are 8 ligand resonances observed with DMSALEN and 9 resonances observed with EtSALEN. In addition to these resonances two further resonances are seen between δ 0 and –10 ppm corresponding to the two Al–Me groups within the complexes. Full details of the ^{1}H and ^{13}C N.M.R. spectra of these complexes are reported in the experimental section of this Chapter.

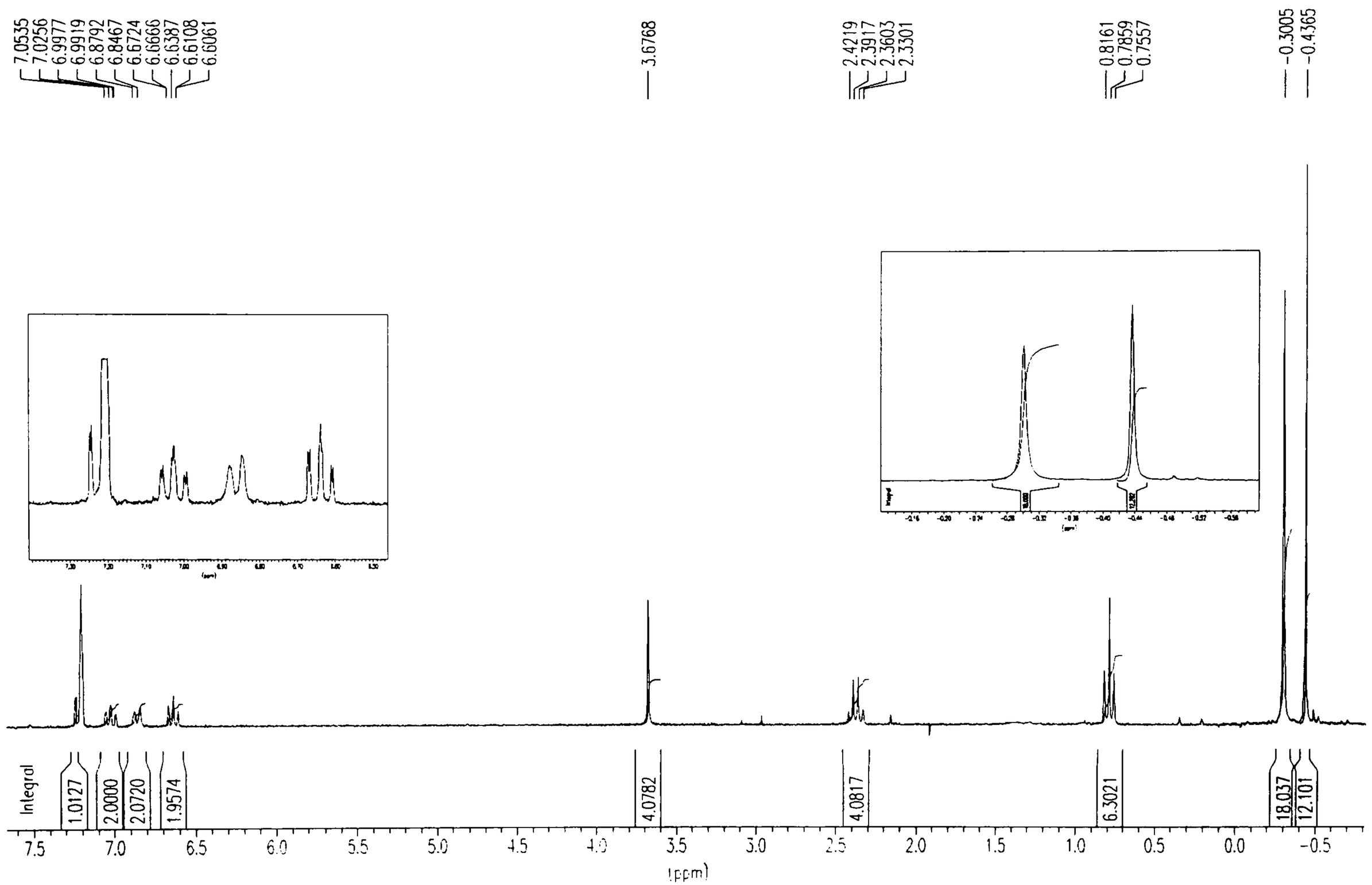

Figure 3.18 The ^{1}H N.M.R spectrum of $[(AlMe_2)_2(AlMe_3)_2(EtSALEN)]$.

Attempted alkylation of $[M(L)Cl_2]$ by reaction with RMgX

Alkylation of $[M(L)Cl_2]$ Group 4 tetradentate Schiff base complexes was attempted to produce new complexes of the type $[(L)MR_2]$. Despite the availability of $[M(L)Cl_2]$ complexes, alkyl derivatives are rare. Floriani *et al*[114] found that the alkylation chemistry of $[Ti(SALEN)Cl_2]$ is highly dependent on the nature of the alkylating agent and solvent. Thus reaction of $[Ti(SALEN)Cl_2]$ with MeLi in non–polar aromatic solvents yields the thermally unstable dimethyl derivative *trans*–$[Ti(SALEN)Me_2]$. However, the use of Grignard reagents leads to alkylation of the SALEN imine carbon or the formation of reduced Ti(III) products depending on the polarity of the solvent.

In order to prevent possible reduction products all attempted reactions were carried out with $[Zr(L)Cl_2]$, and ligands with a substituent (ethyl, phenyl etc.) on the imine carbon were used in the hope that steric effects from this substitution would prevent the alkylation of the ligand.

These reactions were carried out in a variety of solvents (toluene, THF, hexane) and at a range of temperatures (0–120 °C) using both MeLi and Grignard reagents (e.g. $PhCH_2MgCl$) as the alkylating reagent. Unfortunately, these reactions afforded a mixture of products which could not be separated or properly characterised. It is likely that the products contain both cis and trans isomers as well as alkyl migration products described in Chapter 2. The N.M.R. spectra show that complex product mixtures are formed. Similar problems with the ligand H_2ACEN have also been encountered by Jordan *et al*.[83]

Experimental

Again all reactions were carried out in a dry nitrogen or argon atmosphere using conventional Schlenk apparatus and techniques. All solvents were carefully dried using either calcium hydride or sodium metal,and glassware was stored in a hot oven.

Preparation of [(L)$MCl_2Al_2Me_6$] *complexes (where M* = Ti, Zr*; L* = DMSALEN, EtSALEN)

The Group 4 metal complex [M(L)Cl_2], (0.5 g) was placed into a dry Schlenk tube charged with a magnetic follower and suspended in dry toluene (30 cm^3). This solution was then cooled to –5 °C. To this suspension was slowly added 2 molar equivalents of $AlMe_3$ using a syringe. After complete addition the Group 4 metal complex completely dissolved, yielding a deep red solution. This solution was stirred at 0 °C for 1 h, after which time the solution was filtered (cold) to remove any impurities, and the filtrate was evaporated to dryness. This yielded a brown solid (40%)

[Zr(DMSALEN)$Cl_2(AlMe_3)_2$]:

^{1}H N.M.R (C_6D_6) δ/ppm: 7.37–7.21 (m, 8H); 4.14 (s, 4H); 2.82 (s, 6H); –0.68 (s, 9H); –0.77 (s, 9H): ^{13}C N.M.R (C_6D_6) δ/ppm: 118.42, 135.10, 129.81, 129.09, 128.29, 125.37, 125.22, 48.75, 21.29, –6.87, –10.66

[Ti(DMSALEN)$Cl_2(AlMe_3)_2$]:

^{1}H N.M.R (C_6D_6) δ/ppm: 7.15–6.62 (m, 8H); 4.11 (s, 4H); 2.54 (s, 6H); –0.34 (s, 9H); –0.53 (s, 9H): ^{13}C N.M.R (C_6D_6) δ/ppm: 180.29,134.90, 129.33, 128.64, 125.83, 124.32, 124.04, 48.41, 20.96, –6.94, –10.03

[Zr(EtSALEN)$Cl_2(AlMe_3)_2$]:

^{1}H N.M.R (C_6D_6) δ/ppm: 7.71–7.19 (m, 8H); 4.15 (s, 4H); 3.19–3.10 (q, 4H); 1.35–1.29 (t, 6H); –0.67 (s, 9H); –0.78 (s, 9H): ^{13}C N.M.R (C_6D_6) δ/ppm: 186.05, 135.13, 129.53, 129.10, 128.29, 125.36, 125.30, 48.84, 25.62, 12.18, –10.52, –10.63

[Ti(EtSALEN)Cl_2($AlMe_3$)$_2$]:

^{1}H N.M.R (C_6D_6) δ/ppm: 7.20–6.65 (m, 8H); 4.05 (s, 4H); 2.55–2.46 (q, 4H); 1.00–0.92 (t, 6H); –0.21 (s, 9H); –0.41 (s, 9H): ^{13}C N.M.R (C_6D_6) δ/ppm: 185.97, 134.51, 128.77, 128.07, 125.03, 124.81, 124.32, 48.56, 24.99, 11.74, –6.33, –10.43

General method for the preparation of* [Al(L)R] *complexes

The free ligand, L, (1.0 g) was placed into a dry Schlenk tube charged with a magnetic follower and suspended in dry toluene (30 cm^3). This solution was then cooled to –78 °C. An equimolar amount of AlR_3 (R = Me, Et) was added slowly via a syringe, and the reaction mixture allowed to warm to room temperature. The solution was then refluxed for 2 h, cooled and the product filtered off and dried *in vacuo*. This crude product was recrystallised from benzene, and the 1:1 product isolated and characterised by the usual methods.

***Preparation of* [Al(DMSALEN)Me]**

Procedure as for [Al(L)R] above, using H_2DMSALEN and aluminium trimethyl.

^{1}H N.M.R ($CDCl_3$) δ/ppm: 7.53–6.65 (m, 8H); 3.94–3.75 (m, 4H); 2.51 (s, 6H); –1.15 (s, 3H): ^{13}C N.M.R ($CDCl_3$) δ/ppm: 175.02, 164.94, 134.28, 129.11, 123.73, 120.47, 115.81, 48.29, 18.29, 3.24

***Preparation of* [Al(DMSALEN)Et]**

Procedure as for [Al(L)R] above, using H_2DMSALEN and aluminium triethyl.

^{1}H N.M.R ($CDCl_3$) δ/ppm: 7.51–6.66 (m, 8H); 3.89–3.74 (m, 4H); 2.48 (s, 6H); 0.75–0.69 (q, 4H); –0.28–(–0.40) (t, 6H): ^{13}C N.M.R ($CDCl_3$) δ/ppm: 175.76, 164.86, 134.08, 129.23, 123.54, 120.34, 116.02, 47.99, 18.40, 10.41, 9.92

***Preparation of* [Al(EtSALEN)Me]**

Procedure as for [Al(L)R] above, using H_2EtSALEN and aluminium trimethyl.

^{1}H N.M.R ($CDCl_3$) δ/ppm: 7.29–6.65 (m, 8H); 4.00–3.74 (m, 4H); 2.99–2.84 (m, 4H); 1.32–1.25 (m, 6H); –1.10 (s, 3H): ^{13}C N.M.R ($CDCl_3$) δ/ppm: 179.18, 165.66, 134.31, 128.97, 124.03, 118.83, 115.94, 47.62, 23.97, 11.95, 7.09

***Preparation of* [Al(EtSALEN)Et]**

Procedure as for [Al(L)R] above, using H_2EtSALEN and aluminium triethyl.

^{1}H N.M.R ($CDCl_3$) δ/ppm: 7.23–6.58 (m, 8H); 3.97–3.75 (m, 4H); 3.00–2.84 (m, 4H); 1.33–1.27 (m, 6H); 0.71–0.65 (q, 4H); –0.34–(–0.44) (t, 6H): ^{13}C N.M.R ($CDCl_3$) δ/ppm: 179.38, 165.95, 134.28, 128.93, 123.96, 118.96, 115.86, 47.72, 24.01, 12.00, 10.19

***Preparation of* [Al(PhSALEN)Me]**

Procedure as for [Al(L)R] above, using H_2PhSALEN and aluminium trimethyl.

^{1}H N.M.R ($CDCl_3$) δ/ppm: 7.34–6.48 (m, 8H); 3.60–3.46 (m, 2H); 3.25–3.11 (m, 2H); 7.49–7.14 (m, 10H); –0.83 (s, 3H): ^{13}C N.M.R ($CDCl_3$) δ/ppm: 177.25, 166.13, 135.67, 129.05, 123.29, 120.10, 115.65, 50.54, 135.67, 133.18, 128.94, 126.44, 21.38

***Preparation of* [Al(PhSALEN)Et]**

Procedure as for [Al(L)R] above, using H_2PhSALEN and aluminium triethyl.

^{1}H N.M.R ($CDCl_3$) δ/ppm: 7.32–6.46 (m, 8H); 3.56–3.42 (m, 2H); 3.25–3.11 (m, 2H); 7.48–7.06 (m, 10H); 0.94–0.88 (q, 4H); –0.08–(–0.17) (t, 6H): ^{13}C N.M.R ($CDCl_3$) δ/ppm: 177.47, 166.41, 134.87, 133.15, 123.21, 120.19, 115.56, 50.56, 135.72, 129.05, 128.94, 126.44, 10.42, 9.85

Preparation of* [Al_4Me_{10}(L)] *(where L* = H_2DMSALEN, H_2EtSALEN*)

The free ligand, L, (1.0 g) was placed into a dry Schlenk tube charged with a magnetic follower and suspended in dry toluene (50 cm^3). This solution was then cooled to –78 °C. To this solution was slowly added 4 molar equivalents of $AlMe_3$. This reaction mixture was allowed to warm to room temperature yielding a white precipitate. This resultant reaction mixture was then heated at > 80 °C for 3 days resulting in a yellow solution. This solution was filtered warm to remove any impurities and the yellow filtrate was evaporated to dryness resulting in a white solid.

$[Al_4Me_{10}(DMSALEN)]$:

^1H N.M.R (C_6D_6) δ/ppm: 7.42–7.38 (dd, 2H); 7.31–7.25 (dt, 2H); 7.01–6.97 (dd, 2H); 6.62–6.58 (dt, 2H); 3.62 (s, 4H); 2.07 (s, 6H); –0.27 (s, 9H); –0.46 (s, 9H): ^{13}C N.M.R (C_6D_6) δ/ppm: 177.04, 163.75, 134.54, 129.39, 123.31, 120.87, 116.09, 47.14, 18.29, –6.28

$[Al_4Me_{10}(EtSALEN)]$:

^1H N.M.R (C_6D_6) δ/ppm: 7.25–7.20 (dd, 2H); 7.05–6.99 (dt, 2H); 6.87–6.84 (dd, 2H); 6.67–6.60 (dt, 2H); 3.67(s, 4H); 2.42–2.33 (q, 4H); 0.81–0.75 (t, 6H); –0.30 (s, 18H); –0.43 (s, 12H): ^{13}C N.M.R (C_6D_6) δ/ppm: 180.11, 164.86, 134.87, 129.55, 124.19, 118.56, 116.47, 47.93, 22.36, 11.21, –6.07

CHAPTER 4

Group 4 Metal Complexes of Tetraazaannulene Macrocyclic Ligands

CHAPTER 4 Group 4 metal complexes of tetraazaannulene macrocyclic ligands

Introduction

It was mentioned in Chapter 1 that the investigation of other ligand systems, as well as tetradentate Schiff base ligands, would be studied and their potential for use as Ziegler–Natta catalysts investigated. The results obtained from these investigations into the polymerisation of ethene have been compared with results obtained with other ligand systems, and can be found in Chapter 6 of this thesis.

It is believed that such potential catalysts should possess a *cis* configuration of chlorine atoms at the metal centre. Apart from the metallocene compounds such systems are limited. However, one type of ligand system which is capable of producing such a *cis* or pseudo–*cis* configuration at the metal centre is based on macrocyclic ligands (see introduction p.29). One class of macrocyclic ligands which are potentially of interest because of their ability to form *cis* complexes are the tetraazaannulene ligands.

The tetraazaannulene macrocyclic ligands studied in this chapter are 5,7,12,14–tetramethyldibenzo[b,i][1,4,8,11]tetraazacyclotetradecine, (H_2tmtaa) (I) and 2,3,6,8,11,12,15,17–octamethyl–5,14–dihydro–5,9,14,18–tetrazadibenzo–[a,h]–cyclo –tetradecine, (H_2omtaa) (II).

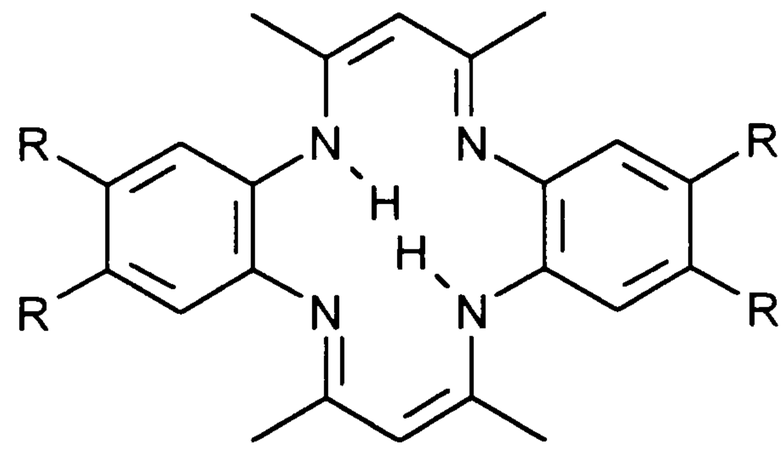

R = H = H_2tmtaa (I)

R = Me = H_2omtaa (II)

Figure 4.1 Diagrammatic representation of the free ligands H_2tmtaa and H_2omtaa

Studies of H_2tmtaa (Figure 4.1) are well documented,[146] and H_2tmtaa has been found to form complexes with both main group and transition metals. In most of these reported complexes, the structure shows the coordinated metal possesses an unusual stereochemistry.

These ligands share a number of common features with porphyrins and phthalocyanine ligands, although they possess some important differences. The principle similarities and differences between H_2tmtaa and porphyrin systems have been summarised.[146,147] The similarities are: (1) the four nitrogen atoms of H_2tmtaa are confined to a planar arrangement. (2) upon metal complexation, the ligand usually loses two protons to form a dianion. (3) this dianion possesses a completely conjugated system of double bonds. The differences are: (1) the 14–membered ring of H_2tmtaa, as compared to the larger 16–membered porphyrin ring, leads to a shorter than ideal metal–nitrogen distance. The N–Ct distance (defined as half the average distance between two diagonally opposite N atoms) for the neutral atom is about 1.902 Å,[146] and for the dianion is expected to lie in the range 1.85–1.87 Å.[148] These values compare with the corresponding value of about 2.01 Å in porphyrins.[149] (2) in contrast to porphyrins, the anionic charges are not delocalised over the entire ligand framework, but are essentially localised within the two six–membered 2,4–pentanediiminato chelate rings. (3) although the ligand framework of the dianion is completely conjugated, the π–system is an antiaromatic (4n) and not, as in the porphyrins, an aromatic (4n+2) π electron system.

The rigid structure of the tmtaa type of ligand imposes a number of interesting steric features which dictate the structure of complexes formed. Ligands (I) and (II) possess three special steric features which dictate their reactivity and coordination geometry: (1) their core size (previously mentioned). (2) a saddle–shape conformation is produced by internal steric restraints between the methyl groups and the benzenoid ring which results in the nitrogen lone pairs pointing out on the same side of the macrocycle as the benzenoid rings. This causes displacement of the coordinated metal from the N_4 plane. (3) because the saddle–shape has the benzenoid rings and the diiminate framework displaced in opposite directions, the two remaining axial coordination positions on the metal are not chemically equivalent.

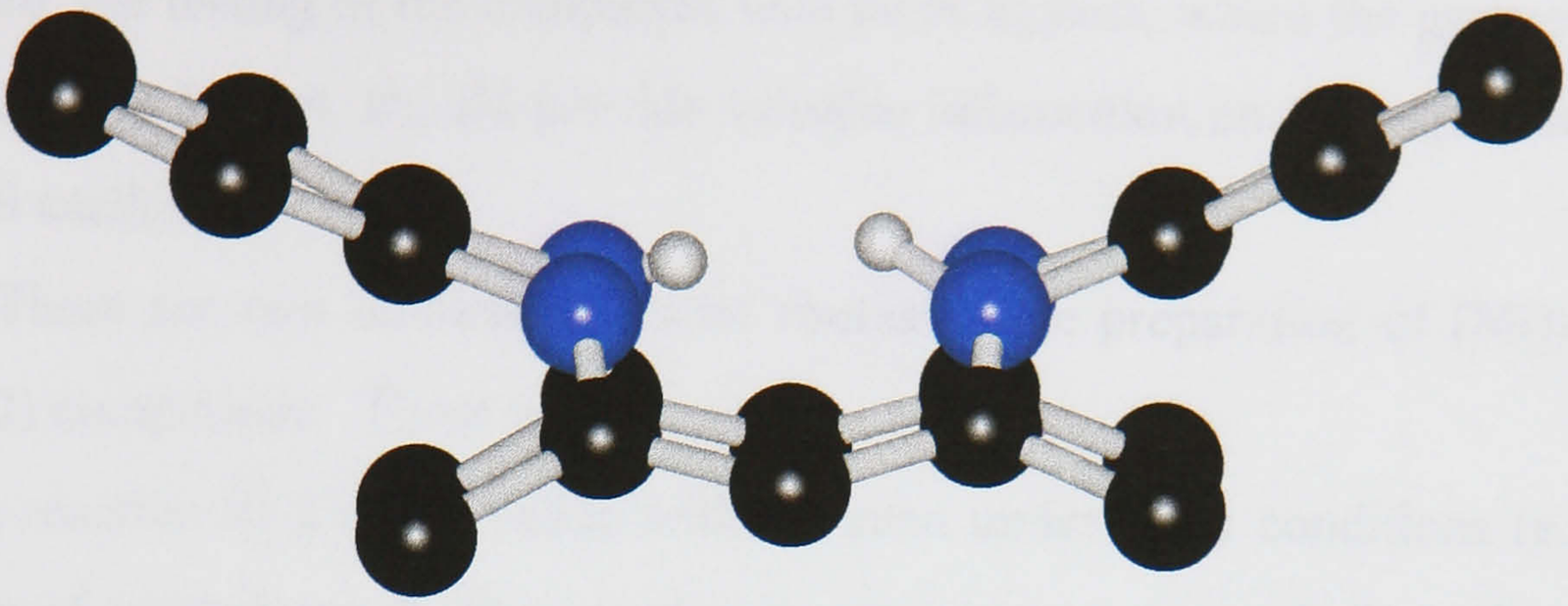

Figure 4.2 The molecular structure of H_2tmtaa showing its saddle–shape

The study of the complexes produced from these ligands provides some insight as to whether increasing steric factors, or the addition of substituents, has any effect on their activity and selectivity as catalysts for polymerisation. There also remains a great deal of scope for further substitution within the ligand framework if interesting or promising results are obtained from the polymerisation studies.

Group 4 transition metal complexes

The main reason behind targeting complexes of these two ligands for their potential as Ziegler–Natta catalysts is because [M(tmtaa)Cl_2] complexes are known to have the two chlorine atoms in a *cis* configuration. In the case of [Ti(tmtaa)Cl_2] the Cl–Ti–Cl bond angle is not exactly 90.0° but is in fact 85.7°.[150] Although these complexes possess a six coordinate metal, the coordination is not octahedral, but instead an unusual stereochemistry is observed due to the steric influences imposed by the ligand, with the metal sitting above the N_4 plane by as much as 1 Å. It is of interest to note that the Ti–Cl bond length of 2.323Å is comparable to the corresponding Ti–Cl bond length of 2.341Å in the metallocene complex [Cp_2TiCl_2],[3] and that the cavity provided for the metal by the two *cis* chlorine atoms and the conformation of the ligand resembles that found in [Cp_2MX_2]complexes.[151,152]

Therefore, the testing of the complexes with these ligands, where the geometry at the metal centre is known, should provide valuable information on the requirements of a potential catalyst.

There are two efficient synthetic routes to the preparation of $[M(tmtaa)Cl_n]$ (n = 1, 2) compounds. These are:

(1) The reaction of a metal halide with H_2tmtaa under basic conditions (e.g. in the presence of triethylamine). The reaction is carried out in acetonitrile under refluxing conditions:

$$MCl_4 + H_2tmtaa \longrightarrow [M(tmtaa)Cl_2] + 2\,(NEt_3H)Cl \qquad (1)$$

(2) The reaction of a metal halide with the dilithio salt, Li_2tmtaa. The lithium salt is formed upon reacting an alkyl lithium (e.g. MeLi) with H_2tmtaa in a 2:1 ratio at –10°C in THF. The dilithium salt need not be isolated and can be used *in situ*:

$$H_2tmtaa + 2\,LiR \longrightarrow Li_2(tmtaa) + 2\,RH \qquad (2)$$

$$Li_2(tmtaa) + MCl_4 \longrightarrow [M(tmtaa)Cl_2] + 2\,LiCl \qquad (3)$$

Goedken and co–workers synthesised $[Ti(tmtaa)Cl_2]$[150] and other $[Ti(tmtaa)(R)_n]$[153] type compounds (where R = O, S; n = 1 or 2). The synthesis of $[Ti(tmtaa)Cl_2]$ was carried out by the reaction of $TiCl_4$ with H_2tmtaa under basic conditions resulting in the formation of molecular $[Ti(tmtaa)Cl_2]$ (equation (1), M = Ti). This moisture–sensitive complex, then undergoes a variety of reported reactions under different reaction conditions (Scheme 4.1)

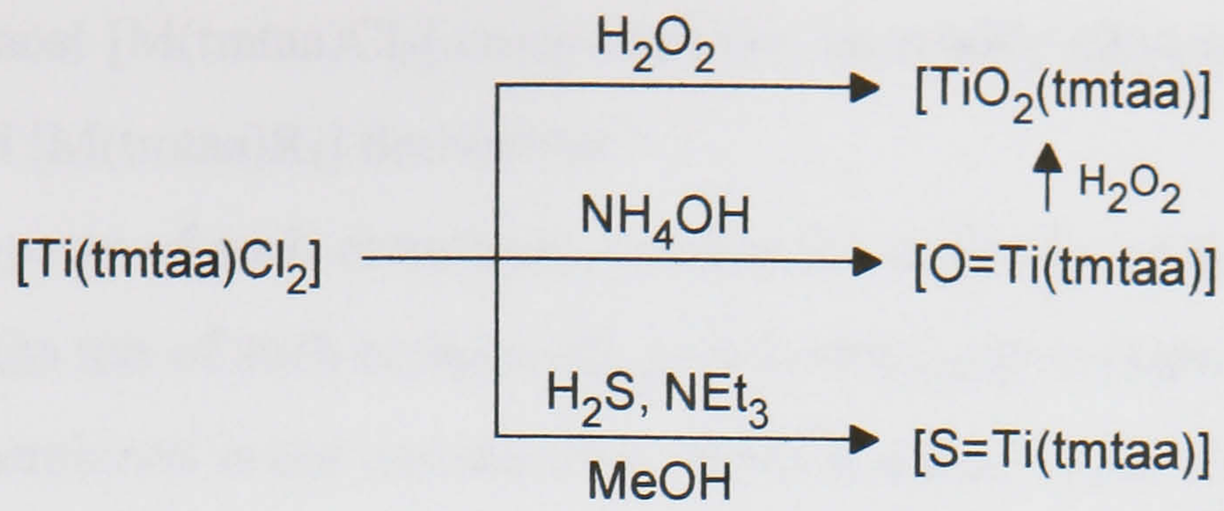

Scheme 4.1 Some of the reactions of $[Ti(tmtaa)Cl_2]$

Since then, more early transition metal complexes of the type $[M(tmtaa)Cl_2]$ (M = Zr, Nb, etc.) have been synthesised.[154-159]

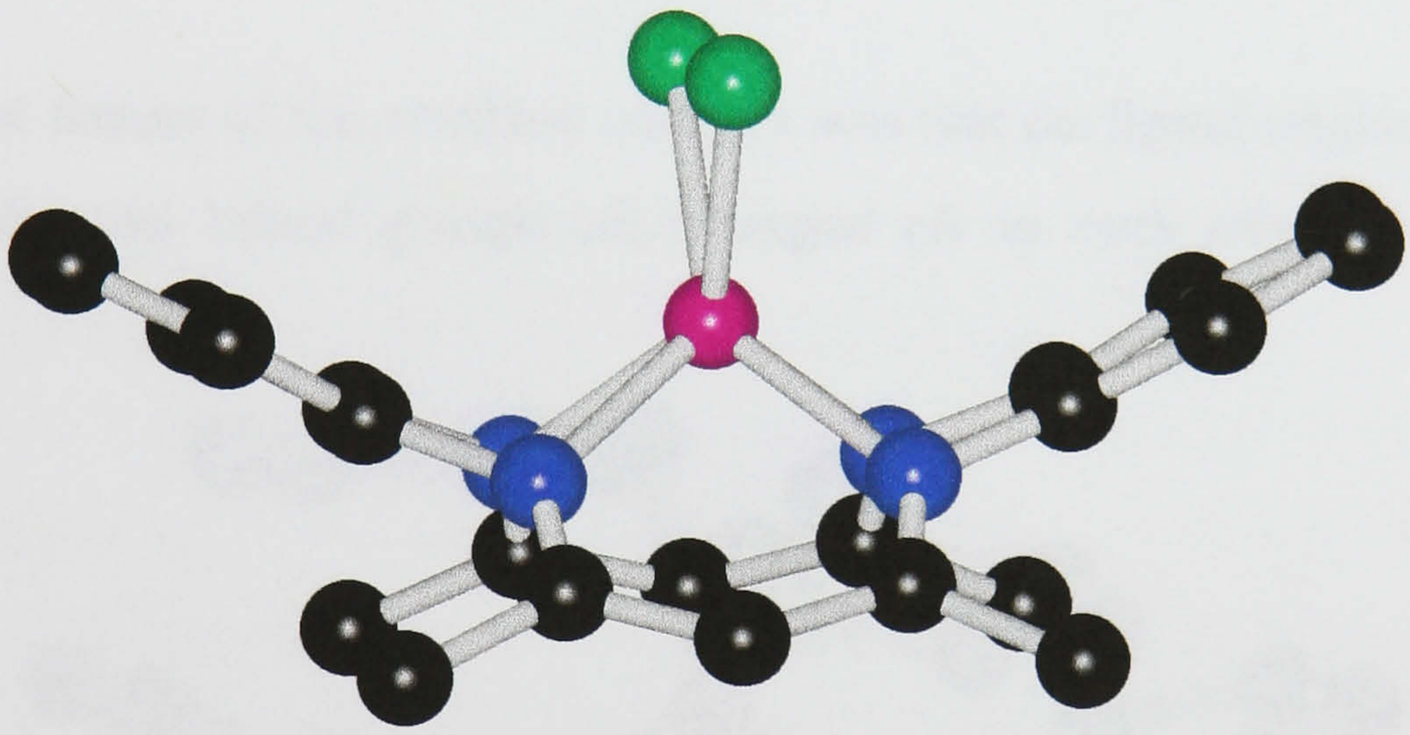

Figure 4.3 The molecular structure of $[Ti(tmtaa)Cl_2]$[138]

These complexes possess two important features, the first is that the metal cannot be accommodated within the N_4 plane of the ligand and therefore lies out of the N_4 plane. This feature of the ligand, as has been mentioned earlier, is due to the steric interactions between the methyl and phenyl groups of the ligand causing the saddle–shape of the ligand which forces the metal out of the N_4 plane. The degree of the metal displacement is a function of the size of the metal ion, the larger the metal ion the larger the displacement. This can be seen by comparing the complexes $[Zr(tmtaa)Cl_2]$ and $[Ti(tmtaa)Cl_2]$, where the zirconium is displaced 1.070 Å out of the N_4 plane whereas the smaller titanium is only displaced by 0.91 Å. The second

feature is that most [M(tmtaa)Cl_2] complexes can be readily alkylated with Grignard reagents to yield [M(tmtaa)R_2] derivatives.

This property of such complexes, namely the reactivity of the M–Cl bond, is of relevance to the use of such compounds as potential polymerisation catalysts. This is because, as mentioned in the introduction, MAO is added to the Group 4 derivative in the polymerisation reaction, and as a result the formation of Group 4 metal alkyl complexes is facilitated under these conditions, which aids polymerisation. Floriani *et al* first observed this with Group 4 transition metals when they reported the synthesis of [Zr(tmtaa)Cl_2] and its alkylation with $PhCH_2MgCl$.[154]

$$[Zr(tmtaa)Cl_2] + PhCH_2MgCl \longrightarrow [Zr(tmtaa)(CH_2Ph)_2] + MgCl_2 \quad (4)$$

An important feature of this resultant complex was that the ligand retained its saddle–shape and the two benzyl groups are arranged *cis* to each other at an angle of 80.1(4)°.

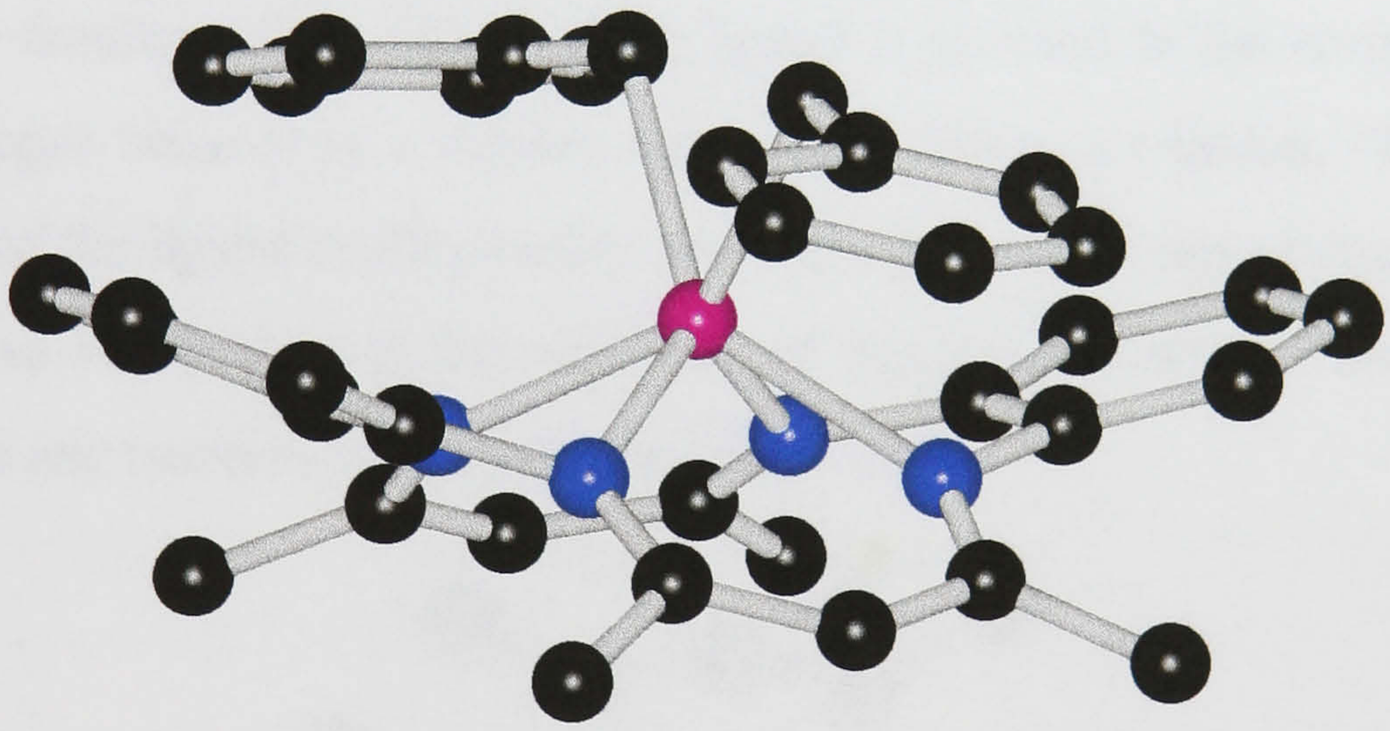

Figure 4.4 The molecular structure of [Zr(tmtaa)$(CH_2Ph)_2$]

This retention of conformation upon alkylation of the M–Cl bond was seen as further proof that these ligands could be of great potential as Ziegler–Natta catalysts. One of the reasons for the resilience of these ligands and their resulting complexes is the macrocyclic effect (see introduction). In this study, the complexes [Ti(tmtaa)Cl_2], [Zr(tmtaa)Cl_2], [Ti(omtaa)Cl_2] and [Zr(omtaa)Cl_2] have been studied for their catalytic ability, and we have found that these compounds do act as polymerisation catalysts. The results are reported in Chapter 6. Since Floriani *et al*[154] reported the

reactions in Scheme 4.1 and equation (4), a variety of other reactions have been reported.[160,161] These include the reactions of NH_4OH and H_2S with $[Ti(tmtaa)Cl_2]$ producing the nucleophilic oxo and sulphido complexes, [(tmtaa)Ti=O] and [(tmtaa)Ti=S] respectively, from which compounds further derivative chemistry has been studied.

In view of the earlier investigations of this type, it came as a surprise that during the attempted alkylation of $[Zr(tmtaa)Cl_2]$ with MeMgI by Floriani *et al*,[156] it was discovered that instead of the expected alkylation of the two Zr–Cl bonds the ligand itself undergoes a transformation (equation 5).

$$[Zr(tmtaa)Cl_2] + MeMgI \longrightarrow [(Me)Zr(tmtaa\text{–}\overset{*}{Me})(THF)] + MgCl_2 \quad (5)$$

The reaction results in the methylation of an imine carbon within the ligand, and the formation of [(Me)Zr(tmtaa–$\overset{*}{Me}$)(THF)] (Figure 4.5). It is not known whether this is direct alkylation at the imino group or of a methyl migration from the metal to the ligand. The familiar saddle–shape of the ligand is retained in the complex, but the ligand no longer behaves as a dianion but instead acts as a trianion. This potential methylation of the ligand could possibly provide a problem in any attempted catalytic polymerisation reactions, and the reactivity of the imine bond has therefore to be recognised in any reactions of these complexes.

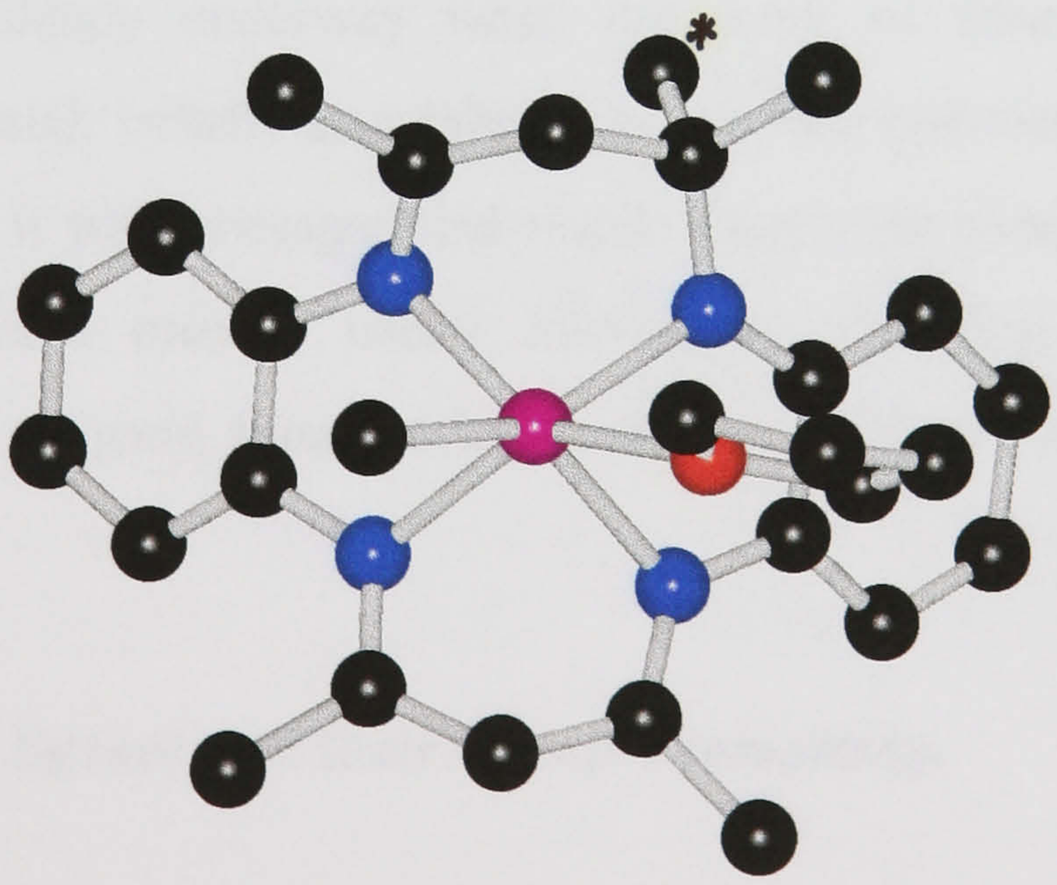

Figure 4.5 The molecular structure of [(Me)Zr(tmtaa–Me*) (THF)]

(Me* = methyl group substituted into the ligand backbone)

More recently the work of Jordan *et al*[82] has involved the study of tetraazamacrocycles as ancillary ligands in early metal alkyl chemistry. The work involves studies with both H_2Me_4taen (Figure 4.6(a)) and H_2omtaa (Figure 4.6(b))

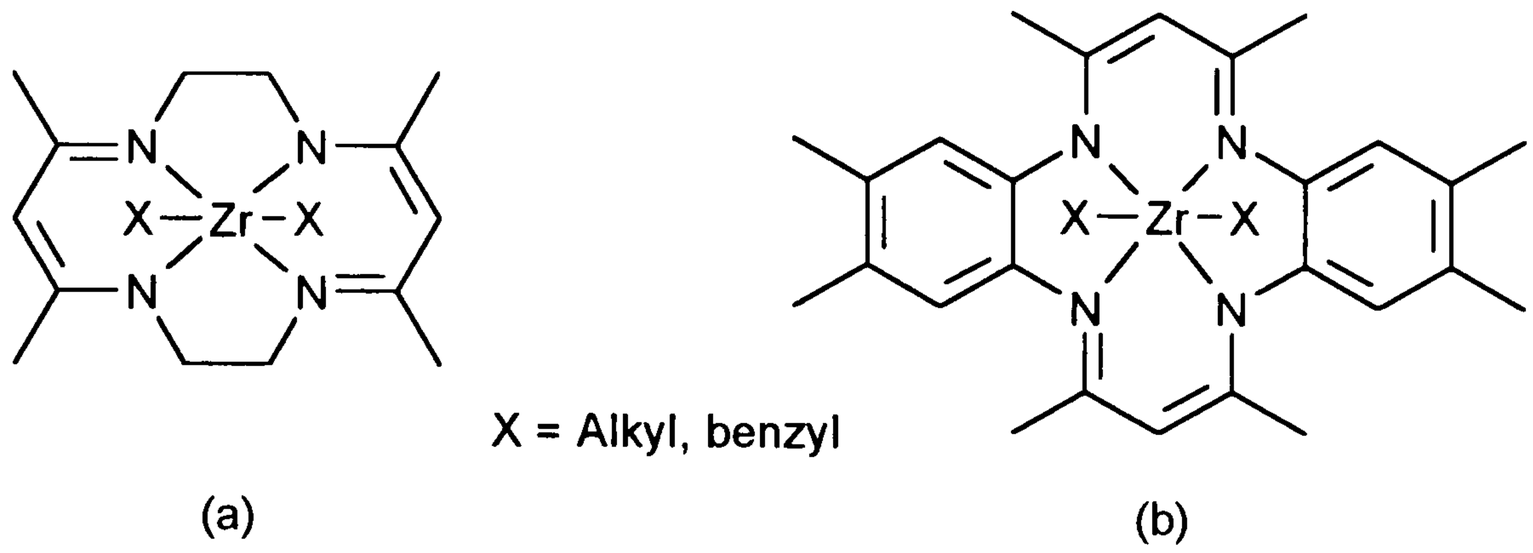

Figure 4.6 A diagrammatic representation of the ZrX_2 complexes formed with the ligands (a) H_2Me_4taen and (b) H_2omtaa

In this work the synthesis of zirconium dialkyl complexes has been carried out by the reaction of the free ligands with the metal tetraalkyl species, which results in the desired complex by direct alkyl elimination. Protonolysis of these complexes with ammonium reagents has yielded $[(L)M(R)]^+$ cations which have been found to insert alkynes and polymerise ethene.

In the present work attempts to synthesise the known $[Ti(tmtaa)Cl_2]$ and $[Zr(tmtaa)Cl_2]$ complexes along with the unknown $[Ti(omtaa)Cl_2]$ and $[Zr(omtaa)Cl_2]$ complexes were already underway when the work of Jordan appeared. The complexes were tested, initially as catalysts for ethylene polymerisation, using MAO as the co–catalyst. It was envisaged that results from these complexes with a known stereochemistry would provide useful information regarding the influence that substitution within a ligand framework has on the catalyst activity and/or rate of polymerisation.

Preparation of the ligands and their Group 4 complexes.

The synthesis of the neutral free ligand H_2tmtaa was carried out by the reported Ni(II) template reaction (Scheme 4.2).[162]

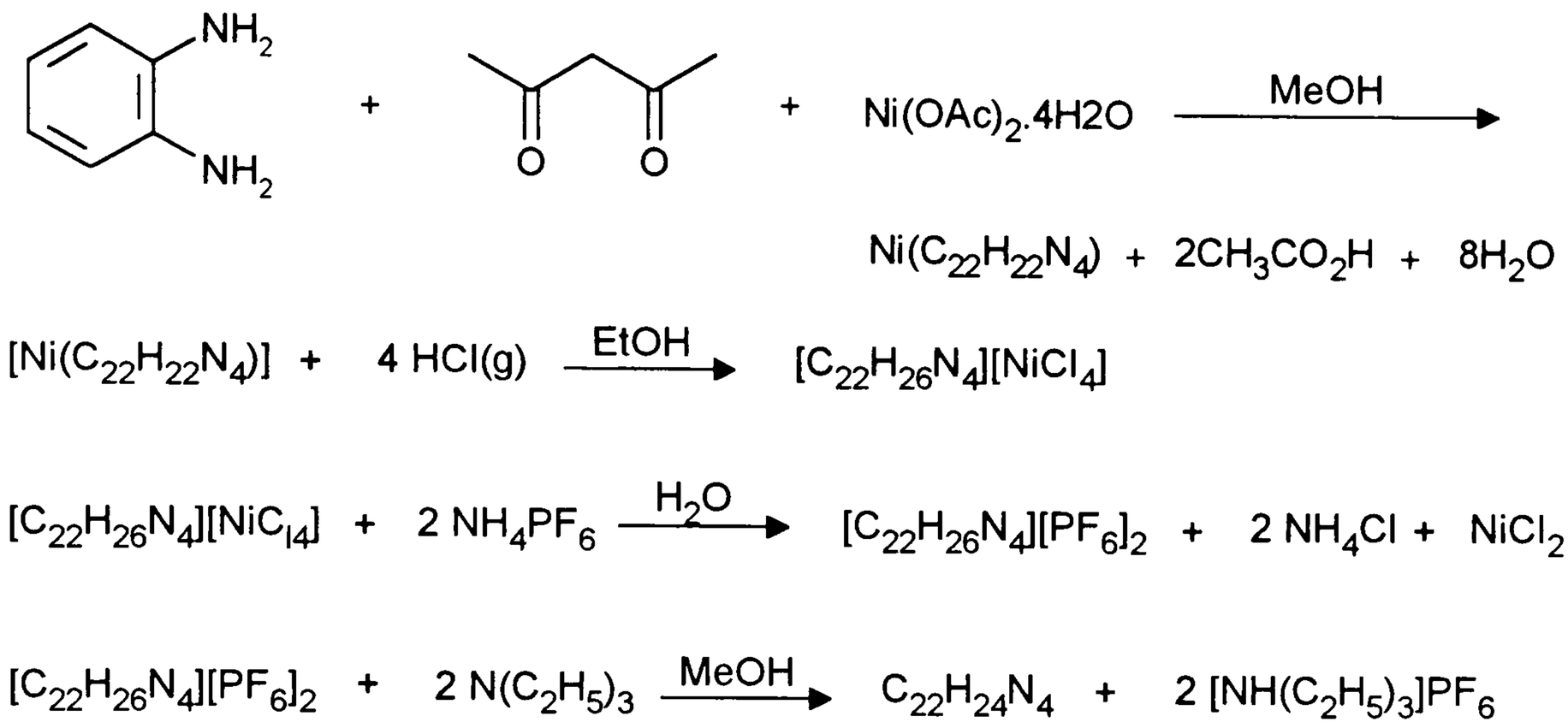

Scheme 4.2 Showing the synthetic route for the preparation of H_2tmtaa

The free ligand is isolated as yellow/orange crystals and has been fully characterised in this work by ^{1}H and ^{13}C N.M.R. spectroscopy, elemental analysis and mass spectrometry. The ^{1}H and ^{13}C N.M.R. spectra of these ligands consist of only a few resonances due to the high symmetry. Initial efforts were then concentrated on the deprotonation of the ligand

$$H_2tmtaa + 2\,LiR \longrightarrow Li_2(tmtaa) + 2\,RH$$

Time and effort was spent on the preparation and isolation of the dilithium salt of the ligand, Li_2(tmtaa). The reason for this was that the complete conversion to the dilithium salt is essential for the complexation reaction to proceed; however, excess LiR could not be present in the reaction as alkylation at the imine carbon could then complicate the reaction. For this reason the best reaction conditions (temperature, time, solvent, etc.) for the preparation and isolation of the dilithium salt of the ligand, Li_2(tmtaa) were determined. To eliminate any error the alkyllithium solution was always titrated against diphenylacetic acid immediately prior to use to establish the true molarity of the solution.[163] For complete lithiation to occur it was found that exactly 2 moles of MeLi (MeLi due to its greater reactivity was found to work much quicker and cleaner than ^{n}BuLi) with gentle heating (40–50 °C) for 4 hours was

required irrespective of which solvent was used. The dilithium compound, Li_2(tmtaa), is extremely moisture sensitive and therefore great care had to be taken to ensure that all reactions and characterisations were performed using dry solvents and under an inert, dry nitrogen or argon atmosphere. The dilithium complex was isolated as a deep red crystalline solid which readily reforms to the free ligand, H_2tmtaa, if exposed to the air. The dilithium compound was characterised by ^{1}H and ^{13}C N.M.R. spectroscopy and by elemental analyses which confirm the preparation of Li_2tmtaa. The N.M.R. spectra indicate that in Li_2tmtaa the ligand has retained its saddle–shape; Floriani found that recrystallisation from DME results in the structure, [(tmtaa)$_2$Li$_2$(DME)$_3$] which is the only reported structure of a lithium compound with tmtaa.[154]

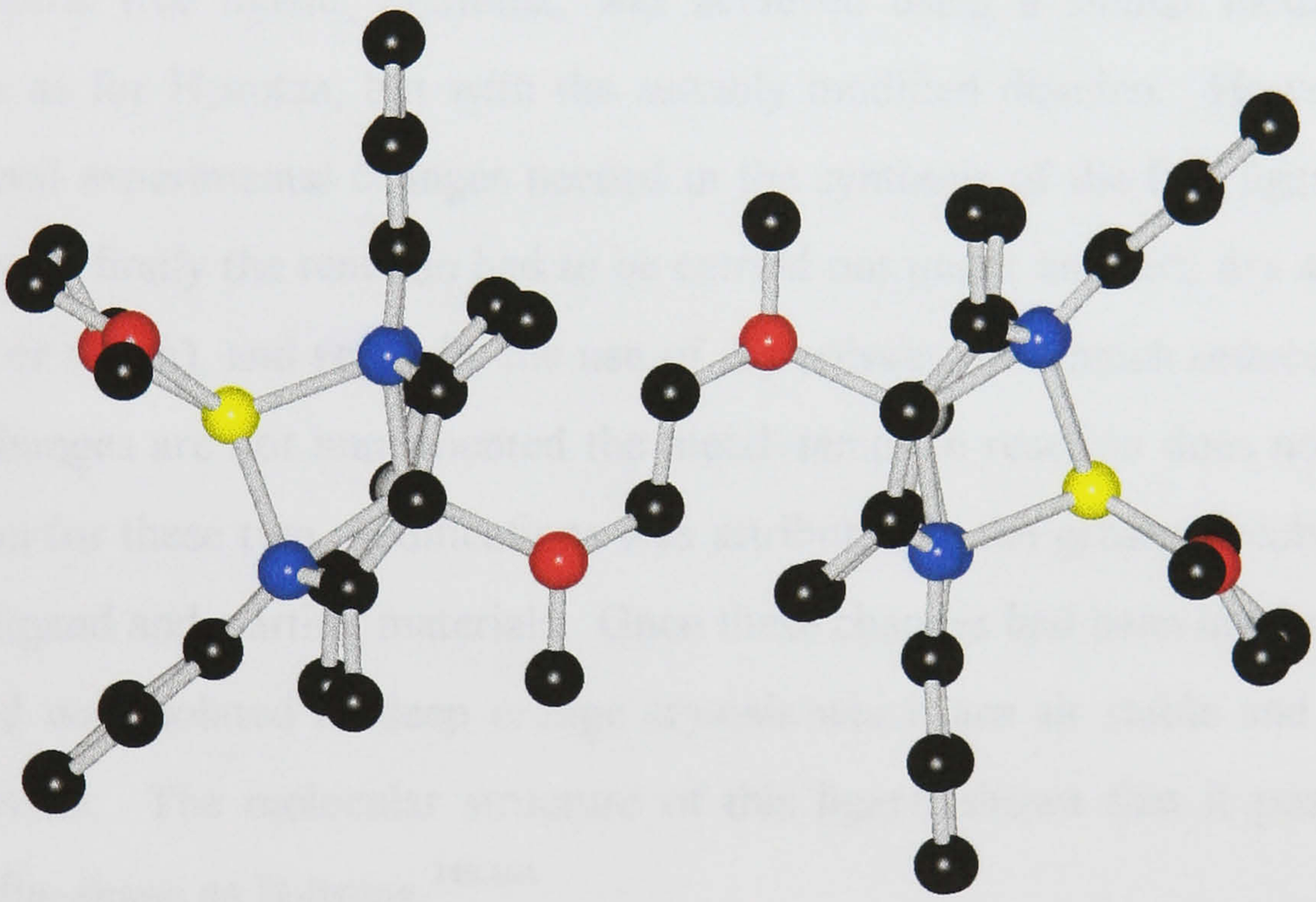

Figure 4.7 The molecular structure of [(tmtaa)$_2$Li$_2$(DME)$_3$] (lithium = yellow)

The *cis* dihalide complexes [Ti(tmtaa)Cl$_2$] and [Zr(tmtaa)Cl$_2$] were then synthesised by the reaction of Li_2(tmtaa) with MCl$_4$.2THF (M = Ti, Zr). The method adopted here is similar to that described elsewhere.[154] These complexes are air sensitive compounds and therefore dry solvents and Schlenk techniques were employed in their preparation using a dry nitrogen or argon atmosphere.

$$H_2\text{tmtaa} + 2\,\text{LiR} \longrightarrow Li_2(\text{tmtaa}) + 2\,\text{RH}$$

$$Li_2(tmtaa) + MCl_4.2THF \longrightarrow [M(tmtaa)Cl_2] + 2\,LiCl$$

(M = Ti, Zr; R = Me)

The THF adduct of the metal tetrahalide ($MCl_4.2THF$) is again used in the complexation reaction, and the solvent of the reaction is dependent upon which metal complex is being prepared. In the case of $[Ti(tmtaa)Cl_2]$ dry benzene solvent is used with the reactant refluxed for 20 h, and for $[Zr(tmtaa)Cl_2]$ dry THF is used as the reaction solvent for 12 h. A problem that was encountered with these complexes was that they had poor solubility in most solvents including CH_2Cl_2.

It was believed that this problem of solubility would be alleviated by the use of the ligand H_2omtaa, due to the presence of the extra methyl groups. The preparation of the neutral free ligand, H_2omtaa, was achieved using a similar metal template procedure as for H_2tmtaa, but with the suitably modified diamine. However, there were several experimental changes needed in the synthesis of the free ligand. These changes were firstly the reaction had to be carried out under an inert, dry atmosphere (nitrogen or argon), and secondly the use of dry solvents in a much reduced volume. If these changes are not implemented the metal–template reaction does not proceed. The reason for these two modifications was attributed to the greater solubility of the resultant ligand and starting materials. Once these changes had been implemented the free ligand was isolated as deep orange crystals which are air stable and soluble in most solvents. The molecular structure of this ligand shows that it possesses the same saddle–shape as H_2tmtaa.[148,164]

The same strategy was used for the preparation of the presumed *cis* dihalide complexes $[Ti(omtaa)Cl_2]$ and $[Zr(omtaa)Cl_2]$.

$$H_2omtaa + 2\,LiMe \longrightarrow Li_2(omtaa) + 2\,CH_4$$

$$Li_2(omtaa) + MCl_4.2THF \longrightarrow [M(omtaa)Cl_2] + 2\,LiCl$$

(M = Ti and Zr)

The preparation of the dilithium salt, $Li_2(omtaa)$, was achieved using the same procedure as for H_2tmtaa. Again time and effort was spent on obtaining the dilithium salt in a pure form by a method that was readily repeated. The dilithium salt was

again isolated as bright red crystals. The best solvent for the reaction was found to be diethyl ether, and again the dilithiating agent used was MeLi. Li_2(omtaa) was again found to be extremely air–sensitive and readily reforms the free ligand if exposed to the air or moisture. The dilithium salt was characterised by ^{1}H and ^{13}C N.M.R. spectroscopy and by elemental analyses which confirm its synthesis. The N.M.R. spectra indicate that the saddle–shape is retained.

Once the dilithiation procedure was established, the synthesis of the two complexes [Ti(omtaa)Cl_2] and [Zr(omtaa)Cl_2] were attempted. Initially the same reaction conditions used for the preparation of the tmtaa complexes were used; however, these conditions were unsuccessful in the isolation of the dihalide metal complexes, and the reasons for this have not been successfully established. These complexes were eventually prepared by the treatment of a diethyl ether suspension of [MCl_4.2THF] chilled at –78 °C with a diethyl ether solution of 2 moles of Li_2(omtaa). On heating this solution, elimination of 2 moles of LiCl occurs, and the metal complexes [M(omtaa)Cl_2] are precipitated. These complexes and lithium chloride are filtered off, and the pure complex is obtained by extensive washing with THF. [Ti(omtaa)Cl_2] is a brown solid at room temperature, whereas [Zr(omtaa)Cl_2] is a golden yellow solid. These compounds were found to be more soluble in solvents, such as $CHCl_3$, CH_2Cl_2, than the corresponding tmtaa compounds, although they still were only moderately soluble in these solvents.

Spectroscopic Properties

N.M.R. Spectra.

The ^{1}H and ^{13}C N.M.R spectra of the compounds provide clear information regarding their symmetry and their purity. Full details of the ^{1}H and ^{13}C N.M.R spectra for individual compounds are given in the experimental section. The ^{1}H spectra of [Zr(tmtaa)Cl_2] and the ^{1}H and ^{13}C spectra of [Zr(omtaa)Cl_2] are shown in Figures 4.8, 4.9 and 4.10. Summaries of the resonances and assignments are given in Tables 4.1 and 4.2.

Table 4.1 Summary of the ^{1}H N.M.R. data (δ/ppm.) for the tmtaa and omtaa compounds. Integrals are given in parenthesis

Compound	NH	ArH	Methine	CH_3	ArMe
H_2tmtaa	12.58(2H)	6.99(8H)	4.87(2H)	2.12(12H)	–
Li_2tmtaa	–	7.00(8H)	4.75(2H)	2.28(12H)	–
[Ti(tmtaa)Cl_2]	–	7.62–7.57(8H)	5.88(2H)	2.65(12H)	–
[Zr(tmtaa)Cl_2]	–	7.64–7.49; 7.23–7.15	5.65; 5.83	2.50(8H); 2.76(4H)	–
H_2omtaa	12.56(2H)	6.76(4H)	4.83(2H)	2.13(12H)	2.22(12H)
Li_2omtaa	–	6.64(4H)	4.52(2H)	2.26(12H)	2.34(12H)
[Ti(omtaa)Cl_2]	–	7.40(4H)	5.82(2H)	2.38(12H)	2.62(12H)
[Zr(omtaa)Cl_2]	–	7.38(4H)	5.59(2H)	2.36(12H)	2.47(12H)

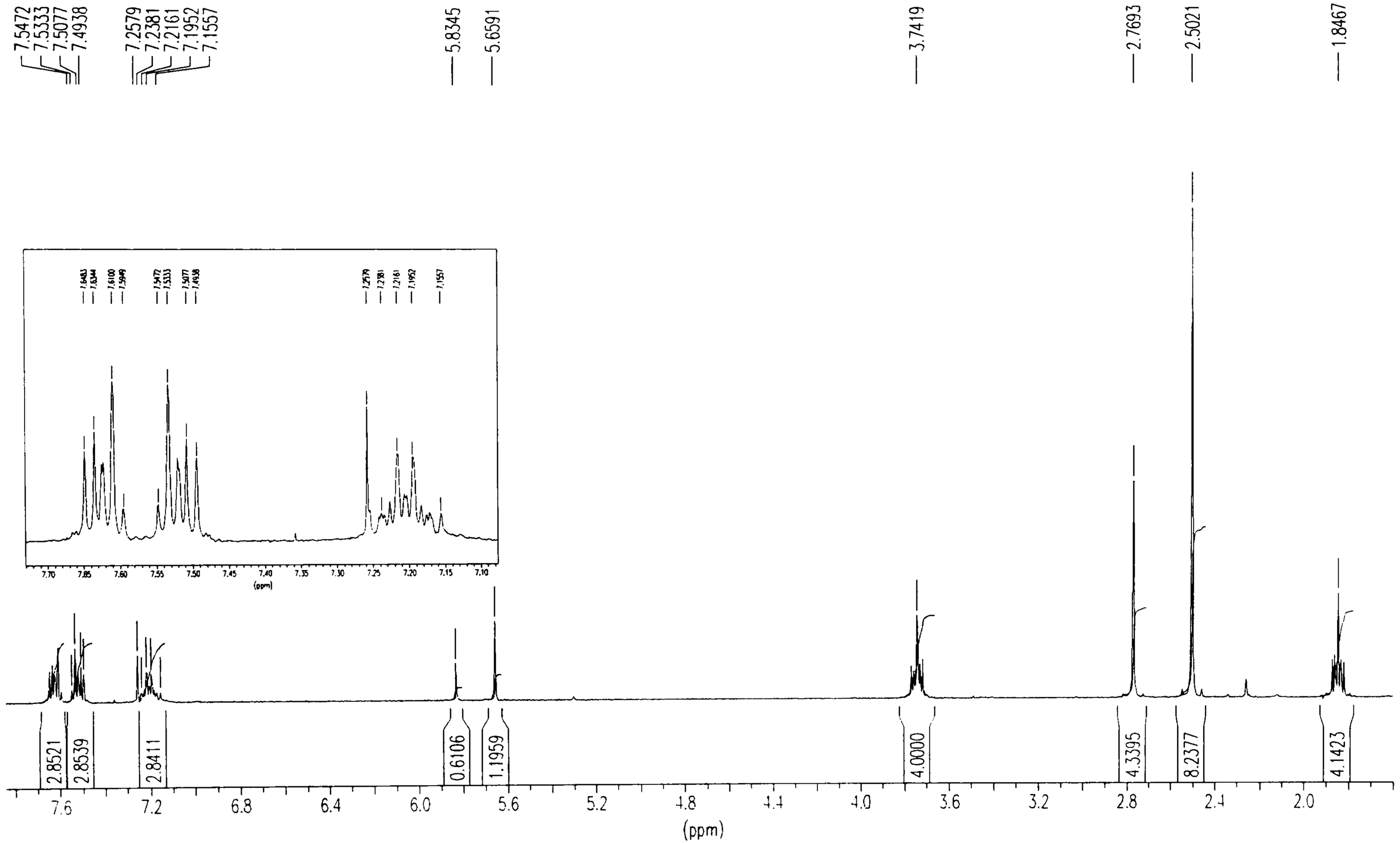

Figure 4.8 The ^{1}H N.M.R. spectrum of $[Zr(tmtaa)Cl_2].2THF$

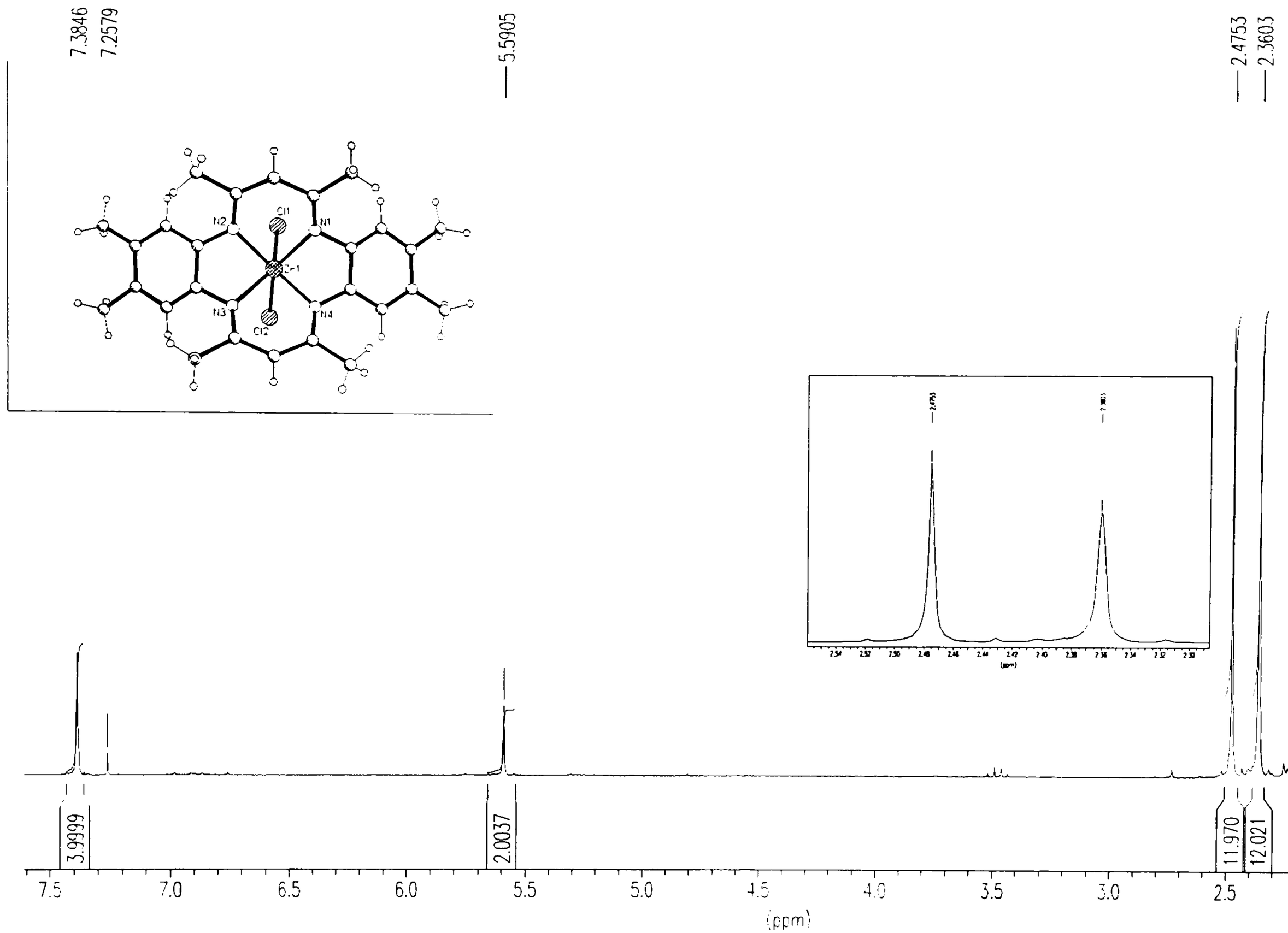

Figure 4.9 The ^{1}H N.M.R. spectrum of $[Zr(omtaa)Cl_2]$

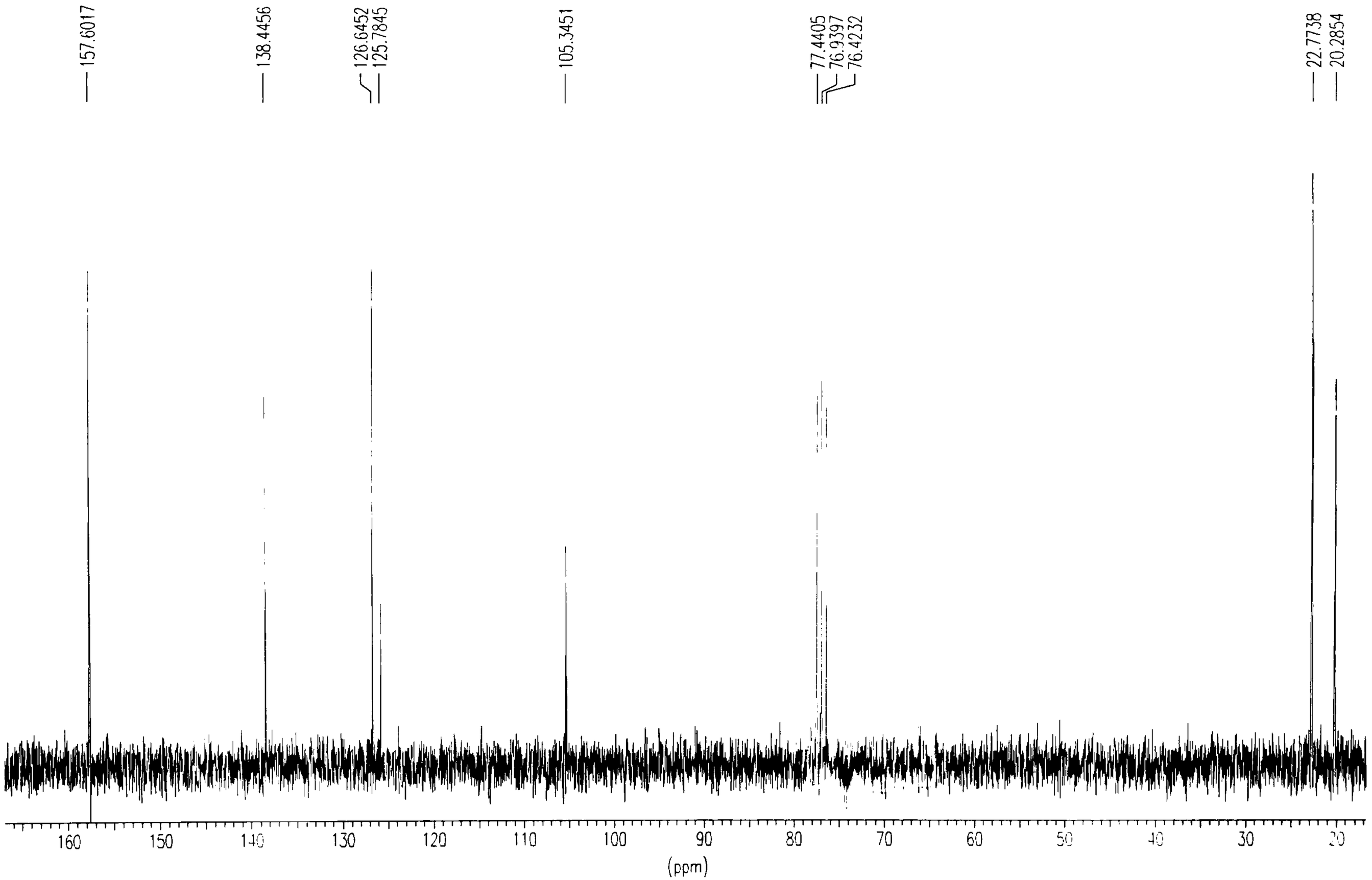

Figure 4.10 The ^{13}C N.M.R. spectrum of $[Zr(omtaa)Cl_2]$ in $CDCl_3$

Table 4.2 Summary of proton decoupled ^{13}C N.M.R shifts (δ/ppm.) for tmtaa and omtaa compounds

Compound	C–N	aromatic–CN	aromatic–CH	methine–CH	methyl–C	aromatic–Me
H_2tmtaa	158.84	138.00	122.79, 123.00	97.84	20.81	–
Li_2tmtaa	160.41	145.95	121.10, 120.74	98.81	22.38	–
[Ti(tmtaa)Cl_2]	156.83	129.35	124.73, 128.21	106.58	23.55	–
[Zr(tmtaa)Cl_2]	158.39	128.77	126.70, 124.87	105.84	22.82	–
H_2omtaa	158.57	136.10	130.87, 123.98	97.31	20.80	19.43
Li_2omtaa	161.02	140.57	128.64, 125.43	98.77	22.35	20.13
[Ti(omtaa)Cl_2]	157.35	138.53	127.65, 124.96	105.88	23.01	20.44
[Zr(omtaa)Cl_2]	158.22	139.02	126.73, 125.89	105.08	22.77	20.25

The ^{1}H N.M.R. spectra of the two free ligands H_2tmtaa and H_2omtaa show that in these ligands there is high symmetry, and as a result the spectra show four singlet resonances in H_2tmtaa and five singlet resonances in H_2omtaa, the extra resonance arising from the four extra methyl groups.

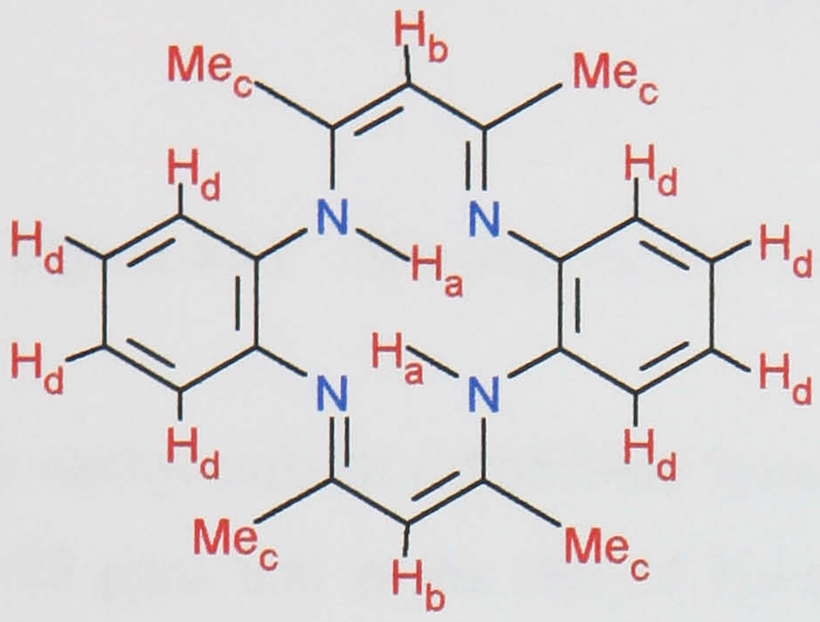

H_2tmtaa

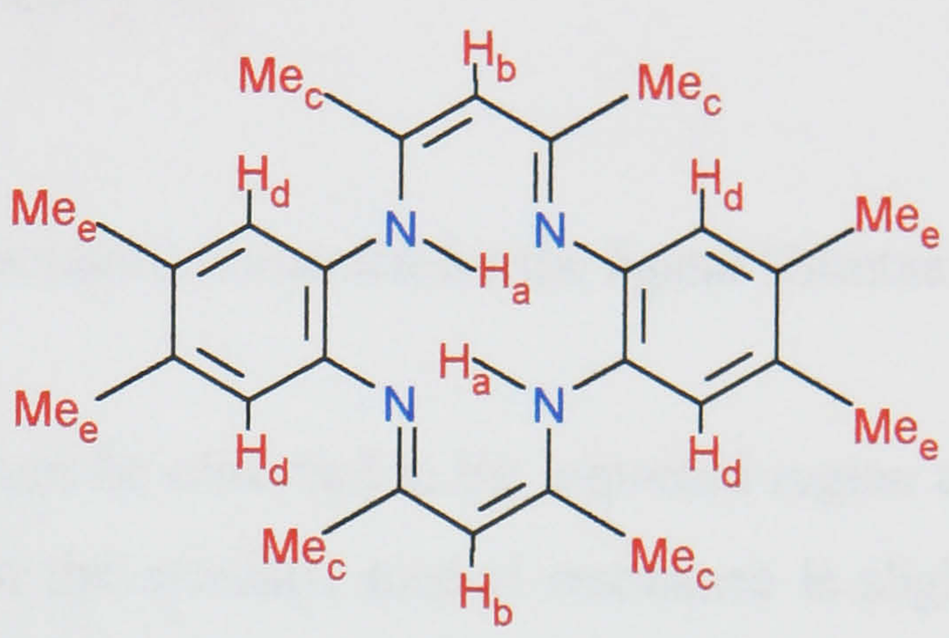

H_2omtaa

Figure 4.11 The symmetry of the ligands H_2tmtaa and H_2omtaa confirmed by ^{1}H N.M.R spectroscopy

The methyl protons of these ligands (H_c and H_e) are seen as singlets and are found in the expected region between δ 2.0 and 2.5 ppm. The methine CH protons (H_b) are also seen as a singlet at δ 4.5–5.0 ppm. The aromatic protons (H_c) resonance is seen in the expected region between δ 6 and 7 ppm, but surprisingly do not show any splitting patterns and are observed as a singlet. The NH resonance (H_a) is seen at δ 12.5–12.6 ppm. and the absence of this resonance in the spectra of the complexes is essential for the desired dihalide complex to have been formed. This high symmetry within the ligand is also evident from the ^{13}C N.M.R spectra of these compounds. The ^{13}C N.M.R spectrum of H_2tmtaa has only six resonances and that of H_2omtaa has seven resonances due to the extra methyl groups on the aromatic rings. These observations are as expected due to the high degree of symmetry within the ligand (Figure 4.12).

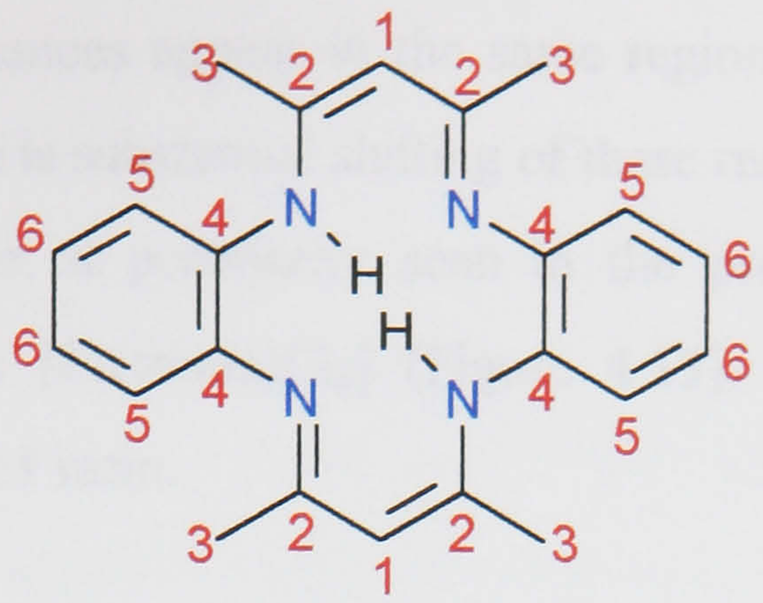

Figure 4.12 Showing the six ^{13}C resonances expected for the ligand H_2tmtaa

The methyl carbons (3) of these ligands can be observed in the expected region at δ 15–25 ppm, and in the case of H_2omtaa the aromatic methyl resonance is slightly further upfield than the non–aromatic methyl resonance. The methine carbon (1) is seen around δ 100 ppm. The C–N carbon (2) is the most downfield resonance and is seen around δ 160 ppm. The aromatic carbons (5+6) are seen in the expected aromatic region at δ 120–130 ppm, the aromatic C–N (4) resonance is shifted downfield and seen at approximately δ 140 ppm.

The high symmetry within the ligands is also retained in the dilithium salts and in the Group 4 metal complexes, as can be seen in their ^{1}H and ^{13}C N.M.R spectra. The NH resonance disappears in the spectra of these compounds showing the loss of the two NH protons, and that the reaction has proceeded to completion. The ^{1}H N.M.R. spectra of these compounds show the same number of resonances, apart from the NH resonance, as in the free ligands. This shows that the symmetry of the free ligand is retained upon complexation of the metal. In the complexes the resonances are shifted in general downfield from those of the free ligands, and are seen to shift by as much as 1 ppm (Table 4.1), and this provides good evidence that the complexes have been formed. One other difference in these compounds is that in some cases the aromatic region is split into a multiplet rather than a singlet as seen in the free ligands. The ^{13}C N.M.R spectra of these compounds also show the same resonances as their free ligands providing further evidence that the symmetry within the complexes is the same as that within the free ligands. The ^{13}C N.M.R spectra of the tmtaa compounds show six resonances and the ^{13}C N.M.R spectra of the omtaa compounds show seven

resonances. These resonances appear in the same regions as the as the free ligand resonances although there is substantial shifting of these resonances (Table 4.2).

There is, however, a peculiarity seen in the proton N.M.R. spectrum of [Zr(tmtaa)Cl_2].2THF and [Zr(tmtaa)Cl_2] (Figure 4.13). In these spectra all the resonances are split in a 3:1 ratio.

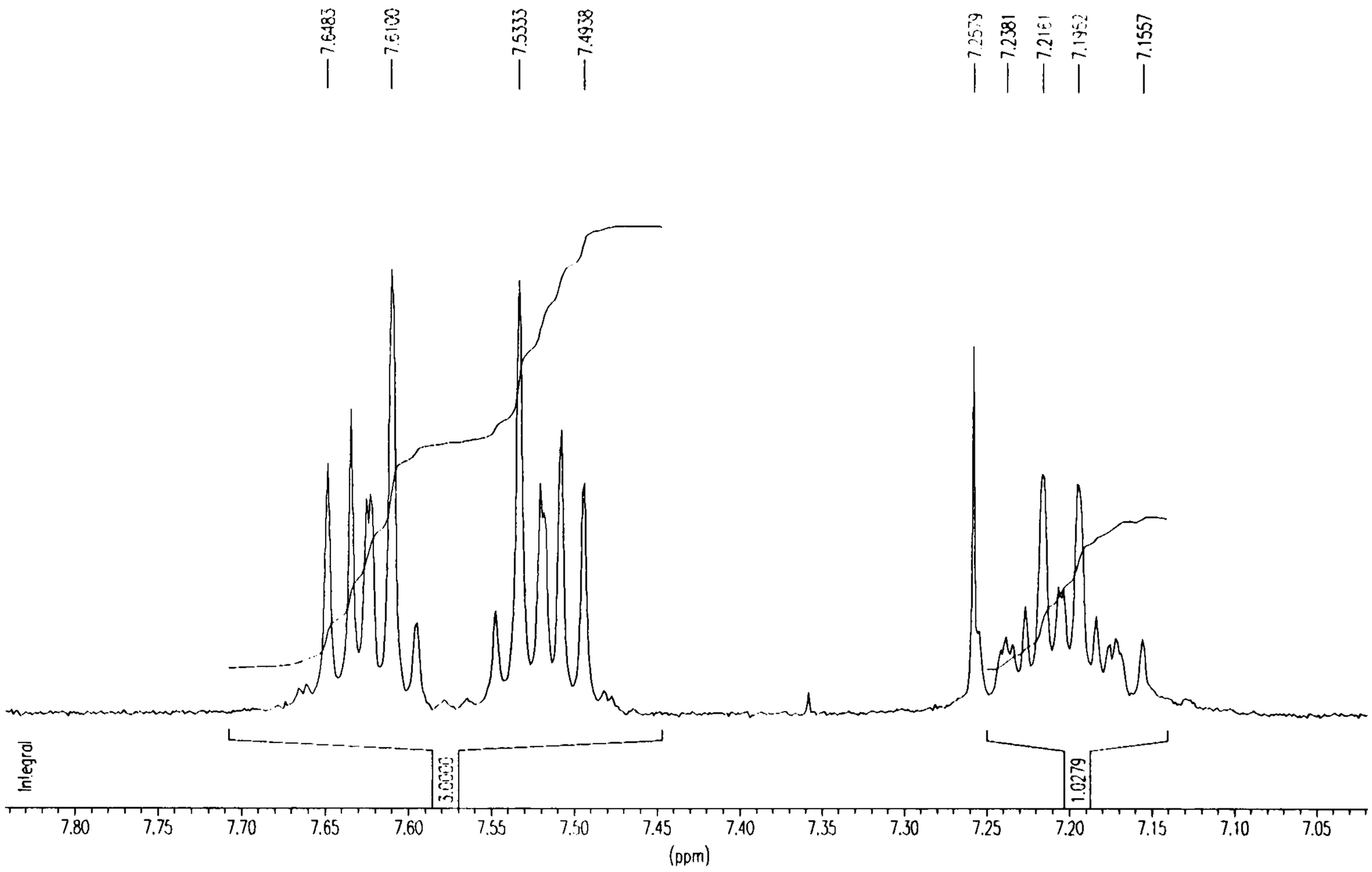

Figure 4.13 Showing the splitting of the aromatic resonance in [Zr(tmtaa)Cl_2].2THF and [Zr(tmtaa)Cl_2].

Floriani *et al*[154] reported that the two forms observed in the ^{1}H N.M.R. spectrum are two saddle–shape conformations of the ligand, with a different out of N_4 plane distance of the metal. The two forms are in a slow equilibrium determined by the nature of the solvent, but independent of its binding ability. This was also reported to be the case with [Ti(tmtaa)Cl_2], although such splitting was never seen in the spectrum of this complex no matter which solvent was used. This splitting was not evident in any of the complexes synthesised with the ligand H_2omtaa.

Infra–red Spectra

The infra–red spectra of all the compounds have been recorded as Nujol mulls with the important peaks listed in the experimental section. The spectra are complex and only the main features are discussed here. The NH bonds of the free ligands, expected at 3300 cm^{-1} are not detected, the reason for this is probably because of hydrogen–bonding involving the nitrogen atoms. The spectra of both the free ligands and their metal complexes contain strong absorptions near 1620 and 1595 cm^{-1}, and these bands are assigned to C=N and C=C stretching frequencies.

The infra–red spectra of the complexes provide the most important information. The region below 400 cm^{-1} is the region where the M–Cl stretch is observed. In all the complexes the M–Cl stretch was seen between 350 and 250 cm^{-1} and in some cases provided information on the stereochemistry of the metal because two peaks were visible indicating that *cis* chlorines were present.

Mass Spectra

E.I. and C.I. mass spectra have been obtained for both the free ligands and their corresponding titanium and zirconium complexes. These spectra have provided valuable evidence that the intended products have been formed. All the spectra of these compounds were obtained at a source temperature of typically 150 °C.

In the case of the free ligands the molecular ion was readily detected at high intensity, however, in the case of the metal complexes the molecular ion was not detected. The spectra of the complexes showed the loss of a chlorine atom and/or the loss of methyl groups from the ligand. Further fragmentation of the complexes occurs with the loss of the metal, as shown by the prominent molecular ion from the free ligand, and numerous lower mass peaks arise from fragmentation of the macrocyclic ring. Table 4.3 below summarises the important high mass peaks recorded in the E.I. mass spectra of the free ligands and their complexes.

Table 4.3 Summary of the E.I. Mass Spectra of H_2tmtaa, H_2omtaa and their titanium(IV) and zirconium (IV) complexes

Compound	m/z	Relative intensity (%)	Assignment
H_2tmtaa	344	100	M^+
	343	5.8	$[M–H]^+$
	329	86.3	$[M–CH_3]^+$
H_2omtaa	400	25.0	M^+
	399	100.0	$[M–H]^+$
[Ti(tmtaa)Cl_2]	425	1.2	$[M–Cl]^+$
	401	0.8	$[M–(4CH_3)]^+$
[Zr(tmtaa)Cl_2]	445	0.9	$[M–(4CH_3)]^+$
	394	0.4	$[M–(8CH_3)]^+$
[Ti(omtaa)Cl_2]	481	0.7	$[M–Cl]^+$
	445	0.2	$[M–2Cl]^+$
[Zr(omtaa)Cl_2]	524	1.8	$[M–Cl]^+$
	500	1.2	$[M–(4CH_3)]^+$

X–ray Crystallographic Studies

The molecular and crystal structure of the complex, [Zr(omtaa)Cl_2] was determined by a single crystal X–ray diffraction study. The complex consists of discrete [Zr(omtaa)Cl_2] molecules and disordered THF solvent molecules of crystallisation in a complex/solvent molar ratio of 1:0.5.

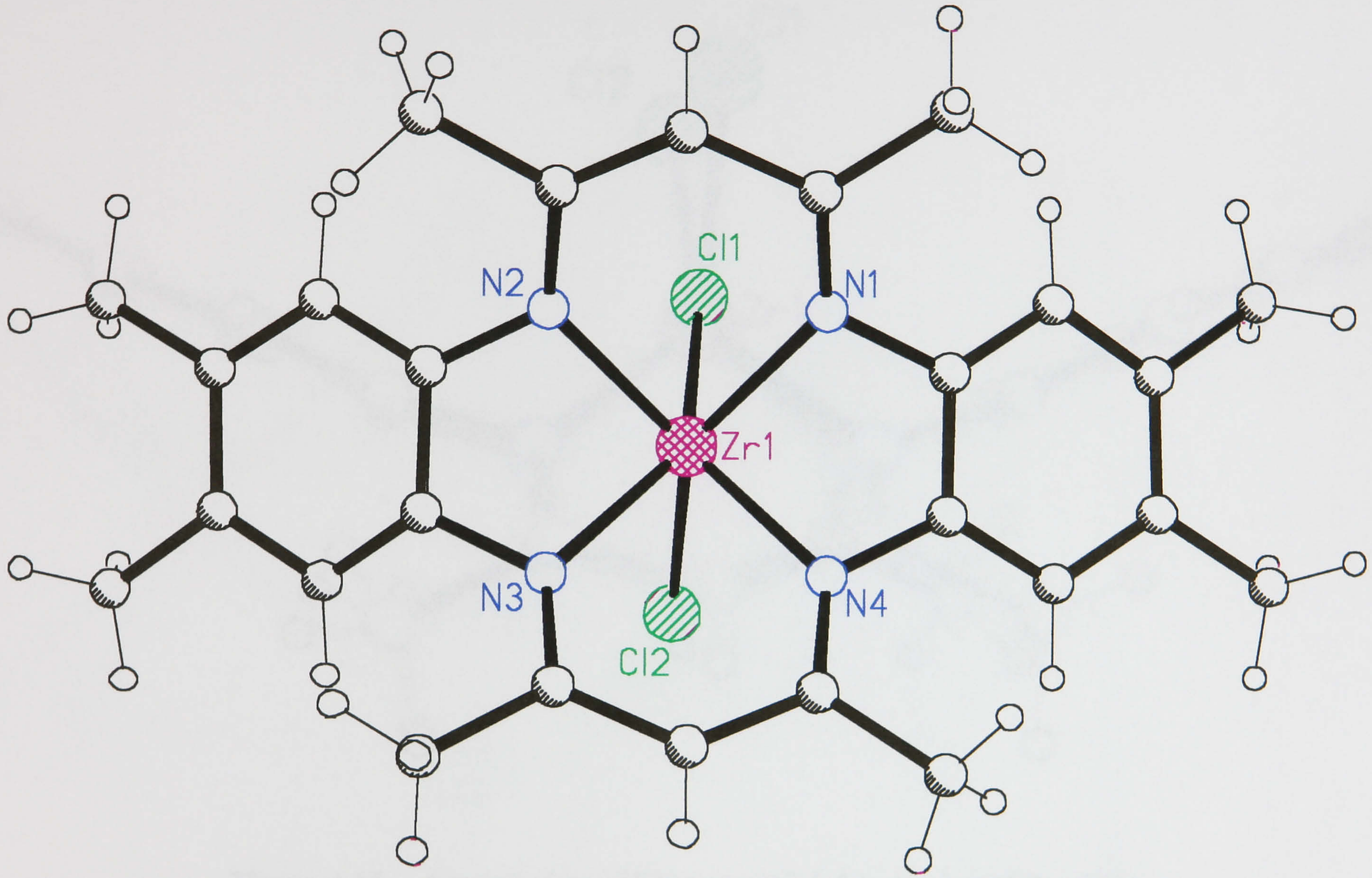

Figure 4.14 The molecular structure of $[Zr(omtaa)Cl_2]$ showing its symmetry.

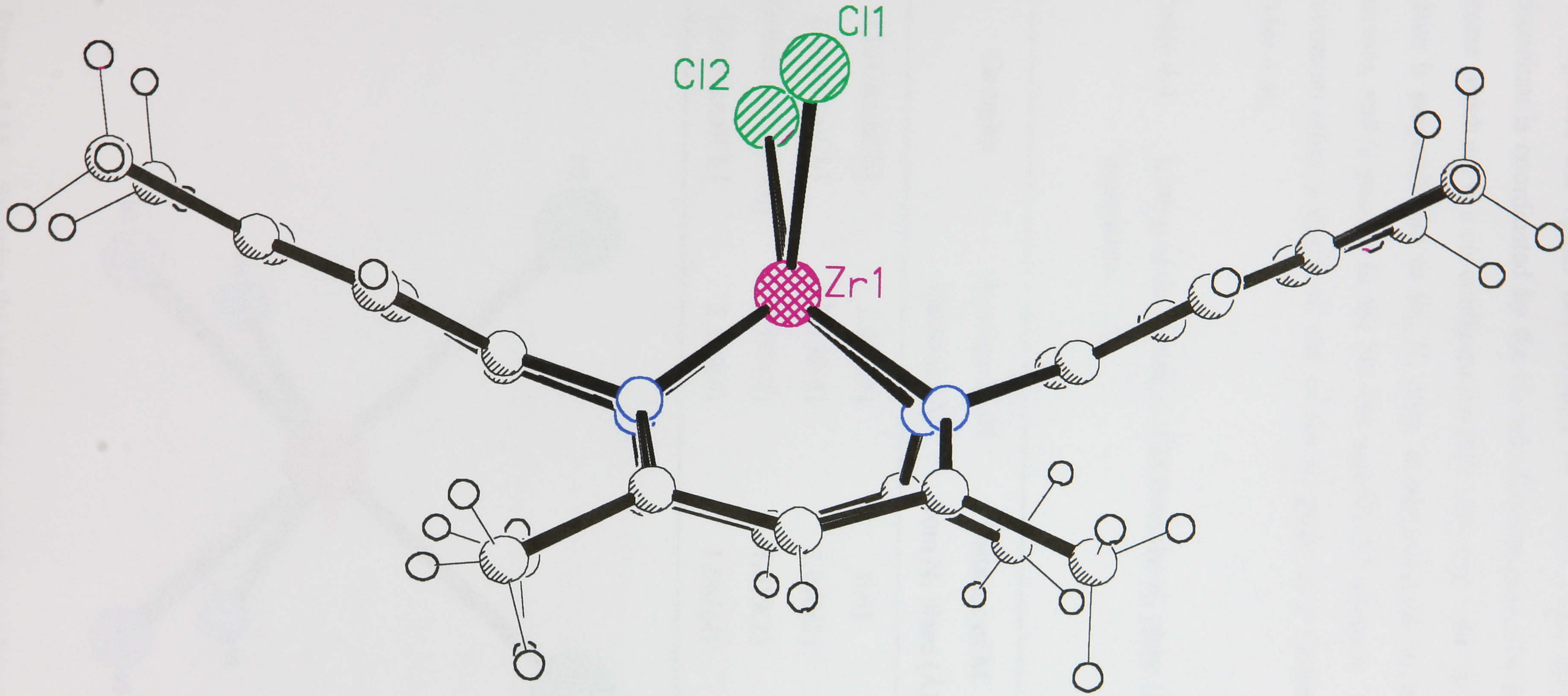

Figure 4.15 Another view of [Zr(omtaa)Cl_2] showing its saddle–shape.

As expected the ligand has retained its saddle–shape upon complexation. The zirconium is coordinated by the N_4 set of atoms from the ligand and two chlorine atoms which are in a *cis* configuration (Cl1–Zr1–Cl2 = 84.75(9)°). The Cl1–Zr1–Cl2 plane is perpendicular to the N_4 core, is perpendicular to the N1–N2 and N3–N4 vectors, and is parallel to the N1–N4 and N2-N3 vectors. Again, as expected the zirconium atom is displaced out of the N_4 plane by a distance of 1.061(4) Å (see Table 4.4).

Table 4.4 Listing of the distance of M from the N_4 plane (Å) in $[M(L)Cl_2]$ complexes

Complex	Average M–N distance (Å)	Distance of M from N_4 plane (Å)	Reference
$[Ti(tmtaa)Cl_2]$	2.042(4)	0.91	150
$[Zr(tmtaa)Cl_2]$	2.132(8)	1.070(2)	154
$[Zr(tmtaa)(CH_2Ph)_2]$	2.189(8)	1.019(2)	154
$[Zr(omtaa)Cl_2]$	2.167(4)	1.061(4)	This work

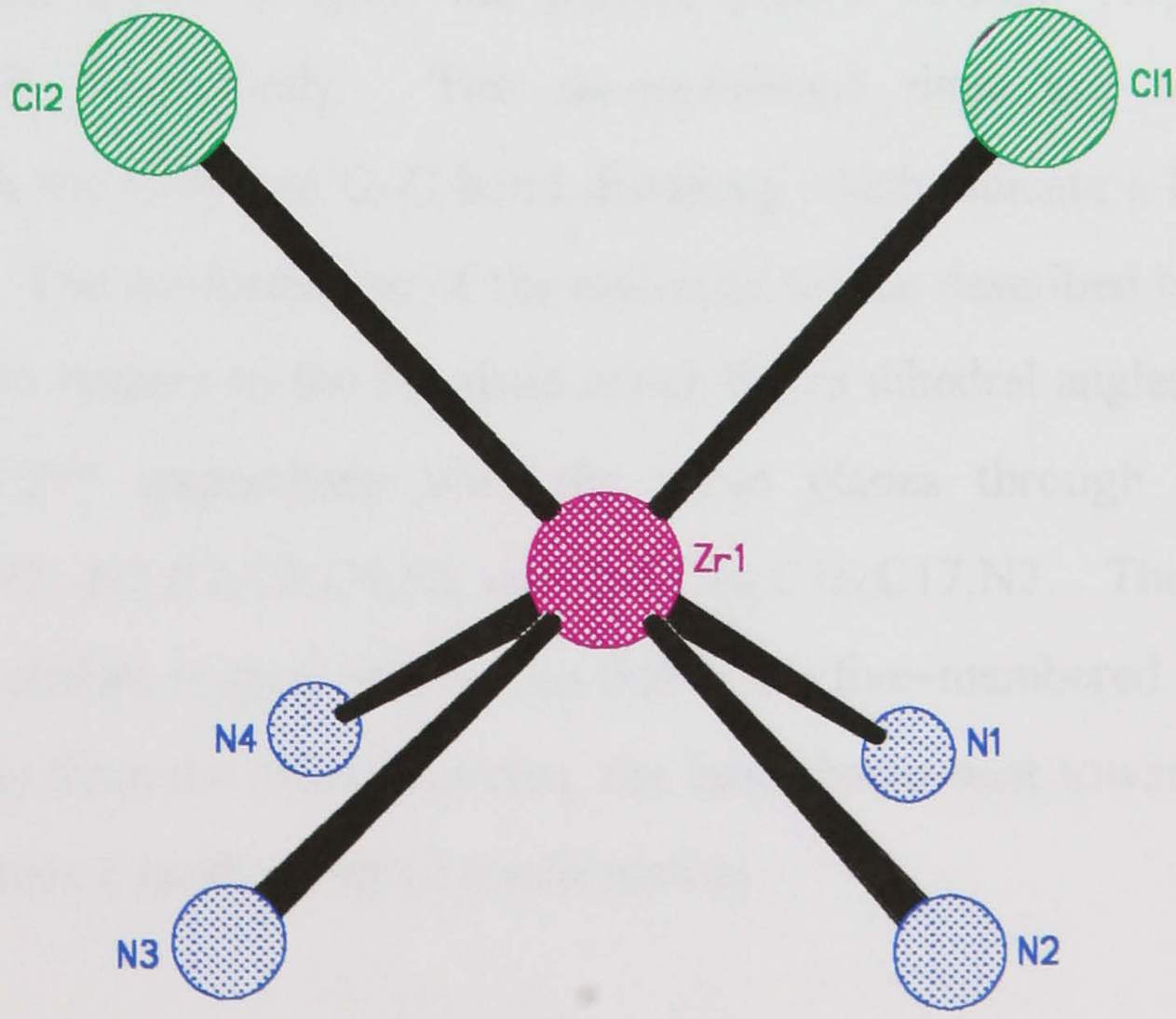

Figure 4.16 Showing the coordination around zirconium in $[Zr(omtaa)Cl_2]$

Table 4.5 Selected bond angles (°) for $[Zr(omtaa)Cl_2]$

Cl1–Zr1–Cl2	84.75(9)	N3–Zr1–N4	78.7(2)
N3–Zr1–N2	73.6(2)	N1–Zr1–N4	74.0(2)
N1–Zr1–N2	77.4(2)	N2–Zr1–Cl1	90.0(2)
N1–Zr1–Cl1	87.4(2)	N3–Zr1–Cl2	85.3(2)
N4–Zr1–Cl2	88.3(2)	N2–Zr1–N4	122.0(2)
N3–Zr1–Cl1	142.7(2)	N2–Zr1–Cl2	137.3(2)

The coordination around the zirconium atom, although six coordinate, is not octahedral but instead trigonal prismatic and has bond angles, around the zirconium, varying from 90.0(2) to 73.6(2)°. The bond lengths and angles within the complex are as expected for compounds of this type. The Zr–Cl bond lengths are 2.498(3) and 2.509(3) Å which can be compared with bond lengths of 2.493(2) and 2.490(2) Å in $[Zr(tmtaa)Cl_2]$.

Coordination of the ligand results in two five–membered and two six–membered rings. The first two have an envelope conformation with the zirconium lying 1.296 and 1.304 Å from the perfect planes through N1,C6,C13,N4 and N2,C26,C19,N3 respectively. The six–membered rings are nearly planar in agreement with the C–N and C–C bond distances which indicate a high degree of π delocalisation. The conformation of the molecule can be described by the bending of its portions with respect to the N_4 plane which forms dihedral angles of 25.17, 6.49, 35.36 and 35.19° respectively with the mean planes through N1,C6–C13,N4; N3,C19–C26,N2; N2,C2,C3,C4,N1 and N4,C14,C16,C17,N3. The bending of the six–membered chelate rings is opposite to that of the five–membered rings, the former being bent away from the chlorine atoms, the latter being bent towards them, so that the ligand assumes a saddle–shaped conformation.

Further reactions of [M(omtaa)Cl_2] complexes

The two complexes [Ti(omtaa)Cl_2] and [Zr(omtaa)Cl_2] have been reacted with a variety of reagents in an attempt to produce new novel compounds. As this was not the main aim of the project only a limited amount of time was spent on these reactions in an attempt to ascertain the reactivity of these compounds.

It is well documented that complexes of the type [M(tmtaa)Cl_n] are readily alkylated with Grignard reagents.[154-159] Therefore, the alkylation of the two complexes [Ti(omtaa)Cl_2] and [Zr(omtaa)Cl_2] were attempted. Initial efforts were concentrated on the preparation of complexes of the type [M(omtaa)R_2] (where R = benzyl, methyl).

$$[M(omtaa)Cl_2] + 2\,RMgX \longrightarrow [M(omtaa)R_2] + 2\,MgCl_2$$

(R = $PhCH_2$, Me; M = Ti, Zr)

These reactions were carried out in a variety of solvents (toluene, THF, benzene, hexane) and at a range of temperatures (0–120 °C). However, although the desired reaction was believed to have taken place , it was not found possible to isolate a pure complex. The reason for this was believed to be that as a small side reaction the ligand was alkylated, and as a result the desired complex and the side reaction complex were almost impossible to separate. A major problem involved in the purification of the products was their insolubility in most solvents. This insolubility proved to be a major problem in both the purification and characterisation procedures. One possible way to overcome this problem is to use an alkylating Grignard reagent which, upon complexation, will make the resultant complex much more soluble. One such Grignard reagent which could be used is $(CH_3)_3SiCH_2MgCl$.

Another reaction that was attempted was the substitution of one or two Cl atoms with one or two cyclopentadienyl (Cp) groups. Goedken *et al*[157] reported that the reaction of [Ti(tmtaa)Cl_2] with NaC_5H_5 (NaCp) in THF resulted in the reduction of Ti(IV) to Ti(III) and the formation of [Ti(tmtaa)(Cp)]. As a result of this the attempted preparation of [Ti(omtaa)(Cp)] using the same experimental procedure was undertaken. However, using these conditions no reduction of the titanium was seen

and the only product recovered from the reaction was unreacted [Ti(omtaa)Cl_2]. As no reduction was detected more forcing conditions were used in order to bring about one of the following reactions:

$$[M(omtaa)Cl_2] + NaCp \longrightarrow [M(omtaa)(Cp)Cl] + NaCl$$

$$[M(omtaa)Cl_2] + 2\,NaCp \longrightarrow [M(omtaa)(Cp)_2] + 2\,NaCl$$

(M = Ti, Zr)

These reactions were attempted initially using THF as solvent at room temperature but no reaction was seen under these conditions. Subsequently these reactions were carried out using toluene as solvent and under refluxing conditions, but again no significant reaction was seen, and the major product from the reaction was pure, unreacted starting material [M(omtaa)Cl_2]. From these results it would appear that the Cp group is too large to be accommodated at the metal with another group in a *cis* manner.

Experimental

Again all reactions were carried out in a dry nitrogen or argon atmosphere using conventional Schlenk apparatus and techniques. All solvents were carefully dried using either calcium hydride or sodium metal,and glassware was stored in a hot oven.

Preparation of 5,7,12,14–tetramethyldibenzo[b,i][1,4,8,11]tetraazacyclotetradecine (*H_2*tmtaa)

Nickel diacetate tetrahydrate (50.0 g, 1 eq), o–phenylenediamine (43.5 g, 2 eq) and 2,4–pentadione (40.23 g, 2 eq) were added to anhydrous methanol (500 cm^3) in a 1 litre flask, and the mixture was stirred and refluxed for 48 h under nitrogen. The colour of the solution changed from a pale green to deep–purple to a blue–green. After refluxing, the solution was cooled, filtered, and the solid residue washed with generous volumes of methanol until the effluent was light green to colourless.

Yield = 28.3 g (26%).

Anhydrous hydrogen chloride was bubbled at a moderate rate through a constantly stirred suspension of $[Ni(C_{22}H_{22}N_4)]$ (15 g) in anhydrous methanol (500 cm^3). The reaction mixture became hot and the colour of the solution turned from a blue–green to green to a brownish purple. The solution was then cooled in an ice bath for one hour. The solid product was filtered, washed with the minimum amount of methanol, and dried.

Yield = 95 %

$[C_{22}H_{26}N_4][NiCl_4]$ (10 g)was dissolved in the minimum amount of H_2O (~100 cm^3), and of ammonium hexafluorophosphate [9.0 g (1.5 molar excess)], that had also been dissolved in the minimum amount of H_2O (~8 cm^3) was added slowly. A colourless precipitate developed which was filtered, washed with H_2O, and dried.

Yield = quantitative.

The free ligand was obtained by neutralising a suspension of 10 g of $[C_{22}H_{26}N_4][PF_6]_2$ in anhydrous methanol by the addition of a slight excess (5.0 cm^3) of triethylamine (any amine base e.g. pyridine may be used). A bright yellow product crystallised immediately which was then filtered, washed with methanol and dried.

Yield = 92 %

^{1}H N.M.R ($CDCl_3$) δ/ppm: 2.16 (s, 12H); 4.90 (s, 2H); 7.01 (s, 8H); 12.6 (s, NHx2).

^{13}C N.M.R ($CDCl_3$) δ/ppm: 20.81 (CH_3) ;97.84 (methine CH); 122.79 (C–C); 123.00 (aromatic C–C); 138.38 (aromatic C–N); 158.84 (C=N)

Preparation of 2,3,6,8,11,12,15,17–octamethyl–5,14–dihydro–5,9,14,18–tetraza–dibenzo–[a,h]–cyclotetradecine (*H_2*omtaa).

Nickel diacetate tetrahydrate (4.73 g, 1 eq) ,4,5–Dimethyl–1,2phenylene–diamine (5.18 g, 2 eq) and 2,4–pentanedione (3.81 g, 2 eq) were added to 50 cm^3 of anhydrous methanol in a 250 cm^3 flask and refluxed under nitrogen for 3 d. After this time the solution was cooled and the product, a finely divided dark violet solid, filtered, washed with generous volumes of methanol, and dried.

Yield = 2 g

Anhydrous HCl was bubbled at a moderate rate through a constantly stirred suspension of 2 g of $[Ni(C_{26}H_{30}N_4)]$ in 50 cm^3 of dry methanol (dried by distillation over magnesium turnings) until the solution became strongly acidic. After the solution had cooled, it was placed at –20°C for 1 d. The product was filtered whilst still cold and dried *in vacuo*.

1.6 g of $[C_{26}H_{34}N_4][NiCl_4]$ was dissolved in a minimum amount (~15 cm^3) of water and 1.44 g (1.5 excess) of ammonium hexaflourophosphate, which was also dissolved in a minimum amount of water (~2.5 cm^3), was slowly added. A coloured precipitate was formed $[C_{26}H_{34}N_4][PF_6]_2$. This product was filtered, washed with water, and dried.

A suspension of 2.4 g of $[C_{26}H_{34}N_4][PF_6]_2$ in anhydrous MeOH was neutralised by the addition of a slight excess of triethylamine (2.5 cm^3). A bright orange solid crystallised immediately. This was filtered, washed with methanol, and dried. Yield = 1.15 g

^{1}H N.M.R ($CDCl_3$) δ/ppm: 2.10 (s, 12H); 2.20 (s, 12H); 4.81 (s, 2H); 6.76 (s, 4H); 12.56 (s, NHx2): ^{13}C N.M.R ($CDCl_3$) δ/ppm: N=C 158.57; N–C 136.10; C–C 130.87; C–C 123.98; methine 97.31; CH_3 20.79; CH_3 19.43.

Preparation and isolation of **Li_2[tmtaa].**

MeLi (1.25 cm^3, 2.1 eq) was added dropwise to a cooled (–78°C) THF solution (7.5 cm^3) of H_2tmtaa (0.25 g, 1 eq). The resultant red solution was allowed to warm to RT and then heated to 50 °C for 4 h. After 4 h the solution was allowed to cool and then evaporated to dryness *in vacuo* resulting in a deep red solid.

^{1}H N.M.R ($CDCl_3$) δ/ppm: 1.27 + 3.38 THF; 2.28 (s, 12H); 4.75 (s, 2H) 6.99 – 7.00 (m, 8H): ^{13}C N.M.R ($CDCl_3$) δ/ppm: 160.41, 145.95, 121.10, 120.74, 98.81, 22.38

Preparation and isolation of **Li_2[omtaa].**

MeLi (1.25 cm^3, 2.1 eq) was added dropwise to a cooled (–78°C) Et_2O solution (7.5 cm^3) of H_2omtaa (0.25 g, 1 eq). The resultant red solution was allowed

to warm to RT and then heated to 30 °C for 2 h. After 2 h the solution was evaporated to dryness *in vacuo* resulting in a deep red solid.

^{1}H N.M.R ($CDCl_3$) δ/ppm: 6.64 (s, 6H0; 4.52 (s, 2H); 2.26 (s, 12H); 2.34 (s, 12H)

^{13}C N.M.R ($CDCl_3$) δ/ppm: 161.02, 140.57, 128.64, 125.43, 98.77, 22.35, 20.13.

Preparation of tetrachlorobis(tetrahydrofuran)titanium(IV), **[$TiCl_4(THF)_2$]**

Into a Schlenk tube was placed 5.0 g (26 mmol) of titanium tetrachloride dissolved in 50 cm^3 of dichloromethane. Anhydrous tetrahydrofuran (7.62 g, 0.10 mole) was added dropwise (slowly), and the solution stirred at room temperature under nitrogen for 15 min. Dry pentane (50 cm^3) was added and the solution was chilled to –25°C for 1 h. The resultant bright yellow solid was collected on a filter stick and washed with 25 cm^3 dry pentane.

Yield = 80 %; mp = 126–128 °C; IR: strong sharp peak 990 cm^{-1}, strong broad peak 825 – 845 cm^{-1}

Preparation of tetrachlorobis(tetrahydrofuran)zirconium(IV), **[$ZrCl_4(THF)_2$]**

Into a Schlenk tube, equipped with a magnetic stirrer bar, was placed zirconium tetrachloride (23.3 g, 100 mmol) in 300 cm^3 of dichloromethane at room temperature. Anhydrous tetrahydrofuran (14.42 g, 200 mmol) was added dropwise to the suspension causing an exothermic reaction strong enough to reflux the dichloromethane. As the tetrahydrofuran was added, the zirconium tetrachloride dissolved giving a slightly turbid, colourless solution at the end of the addition. The solution was filtered and to the filtrate was added 250 cm^3 of dry hexane. The solution was chilled to –25°C for 2h. The product was collected on a medium fritted filter stick, washed with 50 cm^3 of dry hexane and dried *in vacuo*. The product was a white crystalline solid.

Yield = 89 %; mp = 170 – 172 °C; IR: strong sharp peak 990 cm^{-1}, strong sharp peak 820 – 840 cm^{-1}.

***The general preparation of* [M(omtaa)Cl_2] *complexes* (M = Ti, Zr)**

To a solution of H_2omtaa ($C_{30}H_{38}N_4$, 0.5 g, 1 eq) in Et_2O (30 cm^3) at –78 °C was added dropwise LiMe (a 1.2 mol dm^{-3} solution in Et_2O, 2 eq). The resultant red solution was stirred at 40 –50°C for 3.5 h. The Li_2[omtaa] solution was transferred to a solution of [$MCl_2(THF)_2$] (M = Ti, Zr) (1 eq) in Et_2O (30 cm^3). The suspension was heated gently at 35 °C for 5 h and the resultant solid which formed was collected, washed with hexane and dried *in vacuo* (yield = 50%).

[Ti(omtaa)Cl_2]

^{1}H N.M.R ($CDCl_3$) δ/ppm: 7.40 (s, 4H); 5.82 (s, 2H); 2.38 (s, 12H); 2.62 (s, 12H): ^{13}C N.M.R ($CDCl_3$) δ/ppm: 157.35, 138.53, 127.65, 124.96, 105.88, 23.01, 20.44. Analysis, calculated for $C_{26}H_{30}N_4TiCl_2$ (M.W. 517.34): C, 60.36; H, 5.84; N, 10.83%. Found: C, 60.58; H, 5.90; N, 11.05%.

[Zr(omtaa)Cl_2]

^{1}H N.M.R ($CDCl_3$) δ/ppm: 7.38 (s, 4H); 5.59 (s, 2H); 2.36 (s, 12H); 2.47 (s, 12H): ^{13}C N.M.R ($CDCl_3$) δ/ppm: 158.22, 139.02, 126.73, 125.89, 105.08, 22.77, 20.25. Analysis, calculated for $C_{26}H_{30}N_4ZrCl_2$ (M.W. 560.68): C, 55.70; H, 5.39; N, 9.99%. Found: C, 55.91; H, 5.43; N, 10.24%.

***Preparation of* [(tmtaa)Zr(Cl_2)]THF**

To a solution of H_2tmtaa ($C_{26}H_{30}N_4$, 0.75 g, 1 eq) in Et_2O (20 cm^3) at –78 °C was added dropwise LiMe (3.75 cm^3 of a 1.2 mol dm^{-3} solution in Et_2O, 2.2 eq). The resultant red solution was stirred at 40–50 °C for 3.5 h. The Li_2[tmtaa] was transferred to a solution of [$ZrCl_4(THF)_2$] (0.822 g, 1 eq) in THF (20 cm^3). The suspension was refluxed overnight, and the yellow solid which formed was collected, washed with hexane, and dried *in vacuo* (yield = 80%).

^{1}H N.M.R ($CDCl_3$) δ/ppm: 7.64–7.15 (m, 8H); 5.65 +5.83 (s, 2H); 2.50 + 2.76 (s, 12H): ^{13}C N.M.R ($CDCl_3$) δ/ppm: 158.39, 128.77, 126.70, 124.87, 105.84, 22.82. Analysis, calculated for $C_{24}H_{22}N_4ZrCl_2.C_4H_8O$ (M.W. 576.68): C, 54.15; H, 5.24; N, 9.72%. Found: C, 55.34; H, 5.19; N, 9.90%.

***Preparation of* [(tmtaa)Ti(Cl_2))]C_6H_6.**

To a stirred solution of H_2tmtaa (1.0 g, 1 eq) in benzene (25 cm^3) at 0 °C was added dropwise LiMe (5 cm^3 of a 1.25 mol dm^{-3} solution in Et_2O, 2.1 eq). The solution turned to a red colour and a gas was evolved. The solution was stirred for 4 h at 40 ° C and then transferred to a solution of [$TiCl_4(THF)_2$] (0.98 g, 1 eq) in benzene (50 cm^3) at 0°C. The resultant brown suspension was refluxed for 6 h. The resulting brown solid was extracted for 3 d with the mother liquor, using a soxlet apparatus. The resultant brown liquid was evaporated to dryness to yield a brown solid (yield = 35%).

^{1}H N.M.R ($CDCl_3$) δ/ppm: 7.62–7.57 (m, 8H); 5.88 (s, 2H); 2.65 (s, 12H): ^{13}C N.M.R ($CDCl_3$) δ/ppm: 156.83, 129.35, 124.73, 128.21, 106.58, 23.55:

Analysis, calculated for $C_{24}H_{22}N_4TiCl_2.C_6H_6$ (M.W. 539.34): C, 62.36; H, 5.23; N, 10.39%. Found: C, 62.51; H, 5.13; N, 10.55%:

CHAPTER 5

Reactions of Pyridine-containing Tetraazamacrocycles and Group 4 Transition Metals

CHAPTER 5 Reactions of Pyridine-containing Teteraazamacrocycles and Group 4 Transition Metals

Introduction

It was mentioned in Chapter 1 that the proposed ideal compounds desired for catalysis would contain two chlorine atoms in a *cis* configuration. The work of Busch[165] and Schröder[166] on the pyridine containing tetraazamacrocycles (Figure 5.2) reveals that upon complexation these ligands can produce *cis* complexes of the type shown in Figure 5.1.

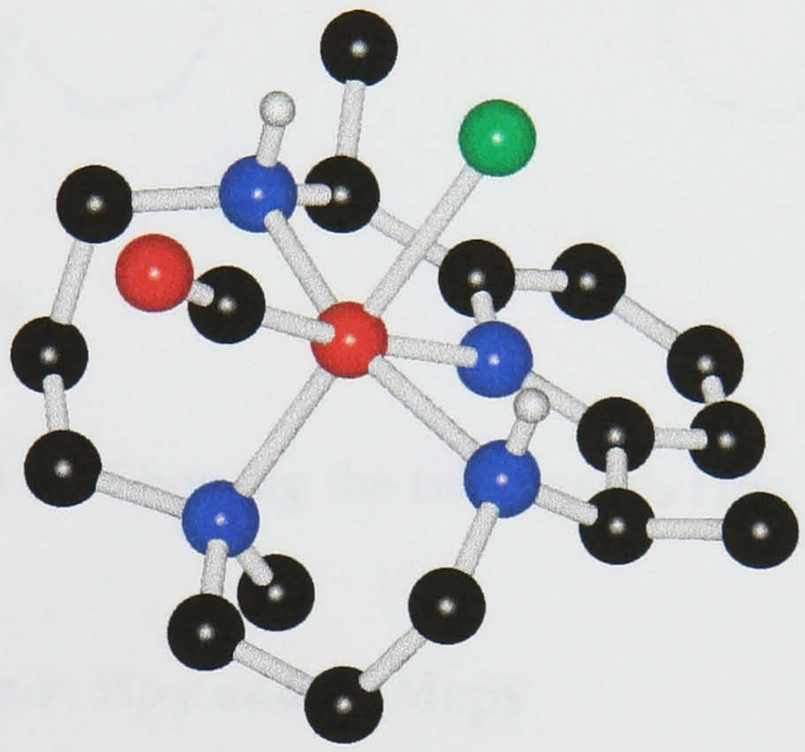

Figure 5.1 The molecular structure of [(DMMepy)Ru(Cl)(CO)]

These pyridine containing macrocycles also possess great scope for ligand modification by the addition of substituent groups, R, shown in Figure 5.2. In this way both the steric and electronic effects altered by such substitution can be studied to gain an insight to the effect, if any, this has on the catalytic properties of the metal complexes.

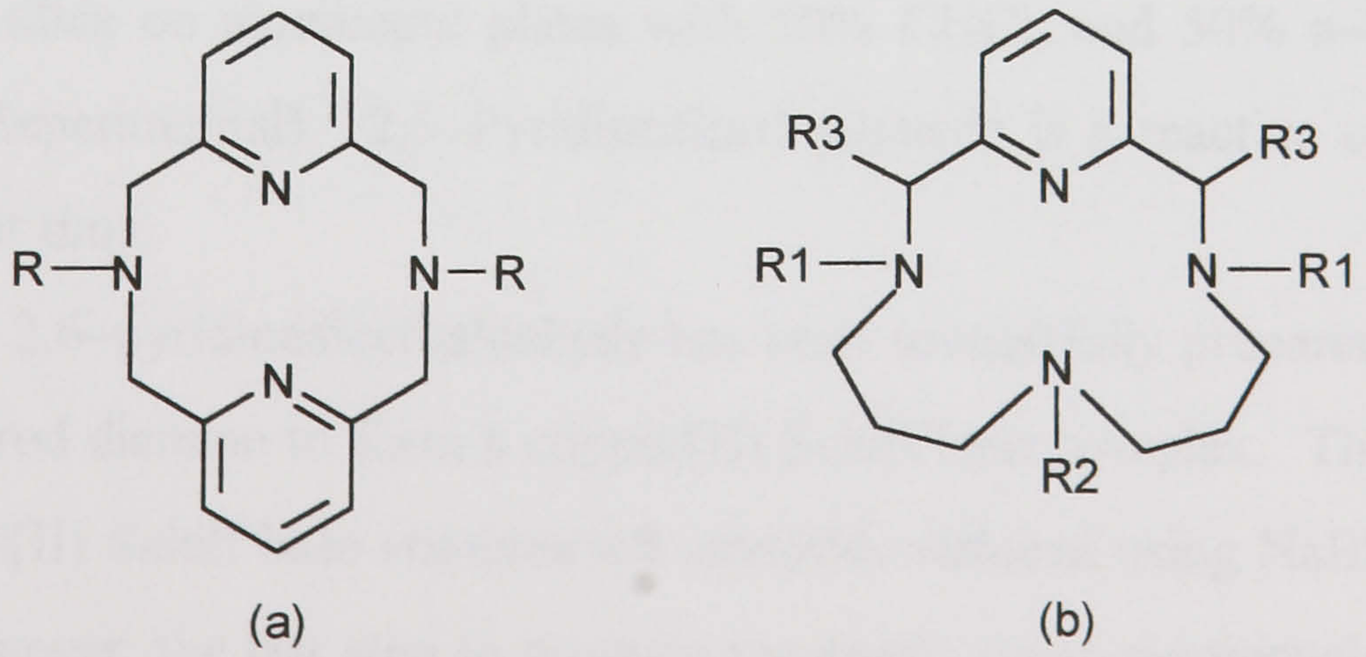

Figure 5.2 Showing the pyridine based macrocycles (a)[167] and (b)[168-174]

In this work initial studies were focused on the two ligands Hpy and H_2Mepy (Figure 5.3). The synthesis of these two ligands has previously been reported in 1986 (H_2Mepy)[175] and 1987 (Hpy)[176] and are prepared (Scheme 5.1) by using Cu(II) as a template metal ion.[177]

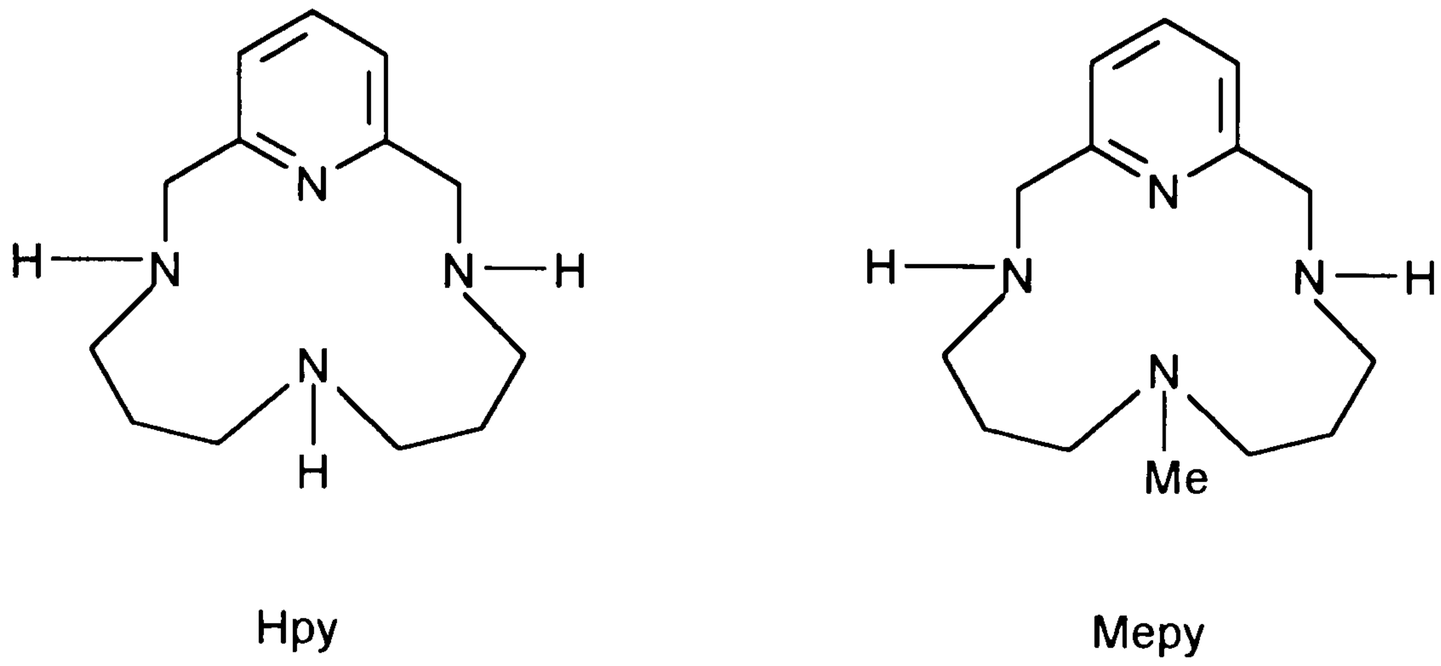

Hpy Mepy

Figure 5.3 Showing the two ligands Hpy and H_2Mepy

Preparation of the ligands Hpy and H_2Mepy

The procedure for the preparation of the two ligands is shown in Scheme 5.1. The first step of the preparation involves the conversion of 2,6–pyridinedimethanol to 2,6–pyridinedicarbaldehyde; the reported method for this conversion involves the use of selenium dioxide in dioxane, but, poor yields were obtained following the literature method. Improved yields were obtained when toluene was used as the solvent and fresh SeO_2 was used in the reaction. The reaction can be followed conveniently by TLC (using silica on aluminium plates with 50% $CHCl_2$ and 50% n–hexane as the eluent; see Experimental). 2,6–Pyridinedicarbaldehyde is a reactive compound and degrades over time.

Once 2,6–pyridinedicarbaldehyde has been successfully prepared, it is reacted with the desired diamine to form a copper(II) Schiff base complex. The imine bonds of the copper(II) Schiff base complex are smoothly reduced using $NaBH_4$ in aqueous ethanol. However, the last step to produce the cyclic amine macrocycle by removing the copper with Na_2S is not so straightforward. Instead of a white solid resulting, a

brown gel was obtained which contains the macrocycle and an unknown impurity. All attempts to dissolve this gel and precipitate out the desired macrocyclic ligands proved unsuccessful. In the end pure ligand was eventually obtained, in reasonable yields, from the sublimation of this gel at 120 °C under vacuum.

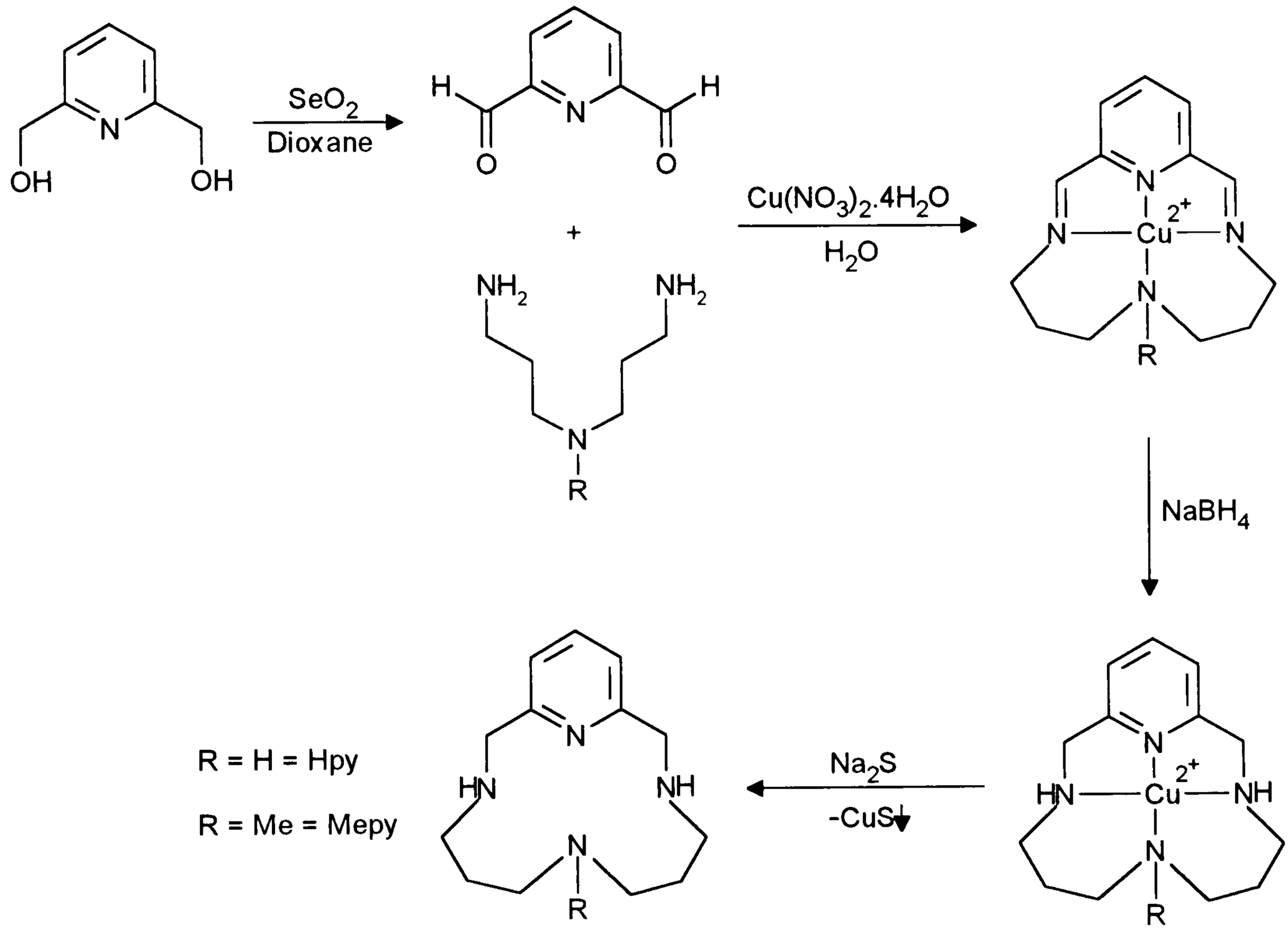

Scheme 5.1 Showing the route to the synthesis of the ligands Hpy and H_2Mepy

Spectroscopic Properties

N.M.R. Spectra

The two macrocyclic ligands Hpy and H_2Mepy have a plane of symmetry through the pyridine nitrogen atom and the N–R group as shown in Figure 5.6. This symmetry is reflected in both the ^{1}H and ^{13}C N.M.R. spectra of these ligands. Full details of the ^{1}H and ^{13}C N.M.R. are given in the experimental section, and were recorded in both $CDCl_3$ and C_6D_6. The ^{1}H and ^{13}C N.M.R. spectra of H_2Mepy can be seen in Figures 5.4 and 5.5.

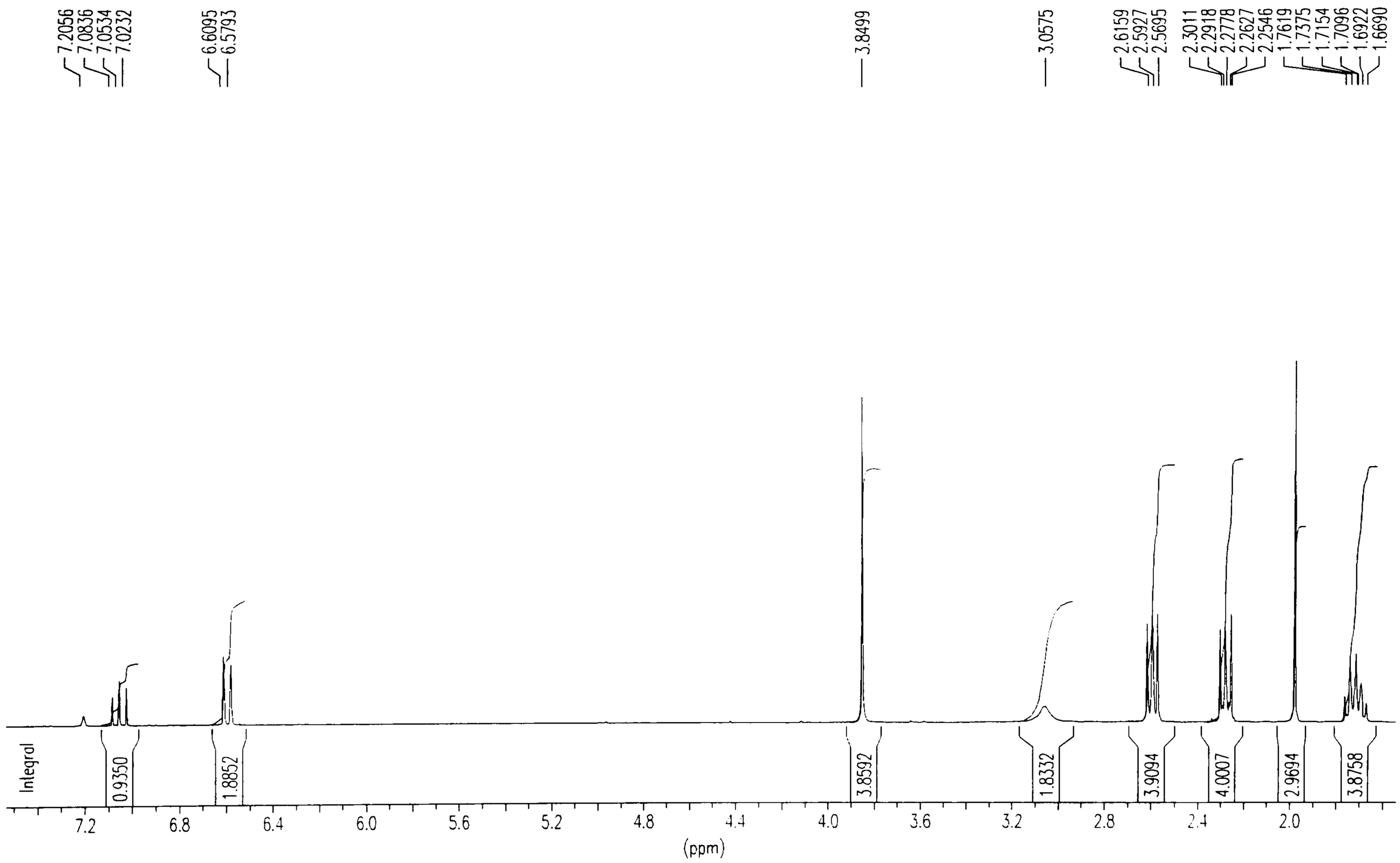

Figure 5.4 The ^{1}H N.M.R. spectrum of the free ligand H_2Mepy in C_6D_6

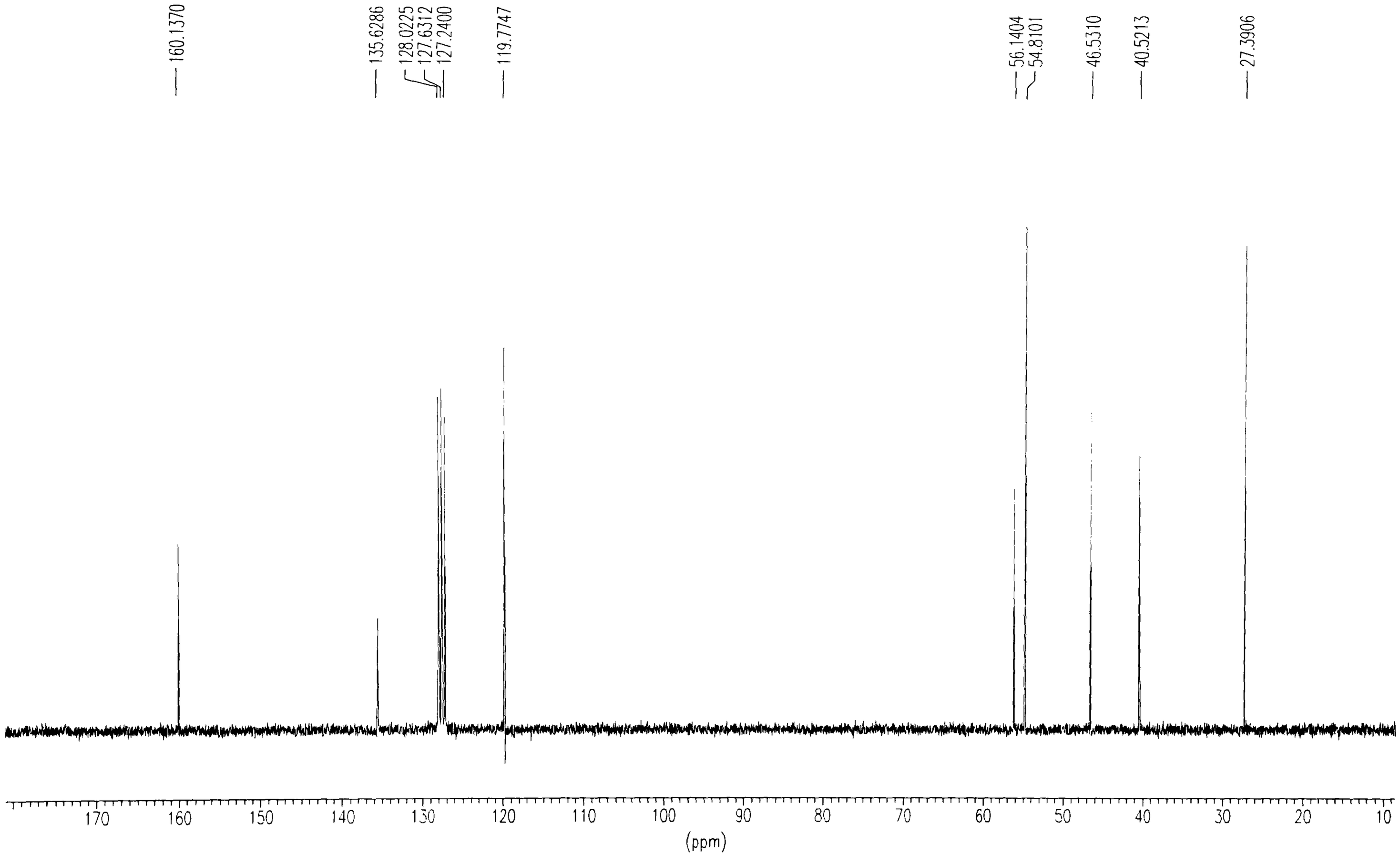

Figure 5.5 The proton decoupled ^{13}C N.M.R. spectrum of the free ligand H_2Mepy in C_6D_6

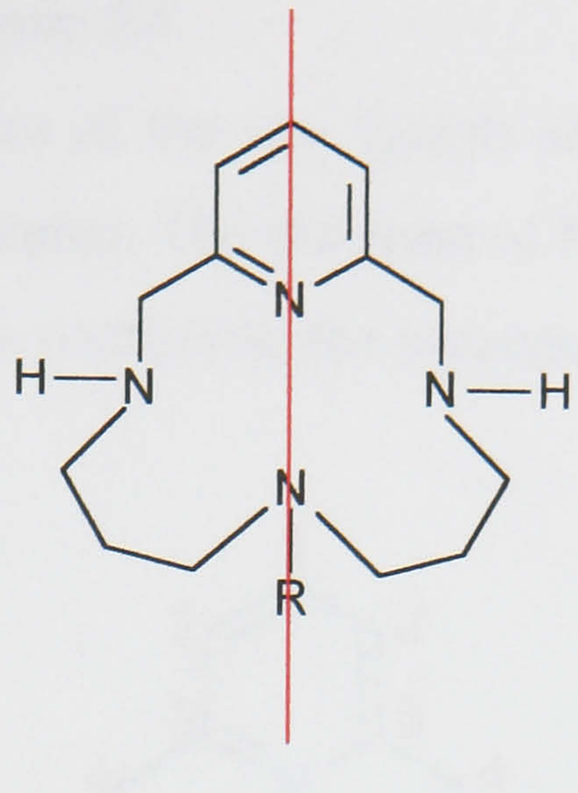

Figure 5.6 Showing the plane of symmetry in the ligands Hpy and H_2Mepy

The ^{1}H N.M.R. spectra of the two ligands are, as expected, remarkably similar. The only difference is the presence of a methyl resonance in the spectrum of H_2Mepy (at δ 2 ppm).

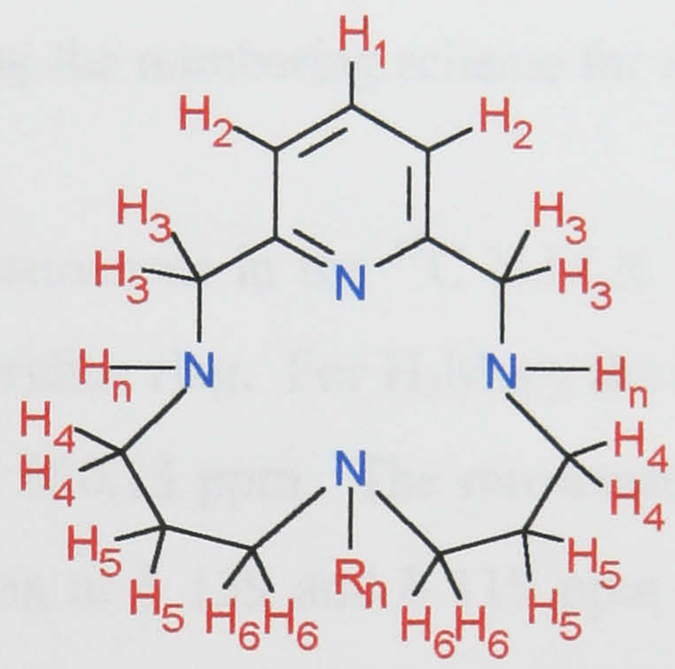

Figure 5.7 Showing the different protons in Hpy and H_2Mepy

The three protons associated with pyridine (H_1 and H_2) are split into a doublet and a triplet, integrating for 1 and 2 protons respectively in the region δ 6.57–7.08. The two CH_2 groups (H_3) are the most downfield CH_2's and are seen as a singlet at δ 3.8 ppm. The CH_2 groups (H_4 and H_6) resonances are seen between δ 2.3 and 2.6 ppm as two sets of triplets each integrating for four protons, and the remaining CH_2 groups (H_5) the most upfield resonance and are seen as a quintet at δ 1.7 ppm. The NH protons (H_n and/or R_n) are seen as a broad singlet resonance at δ 2.9 ppm integrating

for two protons in H_2Mepy and three in Hpy. The ^{1}H N.M.R. spectrum of the free ligand H_2Mepy is shown in Figure 5.4.

The ^{13}C N.M.R. spectra of the two ligands are similar except for the extra resonance due to the N-R grouping. The spectrum of H_2Mepy is shown in Figure 5.5 and has eight resonances again confirming the symmetry within these ligands (Figure 5.8).

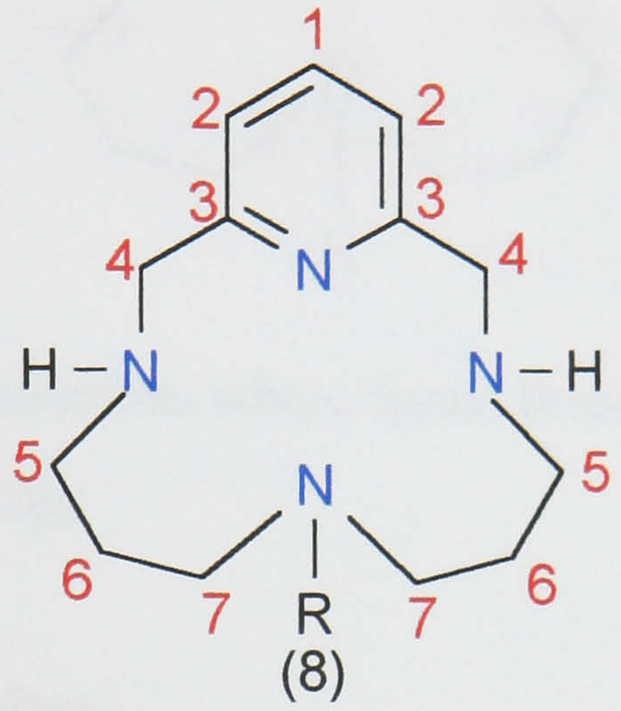

Figure 5.8 Showing the numbering scheme for the ligand carbon atoms

In general the downfield resonances in the ^{13}C N.M.R. spectra of these ligands are those associated with the pyridine ring. For H_2Mepy the resonance for C3 is the most downfield and is found at δ 160.13 ppm. The resonances for the other two pyridine carbons, C1 and C2 are seen at δ 139 and δ 119 ppm respectively. The two CH_2 groups, C4 and C5 are observed at δ 56 and δ 54 ppm respectively, and the CH_2 carbon, C7, is observed at δ 46.85 ppm. The CH_2, C6, carbon is the most upfield resonance and is seen at δ 27.39 ppm with the N-Me resonance observed at δ 40.52 ppm.

Mass Spectra

E.I. and C.I. mass spectra have been obtained for the two free ligands Hpy and H_2Mepy.

These mass spectra were obtained at source temperatures typically ranging from ca. 50–100 °C and show peaks corresponding to the molecular ions. The

fragmentation of these two ligands is, as expected, the same and involves the breakage of the ring at various sites with subsequent fragmentation.

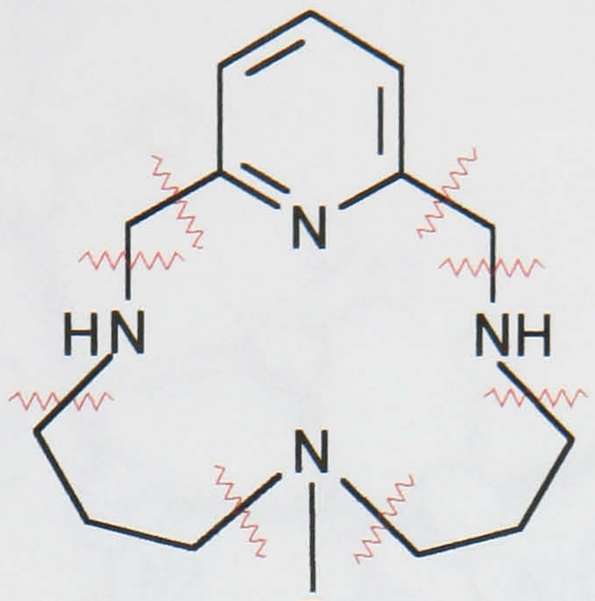

Figure 5.9 Showing the positions where ligand breakage occurs in the ligands H_2Mepy and Hpy

X–ray Crystallography studies

The molecular structure of the free ligand H_2Mepy can be seen below in Figures 5.10, 5.11, and 5.12. The unit cell contains half a molecule.

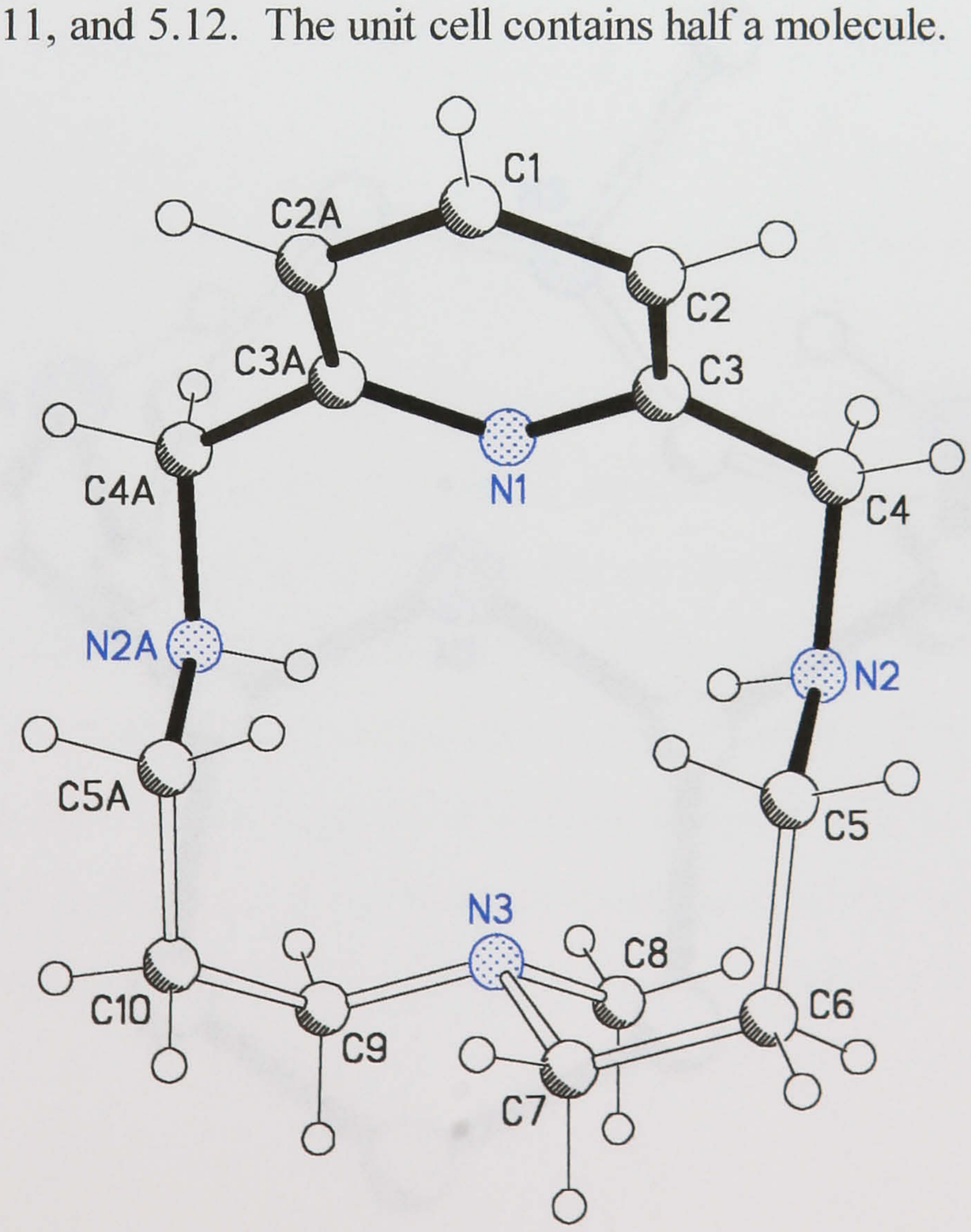

Figure 5.10 The molecular structure of the free ligand H_2Mepy

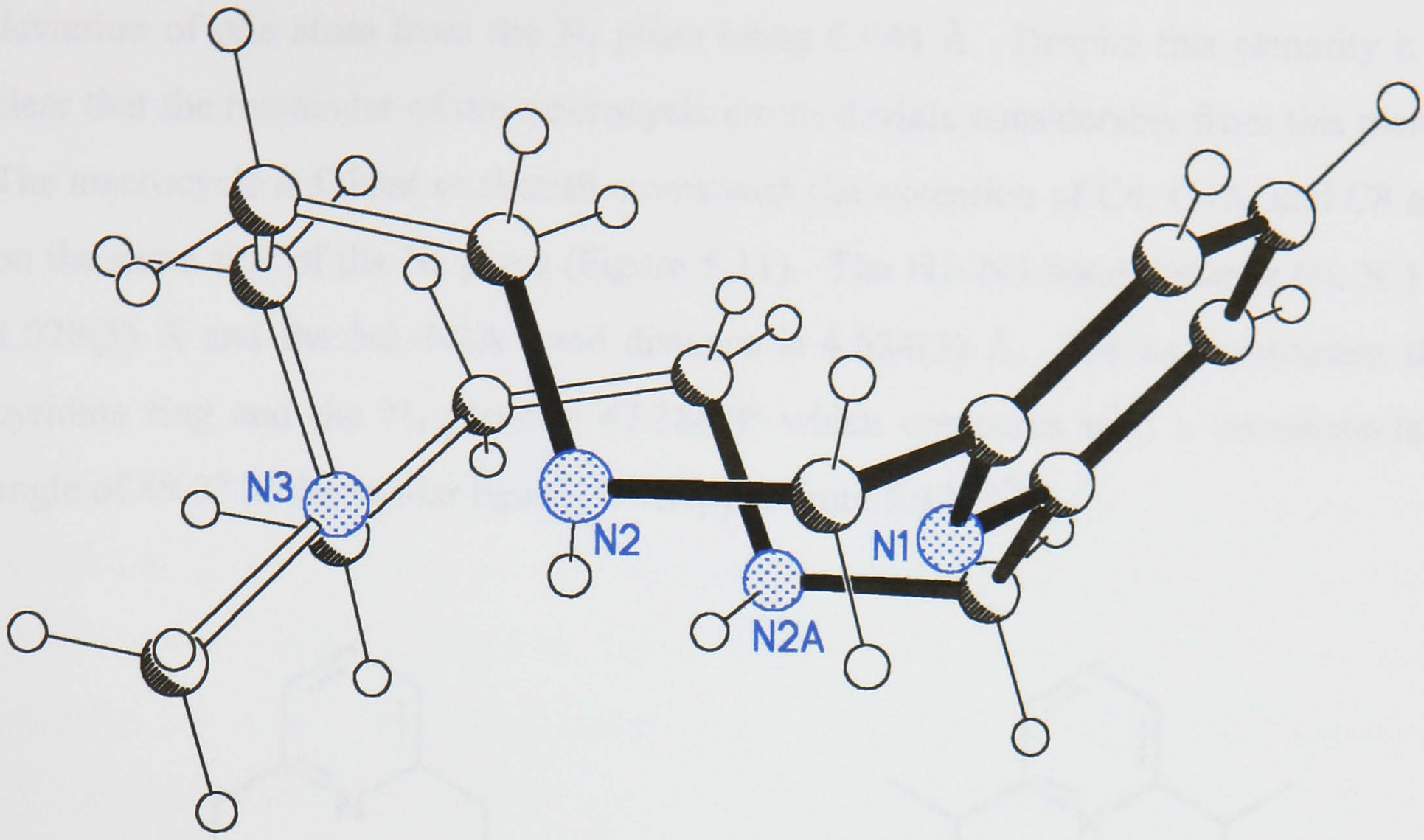

Figure 5.11 Another view of the molecular structure of H_2Mepy

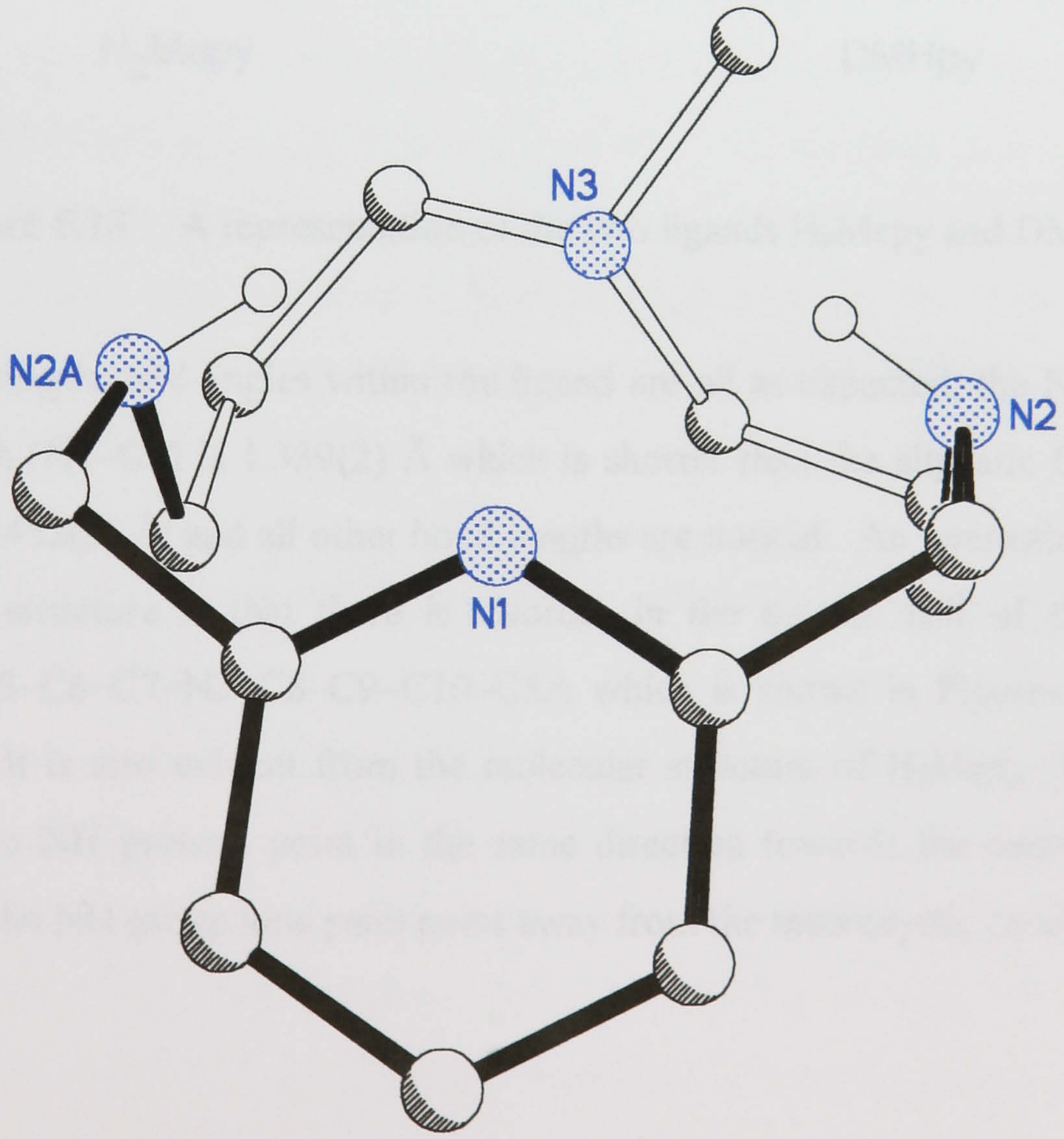

Figure 5.12 Another view of H_2Mepy showing the direction of the N–H protons

In the free macrocycle the four nitrogen atoms are closely planar with the maximum deviation of one atom from the N_4 plane being 0.044 Å. Despite this planarity it is clear that the remainder of the macrocycle atoms deviate considerably from this plane. The macrocycle is folded so that all atoms with the exception of C4, C4A, and C8 are on the same side of the N_4 plane (Figure 5.11). The N1–N3 bond distance (N..N) is 3.928(3) Å and the N2–N2A bond distance is 4.624(3) Å. The angle between the pyridine ring and the N_4 plane is 47.38(8)° which compares with a corresponding angle of 49.2° in the similar ligand, DMHpy (Figure 5.13).[178]

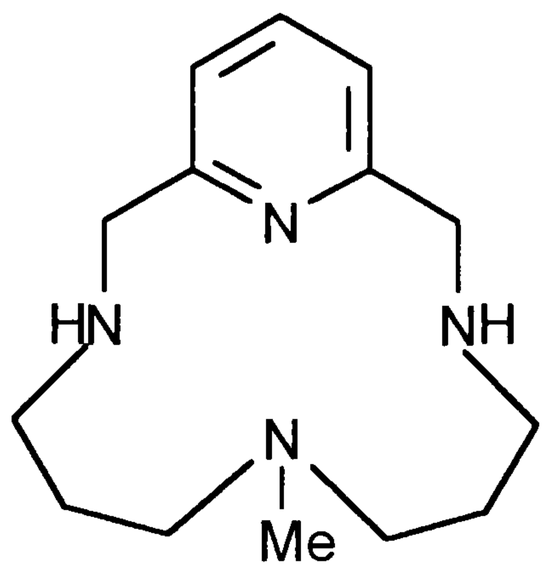

H_2Mepy

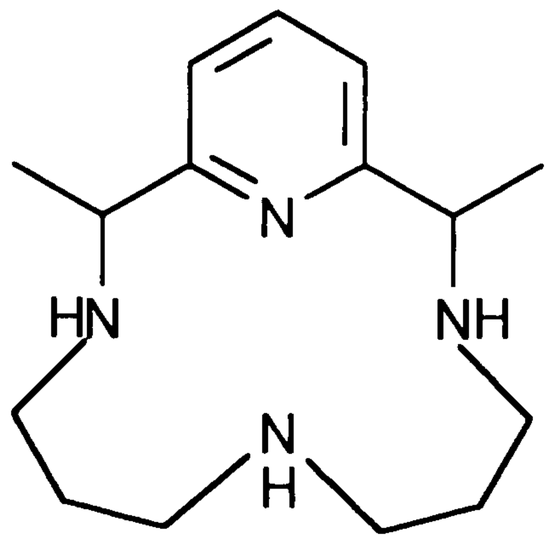

DMHpy

Figure 5.13 A representation of the two ligands H_2Mepy and DMHpy.

The bond lengths and angles within the ligand are all as expected; the N–C pyridine bond length (N1–C3) is 1.339(2) Å which is shorter than the aliphatic C5–N2 bond length of 1.452(3) Å; and all other bond lengths are normal. An interesting feature of the ligand structure is that there is disorder in the bottom half of the molecule between C5–C6–C7–N3–C8–C9–C10–C5A which is shown in Figures 5.10, 5.11, and 5.12. It is also evident from the molecular structure of H_2Mepy (Figure 5.12) that the two NH protons point in the same direction towards the centre of the N_4 plane, and the NH group lone pairs point away from the macrocyclic cavity.

Reactions of Mepy with aluminium(III) alkyls

Initial studies with these ligands were directed towards the removal of the slightly acidic NH protons. By comparison with the studies of Robinson[179] on reactions of $GaMe_3$ and $AlMe_3$ on cyclam, it was believed that that reactions of H_2Mepy with aluminium(III) alkyls would provide the relevant information on the reactivity of the N–H protons within these ligands.

Reactions were carried out on H_2Mepy, and not Hpy, to eliminate any complications that might arise from having two different amine protons. The initial experiment was to react the free ligand H_2Mepy in a molar ratio with aluminium trimethyl ($AlMe_3$). This reaction was carried out using both toluene and hexane as the solvent at room temperature.

$$H_2Mepy + AlMe_3 \xrightarrow[RT]{\text{toluene or hexane}} [H_2MepyAlMe_3] \qquad (1)$$

In this reaction there was no loss of an amine proton from the ligand, but an aluminium–ligand complex of the type represented in equation (1) is believed to result from the spectroscopic analysis of the product. As one mole of $AlMe_3$ did not remove an amine proton from the ligand H_2Mepy, it was decided that the reaction of 2 moles of $AlMe_3$ with one mole of H_2Mepy might result in the desired loss of an amine proton. These reactions were again carried out in both toluene and hexane and again at room temperature.

$$H_2Mepy + 2AlMe_3 \xrightarrow[RT]{\text{toluene or hexane}} [H_2MepyAlMe_3] + AlMe_3 \qquad (2)$$

These reactions resulted in exactly the same product as in the 1:1 mole ratio reactions, with no loss of an amine proton (equation 2). It was then decided to heat the reactions to refluxing temperature in an attempt to force a reaction at the N–H proton. In all the reactions in hexane the use of heat had no affect on the reaction, however, with reactions in toluene these extra forcing conditions resulted in the loss

of an amine proton. This loss of the amine proton could be detected by ^{1}H N.M.R. spectroscopy.

$$H_2Mepy + AlMe_3 \xrightarrow[\text{reflux}]{\text{toluene}} [HMepyAlMe_2] + CH_4 \qquad (3)$$

$$H_2Mepy + 2AlMe_3 \xrightarrow[\text{reflux}]{\text{toluene}} [HMepyAlMe_2] + AlMe_3 + CH_4 \qquad (4)$$

In refluxing toluene the ligand loses an N–H proton upon reaction with $AlMe_3$ and a gas assumed to be CH_4 is evolved (equations 3 and 4). In order to determine whether similar products are obtained with other aluminium alkyls these reactions were carried out using aluminium triethyl ($AlEt_3$). The initial reaction was again to react H_2Mepy in a 1:1 mole ratio with $AlEt_3$ in both toluene and hexane at room temperature.

$$H_2Mepy + AlEt_3 \xrightarrow[\text{RT}]{\text{toluene or hexane}} [HMepyAlEt_2] + C_2H_6 \qquad (5)$$

This time the reaction involved the loss of an amine proton (detected by ^{1}H N.M.R. spectroscopy) without any heat being necessary and is independent of which solvent is used. The reason for this difference in reaction between $AlMe_3$ and $AlEt_3$ is not known unless steric factors are involved, or whether Al_2Me_6 is a more stable dimer than Al_2Et_6 under the reaction conditions, and the reactive unit in these reactions is $AlMe_3$ and $AlEt_3$ respectively.

Spectroscopic Properties

N.M.R. Spectra

The ^{1}H and ^{13}C N.M.R. spectra of all resultant compounds from the above reactions were recorded in C_6D_6 solution as this was considered to be an inert solvent to avoid further reaction in the N.M.R. solution. Full details of the ^{1}H and ^{13}C N.M.R. spectra of these compounds are given in the experimental section. The ^{1}H N.M.R. spectra of these complexes can be seen in Figures 5.14, 5.15 and 5.16.

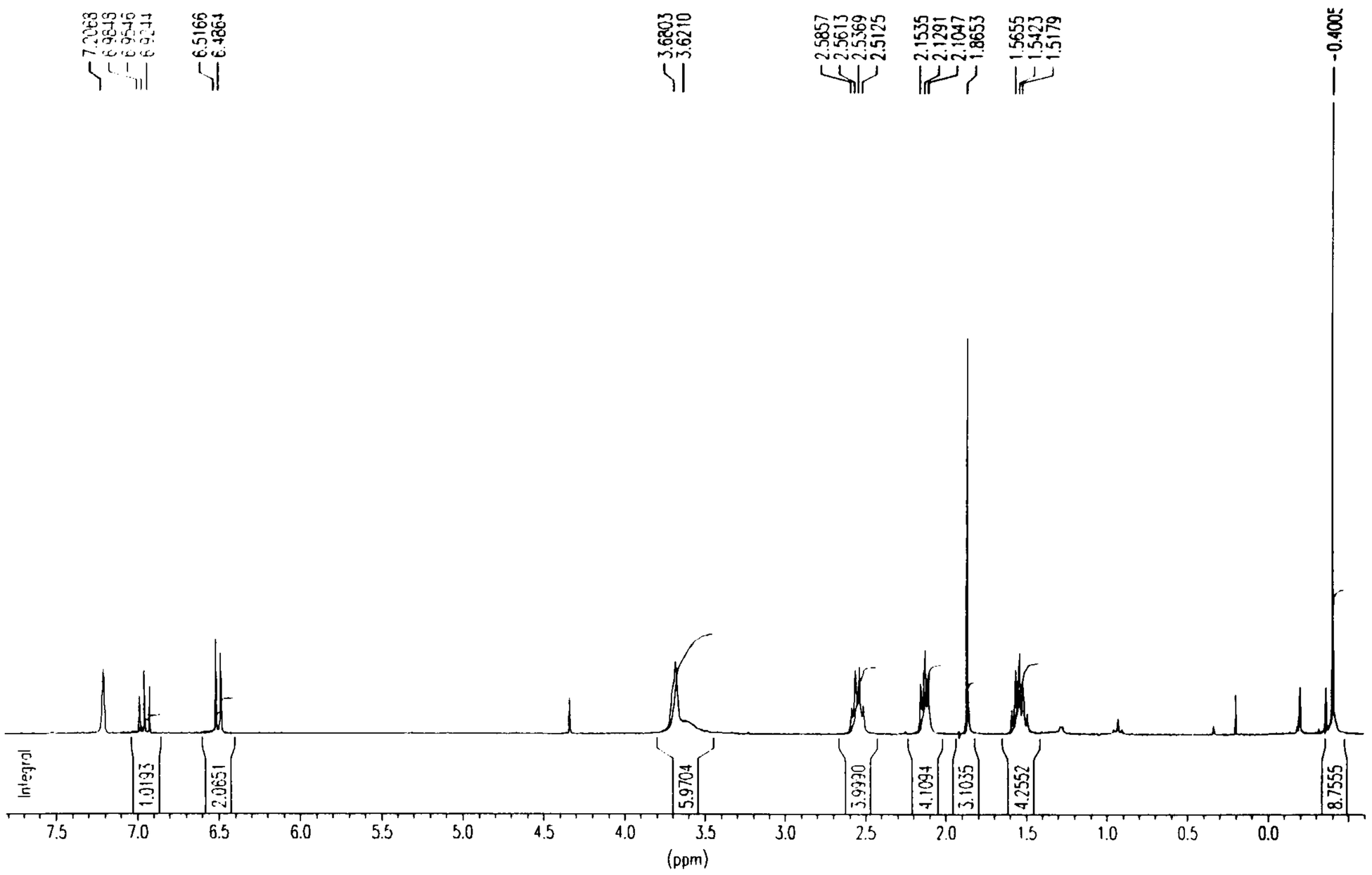

Figure 5.14 The ^{1}H N.M.R. spectrum of the complex $[(H_2Mepy)AlMe_3]$

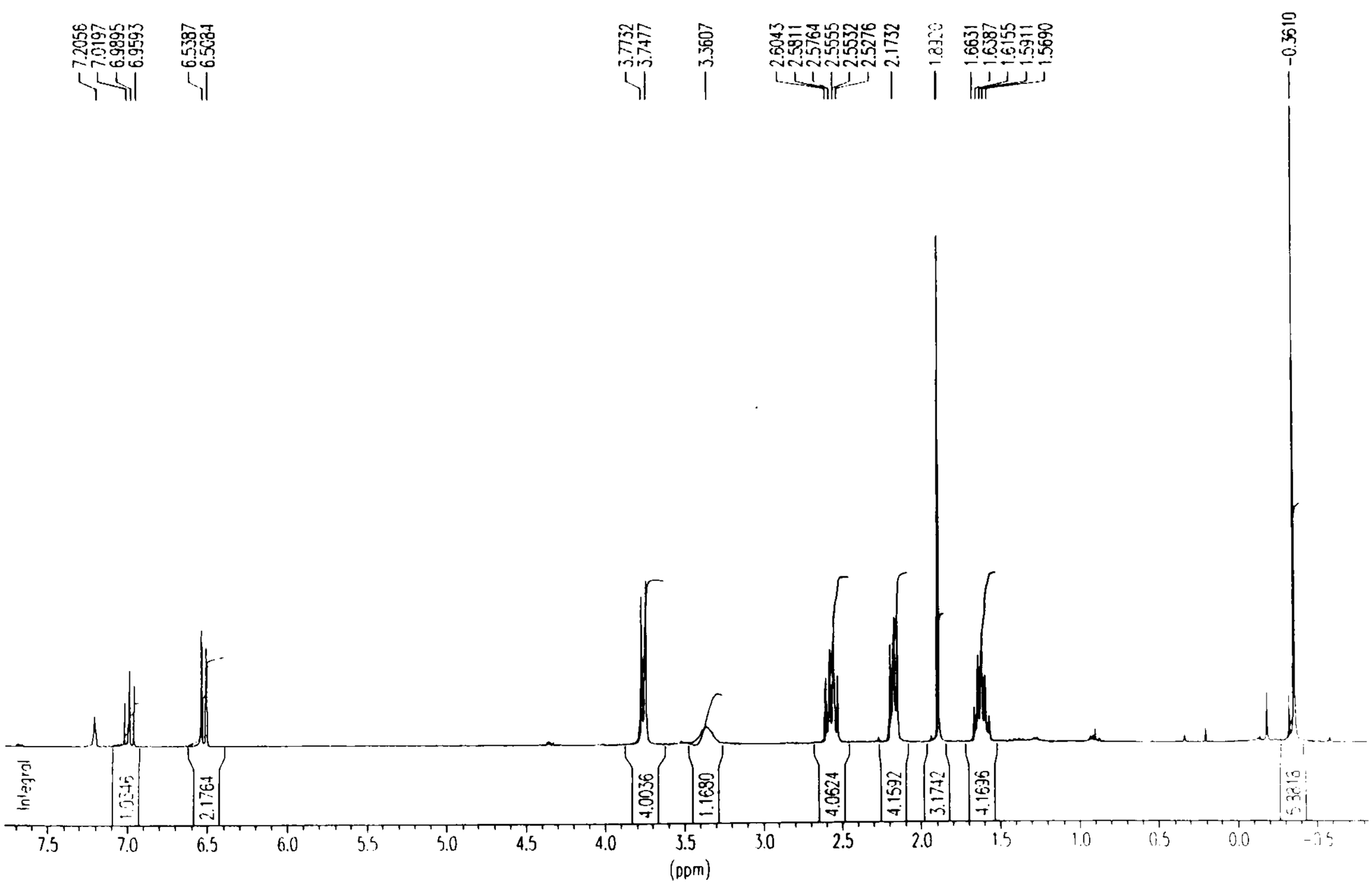

Figure 5.15 The ^{1}H N.M.R. spectrum of the complex $[(HMepy)AlMe_2]$

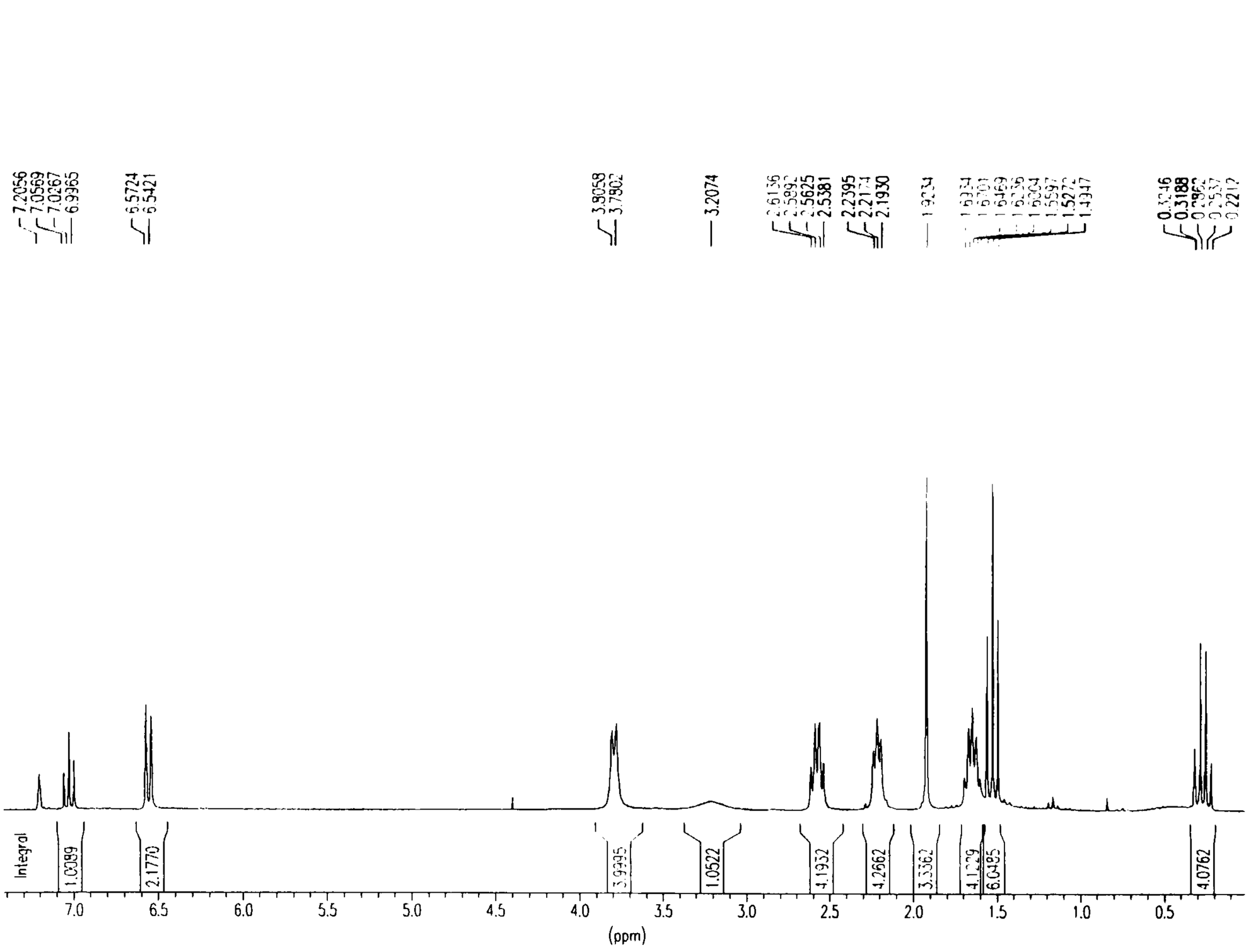

Figure 5.16 The ^{1}H N.M.R. spectrum of the complex [(HMepy)$AlEt_2$]

These ^{1}H N.M.R. spectra remain almost identical to the ^{1}H N.M.R. spectra of the free ligand with the addition of the Al–R resonances. The splitting pattern for the ligand resonances remains the same in most instances and these resonances are observed in the same regions although considerable shifts in these resonances are observed. The two most important resonances in the spectra of these complexes are firstly the NH resonance observed between δ 3 and 4 ppm, and its integral (either 1 or 2 protons depending upon whether a proton has been lost due to reaction with Al-R): as well as the Al-R resonance the integral of which also indicates whether RH has been lost due to reaction at the amine.

The ^{13}C N.M.R. spectra are also similar to that of the free ligand. Upon forming the aluminium complex the symmetry within the ligand is still retained and can be described as in Figure 5.8 (p.203). The assignment of the ^{13}C N.M.R. resonances are given in Table 5.1.

From the ^{1}H and ^{13}C N.M.R. spectra it is apparent that the symmetry within these complexes is the same as within the free ligand. Therefore AlR_3 must add to the complex in such a way that the symmetry within the ligand is retained.

Table 5.1 Summary of proton decoupled ^{13}C N.M.R shifts (δ/ppm.) for H_2Mepy and its Al(III) complexes

Compound	C(1)	C(2)	C(3)	C(4)	C(5)	C(6)	C(7)	N–Me	Al–R
H_2Mepy	135.62	119.77	160.13	56.14	54.81	27.39	46.53	40.52	–
$[(H_2Mepy)AlMe_3]$	136.45	120.77	157.70	55.93	53.77	25.95	47.25	41.25	–8.52
$[(HMepy)AlMe_2]$	136.14	120.38	158.33	55.89	54.12	26.59	46.85	41.03	–8.03
$[(HMepy)AlEt_2]$	135.98	120.15	158.97	55.93	54.35	26.92	46.13	40.95	10.31, –0.06

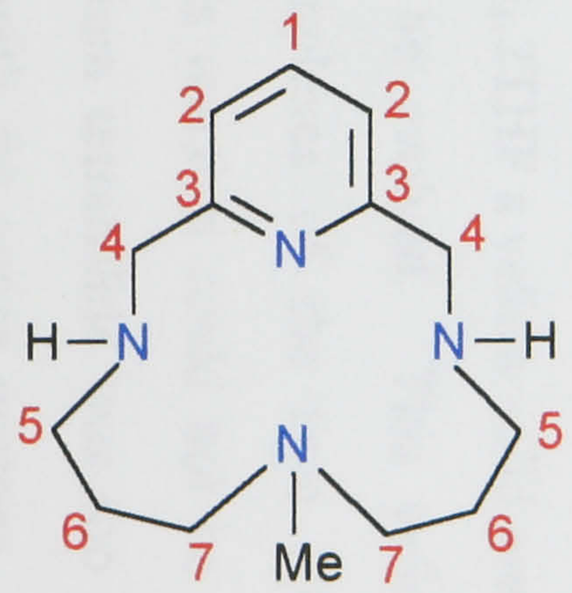

Reactions of H_2Mepy with Group 4 transition metals

Once it had been established that one of the NH protons could be removed reactions were then carried out with the Group 4 transition metals. It was decided to again use the THF adduct of the Group 4 tetrahalides ($MCl_4.2THF$) in these reactions. Initially, the straight reaction of the Group 4 tetrahalide and the free ligand was attempted

$$H_2Mepy + MCl_4.2THF \longrightarrow [(Mepy)MCl_2] + 2HCl + 2THF \quad (1)$$

(M = Ti, Zr, Hf)

It was hoped that the respective Group 4 tetrahalide would be reactive enough to remove both the NH protons and form the desired complex (equation 1). These reactions were carried out in toluene with heating (50 °C). In the reactions with zirconium and hafnium, on addition of the $MCl_4.2THF$ a yellow solid precipitated and a gas (assumed to be HCl) was seen to be evolved. This yellow solid on spectroscopic analyses appeared to be complexes of the type $[(Mepy)MCl_2]$. However with titanium the product from this reaction could not be satisfactorily identified, and it was believed that the titanium tetrahalide was too reactive and breaks down the ligand as well as reacting with the amine protons. In order to produce the complex $[(Mepy)TiCl_2]$ it was decided to remove the NH protons by making the dilithium salt of the ligand and then reacting the dilithium salt with titanium tetrahalide

$$H_2Mepy + 2LiMe \longrightarrow Li_2Mepy + 2CH_4 \quad (2)$$

$$Li_2Mepy + TiCl_4.2THF \longrightarrow [(Mepy)TiCl_2] + 2LiCl \quad (3)$$

Despite numerous attempts to isolate the dilithium salt of the ligand (equation 2) this was not possible due to the extreme reactivity of the compound. However, it is assumed that the dilithium salt is formed due to the deep red solid resulting from the reaction which is consistent with dilithium salts of other tetraazamacrocycles. As a result of this the dilithium salt was used in situ and the titanium tetrahalide was slowly

added to a toluene solution of the dilithium salt. This reaction mixture was heated to 50 °C which resulted in the precipitation of a brown solid. The problem of removing the lithium chloride which is also precipitated was overcome by numerous washings of the solid with dry THF. The spectroscopic and elemental analyses of the resultant solid indicated that the reaction had proceeded as in equations 2 and 3 yielding the desired complex [(Mepy)$TiCl_2$]. The predicted structure of [(Mepy)$TiCl_2$] is shown below in Figure 5.17.

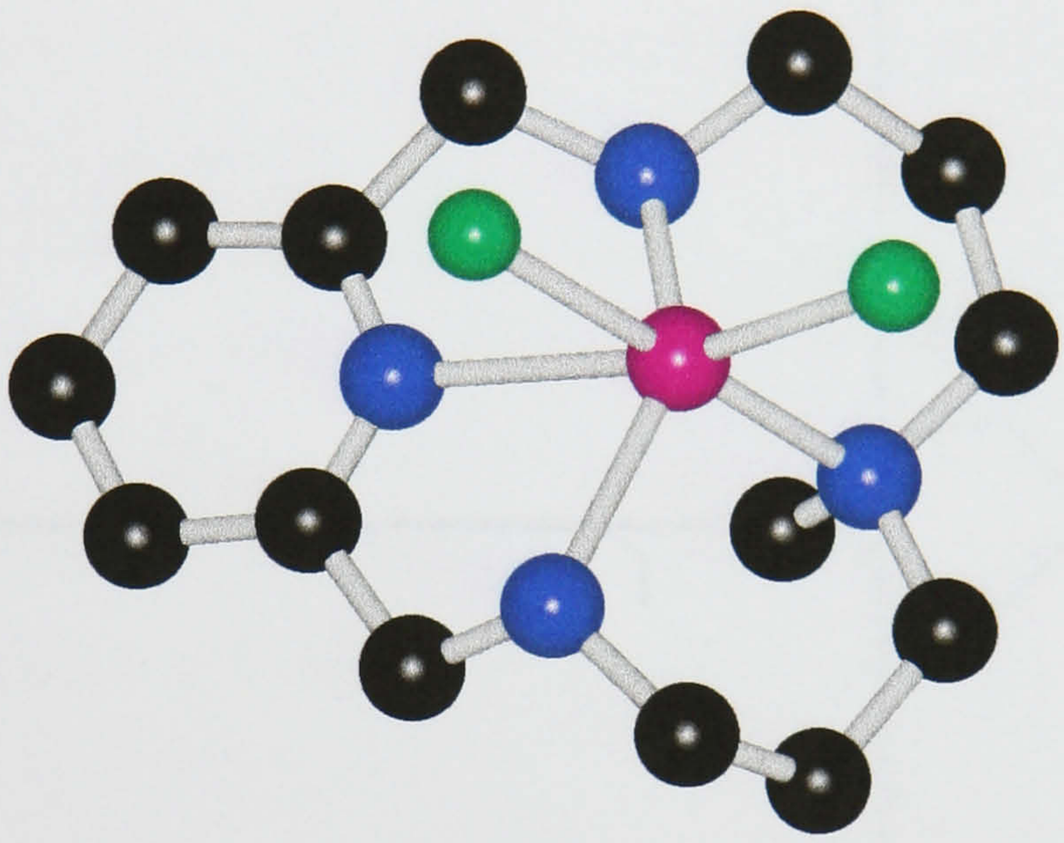

Figure 5.17 The predicted structure of [(Mepy)$TiCl_2$].

Spectroscopic Properties

N.M.R. Spectra

The ^{1}H N.M.R. spectra of the [(Mepy)MCl_2] complexes (M = Ti, Zr, Hf) have been recorded and confirm the loss of both the NH protons from the ligand. All the other ligand resonances show a very similar profile to those of the free ligand. The ^{1}H N.M.R. spectrum of [(Mepy)$HfCl_2$] is shown in Figure 5.18 as a typical example.

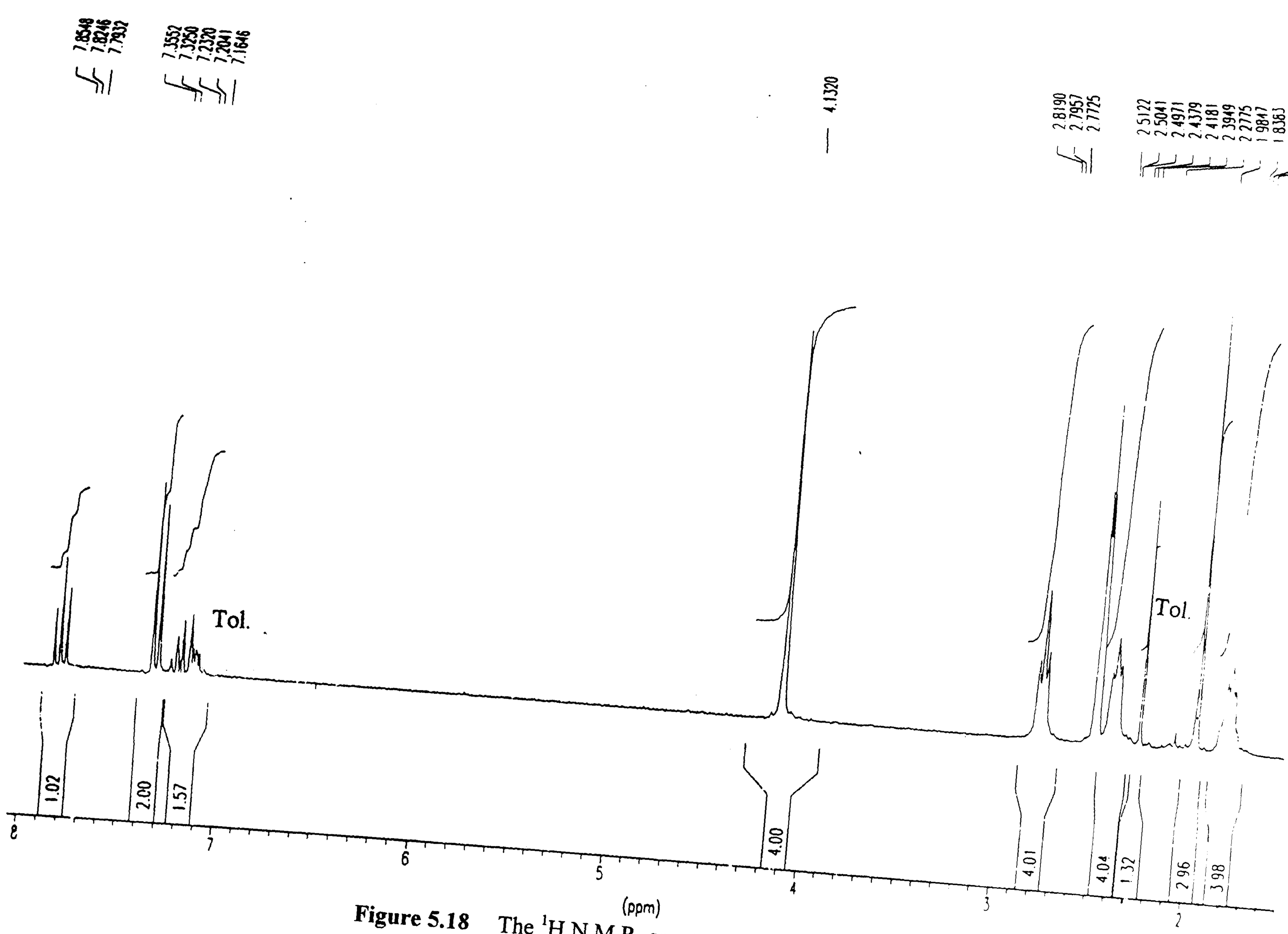

Figure 5.18 The ^{1}H N.M.R. spectrum of [(Mepy)$HfCl_2$]

Experimental

Again all reactions were carried out in a dry nitrogen or argon atmosphere using conventional Schlenk apparatus and techniques. All solvents were carefully dried using either calcium hydride or sodium metal,and glassware was stored in a hot oven.

Preparation of 2,6-Pyridinedicarbaldehyde

2,6-Pyridinedimethanol (19 g, 0.137 mol) an selenium dioxide (15.15 g, 0.137 mol) were dissolved in toluene (300 cm^3) and heated to 80°C whilst stirring vigorously. The reaction was followed by TLC (aluminium plates and 50 % CH_2Cl_2 and 50 % hexane) and after 4 h selenium dioxide (15.15 g, 0.137 mol) was added and stirred at 80°C for a further 3 h to ensure a complete reaction occurred. The solution was allowed to cool and was then filtered through a bed of Celite and the solvent was removed from the filtrate by evaporation. Yield = 16 g (85 %). ^1H N.M.R. ($CDCl_3$): δ/ppm. 8.15 (3H, m), 10.16 (2H, s)

Preparation of H_2Mepy

To a stirred solution of freshly prepared 2,6-pyridinedicarbaldehyde (9.81 g, 72.7 mmol) in ethanol (150 cm^3) was added a solution of $Cu(NO_3)_2.4H_2O$ (17.56 g, 72.7 mmol) in water (150 cm^3). To the resulting pale green solution was added dropwise, with stirring, a solution of 1,7-diamino-4-methyl-4-azaheptane (9.54 g, 72.7 mmol) in ethanol (30 cm^3). The resulting deep blue solution was stirred whilst heating under reflux for 2 h, during which time an intense violet colour develops. The solution is then placed under a dry nitrogen atmosphere and cooled to 5°C. Sodium tetrahydroborate (7 g, 184.2 mmol) was added in small portions over a period of 30 min. The solution was stirred at room temperature for 30 min, and then heated to reflux for a further 30 min, before being left to stir overnight at room temperature. The copper was removed by treating the mixture with $Na_2S.9H_2O$ (40 g, 167 mmol) followed by heating to reflux for 30 min. The solution was then cooled, and the black copper sulphide removed by filtration through a bed of Celite. The filtrate was

extracted with dichloromethane (7 × 200 cm^3), the combined extracts dried with anhydrous $MgSO_4$, and the dichloromethane removed by evaporation to leave an orange/white gel. The pure ligand was obtained by the sublimation of the gel. Yield = 5 g.

^{1}H N.M.R. (C_6D_6) δ/ppm: 7.08–7.02 (t, 1H); 6.60–6.57 (d, 2H); 3.84 (s, 4H); 3.05 (s, 2xNH); 2.61–2.56 (t, 4H); 2.30–2.25 (t, 4H); 1.97 (s, 3H); 1.76–1.66 (qu, 4H):

^{13}C N.M.R (C_6D_6) δ/ppm: 160.13, 135.62, 119.77, 56.14, 54.81, 46.53, 40.52, 27.39.

Analysis, calculated for $C_{14}H_{24}N_4$ (M.W. 248.37): C, 67.70; H, 9.74: N, 22.56%. Found: C, 67.82; H, 9.68; N, 22.71%.

***Preparation of* Hpy**

The ligand Hpy was prepared using the same procedure as for H_2Mepy, replacing 1,7-diamino-4-methyl-4-azaheptane with 1,7-diamino-4-azaheptane. Yield = 3g.

^{1}H N.M.R. (C_6D_6) δ/ppm: 7.06–7.00 (t, 1H); 6.60–6.57 (d, 2H); 3.80 (s, 4H); 3.00–2.70 (br s, 3xNH); 2.64–2.60 (t, 4H); 2.58–2.54 (t, 4H); 1.71–1.62 (qu, 4H):

^{13}C N.M.R (C_6D_6) δ/ppm: 159.77, 135.80, 119.89, 54.59, 47.83, 46.89, 29.36.

Analysis, calculated for $C_{13}H_{22}N_4$ (M.W. 234.34): C, 66.63; H, 9.46: N, 23.91%. Found: C, 66.80; H, 9.48; N, 24.03%.

***Preparation of* [(H_2Mepy)$AlMe_3$]**

To a stirred solution of H_2Mepy (0.5 g, 1 eq) in toluene (40 cm^3) at –78 °C was slowly added via a syringe an equimolar amount of a 2.0 $moldm^{-3}$ solution of $AlMe_3$ (1.1 cm^3) in hexane. The solution was allowed to warm to room temperature, then stirred at 50 °C for 2 h. After this time the solution was allowed to cool and then evaporated to dryness. The resultant yellow solid was washed with dry hexane (30cm^3) and dried under vacuo.

^{1}H N.M.R. (C_6D_6) δ/ppm: 6.98–6.92 (t, 1H); 6.51–6.48 (d, 2H); 3.67 (s, 4H); 3.61 (br s, 2xNH); 2.58–2.51 (q, 4H); 2.15–2.10 (t, 4H); 1.86 (s, 3H); 1.58–1.49 (qu, 4H); –0.40 (s, 9H): ^{13}C N.M.R (C_6D_6) δ/ppm: 157.70, 136.45, 120.77, 55.93, 53.77, 47.25, 41.25, 25.95, –8.52.

***Preparation of* [(HMepy)AlMe$_2$]**

To a stirred solution of H_2Mepy (0.5 g) in toluene (30 cm^3) at –78°C was slowly added using a syringe a 2 molar amount of a 2.0 moldm^{-3} solution of $AlMe_3$ (2.2 cm^3) in hexane. The solution was allowed to warm to room temperature, then refluxed at 120°C for 4 h. After this time the solution was allowed to cool and then evaporated to dryness. The resultant yellow solid was washed with dry hexane (30 cm^3) and dried under vacuo.

^{1}H N.M.R. (C_6D_6) δ/ppm: 7.01–6.95 (t, 1H); 6.53–6.50 (d, 2H); 3.77–3.74 (d, 4H); 3.35 (s, NH); 2.60–2.52 (q, 4H); 2.19–2.14 (t, 4H); 1.89 (s, 3H); 1.66–1.56 (qu, 4H) –0.36 (s, 9H): ^{13}C N.M.R (C_6D_6) δ/ppm: 158.33, 136.14, 120.38, 55.89, 54.12, 46.85, 41.03, 26.59, –8.03.

***Preparation of* [(HMepy)AlEt$_2$]**

To a stirred solution of H_2Mepy (0.3 g, 1 eq) in toluene (40 cm^3) at –78°C was slowly added using a syringe a 2 molar amount of a 2.0 moldm^{-3} solution of $AlEt_3$ (2.5 cm^3) in hexane. The solution was allowed to warm to room temperature, then stirred at 50°C for 2 h. After this time the solution was allowed to cool and then evaporated to dryness. The resultant yellow solid was washed with dry hexane (30 cm^3) and dried under vacuo.

^{1}H N.M.R. (C_6D_6) δ/ppm: 7.05–6.99 (t, 1H); 6.57–6.54 (d, 2H); 3.80–3.78 (d, 4H); 3.20 (s, NH); 2.61–2.53 (q, 4H); 2.24–2.19 (t, 4H); 1.92 (s, 3H); 1.69–1.60 (qu, 4H) 1.55–1.49 (t, 6H); 0.32–0.22 (q, 4H): ^{13}C N.M.R (C_6D_6) δ/ppm: 158.97, 135.98, 120.15, 55.93, 54.35, 46.13, 40.95, 26.92, 10.31, –0.06.

***Preparation of* [M(Mepy)Cl$_2$] *(M* = Zr, Hf).**

To a stirred solution of H_2Mepy (0.5g, 1 eq) in toluene (40 cm^3) at –78°C was slowly added an equimolar amount of MCl_4.2THF in toluene (30 cm^3). On addition a yellow solid precipitated and a gas was seen to be evolved. The suspension was allowed to warm to room temperature, then stirred at 50°C for 2 h. After this time the yellow solid was filtered from the solution and dried *in vacuo*

[Zr(Mepy)Cl_2]:

^{1}H N.M.R. (d^6–DMSO) δ/ppm: 7.81–7.73 (t, 1H); 7.30–7.27 (d, 2H); 4.04 (s, 4H); 2.72–2.67 (t, 4H); 2.39–2.35 (t, 4H); 1.97 (s, 3H); 1.77–1.70 (qu, 4H):

Analysis, calculated for $C_{14}H_{22}N_4ZrCl_2$ (M.W.): C, 41.17; H, 5.43; N, 13.72%. Found: C, 41.46; H, 5.38; N, 14.01%.

[Hf(Mepy)Cl_2]:

^{1}H N.M.R. (d^6–DMSO) δ/ppm: 7.85–7.79 (t, 1H); 7.35–7.32 (d, 2H); 4.13 (s, 4H); 2.81–2.77 (t, 4H); 2.43–2.39 (t, 4H); 1.98 (s, 3H); 1.83–1.79 (qu, 4H):

Analysis, calculated for $C_{14}H_{22}N_4HfCl_2$ (M.W.): C, 33.92; H, 4.47; N, 11.30%. Found: C, 34.00; H, 4.49; N, 11.52%.

Preparation of **[Ti(Mepy)Cl_2]**

To a stirred solution of H_2Mepy (0.5 g, 1 eq) in toluene (40 cm^3) at –78 °C was slowly added LiMe (a 1.25 $moldm^{-3}$ solution in Et_2O, 2 eq). A deep red solution resulted which was stirred at 40 °C for 1 h. After this time it was allowed to cool and then transferred to a solution of [$TiCl_4(THF)_2$] (1 eq) in toluene (30 cm^3) at –78 °C. On addition a brown solid precipitated, this suspension was allowed to warm to room temperature, then stirred at 50 °C for 2 h. After this time the solid was filtered and dried *in vacuo*.

^{1}H N.M.R. (d^6–DMSO) δ/ppm: 7.93–7.87 (t, 1H); 7.44–7.40 (d, 2H); 4.28 (s, 4H); 2.97–2.93 (t, 4H); 2.51–2.49 (t, 4H); 2.00 (s, 3H); 1.97–1.91 (qu, 4H):

Analysis, calculated for $C_{14}H_{22}N_4TiCl_2$ (M.W.): C, 46.05; H, 6.07; N, 15.34%. Found: C, 46.21; H, 6.12; N, 15.55%.

CHAPTER 6

Polymerisation Studies

CHAPTER 6 Polymerisation Studies

Introduction

The aim of this research project was to investigate the coordination chemistry of the early transition metals with ligands other than those containing the cyclopentadienyl group, and at the same time to recognise the role that such compounds play in the synthesis and design of potential Ziegler-Natta polymerisation catalysts. Initially these complexes were examined for their use as ethylene polymerisation catalysts, although, their use in propylene and styrene polymerisation would also be of interest.

Initially the testing of the complexes prepared within this research was performed within the chemistry department at the University of Warwick using a specially built polymerisation rig (See Figure 6.1). If any of these complexes were found to be catalytically active, or interesting then further, more detailed, testing of these complexes was to be performed at BP Chemicals, Sunbury using their small scale testing rig, operating at constant higher pressures and temperatures nearer to those used on the industrial plant.

The polymerisation rig in Warwick was designed in such a way that both ethylene and propylene monomers could easily be used in the polymerisation reaction. It was also essential that the rig had a detachable reaction vessel which could be attached to a Schlenk line due to the air and moisture sensitivity of both the catalysts and the cocatalyst methylaluminoxane, MAO. A schematic representation of the polymerisation rig is shown in Figure 6.1. The reservoir contains either the ethylene or the propylene prior to their addition to the reaction vessel. The reaction vessel is made from borosilicate glass and has a volume of 350 cm^3. The remainder of the apparatus is constructed from stainless steel (i.e. the tubing, gas containers and pressure valves). The rig was designed and built by Drs. A. McCamley and D. Duncalf, and is interfaced to a PC to allow a continuous monitoring of the pressure and temperature throughout a run. Unlike the pressure rig at BP, which operates at a fixed pressure of alkene gas, the rig described here uses a fixed volume (500 cm^3) in the reservoir vessel so that as the polymerisation proceeds there is a fall in the

pressure inside the reaction vessel. Such an arrangement, although not ideal, is a compromise to avoid the extra complexity and expense which would be necessary to introduce the alkene gas via special valves, coupled to a monitoring system to maintain a constant pressure. In spite of these limitations the rig proved to be extremely successful in monitoring the relative effectiveness of the catalysts, and gave results which corresponded to the overall order of effectiveness obtained using the industrial rig.

A typical test performed on the rig is as follows. A standard solution of the catalyst was made in toluene and on each polymerisation run only 10 mg of catalyst was used unless otherwise stated. The reaction vessel was attached to a Schlenk line and purged with argon before use. Toluene and MAO (typically 1000:1, MAO:catalyst) are added to the reaction vessel via a syringe and allowed to stir for ca 15 minutes to allow further drying of the toluene before the addition of a toluene solution of the catalyst. The vessel is then sealed by closing tap G and attached to the polymerisation rig. All the equipment on the rig is attached to a vacuum pump enabling the system to be left under vacuum to remove any air or moisture from the connecting pipework once the reaction vessel is attached to the polymerisation rig. The system is then sealed from the vacuum by closing tap H. The monomer then flows through tap A or tap B to the scrubber which contains potassium sublimed onto glass wool to remove any moisture. The pressure of the monomer gas can be varied but the system is usually run at 40 psi for all reactions. The monomer gas flows via tap C or tap D into the reservoir where it is kept until required for the reaction. To avoid any contamination the scrubbers are sealed from the main system by closing taps A-D, and the monomer is then allowed to enter the reaction vessel by opening tap G. The initiation of the polymerisation reaction can usually be observed visually by the formation of colourless solid polymer in the reaction vessel. The reaction pressure and temperature are monitored over the reaction run via gauges which are linked to a PC. When the run is finished taps F and G are closed and the reaction vessel is removed from the rig. Tap E to the reservoir is closed and the residual gases in the system are removed under vacuum by opening tap H, so that the system remains under vacuum until the next time the rig is used.

Any excess gas from the reaction which remains in the reaction vessel is vented into a fumehood by opening tap G, then the reaction mixture is quenched by the addition of acidified methanol. The polymer, which is usually obtained as colourless granular particles, is then removed from the solvent, washed and dried in an oven.

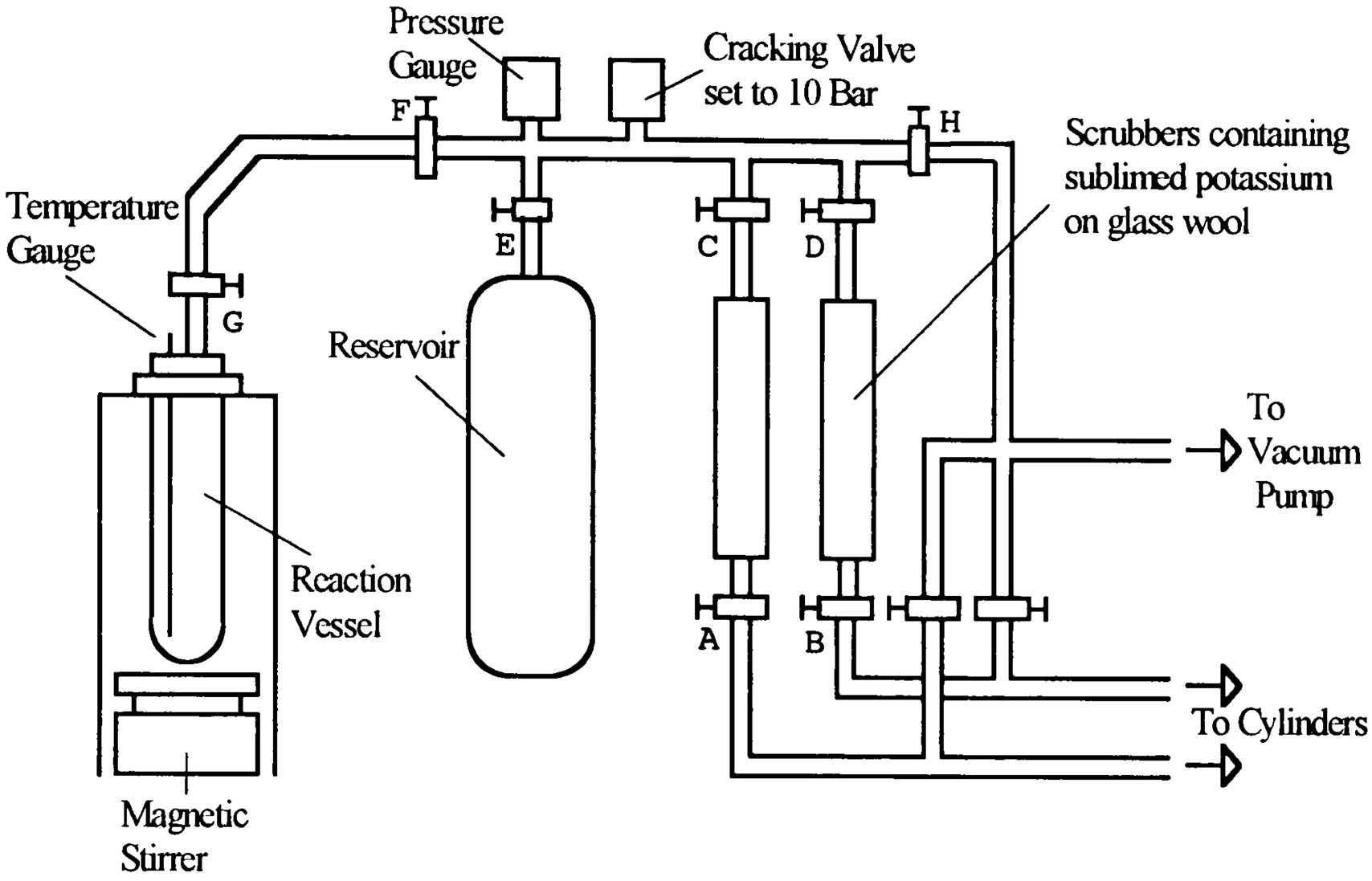

Specifications

Reaction Vessel max P= 10 Bar
max T=200C
max ΔT=50K

Computer monitors temperature and pressure

Figure 6.1 Schematic representation of the high pressure polymerisation test rig

Ethylene polymerisation Studies

Testing procedure:

The weights of the respective reagents used are calculated from the corresponding molecular weights of the reagents with the empirical formula of MAO assumed to be (MeAlO).

To methyl aluminoxane (MAO, 1000 eqv) in toluene (*ca* 100 cm^3) is added a toluene solution (20 cm^3) of the catalyst (10 mg, 1 eqv). This mixture is then placed on the

rig at room temperature (23 °C) and under a pressure of ethene (30 psi) and left stirring for 1 h. After 1 h the reaction is quenched with methanol (100 cm^3) containing HCl (4 drops of concentrated acid) and the polyethylene is filtered off, dried and weighed.

Table 6.1 The results of ethylene polymerisation tests with Group 4 complexes

Complex	**Ratio of Complex : MAO**	**Yield of Polyethylene (g polymer per mmol catalyst)**
$[Zr(omtaa)Cl_2]$	1:1000	56.2
$[Ti(omtaa)Cl_2]$	1:100	18.1
$[Ti(EtSLPN)Cl_2]$	1:1000	97.1
$[Ti(PhSLPN)Cl_2]$	1:1000	69.7
$[Ti(EtCycH)Cl_2]$	1:1000	19.9
$[Ti(PhCycH)Cl_2]$	1:1000	15.8
$[Zr(PhSLPN)Cl_2]$	1:1000	14.8
$[Zr(EtCycH)Cl_2]$	1:1000	15.3
$[Zr(HCycH)Cl_2]$	1:1000	4.9
$[Zr(PhSALEN)Cl_2]$	1:1000	14.5
$[Ti(DMSALEN)Cl_2]$	1:1000	-
$[Ti(EtSALEN)Cl_2]$	1:1000	-

From the results in Table 6.1 it can be seen that both the Schiff base complexes and the macrocyclic tetraazannulene complexes act as polymerisation catalysts to some degree. There are several points of interest with these results that are discussed below

The first, and probably the most significant finding is that ***trans*** complexes ([Ti(DMSALEN)Cl_2] and [Ti(EtSALEN)Cl_2]) were found to be non-catalytic and the corresponding ***cis*** complexes to be catalytic for alkene polymerisation. This result is as expected from the theories about the mechanism of catalysis and is consistent with current proposals that a *cis* configuration at the metal is desirable for alkene polymerisation to occur. The inability of a *trans* complex to produce polymer might also be used to verify the conformation of complexes where suitable crystals for X-ray crystallography cannot be grown.

There also appears to be a pattern with the Schiff base complexes as to which backbone and substitution produce the best catalyst (see Figure 6.2).

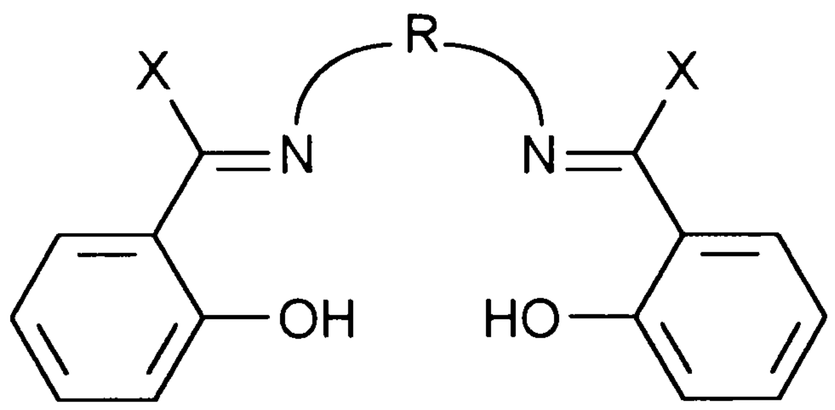

Figure 6.2 A diagrammatic representation of a tetradentate Schiff base ligand showing the sites of ligand modification (R, X).

From the results obtained it was found that for the backbone R, the 2,2-dimethyl propyl group produced more polymer than the cyclohexyl group which produced more polymer than the CH_2CH_2 group. As for the substitution X, the ethyl group was better than the phenyl, followed by methyl and finally a hydrogen. The relative efficiencies of the catalysts may therefore be summarised as:

R group	$-CH_2C(Me_2)CH_3 > C_6H_{11} > CH_2CH_2$
X group	Et > Ph > Me > H

These findings can be attributed to steric influences on the complex. It was also observed that the titanium catalysts produce more polymer than the corresponding zirconium catalysts.

The polymerisations also showed the expected pattern during the polymerisation reaction i.e. an increase in temperature and a loss in pressure. A typical trace can be seen in Figure 6.3.

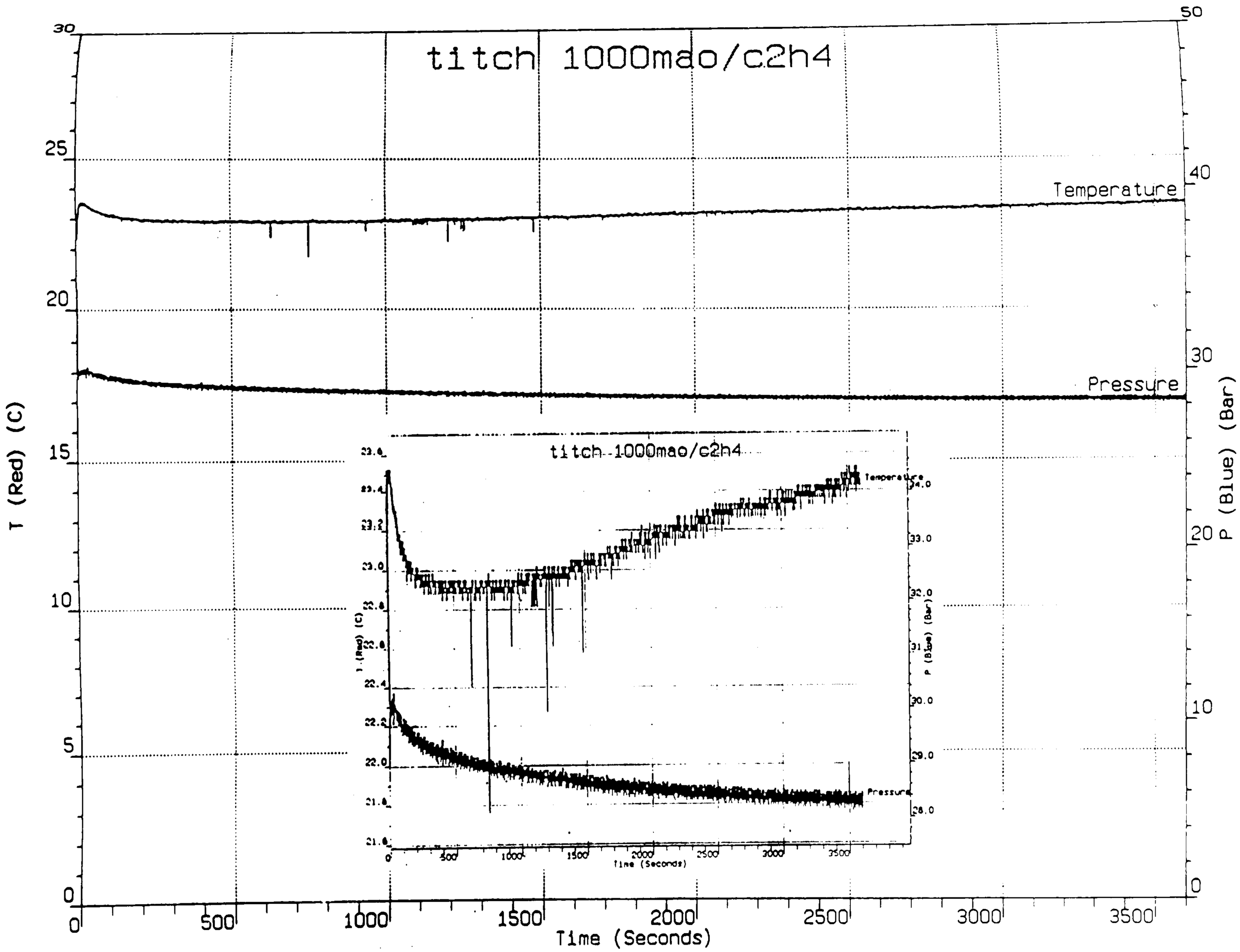

Figure 6.3 Showing a typical trace of temperature and pressure in the polymerisation reaction

The polymer that was produced in these polymerisation reactions was sent to BP Chemicals, Sunbury for analysis by GPC. A table of the results obtained from these analyses can be seen below in Table 6.2.

Table 6.2 Results of the GPC analyses on the polyethylene products

Complex	M_n*	M_w*	M_w/M_n	M_{pk}*
$[Zr(omtaa)Cl_2]$	465000	1335000	2.9	1267000
$[Ti(omtaa)Cl_2]$	-	>2000000	-	-
$[Ti(EtSLPN)Cl_2]$	-	>2000000	-	-
$[Ti(PhSLPN)Cl_2]$	-	>2000000	-	-
$[Ti(EtCycH)Cl_2]$	9000	334000	38.6	116000
$[Ti(PhCycH)Cl_2]$	-	>2000000	-	-
$[Zr(PhSLPN)Cl_2]$	4000	131000	32.3	118000
$[Zr(EtCycH)Cl_2]$	2000	19000	10.6	7000
$[Zr(HCycH)Cl_2]$	4000	47000	10.9	24000
$[Zr(PhSALEN)Cl_2]$	416000	1043000	2.5	923000

* Figures rounded to the nearest 1000.

As can be seen from Table 6.2, some of the titanium catalysts gave polymer with a MW too high to be measured i.e. $M_w > 2000000$. $[Zr(PhSALEN)Cl_2]$ also gave very high MW polyethylene whose molecular weight was just measurable, although all the highest MW material was probably not measured as it remained undissolved. $[Zr(omtaa)Cl_2]$ also gave very high MW which gave a good trace, the other samples gave low or broad traces.

The GPC trace for the polymer obtained with $[Ti(EtCycH)Cl_2]$ can be seen in Figure 6.4. The GPC peak is seen to be centred on 116000 but is skewed strongly to low MW, with considerable deviation from symmetrical the log normal distribution

normally observed for a single site catalyst. The reason for this is probably ethylene diffusion limitation following early stages of the reaction, which inhibits propagation without inhibiting termination. In the polymerisation rig this can occur with falling ethylene concentration in solution combined with poor ethylene diffusion into the solvent. These results indicate that the catalyst is potentially more active than actually measured. The process limitation means that M_w and M_n will be lower than their true values and the MW distribution (polydispersity) M_w/M_n will be higher. However, whether it is actually 2 (the theoretical value for a single site catalyst) or higher is not possible to say.

$M_w = \frac{\sum N_i M_i}{\sum N_i}$ = The *weight average molar mass* defined as 'the sum of the products of the molar mass of each fraction multiplied by its weight fraction'.

$M_n = \frac{\sum N_i M_i^2}{\sum N_i M_i}$ = The *number average molar mass* defined as 'the sum of the products of the molar mass of each fraction multiplied by its mole fraction'.

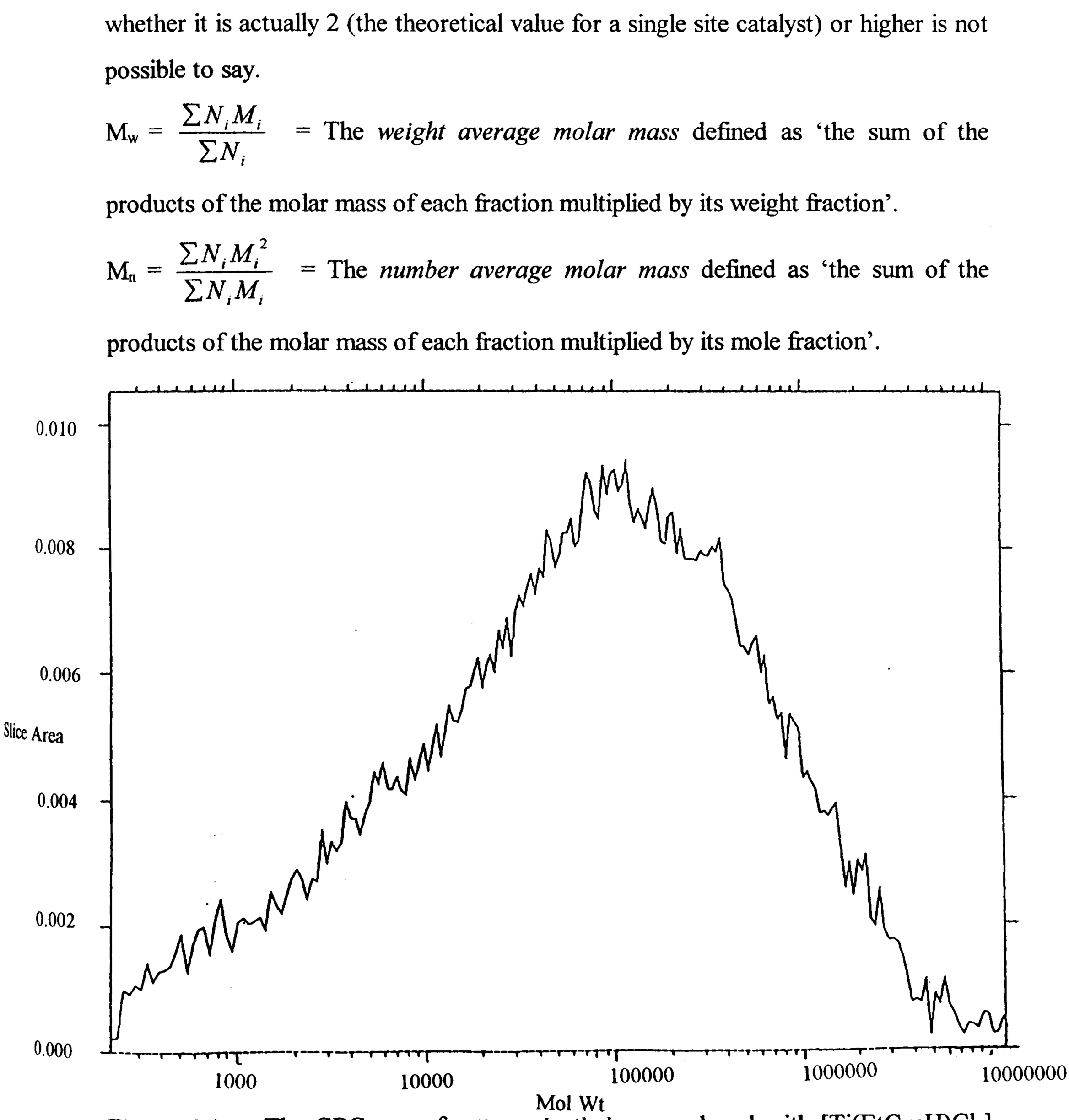

Figure 6.4 The GPC trace for the polyethylene produced with [Ti(EtCycH)Cl_2].

Styrene polymerisation Studies

A brief study of these complexes for their use as potential styrene polymerisation catalysts was also undertaken. The four complexes used in this study were [Ti(EtCycH)Cl_2], [Ti(omtaa)Cl_2], [Zr(omtaa)Cl_2] and [Zr(PhSALEN)Cl_2]. These studies were not carried out on the polymerisation rig, but in Schlenk tubes on a Schlenk line.

Testing procedure:

To methyl aluminoxane (MAO, 500 eq) in toluene (*ca* 50 cm^3) is added styrene (5 cm^3) and the solution is stirred for 20 minutes after which time a toluene solution (20 cm^3) of the catalyst (10 mg, 1eq) is added. The reaction was then left for 21 hours after which time the polymer produced was filtered, washed and dried.

Table 6.3 Showing the results of styrene polymerisation tests with Group 4 complexes

Complex	**Ratio of Complex : MAO**	**Yield of Polystyrene**
[Zr(omtaa)Cl_2]	1:500	0g
[Ti(omtaa)Cl_2]	1:500	0.1g
[Ti(EtCycH)Cl_2]	1:500	0.3g
[Zr(PhSALEN)Cl_2]	1:500	0.3g

These results show that these complexes are poor catalysts for the polymerisation of styrene. One explanation for this is the steric bulk of the styrene is too great to for effective polymerisation to occur.

REFERENCES

REFERENCES

1 R. R. Schrock, *Inorg. Chem.*, 1981, **20**, 1844.

2 R. J. H. Clark, *The Chemistry of Titanium and Vanadium*, Elsevier, Amsterdam, 1968; R. J. H. Clark, *Comprehensive Inorganic Chemistry*, Vol.3, Chapter 32, Pergamon Press, Oxford, 1973; C. A. McAuliffe and D.S. Barratt, *Comprehensive Coordination Chemistry*, Vol.3, Chapter 31, Pergamon Press, Oxford, 1987; R. S. P. Coutts and P. C. Wailes, *Adv. Organomet. Chem.*, 1970, **9**, 135.

3 A. Clearfield, D. K. Warner, C. H. Saldarriaga-Molina, and R. Ropal, *Can. J. Chem.*, 1975, **53**, 1622.

4 Houben-Wehl, *Methods in Organic Chemistry*, Vol.13, Part 7, Thieme, 1976; P. C. Wailes, R. S. P. Coutts and H. Weigold, *Organometallic Chemistry of Titanium, Zirconium and Hafnium*, Academic Press, 1974; R. Feld and P. L. Cowe, *The Organic Chemistry of Titanium*, Butterworth, London and Washington D. C. (1965); M. Bottrill, P. D. Gavens, J. W. Kelland and J. McMeeking, *Comprehensive Organometallic Chemistry*, Vol.3, Chapters 22.1, 22.2, 22.3 and 22.4, (Ed. G. Wilkinson, F. G. A. Stone and E. W. Abel) Pergamon Press, Oxford, 1982.

5 W. Kroll, *Metall. und Erz.*, 1939, **36**, 101, 125.

6 R. D. Euler and E. F. Westrum, *J. Phys. Chem.*, 1961, **65**, 132.

7 G. W. A. Fowles and R. A. Hoodless, *J. Chem. Soc.*, 1963, 33.

8 J. B. Everhart and B. S. Ault, *Inorg. Chem.*, 1995, **34**, 4379.

9 C. I. Brändén, *Acta Chem. Scand.*, 1962, **16**, 1806.

10 S. I. Troyanov, G. N. Mazo and M. A. Simonov, *Koord. Khim.*, 1985, **11**, 1147 (Chem. Abstr., **103**, 151297y).

11 Guo Guolin, Pan Zuohua and Zhang Zeying, *Wuli Huaxue Xeubao* (*Acta Phys.-Chim. Sin.*), 1986, **2**, 278 (Chem. Abstr., **105**, 181782m).

12 L. E. Manzer, *Inorg. Synth.*, 1982, **21**, 135.

13 Guo Guolin, Xie Youchang and Tang Youqi, *Sci. Sin. Ser. B*, (*Engl. Ed*), 1984, **27**, 1 (Chem. Abstr., **101**, 60874b).

14 G. Mazo, A. Bobilev and S. Troyanov, *Vestn. Mosk. Univ. Ser. 2: Khim.*, 1987, **28**, 459 (Chem. Abstr., **108**, 105196v).

15 M. Boyer and Y. Jeannin, *J. Coord. Chem.*, 1978, **7**, 219.

16 L. Brun, *Acta Crystallogr.*, 1966, **20**, 739.

17 D. C. Bradley and C. E. Holloway, *J. Chem. Soc.* (A), 1969, 282.

18 G. R. Willey, M. L. Butcher, M. McPartlin and I. J. Scowen, *J. Chem. Soc. Dalton Trans.*, 1994, 305.

19 P. Sobota, J. Utko and T. Lis, *J. Organomet. Chem.*, 1990, **393**, 349.

20 G, Maler, U. Siepp and R. Boese, *Tetrahedron Lett.*, 1987, **28**, 4515.

21 D. C. Bradley, *Adv. Inorg. Chem. Radiochem.*, 1972, **15**, 259.

22 B. A. Wright and D. A. Williams, *Acta Crystallogr., Sect. B*, 1968, **24**, 1107.

23 J. A. Ibers, *Nature*, 1963, **197**, 686.

24 R. D. Witters and C. N. Caughlan, *Nature*, 1965, **205**, 1312.

25 M. S. Bains and D. C. Bradley, *Can. J. Chem.*, 1962, **40**, 1350; *ibid.*, 2218; R. Masthoff, H. Köhler, H. Böhland and F. Schmeil, *Z. Chem.*, 1965, **5**, 122.

26 V. W. Day, T. A. Eberspacher, W. G. Klemperer, C. W. Park and F. S. Rosenberg, *J. Am. Chem. Soc.*, 1991, **113**, 8190.

27 K. Watenpaugh and C. N. Caughlan, *J. Chem. Soc., Chem. Commun.*, 1967, 76.

28 W. Haase and H. Hoppe, *Acta Crystallogr., Sect. B*, 1968, **24**, 281.

29 N. Serpone, P. H. Bird, D. G. Bickley and D. W. Thompson, *J. Chem. Soc., Chem. Commun.*, 1972, 217.

30 M. Bottrill, P. D. Gavens, J. W. Kelland and J. McMeeking, *Comprehensive Organometallic Chemistry*, Vol.3, Chapter 22.5 (Ed. G. Wilkinson, F. G. A. Stone and E. W. Abel), Pergamon Press, Oxford, 1982.

31 K. Ziegler, E. Holzkamp, H. Breil, K Martin, *Angew. Chem.*, 1955, **67**, 541; K. Ziegler, *Angew. Chem.*, 1964, **76**, 545.

32 G. Natta, *Angew. Chem.*, 1956, **68**, 393; *ibid.* 1964, **76**, 553.

33 P. Cossee, *J. Catal.*, 1964, **3**, 80; E. J. Arlman, *J. Catal.*, 1964, 3, 89; E. J.

Arlman and P. Cossee, *J. Catal.*, 1964, **3**, 99.

34 *Ziegler Catalysts*, (Ed. G. Fink, R. Mülhaupt and H. H. Brintzinger), Springer, Berlin, 1995.

35 F. Patat and H. Sinn, *Angew. Chem.*, 1958, **70**, 496.

36 G. Wilkinson, P. L. Pauson, J. M. Birmingham and F. A. Cotton, *J. Am. Chem. Soc.*,1953, **75**, 1011.

37 D. S. Breslow and N. R. Newburg, *J. Am. Chem. Soc.*, 1957, **79**, 5072.

38 G. Natta, P. Pino, G. Mazzanti, U. Giannini, E. Mantica and M. Peraldo, *Chim. Ind.*, (Paris), 1957, **39**, 19; G. Natta, P. Pino, G. Mazzanti, U. Giannini and E. Mantica, *J. Am. Chem. Soc.*, 1957, **79**, 2975.

39 D. S. Breslow and N. R. Newburg, *J. Am. Chem. Soc.*, 1959, **81**, 81.

40 J. C. W. Chien, *J. Am. Chem. Soc.*, 1959, **81**, 86.

41 G. Natta, and G. Mazzanti, *Tetrahedron.*, 1960, **8**, 86.

42 F. Patat and H. Sinn, *Angew. Chem.*, 1963, **75**, 805.

43 K. H. Reichert and E. Schubert, *Macromol. Chem.*, 1969, **123**, 58; K. H. Reichert, J. Berthold and V. Dornow, *ibid.*, 1969, **121**, 258; K. Meyer and K. H. Reichert, *Angew. Macromol. Chem.*, 1970, **12**, 175; K. H. Reichert, *ibid.*, 1970, **13**, 177.

44 G. Henrici-Olivé and S. Olivé, *Angew. Chem. Int. Ed. Engl.*, 1967, **6**, 790.

45 A. K. Zelfirova and A. E. Shilov, *Dokl. Chem. (Engl. Transl.),* 1961, **136**, 77; F. S. Dyachkovskii, A. K. Shilov and A. E. Shilov, *J. Polym. Sci. Part C.*, 1967, **16**, 2333.

46 J. J. Eisch, A. M. Piotrowski, S. K. Brownstein, E. J. Gabe and F. L. Lee, *J. Am. Chem. Soc.*, 1985, **107**, 7219.

47 R. F. Jordan, W. E. Dasher and S. F. Echols, *J. Am. Chem. Soc.*, 1986, **108**, 1718; R. F. Jordan, C. S. Bajgur, W. E. Dasher and A. L. Rheingold, *Organometallics*, 1987, **6**, 1041.

48 M. Bochmann and L. M. Wilson, *J. Chem. Soc., Chem. Commun.*, 1986, 1610; M. Bochmann, L. M. Wilson, M. B. Hursthouse and R. L. Short, *Organometallics*, 1987, **6**, 2556.

49 J. J. W. Eshius, Y. Y. Tan, A. Meetsma, J. H. Teuben, J. Renkema and G.

G. Evens, *Organometallics*, 1992, **11**, 362.

50 R. Taube and L. Krukowka, *J. Organomet. Chem.*, 1988, **347**, C9.

51 J. W. Lauher and R. Hoffmann, *J. Am. Chem. Soc.*, 1976, **98**, 1729.

52 M. Brookhart and M. H. Green, *J. Organomet. Chem.*, 1983, **250**, 395.

53 H. Krauledat and H. H. Brintzinger, *Angew. Chem. Int. Ed. Engl.*, 1990, **29**, 1412.

54 W. E. Piers and J. E. Bercaw, *J. Am. Chem. Soc.*, 1990, **112**, 9406.

55 L. A. Castonguay and A. K. Rappé, *J. Am. Chem. Soc.*, 1992, **114**, 5832; T. K. Woo, L. Fan and T. Ziegler, *Organometallics*, 1994, **13**, 2252; H. Weiss, M. Ehrig and R. Ahlrichs, *J. Am. Chem. Soc.*, 1994, **116**, 4919.

56 K. H. Reichert and K. R. Meyer, *Macromol. Chem.*, 1973, **169**, 163.

57 W. P. Long and D. S. Breslow, *Liebigs Ann. Chem.*, 1975, 463.

58 A. A. Anderson, H. G. Cordes, J. Herwig, W. Kaminsky, A. Merck, R. Motweiller, J. Pein, H. Sinn and H. J. Vollmer, *Angew. Chem.*, 1976, **88**, 689; *Angew. Chem. Int. Ed. Engl.*, 1976, **15**, 630.

59 H. Sinn, W. Kaminsky, H. J. Vollmer and R. Woldt, *Angew. Chem.*, 1980, **92**, 396; *Angew. Chem. Int. Ed. Engl.*, 1980, **19**, 396.

60 H. Sinn and W. Kaminsky, *Adv. Organomet. Chem.*, 1980, **18**, 99.

61 J. A. Smith, J. v. Seyerl, G. Huttner and H. H. Brintzinger, *J. Organomet. Chem.*, 1979, **173**, 175.

62 M. D. Fryzuk and B. Bosnich, *J. Am. Chem. Soc.*, 1978, **100**, 5491.

63 F. R. W. P. Wild, L. Zsolnai, G. Huttner and H. H. Brintzinger, *J. Organomet. Chem.*, 1982, **232**, 233; J. A. Ewen, L. Haspeslagh, J. L. Atwood and H. Zhang, *J. Am. Chem. Soc.*, 1987, **109**, 6544.

64 J. A. Ewen, *J. Am. Chem. Soc.*, 1984, **106**, 6355.

65 W. Kaminsky, K. Külper, H. H. Brintzinger and F. R.W. P. Wild, *Angew. Chem.*, 1985, **97**, 507; *Angew. Chem. Int. Ed. Engl.*, 1985, **24**, 507.

66 W. Röll, H. H. Brintzinger, B. Rieger and R. Zolk, *Angew. Chem.*, 1990, **102**, 339; *Angew. Chem. Int. Ed. Engl.*, 1990, **29**, 279.

67 B. Rieger, A. Reinmuth, W. Röll and H. H. Brintzinger, *J. Mol. Catal.*, 1993, **82**, 67.

68 J. A. Ewen, M. J. Elder, R. L. Jones, L. Haspeslagh, J. L. Atwood, S. G. Bott and K. Robinson, *Macromol. Chem. Macromol. Symp.*, 1991, 48/49, 253.

69 W. Kaminsky, R. Engehausen, K. Zoumis, W. Spaleck and J. Rohrmann, *Makromol. Chem.*, 1992, **193**, 1643.

70 W. Röll, L. Zsolnai, G. Huttner and H. H. Brintzinger, *J. Organomet. Chem.*, 1987, **322**, 65.

71 M. L. H. Green, I. M. Gardner and K. Prout, *J. Chem. Soc. Dalton Trans.*, 1991, 2207.

72 M. E. Huttenloch, J. Diebold, U. Rief, H. H. Brintzinger, A. M. Gilbert and T. J. Katz, *Organometallics*, 1992, **11**, 3600.

73 I. M. Lee, W. J. Gauthier, J. M. Ball, B. Iyengar and S. Collins, *Organometallics.*, 1992, **11**, 2115.

74 H. J. R. de Boer and B. W. Ryan, *J. Mol. Catal.*, 1994, **90**, 171.

75 J. C. Chien and R. Sugimoto, *J. Polym. Sci. Part A.*,1991, **29**, 459.

76 N. Herfert and G. Fink, *Makromol. Chem.*, 1992, **193**, 1359.

77 U. Stehling, J. Diebold, R. Kirsten, W. Röll, H. H. Brintzinger, S. Jüngling, R. Mülhaupt and F. Langhauser, *Organometallics*, 1994, **13**, 964.

78 G. Fink, R. Mülhaupt and H. H. Brintzinger, *Ziegler Catalysts*, P.159, Springer, Berlin, 1995.

79 J. A. Canich, Eur. Pat. Applic., EP420436,1990.

80 J. C. Stevens and D. R. Neithammer, Eur. Pat. Applic., EP418044, 1990.

81 A. N. Chernega, R. Gomez and M. L. H. Green, *J. Chem. Soc., Chem. Commun.*, 1993, 1415.

82 R. Uhrhammer, D. G. Black, T. G. Gardner, J. D. Olsen and R. F. Jordan, *J. Am. Chem. Soc.*, 1993, **115**, 8493; D. G. Black, D. C. Swenson, R. F. Jordan and R. D. Rogers, *Organometallics.*, 1995, **14**, 3539.

83 E. B. Tjaden, D. C. Swenson, R. F. Jordan and J. L. Peterson, *Organometallics*, 1995, **14**, 371.

84 F. G. N. Cloke, P. B. Hitchcock and J. B. Love, *J. Chem. Soc., Dalton Trans.*, 1995, 25.

85 B-J. Deelman, P. B. Hitchcock, M. F. Lappert, H-K. Lee and W-P. Leung, *J. Organomet. Chem.*, 1996, **513**, 281.

86 A. van der Linden, C. J. Schavarien, N. Meijboom, C. Ganter and A. G. Orpen, *J. Am. Chem. Soc.*, 1995, **117**, 3008.

87 J. J. Christensen, D. J. Eatough and R. M. Izatt, *Chem. Rev.*, 1974, **74**, 351.

88 J. S. Bradshaw, G. E. Maas, R. M. Izatt and J. J. Christensen, *Chem. Rev.*, 1979, **79**, 37.

89 L. F. Lindoy, *Chem. Soc. Rev.*, 1975, 4421.

90 N. F. Curtis, *Coord. Chem. Rev.*, 1968, **3**, 3.

91 R. Bhula, P. Osvath and D. C. Weatherburn, *Coord. Chem. Rev.*, 1988, **91**, 89.

92 P. Chavadhuri and K. Weighardt, *Prog. Inorg. Chem.*, 1987, **35**, 329.

93 B. Bosnich, C. K. Poon and M. L. Tobe, *Inorg. Chem.*, 1965, **4**, 1102.

94 J. E. Richman and T. J. Atkins, *J. Am. Chem. Soc.*, 1974, **91**, 2268.

95 D. K. Cabbiness and D. W. Margerum, *J. Am. Chem. Soc.*, 1969, **91**, 6540.

96 H. K. Frensdorff, *J. Am. Chem. Soc.*, 1971, **93**, 600.

97 A. Anichini, L. Fabbrizzi, P. Paoletti and R. M. Clay, *Inorg. Chim. Acta.*, 1977, **22**, L25.

98 L. Fabbrizzi, P. Paoletti and A. B. P. Lever, *Inorg. Chem.*, 1976, **15**, 1502.

99 H. Schiff, *Ann. Chim. (Paris).*, 1864, **131**, 118.

100 B. Pahor, M. Calligaris, G. Nardin and L. Randaccio, *Acta Crystallogr., Sect. B*, 1978, **34**, 1360.

101 D. L. Hughes, U. Kleinkes, G. J. Leigh, M. Maiwald, J. R. Sanders, C. Sudbrake and J. Weisner, *J. Chem. Soc., Dalton Trans.*, 1993, 3039.

102 C. Huilan, H. Deyan, L. Tian, Y. Hang and T. Wenxia, *Inorg. Chem.*, 1996, **35**, 1502.

103 R. H. Heistand, A. L. Roe and L. Que Junior, *Inorg. Chem.*, 1982, **21**, 676.

104 L. G. Marzilli, M. F. Summers, N. Bresciani-Pahor, E. Zangrando, J. P. Charland and L. Randaccio, *J. Am. Chem. Soc.*, 1985, **107**, 6880.

105 R. Atkins, G. Brewer, E. Kokot, G. M. Mockler and E. Sinn, *Inorg. Chem.*, 1985, **24**, 127.

106 W. Zhang, J. L. Loebach, S. R. Wilson and E. N. Jacobsen, *J. Am. Chem. Soc.*, 1990, **112**, 2801; W. Zhang and E. N. Jacobsen, *J. Org. Chem.*, 1991, **56**, 2296; B. D. Brandes and E. N. Jacobsen, *J. Org. Chem.*, 1994, **59**, 4378; H. Sasaki, R. Irie, T. Hamada, K. Susuki and T. Katsuki, *Tetrahedron*, 1994, **50**, 11827.

107 N. S. Biradar and V. H. Kulkarni, *J. Inorg. Nucl. Chem.*, 1971, **33**, 3847.

108 G. Gilli, D. W. J. Cruickshank, R. L. Beddoes and O. S. Mills, *Acta Crystallogr., Sect. B*, 1972, **28**, 1889.

109 M. Pasquali, F. Marchetti, A. Landi and C. Floriani, *J. Chem. Soc., Dalton Trans.*, 1978, 545.

110 R. D. Archer, R. O. Day and M. L. Illingsworth, *Inorg. Chem.*, 1979, **18**, 2908.

111 M. Mazzanti, J-M. Rosset, C. Floriani, A. Chiesi-Villa and C. Gaustini, *J. Chem. Soc., Dalton Trans.*, 1989, 953.

112 C. Floriani, E. Solari, F. Corazza, A. Chiesi-Villa and C. Gaustini, *Angew. Chem. Int. Ed. Engl.*, 1989, **28**, 64.

113 F. Corazza, E. Solari, C. Floriani, A. Chiesi-Villa and C. Gaustini, *J. Chem. Soc., Dalton Trans.*, 1990, 1335.

114 E. Solari, C. Floriani, A. Chiesi-Villa and C. Rizzoli, *J. Chem. Soc., Dalton Trans.*, 1992, 367.

115 M. Calligaris and L. Randaccio, *Comprehensive Coordination Chemistry*, Vol.2, Pergamon Press, Oxford, 1987.

116 N. B. Pahor, M. Calligaris, P. Delise, G. Dodic, G. Nardin and L. Randaccio, *J. Chem. Soc., Dalton Trans.*, 1976, 2478.

117 C. Subrahmanyam, M. Seshasayee and G. Aravamudan, *Cryst. Struct. Chem. Commun.*, 1982, **11,** 1719.

118 Z. Cimerman, N. Galesic and B. Bosner, *J. Mol. Struct.*, 1992, **274**, 131.

119 R. Senn and W. Nowacki, *Z. Kristallogr.*, 1977, **145**, 16.

120 Y. Elerman, I. Svoboda and H. Fuess, *Z. Kristallogr.*, 1991, **196**, 309.

121 A. Bondi, *J. Phys. Chem.*, 1964, **68**, 441.

122 W. P. Schaefer and R. E. Marsh, *Acta Crystallogr., Sect. B*, 1969, **25**, 1675.

123 K. Watenpaugh and C. N. Caughlan, *Inorg. Chem.*, 1967, **6**, 963.

124 B. F. Studd and A. G. Swallow, *J. Chem. Soc., (A)*, 1968, 1961.

125 S. A. Fairhurst, D. L. Hughes, U. Kleinkes and J. G. Leigh, *J. Chem. Soc., Dalton Trans.*, 1995, 321.

126 J. P. Corden, W. Errington, P. Moore and M. G. H. Wallbridge, *Acta Crystallogr., Sect. C*, 1996, **52**, 125.

127 S. Ciurli, C. Floriani, A. Chesi-Villa and C. Gaustini, *J. Chem. Soc., Chem. Commun.*, 1986, 1401.

128 M. D. Hobday and T. D. Smith, *Coord. Chem. Rev.*, 1972, **9**, 311; M. Calligaris, G. Nardin and L. Randaccio, *ibid.*, 1972, **7**, 385.

129 F. Corrazza, C. Floriani and M. Zehnder, *J. Chem. Soc., Dalton Trans.*, 1987, 709.

130 J. C. Cannadine, J. P. Corden, W. Errington, P. Moore and M. G. H. Wallbridge, *Acta Crystallogr., Sect. C*, 1996, **52**, 1014.

131 S. Smith, PhD. Thesis, University of Warwick, 1996.

132 A. G. Orpen, L. Brammer, F. H. Allen, O. Kennard, D. G. Watson and R. Taylor, *J. Chem. Soc., Dalton Trans.*, 1989, 51.

133 P. V. Bernhardt and P. Comba, *Inorg. Chem.*, 1992, **31**, 2638.

134 R. D. Hancock, *Prog. in Inorg. Chem.*, 1989, **37**, 187.

135 "Computational Chemistry", manual for HYPERCHEM version 4, Hypercube Inc., 419 Phillip Street, Waterloo, Ontario, Canada. N2L 3X2.

136 P. Gund, D. C. Barry, J. M. Blaney and N. C. Cohen, *J. Med. Chem.*, 1988, **31**, 2230.

137 D. G. Kelly, A. J. Toner, N. M. Walker, S. J. Coles and M. B. Hursthouse, *Polyhedron*, 1996, **15**, 4307.

138 J. L. Leman, J. Braddock–Wilking, A. J. Coolong and A. R. Barron, *Inorg. Chem.*, 1993, **32**, 4324.

139 V. L. Goedken and S. J. Dzugan, *Inorg. Chem.*, 1986, **25**, 2858.

140 R. G. Vranka and E. L. Amma, *J. Am. Chem. Soc.*, 1967, **89**, 3121.

141 V. L. Goedken, H. Ito and T. J. Ito, *J. Chem Soc., Chem. Commun.*, 1984, 1453.

142 P. L. Gurian, L. K. Cheatham, J. W. Ziller and A. R. Barron, *J. Chem. Soc., Dalton Trans.*, 1991, 1449.

143 D. A. Atwood, J. A. Jegier and D. Rutherford, *Inorg. Chem.*, 1996, **35**, 63.

144 J. C. Cannadine, PhD Thesis, University of Warwick, 1994.

145 K. S. Chong, S. J. Rettig, A. Storr and J. Trotter, *Can. J. Chem.*, 1977, **55**, 2540.

146 V. L. Goedken, J. J. Pluth, S. M. Peng and B. Bursten, *J. Am. Chem. Soc.*, 1976, **98**, 8014.

147 F. A. Cotton and J. Czuchajowska, *Polyhedron*, 1990, **9**, 2553.

148 M. C. Weiss, B. Bursten, S. M. Peng and V. L. Goedken, *J. Am. Chem. Soc.*, 1976, **98**, 8021.

149 J. L. Hoard, *Science*, 1971, **174**, 1295.

150 V. L. Goedken and J. A. Ladd, *J. Chem. Soc., Chem. Commun.*, 1982, 182.

151 I. A. Ronova and N. V. Alekseev, *Dakl. Akad. Nauk. S.S.S.R.*, 1967, **174**, 614.

152 M. A. Bush and G. A. Sim. *J. Chem. Soc.* (A), 1971, 2225.

153 V. L. Goedken and J. A. Ladd, *J. Chem. Soc., Chem. Commun.*, 1991, 145.

154 S. De Angelis, E. Solari, E. Gallo, C. Floriani, A. Chiesi–Villa and C. Rizzoli, *Inorg. Chem.*, 1992, **31**, 2520.

155 C. Floriani, S. Ciurli, A. Chiesi–Villa and C. Guastini, *J. Chem. Soc., Dalton Trans.*, 1988, 1361.

156 C. Floriani, S. Ciurli, A. Chesi-Villa and C. Gaustini, *Angew. Chem. Int. Ed. Engl.*, 1987, **26**, 70.

157 S. Ciurli, C. Floriani, A. Chiesi–Villa and C. Gaustini, *J. Chem. Soc., Chem. Commun.*, 1986, 1401.

158 C.-H. Yang and V. L. Goedken, *J. Chem. Soc., Chem. Commun.*, 1986, 1101.

159 C.-H. Yang, J. A. Ladd and V. L. Goedken, *J. Coord. Chem.*, 1988, **19**, 235.

160 C. E. Housemekerides, R. S. Pilato, G. L. Geoffroy and A. L. Rheingold, *J. Chem. Soc., Chem. Commun.*, 1991, 563.

161 C. E. Housemekerides, D. L. Ramage, C. M. Kretz, J. T. Shontz, R. S. Pilato, G. L. Geoffroy, A. L. Rheingold and B. S. Haggerty, *Inorg. Chem.*, 1992, **31**, 4453.

162 V. L. Goedken and M. C. Weiss, *Inorg. Synth.*, 1980, **20**, 115.

163 W. G. Kofan and L. M. Baclawski, *J. Org. Chem.*, 1976, **41**, 1879.

164 J. C. Cannadine, W. Errington, P. Moore and M. G. H. Wallbridge, *Acta Crystallogr., Sect. C*, **50**, 2037.

165 C. J. Cairns, R. A. Heckman, A. C. Melnyk, W. M. Davis and D. H. Busch, *J. Chem. Soc. Dalton Trans.*, 1987, 2505.

166 A. J. Blake, T. I. Hyde and M. Schröder, *J. Chem. Soc., Dalton Trans.*, 1988, 1165.

167 M. Cesario, J. Guilhem, C. Pascard, E. Anklam, J–M. Lehn and M. Pietraszkiewicz, *Helvetica Chimica Acta*, 1991, **74**, 1157.

168 N. W. Alcock, R. G. Kingston, P. Moore and C. Piermont, *J. Chem. Soc., Dalton Trans.*, 1984, 1937.

169 H. A. A. Omar, P. Moore and N. W. Alcock, *J. Chem. Soc., Dalton Trans.*, 1984, 2631.

170 N. W. Alcock, P. Moore and H. A. A. Omar, *J. Chem. Soc., Chem. Commun.*, 1985, 1058.

171 N. W. Alcock, P. Moore and H. A. A. Omar, *J. Chem. Soc., Dalton Trans.*, 1987, 1107.

172 N. W. Alcock, P. Moore and H. A. A. Omar, *Acta Crystallogr., Sect. C*, 1987, **43**, 2074.

173 N. W. Alcock, K. P. Balakrishnan, A. Berry, P. Moore and C. J. Reader, *J. Chem. Soc., Dalton Trans.*, 1988, 1089.

174 C–M. Che, W–T. Tang, W–O. Lee, W–T. Wong and T–F. Lai, *J. Chem. Soc., Dalton Trans.*, 1989, 2011.

175 N. W. Alcock, P. Moore and H. A. A. Omar, *J. Chem. Soc., Dalton Trans.*, 1986, 985.

176 N. W. Alcock, K. P. Balakrishnan, P. Moore and G. A. Pike, *J. Chem. Soc., Dalton Trans.*, 1987, 889.

177 K. P. Balakrishnan, H. A. A. Omar, P. Moore, N. W. Alcock and G. A. Pike, *J. Chem. Soc., Dalton Trans.*, 1990, 2965.

178 M. G. B. Drew, D. A. Rice, S. bin Silong and P. C. Yates, *J. Chem. Soc., Dalton Trans.*, 1986, 1081.

179 G. H. Robinson, W. T. Pennington, B. Lee, M. F. Self and D. C. Hrncir, *Inorg. Chem.*, 1991, **30**, 809.

APPENDIX

X-Ray Crystallographic Studies

APPENDIX X-Ray Crystallographic Studies

Crystals were grown and mounted by the author. The X-ray crystallographic structure determinations carried out at the University of Warwick described in this work were performed by Dr. W. Errington. The data for the remaining studies described in this work were collected by the EPSRC Crystallographic Service, University of Wales, Cardiff and analysis of the data was carried out by the author and Dr W. Errington.

General Method

All of the free ligand crystals were non air / moisture sensitive and therefore handled and mounted in the air. All the metal complexes were assumed to be air / moisture and were handled as follows. The crystals were placed under dry paraffin oil to protect them from air and moisture exposure and suitable examples were picked using a glass fibre with the aid of a microscope on the bench. The crystals used were mounted under an argon atmosphere in thin walled quartz Lindermann tubes (0.5 and 1.0 mm diameter) and held in place with a trace of silicon grease. The ends of the Lindermann tubes were heat sealed and further protected with wax. This procedure gave good protection from any deterioration of even the more air sensitive crystals used, provided manipulations were rapid.

The diffraction for compound 16 reported within the tables that follow was collected on a Siemens P3R3 four-circle diffractometer in the ω-2θ mode, operating with Mo-Kα graphite monochromatised radiation, λ = 0.71073 Å. Three standard reflections were monitored after every 200 reflections and the data rescaled to correct for any changes in intensity of these standards that occurred during the data collection. Unit cell dimensions and standard deviations were generally obtained by least squares fit to around 15 high angle reflections. For the data collection, all the reflections were used in the refinement of the structures. They were corrected for Lorentz polarisation and absorption effects using the Analytical method. The final refinement by least squares methods, with anisotropic thermal parameters for all non-H atoms. A weighting scheme of the form $w = 1/[\sigma^2(Fo^2)+(aP)^2+bP]$ where $P = (Fo^2+2Fc^2)/3$ was used and shown to be satisfactory by weight analysis. Computing work for structure solution was carried out using SHELXTL PLUS on a DEC MicrovaxII.[a] Refinement was made using SHELXL 93,[b] on a IBM compatible 486

personnel computer. Scattering factors and anomalous dispersion factors were taken fro the literature.[c]

The diffraction data for compounds 1-7, and 9-15, were collected by a Del Instruments FAST TV area detector diffractometer at the EPSRC Crystallographic centr Cardiff, which is run by Professor M. B. Hursthouse. Structure solution and refineme followed a similar procedure to above.

The unit cell data and the data collection parameters for all the compounds are give below. Bond lengths and angles for all non-hydrogen atoms of each compound are listed the tables below. Supplementary material comprising atomic coordinates of all atom thermal parameters and structure factor parameters, can be obtained from Professor M. C H. Wallbridge (University of Warwick).

a G. M. Sheldrick, SHELXTL-PLUS users manual, Nicolet Instr. Co., Madison, Wisconsin, 1990.

b G. M. Sheldrick, L. Appl. Cryst., 1995.

c International Tables for X-ray Crystallography, 1974, Vol IV, Kynoch Press, Birmingham.

	(1)	(2)
Compound	DMSALEN	EtSALEN
Formula	$C_9H_{10}NO$	$C_{20}H_{24}N_2O_2$
Molecular weight	148.18	324.41
Crystal system	Monoclinic	Monoclinic
Space group	P2(1)/n	P2(1)/c
a (Å)	5.707(10)	5.131(5)
b (Å)	20.335(5)	13.261(8)
c (Å)	6.795(2)	12.718(5)
α (°)	90.0	90.0
β (°)	104.647(2)	94.95(8)
γ (°)	90.0	90.0
U ($Å^3$)	763.00(3)	862.1(10)
Temperature (K)	220(2)	150(2)
Z	4	2
D_c (g cm^{-3})	1.290	1.250
μ (mm^{-1})	0.085	0.081
θ_{min}, θ_{max} (°)	2.00, 23.35	2.22, 25.09
Index ranges	-6/6, -22/17, -7/7	-3/5, -14/14, -14/14
Number of data collected	3360	3778
Independant reflections	1103	1324
Absorption correction	-	-
Max., min. transmission	-	-
R1 (F) [I >2σ(I)]	0.0533 (R[int]=0.1378)	0.0423 (R[int]=0.0748)
wR2 (F^2) (all data)	0.1579	0.0927
Goodness of fit on F^2	1.091	0.723
Largest diff. peak & hole (e $Å^{-3}$)	0.200, -0.205	0.190, -0.151
Data, restraints, parameters	1100/0/102	1322/1/111

	(3)	(4)
Compound	PhSALEN	SLPNDM
Formula	$C_{28}H_{24}N_2O_2$	$C_{19}H_{22}N_2O_2$
Molecular weight	420.49	310.39
Crystal system	Orthorhombic	Orthorhombic
Space group	Pna2(1)	P2(1)2(1)2(1)
a (Å)	18.530(8)	6.160(4)
b (Å)	13.443(10)	16.172(6)
c (Å)	17.737(8)	17.307(7)
α (°)	90.0	90.0
β (°)	90.0	90.0
γ (°)	90.0	90.0
U (Å^3)	4418(4)	1724(2)
Temperature (K)	150(2)	293(2)
Z	8	4
D_c (g cm^{-3})	1.264	1.196
μ (mm^{-1})	0.080	0.078
θ_{min}, θ_{max} (°)	1.87, 25.15	2.35, 25.00
Index ranges	-20/20, -14/14, -13/19	-4/6, -18/17, -19/18
Number of data collected	19267	7793
Independant reflections	6357	2678
Absorption correction	-	none
Max., min. transmission	-	-
R1 (F) [I >2σ(I)]	0.0394 (R[int]=0.0918)	0.0376 (R[int]=0.0859)
wR2 (F^2) (all data)	0.0854	0.0768
Goodness of fit on F^2	0.546	0.652
Largest diff. peak & hole (e Å^{-3})	0.148, -0.165	0.114, -0.100
Data, restraints, parameters	6349/5/581	2676/0/208

	(5)	(6)
Compound	EtSLPNDM	PhSLPNDM
Formula	$C_{23}H_{30}N_2O_2$	$C_{31}H_{30}N_2O_2$
Molecular weight	366.49	462.57
Crystal system	Monoclinic	
Space group	P2(1)/c	P-1
a (Å)	12.443(10)	10.261(9)
b (Å)	113.286(9)	10.786(6)
c (Å)	13.033(8)	12.425(5)
α (°)	90.0	99.39(6)
β (°)	108.37(5)	110.22(5)
γ (°)	90.0	99.35(5)
U (Å^3)	2054(3)	1237.0(14)
Temperature (K)	120(2)	120(2)
Z	4	2
D_c (g cm^{-3})	1.185	1.242
μ (mm^{-1})	0.075	0.078
θ_{min}, θ_{max} (°)	2.24, 25.10	1.80, 25.26
Index ranges	-8/14, -15/15, -15/14	-10/11, -11/9, -13/13
Number of data collected	8860	5128
Independant reflections	3248	3510
Absorption correction	none	none
Max., min. transmission	-	-
R1 (F) [I >2σ(I)]	0.0453 (R[int]=0.0730)	0.0514 (R[int]=0.0806)
wR2 (F^2) (all data)	0.1052	0.1402
Goodness of fit on F^2	0.852	0.950
Largest diff. peak & hole (e Å^{-3})	0.196, -0.173	0.229, -0.242
Data, restraints, parameters	3247/2/250	3507/2/320

	(7)	(8)
Compound	DMCycH	EtCycH
Formula	$C_{22}H_{26}N_2O_2$	$C_{24}H_{30}N_2O_2$
Molecular weight	350.45	378.50
Crystal system	Monoclinic	Monoclinic
Space group	P2(1)/c	C2/c
a (Å)	11.832(9)	20.402(8)
b (Å)	13.797(5)	9.595(3)
c (Å)	112.954(7)	11>740(3)
α (°)	90.0	90.0
β (°)	112.51(4)	119.36(3)
γ (°)	90.0	90.0
U (Å^3)	1954(2)	2003.1(12)
Temperature (K)	293(2)	180(2)
Z	4	4
D_c (g cm^{-3})	1.192	1.255
μ (mm^{-1})	0.076	0.080
θ_{min}, θ_{max} (°)	1.86, 24.97	2.29, 28.64
Index ranges	-13/13, -14/15, -14/11	-25/27, -12/10, -15/14
Number of data collected	8708	5955
Independant reflections	2965	2351
Absorption correction	none	none
Max., min. transmission	-	-
R1 (F) [I >2σ(I)]	0.0451 (R[int]=0.0882)	0.0711 (R[int]=0.0598)
wR2 (F^2) (all data)	0.2860	0.1448
Goodness of fit on F^2	0.688	1.129
Largest diff. peak & hole (e Å^{-3})	0.185, -0.186	0.264, -0.226
Data, restraints, parameters	2959/8/239	2351/0/129

	(9)	(10)
Compound	PhCycH	[Ti(DMSALEN)Cl_2]
Formula	$C_{32}H_{30}N_2O_2$	$C_{18}H_{18}Cl_2N_2O_2Ti$
Molecular weight	474.58	413.14
Crystal system	Monoclinic	Monoclinic
Space group	P2(1)/n	P2(1)/c
a (Å)	8.993(6)	12.8657(10)
b (Å)	21.140(5)	10.099(2)
c (Å)	14.290(4)	13.9372(6)
α (°)	90.0	90.0
β (°)	102.26(5)	96.18(2)
γ (°)	90.0	90.0
U ($Å^3$)	2655(2)	1800.3(3)
Temperature (K)	293(2)	150(2)
Z	4	4
D_c (g cm^{-3})	1.187	1.524
μ (mm^{-1})	0.074	0.786
θ_{min}, θ_{max} (°)	1.75, 25.01	2.50, 25.05
Index ranges	-7/10,-24/22,-15/15	-14/14,-11/11,-16/9
Number of data collected	11935	7038
Independant reflections	4098	2750
Absorption correction	none	none
Max., min. transmission	-	-
R1 (F) [I >2σ(I)]	0.0477 (R[int]=0.1400)	0.0329 (R[int]=0.0737)
wR2 (F^2) (all data)	0.1031	0.0704
Goodness of fit on F^2	0.525	0.824
Largest diff. peak & hole (e $Å^{-3}$)	0.128, -0.155	0.311, -0.299
Data, restraints, parameters	4094/2/327	2750/0/228

	(11)	(12)
Compound	[Ti(DMSALEN)Cl_2.THF]	[Ti(PhSALEN)Cl_2.½THF]
Formula	$C_{25}H_{29}N_2O_3Cl_2Ti$	$C_{30}H_{26}Cl_2N_2O_{2.5}Ti$
Molecular weight	524.30	573.33
Crystal system	Monoclinic	Monoclinic
Space group	P2(1)/c	C2/c
a (Å)	13.439(3)	20.0012(10)
b (Å)	13.868(3)	16.170(2)
c (Å)	14.226(3)	19.069(2)
α (°)	90.0	90.0
β (°)	108.61(3)	118.63(3)
γ (°)	90.0	90.0
U ($Å^3$)	2512.7(9)	5413.3
Temperature (K)	293(2)	150(2)
Z	4	8
D_c (g cm^{-3})	1.386	1.407
μ (mm^{-1})	0.582	0.546
θ_{min}, θ_{max} (°)	2.11, 26.06	1.75, 25.00
Index ranges	-15/15,-15/13,-16/16	-23/23,-15/18,-17/21
Number of data collected	11176	11910
Independant reflections	3876	4244
Absorption correction	none	none
Max., min. transmission	-	-
R1 (F) [I >2σ(I)]	0.0471 (R[int]=0.1164)	0.0740 (R[int]=0.1819)
wR2 (F^2) (all data)	0.0920	0.1714
Goodness of fit on F^2	0.739	0.875
Largest diff. peak & hole (e $Å^{-3}$)	0.306, -0.270	0.838, -0.835
Data, restraints, parameters	3868/20/298	4244/1/334

	(13)	(14)
Compound	[Ti(SLPNDM)Cl_2.THF]	[Zr(SLPNDM)Cl_2(THF)]
Formula	$C_{23}H_{28}N_2O_3Cl_2Ti$	$C_{23}H_{28}Cl_2N_2O_3Zr$
Molecular weight	499.27	542.59
Crystal system	Triclinic	Monoclinic
Space group	P-1	P2(1)/c
a (Å)	9.1800(10)	18.002(7)
b (Å)	10.788(2)	11.307(5)
c (Å)	13.5220(10)	11.991(8)
α (°)	103.31(3)	90.0
β (°)	109.360(12)	105.61(5)
γ (°)	100.68(2)	90.0
U ($Å^3$)	1178.5(3)	2351(2)
Temperature (K)	293(2)	240(2)
Z	2	4
D_c (g cm^{-3})	1.407	1.533
μ (mm^{-1})	0.617	0.722
θ_{min}, θ_{max} (°)	2.02, 25.03	2.15, 25.05
Index ranges	-7/10, -12/12, -16/12	-21/20, -13/1, 0/14
Number of data collected	5239	4865
Independant reflections	3387	4164
Absorption correction	none	Analytical
Max., min. transmission	-	0.95, 0.83
R1 (F) [I >2σ(I)]	0.0440 (R[int]=0.0467)	0.0706 (R[int]=0.0587)
wR2 (F^2) (all data)	0.1029	0.1333
Goodness of fit on F^2	0.870	1.046
Largest diff. peak & hole (e $Å^{-3}$)	0.491, -0.234	0.960, -1.217
Data, restraints, parameters	3868/20/298	4159/20/280

	(15)	(16)
Compound	$[Ti(ETCycH)Cl_2].CHCl_3$	$[Zr(omtaa)Cl_2.½THF]$
Formula	$C_{25}H_{29}N_2O_2Cl_5Ti$	$C_{28}H_{34}Cl_2N_4O_{0.5}Zr$
Molecular weight	614.65	596.71
Crystal system	Monoclinic	Triclinic
Space group	P2(1)/c	P-1
a (Å)	16.446(3)	8.958(5)
b (Å)	9.796(2)	13.258(7)
c (Å)	18.160(4)	14.769(8)
α (°)	90.0	71.61(5)
β (°)	111.32(3)	88.37(4)
γ (°)	90.0	70.53(4)
U ($Å^3$)	2725(3)	1564(2)
Temperature (K)	150(2)	293(2)
Z	4	2
D_c (g cm^{-3})	1.498	1.267
μ (mm^{-1})	0.831	0.545
θ_{min}, θ_{max} (°)	2.29, 25.12	1.86, 24.88
Index ranges	-19/18, -8/10, -19/18	-10/10, -15/9, -17/16
Number of data collected	12083	6236
Independant reflections	4286	4082
Absorption correction	none	none
Max., min. transmission	-	-
R1 (F) [I >2σ(I)]	0.0534 (R[int]=0.1856)	0.0540 (R[int]=0.0667)
wR2 (F^2) (all data)	0.0989	0.1271
Goodness of fit on F^2	0.597	0.713
Largest diff. peak & hole (e $Å^{-3}$)	0.485, -0.425	0.582, -0.277
Data, restraints, parameters	4286/6/318	4073/52/343

	(17)	(18)
Compound	[Al(EtSALEN)MeAlMe$_2$.][AlCl$_3$Me]	Mepy
Formula	$C_{24}H_{34}N_2O_2Al_3Cl_3$	$C_{14}H_{24}N_4$
Molecular weight	569.82	248.37
Crystal system	Orthorhombic	Orthorhombic
Space group	Pna2(1)	Pnma
a (Å)	15.707(8)	15.305(4)
b (Å)	9.726(4)	14.574(6)
c (Å)	19.538(7)	6.4175(14)
α (°)	90.0	90.0
β (°)	90.0	90.0
γ (°)	90.0	90.0
U (Å^3)	2985(2)	1431.4(8)
Temperature (K)	230(2)	180(2)
Z	4	4
D_c (g cm^{-3})	1.268	1.153
μ (mm^{-1})	0.418	0.071
θ_{min}, θ_{max} (°)	2.08, 24.99	2.66, 25.49
Index ranges	-20/8, -12/9, -23/26	-17/19, -8/19, -7/7
Number of data collected	6640	3319
Independant reflections	4632	1327
Absorption correction	none	none
Max., min. transmission	-	-
R1 (F) [I >2σ(I)]	0.0983 (R[int]=0.0592)	0.0479 (R[int]=0.0438)
wR2 (F^2) (all data)	0.1949	0.1227
Goodness of fit on F^2	1.233	1.165
Largest diff. peak & hole (e Å^{-3})	0.411, -0.462	0.141, -0.181
Data, restraints, parameters	4632/22/314	1327/0/114

Table 1 Bond lengths [Å] and angles [°] for DMSALEN

O(1)-C(1)	1.340(2)	N(1)-C(7)	1.287(2)
N(1)-C(9)	1.455(2)	C(1)-C(2)	1.389(3)
C(1)-C(6)	1.424(2)	C(2)-C(3)	1.367(3)
C(3)-C(4)	1.396(3)	C(4)-C(5)	1.365(3)
C(5)-C(6)	1.403(3)	C(6)-C(7)	1.466(3)
C(7)-C(8)	1.510(2)	C(9)-C(9)#1	1.505(3)

C(7)-N(1)-C(6)	121.81(14)	O(1)-C(1)-C(2)	118.3(2)
O(1)-C(1)-C(6)	121.4(2)	C(2)-C(1)-C(6)	120.2(2)
C(3)-C(2)-C(1)	120.6(2)	C(2)-C(3)-C(4)	120.2(2)
C(5)-C(4)-C(3)	119.9(2)	C(4)-C(5)-C(6)	121.9(2)
C(5)-C(6)-C(1)	117.1(2)	C(5)-C(6)-C(7)	122.1(2)
C(1)-C(6)-C(7)	120.7(2)	N(1)-C(7)-C(6)	117.8(2)
N(1)-C(7)-C(8)	122.2(2)	C(6)-C(7)-C(8)	119.9(2)
N(1)-C(9)-C(9)#1	109.3(2)		

Symmetry transformations used to generate equivalent atoms: #1 -x-1, -y+1, -z+1

Table 2 Bond lengths [Å] and angles [°] for EtSALEN

O(1)-C(1)	1.351(3)	N(1)-C(7)	1.295(3)
N(1)-C(10)	1.471(3)	C(1)-C(2)	1.394(3)
C(1)-C(6)	1.414(4)	C(2)-C(3)	1.381(3)
C(3)-C(4)	1.365(4)	C(4)-C(5)	1.384(3)
C(5)-C(6)	1.395(3)	C(6)-C(7)	1.471(4)
C(7)-C(8)	1.505(4)	C(8)-C(9)	1.516(3)
C(10)-C(10)#1	1.524(5)		

C(7)-N(1)-C(10)	121.4(2)	O(1)-C(1)-C(2)	118.4(3)
O(1)-C(1)-C(6)	121.6(3)	C(2)-C(1)-C(6)	120.0(2)
C(3)-C(2)-C(1)	120.5(3)	C(4)-C(3)-C(2)	120.1(3)
C(3)-C(4)-C(5)	120.4(3)	C(4)-C(5)-C(6)	121.4(3)
C(5)-C(6)-C(1)	117.6(3)	C(5)-C(6)-C(7)	121.7(3)
C(1)-C(6)-C(7)	120.7(2)	N(1)-C(7)-C(6)	117.3(2)
N(1)-C(7)-C(8)	123.5(3)	C(6)-C(7)-C(8)	119.2(2)
C(7)-C(8)-C(9)	112.2(2)	N(1)-C(10)-C(10)#1	108.4(3)

Symmetry transformations used to generate equivalent atoms: #1 -x, -y, -z

Table 3 Bond lengths [Å] for PhSALEN

O(11)-C(11)	1.350(6)	O(12)-C(128)	1.342(6)
N(11)-C(17)	1.302(6)	N(11)-C(114)	1.480(6)
N(12)-C(116)	1.311(6)	N(12)-C(115)	1.479(6)
C(11)-C(12)	1.409(7)	C(11)-C(16)	1.422(7)
C(12)-C(13)	1.384(8)	C(13)-C(14)	1.393(8)
C(14)-C(15)	1.364(7)	C(15)-C(16)	1.387(7)
C(16)-C(17)	1.484(7)	C(17)-C(18)	1.471(7)
C(18)-C(19)	1.396(7)	C(18)-C(113)	1.395(7)
C(19)-C(110)	1.362(7)	C(110)-C(111)	1.421(9)
C(111)-C(112)	1.385(7)	C(112)-C(113)	1.385(6)
C(114)-C(115)	1.519(7)	C(116)-C(123)	1.470(8)
C(116)-C(117)	1.489(7)	C(117)-C(118)	1.374(7)
C(117)-C(122)	1.396(7)	C(118)-C(119)	1.385(6)
C(119)-C(120)	1.371(8)	C(120)-C(121)	1.385(7)
C(121)-C(122)	1.378(7)	C(123)-C(124)	1.392(7)
C(123)-C(128)	1.405(7)	C(124)-C(125)	1.397(7)
C(125)-C(126)	1.382(7)	C(126)-C(127)	1.382(7)
C(127)-C(128)	1.415(7)		

Table 4 Bond angles [°] for PhSALEN

C(17)-N(11)-C(114)	122.8(5)	C(116)-N(12)-C(115)	120.5(5)
O(11)-C(11)-C(12)	117.2(6)	O(11)-C(11)-C(16)	123.4(5)
C(12)-C(11)-C(16)	119.4(6)	C(13)-C(12)-C(11)	119.1(6)
C(12)-C(13)-C(14)	121.5(6)	C(15)-C(14)-C(13)	119.1(6)
C(14)-C(15)-C(16)	122.2(6)	C(15)-C(16)-C(11)	118.7(5)
C(15)-C(16)-C(17)	121.9(5)	C(11)-C(16)-C(17)	119.4(5)
N(11)-C(17)-C(18)	123.6(5)	N(11)-C(17)-C(16)	116.9(5)
C(18)-C(17)-C(16)	119.5(5)	C(19)-C(18)-C(113)	118.0(5)
C(19)-C(18)-C(17)	120.7(5)	C(113)-C(18)-C(17)	121.3(5)
C(110)-C(19)-C(18)	121.8(6)	C(19)-C(110)-C(111)	119.4(6)
C(112)-C(111)-C(110)	119.9(6)	C(113)-C(112)-C(111)	119.2(6)
C(112)-C(113)-C(18)	121.7(6)	N(11)-C(114)-C(115)	110.0(5)
N(12)-C(115)-C(114)	109.0(5)	N(12)-C(116)-C(123)	118.0(5)
N(12)-C(116)-C(117)	122.5(5)	C(123)-C(116)-C(117)	119.5(5)
C(118)-C(117)-C(122)	118.2(5)	C(118)-C(117)-C(116)	120.6(5)
C(122)-C(117)-C(116)	121.2(5)	C(117)-C(118)-C(119)	121.1(5)
C(120)-C(119)-C(118)	119.9(5)	C(119)-C(120)-C(121)	120.3(6)
C(122)-C(121)-C(120)	119.2(6)	C(121)-C(122)-C(117)	121.3(5)
C(124)-C(123)-C(128)	117.4(6)	C(124)-C(123)-C(116)	120.6(6)
C(128)-C(123)-C(116)	122.0(6)	C(123)-C(124)-C(125)	122.1(6)
C(126)-C(125)-C(124)	119.1(6)	C(127)-C(126)-C(125)	121.5(6)
C(126)-C(127)-C(128)	118.6(6)	O(12)-C(128)-C(123)	121.8(6)
O(12)-C(128)-C(127)	116.7(6)	C(123)-C(128)-C(127)	121.4(5)

Table 5 Bond lengths [Å] and angles [°] for SLPNDM

O(1)-C(1)	1.357(4)	O(2)-C(19)	1.352(3)
N(1)-C(7)	1.284(4)	N(1)-C(8)	1.458(4)
N(2)-C(13)	1.263(3)	N(2)-C(12)	1.450(3)
C(1)-C(2)	1.382(4)	C(1)-C(6)	1.407(4)
C(2)-C(3)	1.375(5)	C(3)-C(4)	1.398(5)
C(4)-C(5)	1.373(5)	C(5)-C(6)	1.404(4)
C(6)-C(7)	1.431(4)	C(8)-C(9)	1.526(4)
C(9)-C(12)	1.528(4)	C(9)-C(10)	1.544(4)
C(9)-C(11)	1.561(4)	C(13)-C(14)	1.458(4)
C(14)-C(15)	1.374(4)	C(14)-C(19)	1.384(4)
C(15)-C(16)	1.369(5)	C(16)-C(17)	1.375(4)
C(17)-C(18)	1.366(4)	C(18)-C(19)	1.379(4)
C(7)-N(1)-C(8)	120.0(3)	C(13)-N(2)-C(12)	120.2(3)
O(1)-C(1)-C(2)	118.8(4)	O(1)-C(1)-C(6)	120.1(4)
C(2)-C(1)-C(6)	121.1(4)	C(3)-C(2)-C(1)	120.1(4)
C(2)-C(3)-C(4)	120.9(4)	C(5)-C(4)-C(3)	118.3(4)
C(4)-C(5)-C(6)	122.8(4)	C(5)-C(6)-C(1)	116.8(3)
C(5)-C(6)-C(7)	120.4(3)	C(1)-C(6)-C(7)	122.7(3)
N(1)-C(7)-C(6)	121.6(3)	N(1)-C(8)-C(9)	112.1(3)
C(8)-C(9)-C(12)	108.7(3)	C(8)-C(9)-C(10)	110.5(3)
C(12)-C(9)-C(10)	110.3(3)	C(8)-C(9)-C(11)	108.5(3)
C(12)-C(9)-C(11)	109.7(3)	C(10)-C(9)-C(11)	109.1(3)
N(2)-C(12)-C(9)	111.9(3)	N(2)-C(13)-C(14)	122.2(3)
C(15)-C(14)-C(19)	117.7(3)	C(15)-C(14)-C(13)	121.9(3)
C(19)-C(14)-C(13)	120.4(3)	C(16)-C(15)-C(14)	122.6(3)
C(15)-C(16)-C(17)	118.3(3)	C(18)-C(17)-C(16)	121.1(4)
C(17)-C(18)-C(19)	119.4(3)	O(2)-C(19)-C(18)	117.4(3)
O(2)-C(19)-C(14)	121.7(3)	C(18)-C(19)-C(14)	120.9(3)

Table 6 Bond lengths[Å] for EtSLPNDM

O(1)-C(1)	1.341(2)	O(2)-C(23)	1.345(2)
N(1)-C(7)	1.288(2)	N(1)-C(10)	1.461(3)
N(2)-C(15)	1.283(2)	N(2)-C(14)	1.467(2)
C(1)-C(2)	1.403(3)	C(1)-C(6)	1.415(3)
C(2)-C(3)	1.374(3)	C(3)-C(4)	1.378(3)
C(4)-C(5)	1.377(3)	C(5)-C(6)	1.399(3)
C(6)-C(7)	1.480(3)	C(7)-C(8)	1.509(3)
C(8)-C(9)	1.528(3)	C(10)-C(11)	1.530(3)
C(11)-C(12)	1.528(3)	C(11)-C(13)	1.529(3)
C(11)-C(14)	1.533(3)	C(15)-C(18)	1.482(3)
C(15)-C(16)	1.511(3)	C(16)-C(17)	1.522(3)
C(18)-C(19)	1.396(3)	C(18)-C(23)	1.410(3)
C(19)-C(20)	1.381(3)	C(20)-C(21)	1.379(3)
C(21)-C(22)	1.376(3)	C(22)-C(23)	1.399(3)

Table 7 Bond angles [°]for EtSPLNDM

C(7)-N(1)-C(10)	124.5(2)	C(15)-N(2)-C(14)	122.9(2)
O(1)-C(1)-C(2)	118.2(2)	O(1)-C(1)-C(6)	122.2(2)
C(2)-C(1)-C(6)	119.6(2)	C(3)-C(2)-C(1)-	120.1(2)
C(2)-C(3)-C(4)	121.0(2)	C(5)-C(4)-C(3)	119.6(2)
C(4)-C(5)-C(6)	121.7(2)	C(5)-C(6)-C(1)	118.0(2)
C(5)-C(6)-C(7)	121.9(2)	C(1)-C(6)-C(7)	120.0(2)
N(1)-C(7)-C(6)	116.1(2)	N(1)-C(7)-C(8)	124.2(2)
C(6)-C(7)-C(8)	119.6(2)	C(7)-C(8)-C(9)	111.5(2)
N(1)-C(10)-C(11)	111.8(2)	C(12)-C(11)-C(13)	108.6(2)
C(12)-C(11)-C(10)	111.1(2)	C(13)-C(11)-C(10)	107.9(2)
C(12)-C(11)-C(14)	108.8(2)	C(13)-C(11)-C(14)	111.0(2)
C(10)-C(11)-C(14)	109.5(2)	N(2)-C(14)-C(11)	110.5(2)
N(2)-C(15)-C(18)	116.4(2)	N(2)-C(16)-C(15)	124.5(2)
C(18)-C(15)-C(16)	119.1(2)	C(15)-C(16)-C(17)	113.1(2)
C(19)-C(18)-C(23)	117.5(2)	C(19)-C(18)-C(15)	121.6(2)
C(23)-C(18)-C(15)	120.9(2)	C(20)-C(19)-C(18)	122.5(2)
C(21)-C(20)-C(19)	118.7(2)	C(22)-C(21)-C(20)	121.3(2)
C(21)-C(22)-C(23)	120.0(2)	O(2)-C(23)-C(22)	118.2(2)
O(2)-C(23)-C(18)	121.7(2)	C(22)-C(23)-C(18)	120.0(2)

Table 8 Bond lengths [Å] for PhSLPNDM

O(1)-C(1)	1.343(3)	O(2)-C(31)	1.344(3)
N(1)-C(7)	1.289(3)	N(1)-C(14)	1.457(3)
N(2)-C(19)	1.296(3)	N(2)-C(18)	1.460(3)
C(1)-C(2)	1.386(3)	C(1)-C(6)	1.416(3)
C(2)-C(3)	1.375(4)	C(3)-C(4)	1.383(4)
C(4)-C(5)	1.376(3)	C(5)-C(6)	1.400(3)
C(6)-C(7)	1.483(3)	C(7)-C(8)	1.492(3)
C(8)-C(13)	1.391(3)	C(8)-C(9)	1.393(3)
C(9)-C(10)	1.378(3)	C(10)-C(11)	1.378(4)
C(11)-C(12)	1.382(3)	C(12)-C(13)	1.373(3)
C(14)-C(15)	1.535(3)	C(15)-C(16)	1.528(3)
C(15)-C(18)	1.530(3)	C(15)-C(17)	1.531(3)
C(19)-C(26)	1.468(3)	C(19)-C(20)	1.497(3)
C(20)-C(25)	1.383(3)	C(20)-C(21)	1.388(3)
C(21)-C(22)	1.381(3)	C(22)-C(23)	1.372(3)
C(23)-C(24)	1.376(3)	C(24)-C(25)	1.389(3)
C(26)-C(27)	1.405(3)	C(26)-C(31)	1.414(3)
C(27)-C(28)	1.375(3)	C(28)-C(29)	1.384(4)
C(29)-C(30)	1.368(4)	C(30)-C(31)	1.388(4)

Table 9 Bond angles[°] for PhSLPNDM

C(7)-N(1)-C(14)	122.4(2)	C(19)-N(2)-C(18)	121.4(2)
O(1)-C(1)-C(2)	118.8(2)	O(1)-C(1)-C(6)	121.8(2)
C(2)-C(1)-C(6)	119.5(2)	C(3)-C(2)-C(1)	121.1(2)
C(2)-C(3)-C(4)	120.3(2)	C(5)-C(4)-C(3)	119.4(2)
C(4)-C(5)-C(6)	121.8(2)	C(5)-C(6)-C(1)	117.9(2)
C(5)-C(6)-C(7)	121.7(2)	C(1)-C(6)-C(7)	120.4(2)
N(1)-C(7)-C(6)	117.8(2)	N(1)-C(7)-C(8)	123.5(2)
C(6)-C(7)-C(8)	118.6(2)	C(13)-C(8)-C(9)	118.4(2)
C(13)-C(8)-C(7)	120.5(2)	C(9)-C(8)-C(7)	121.0(2)
C(10)-C(9)-C(8)	120.4(2)	C(9)-C(10)-C(11)	120.5(2)
C(10)-C(11)-C(12)	119.6(2)	C(13)-C(12)-C(11)	120.2(2)
C(12)-C(13)-C(8)	120.9(2)	N(1)-C(14)-C(15)	112.4(2)
C(16)-C(15)-C(18)	110.8(2)	C(16)-C(15)-C(17)	109.3(2)
C(18)-C(15)-C(17)	107.8(2)	C(16)-C(15)-C(14)	107.7(2)
C(18)-C(15)-C(14)	110.5(2)	C(17)-C(15)-C(14)	110.7(2)
N(2)-C(18)-C(15)	111.4(2)	N(2)-C(19)-C(26)	118.4(2)
N(2)-C(19)-C(20)	121.6(2)	C(26)-C(19)-C(20)	120.0(2)
C(25)-C(20)-C(21)	119.1(2)	C(25)-C(20)-C(19)	121.8(2)
C(21)-C(20)-C(19)	119.1(2)	C(22)-C(21)-C(20)	120.1(2)
C(23)-C(22)-C(21)	120.5(2)	C(22)-C(23)-C(24)	120.1(2)
C(23)-C(24)-C(25)	119.7(2)	C(20)-C(25)-C(24)	120.5(2)
C(27)-C(26)-C(31)	117.6(2)	C(27)-C(26)-C(19)	121.4(2)
C(31)-C(26)-C(19)	121.0(2)	C(28)-C(27)-C(26)	121.8(2)
C(27)-C(28)-C(29)	119.5(3)	C(30)-C(29)-C(28)	120.4(2)
C(29)-C(30)-C(31)	121.1(2)	0(2)-C(31)-C(30)	119.0(2)
O(2)-C(31)-C(26)	121.3(2)	C(30)-C(31)-C(26)	119.7(2)

Table 10 Bond lengths[Å] for DMCycH

O(1)-C(1)	1.346(3)	O(2)-C(22)	1.340.(3)
N(2)-C(15)	1.288(3)	N(1)-C(9)	1.477(3)
C(1)-C(2)	1.391(4)	C(1)-C(6)	1.407(4)
C(2)-C(3)	1.369(4)	C(3)-C(4)	1.380(4)
C(4)-C(5)	1.372(4)	C(5)-C(6)	1.392(4)
C(6)-C(7)	1.471(4)	C(7)-C(8)	1.514(3)
C(9)-C(14)	1.512(4)	C(9)-C(10)	1.522(3)
C(10)-C(11)	1.519(3)	C(11)-C(12)	1.509(3)
C(12)-C(13)	1.533(3)	C(13)-C(14)	1.524(3)
C(15)-C(17)	1.467(4)	C(15)-C(16)	1.497(4)
C(17)-C(18)	1.400(3)	C(17)-C(22)	1.412(4)
C(18)-C(19)	1.377(4)	C(19)-C(20)	1.363(4)
C(20)-C(21)	1.377(4)	C(21)-C(22)	1.389(4)

Table 11 Bond angles [°] for DMCycH

C(7)-N(1)-C(9)	122.4(2)	C(15)-N(2)-C(14)	125.1(2)
O(1)-C(1)-C(2)	117.4(3)	O(1)-C(1)-C(6)	121.7(3)
C(2)-C(1)-C(6)	120.9(3)	C(3)-C(2)-C(1)	120.2(3)
C(2)-C(3)-C(4)	120.3(4)	C(5)-C(4)-C(3)	119.3(4)
C(4)-C(5)-C(6)	122.8(3)	C(5)-C(6)-C(1)	116.5(3)
C(5)-C(6)-C(7)	122.0(3)	C(1)-C(6)-C(7)	121.6(3)
N(1)-C(7)-C(6)	116.8(3)	N(1)-C(7)-C(8)	124.4(3)
C(6)-C(7)-C(8)	118.8(3)	N(1)-C(9)-C(14)	108.5(2)
N(1)-C(9)-C(10)	110.8(2)	C(14)-C(9)-C(10)	110.5(2)
C(11)-C(10)-C(9)	110.9(2)	C(12)-C(11)-C(10)	111.1(2)
C(11)-C(12)-C(13)	111.1(2)	C(14)-C(13)-C(12)	112.3(2)
N(2)-C(14)-C(9)	108.0(2)	N(2)-C(14)-C(13)	108.6(2)
C(9)-C(14)-C(13)	110.9(2)	N(2)-C(15)-C(17)	116.7(3)
N(2)-C(15)-C(16)	124.3(3)	C(17)-C(15)-C(16)	119.0(3)
C(18)-C(17)-C(22)	116.9(3)	C(18)-C(17)-C(15)	121.9(3)
C(22)-C(17)-C(15)	121.2(3)	C(19)-C(18)-C(17)	121.6(3)
C(20)-C(19)-C(18)	120.1(3)	C(19)-C(20)-C(21)	120.9(3)
C(20)-C(21)-C(22)	119.5(3)	O(2)-C(22)-C(21)	117.0(3)
O(2)-C(22)-C(17)	121.9(3)	C(21)-C(22)-C(17)	121.0(3)

Table 12 Bond lengths [Å] an angles [°] for EtCycH

O(1)-C(1)	1.332(3)	N(1)-C(7)	1.291(3)
N(1)-C(10)	1.463(3)	C(1)-C(2)	1.398(3)
C(1)-C(6)	1.420(3)	C(2)-C(3)	1.369(3)
C(3)-C(4)	1.388(3)	C(4)-C(5)	1.375(3)
C(5)-C(6)	1.403(3)	C(6)-C(7)	1.474(3)
C(7)-C(8)	1.508(3)	C(8)-C(9)	1.533(3)
C(10)-C(11)	1.531(3)	C(10)-C(10)#1	1.533(4)
C(11)-C(12)	1.522(3)	C(12)-C(12)#1	1.514(5)

C(7)-N(1)-C(10)	127.3(2)	O(1)-C(1)-C(2)	118.6(2)
O(1)-C(1)-C(6)	122.0(2)	C(2)-C(1)-C(6)	119.4(2)
C(3)-C(2)-C(1)	120.9(2)	C(2)-C(3)-C(4)	120.5(2)
C(5)-C(4)-C(3)	119.5(2)	C(4)-C(5)-C(6)	121.9(2)
C(5)-C(6)-C(1)	117.8(2)	C(5)-C(6)-C(7)	121.7(2)
C(1)-C(6)-C(7)	120.5(2)	N(1)-C(7)-C(6)	115.9(2)
N(1)-C(7)-C(8)	124.9(2)	C(6)-C(7)-C(8)	119.2(2)
C(7)-C(8)-C(9)	112.0(2)	N(1)-C(10)-C(11)	106.7(2)
N(1)-C(10)-C(10)#1	109.1(2)	C(11)-C(10)-C(10)#1	110.5(2)
C(12)-C(11)-C(10)	112.2(2)	C(12)#1-C(12)-C(11)	110.9(2)

Symmetry transformations used to generate equivalent atoms: #1 -x, y, -z+1/2

Table 13 Bond lengths [Å] for PhCycH

O(1)-C(1)	1.358(4)	O(2)-C(32)	1.349(4)
N(1)-C(7)	1.290(4)	N(1)-C(14)	1.456(4)
N(2)-C(20)	1.287(4)	N(2)-C(19)	1.470(4)
C(1)-C(6)	1.384(5)	C(1)-C(2)	1.402(5)
C(2)-C(3)	1.373(5)	C(3)-C(4)	1.380(5)
C(4)-C(5)	1.377(5)	C(5)-C(6)	1.420(5)
C(6)-C(7)	1.465(5)	C(7)-C(8)	1.507(5)
C(8)-C(9)	1.369(5)	C(8)-C(13)	1.373(5)
C(9)-C(10)	1.368(6)	C(10)-C(11)	1.377(6)
C(11)-C(12)	1.335(6)	C(12)-C(13)	1.357(6)
C(14)-C(19)	1.513(5)	C(14)-C(15)	1.525(5)
C(15)-C(16)	1.523(4)	C(16)-C(17)	1.504(5)
C(17)-C(18)	1.508(5)	C(18)-C(19)	1.500(4)
C(20)-C(27)	1.471(5)	C(20)-C(21)	1.483(5)
C(21)-C(26)	1.375(5)	C(21)-C(22)	1.375(5)
C(22)-C(23)	1.376(5)	C(23)-C(24)	1.371(5)
C(24)-C(25)	1.364(5)	C(25)-C(26)	1.394(5)
C(27)-C(32)	1.388(5)	C(27)-C(28)	1.406(5)
C(28)-C(29)	1.369(5)	C(29)-C(30)	1.386(5)
C(30)-C(31)	1.350(5)	C(31)-C(32)	1.389(5)

Table 14 Bond angles [°] for PhCycH

C(7)-N(1)-C(14)	122.9(3)	C(20)-N(2)-C(19)	121.4(4)
O(1)-C(1)-C(6)	122.0(4)	O(1)-C(1)-C(2)	116.7(5)
C(6)-C(1)-C(2)	121.3(4)	C(3)-C(2)-C(1)	119.5(4)
C(2)-C(3)-C(4)	120.8(4)	C(5)-C(4)-C(3)	119.7(5)
C(4)-C(5)-C(6)	121.2(4)	C(1)-C(6)-C(5)	117.4(4)
C(1)-C(6)-C(7)	122.1(4)	C(5)-C(6)-C(7)	120.5(4)
N(1)-C(7)-C(6)	118.6(4)	N(1)-C(7)-C(8)	123.6(4)
C(6)-C(7)-C(8)	117.8(4)	C(9)-C(8)-C(13)	117.2(5)
C(9)-C(8)-C(7)	122.5(5)	C(13)-C(8)-C(7)	120.3(4)
C(10)-C(9)-C(8)	121.6(5)	C(9)-C(10)-C(11)	118.9(5)
C(12)-C(11)-C(10)	120.3(6)	C(11)-C(12)-C(13)	120.3(6)
C(12)-C(13)-C(8)	121.7(5)	N(1)-C(14)-C(19)	108.5(3)
N(1)-C(14)-C(15)	109.8(3)	C(19)-C(14)-C(15)	111.1(3)
C(16)-C(15)-C(14)	111.7(3)	C(17)-C(16)-C(15)	111.2(3)
C(16)-C(17)-C(18)	111.6(4)	C(19)-C(18)-C(17)	111.9(3)
N(2)-C(19)-C(18)	110.0(3)	N(2)-C(19)-C(14)	108.8(3)
C(18)-C(19)-C(14)	110.7(3)	N(2)-C(20)-C(27)	117.6(4)
N(2)-C(20)-C(21)	123.5(4)	C(27)-C(20)-C(21)	118.9(4)
C(26)-C(21)-C(22)	118.2(5)	C(26)-C(21)-C(20)	121.3(4)
C(22)-C(21)-C(20)	120.4(4)	C(21)-C(22)-C(23)	121.7(4)
C(24)-C(23)-C(22)	120.3(5)	C(25)-C(24)-C(23)	118.4(5)
C(24)-C(25)-C(26)	121.6(5)	C(21)-C(26)-C(25)	119.7(5)
C(32)-C(27)-C(28)	116.7(4)	C(32)-C(27)-C(20)	121.8(4)
C(28)-C(27)-C(20)	121.5(4)	C(29)-C(28)-C(27)	122.3(4)
C(28)-C(29)-C(30)	118.8(4)	C(31)-C(30)-C(29)	120.8(5)
C(30)-C(31)-C(32)	120.3(5)	O(2)-C(32)-C(27)	121.3(4)
O(2)-C(32)-C(31)	117.7(5)	C(27)-C(32)-C(31)	121.0(4)

Table 15 Selected bond lengths [Å] and bond angles [°] for [Ti(DMSALEN)Cl_2]

Ti(1)-O(1)	1.817(2)	Ti(1)-O(2)	1.826(2)
Ti(1)-N(2)	2.142(2)	Ti(1)-N(1)	2.168(2)
Ti(1)-Cl(2)	2.3406(10)	Ti(1)-Cl(1)	2.3639(10)
O(1)-C(1)	1.339(3)	O(2)-C(18)	1.339(4)
N(1)-C(7)	1.294(4)	N(1)-C(9)	1.476(4)
N(2)-C(11)	1.292(4)	N(2)-C(10)	1.474(3)
C(1)-C(2)	1.396(4)	C(1)-C(6)	1.418(4)
C(2)-C(3)	1.375(4)	C(3)-C(4)	1.383(5)
C(6)-C(7)	1.473(4)	C(7)-C(8)	1.517(4)
O(1)-Ti(1)-O(2)	109.67(9)	O(1)-Ti(1)-N(2)	164.58(9)
O(2)-Ti(1)-N(2)	85.72(9)	O(1)-Ti(1)-N(1)	85.38(9)
O(2)-Ti(1)-N(1)	164.83(9)	N(2)-Ti(1)-N(1)	79.27(9)
O(1)-Ti(1)-Cl(2)	94.73(7)	O(2)-Ti(1)-Cl(2)	91.47(8)
N(2)-Ti(1)-Cl(2)	85.47(7)	N(1)-Ti(1)-Cl(2)	85.18(7)
O(1)-Ti(1)-Cl(1)	92.65(7)	O(2)-Ti(1)-Cl(1)	94.51(8)
N(2)-Ti(1)-Cl(1)	85.02(7)	N(1)-Ti(1)-Cl(1)	86.46(7)
Cl(2)-Ti(1)-Cl(1)	168.36(3)	C(1)-O(1)-Ti(1)	138.8(2)
C(18)-O(2)-Ti(1)	135.0(2)	C(7)-N(1)-C(9)	120.2(2)
C(7)-N(1)-Ti(1)	127.9(2)	C(9)-N(1)-Ti(1)	111.5(2)
C(11)-N(2)-C(10)	120.8(2)	C(11)-N(2)-Ti(1)	127.7(2)
C(10)-N(2)-Ti(1)	111.3(2)	O(1)-C(1)-C(2)	117.6(3)
O(1)-C(1)-C(6)	121.4(3)	C(2)-C(1)-C(6)	121.0(3)
C(3)-C(2)-C(1)	120.3(3)	C(2)-C(3)-C(4)	120.0(3)
C(1)-C(6)-C(7)	123.3(3)	N(1)-C(7)-C(6)	122.3(3)
N(1)-C(7)-C(8)	120.0(3)	C(6)-C(7)-C(8)	117.7(3)
N(1)-C(9)-C(10)	110.6(2)	N(2)-C(10)-C(9)	109.3(2)
N(2)-C(11)-C(13)	121.7(3)	N(2)-C(11)-C(12)	120.2(3)
O(2)-C(18)-C(17)	118.2(3)	O(2)-C(18)-C(13)	121.3(3)

Table 16 Selected bond lengths [Å] and angles [°] for [Ti(PhSALEN)Cl_2.½THF]

Ti(1)-O(2)	1.805(4)	Ti(1)-O(1)	1.811(4)
Ti(1)-N(2)	2.140(5)	Ti(1)-N(1)	2.162(5)
Ti(1)-Cl(1)	2.329(2)	Ti(1)-Cl(2)	2.356(2)
O(1)-C(1)	1.347(8)	O(2)-C(28)	1.331(7)
N(1)-C(7)	1.298(8)	N(1)-C(14)	1.484(8)
N(2)-C(16)	1.294(8)	N(2)-C(15)	1.457(8)
C(1)-C(2)	1.399(9)	C(1)-C(6)	1.409(9)
C(2)-C(3)	1.339(9)	C(3)-C(4)	1.407(9)
C(27)-C(28)	1.397(9)	C(1S)-0(1S)	1.501(8)
C(1S)-C(2S)	1.630(13)	C(2S)-C(2S)#1	1.71(2)
O(1S)-C(1S)#1	1.501(8)		

Symmetry transformations used to generate equivalent atoms: #1 -x+1, y, _z+1/2

O(2)-Ti(1)-O(1)	110.1(2)	O(2)-Ti(1)-N(2)	85.9(2)
O(1)-Ti(1)-N(2)	162.8(2)	O(2)-Ti(1)-N(1)	164.1(2)
O(1)-Ti(1)-N(1)	85.4(2)	N(2)-Ti(1)-N(1)	78.3(2)
O(2)-Ti(1)-Cl(1)	94.3(2)	O(1)-Ti(1)-Cl(1)	97.5(2)
N(2)-Ti(1)-Cl(1)	87.0(2)	N(1)-Ti(1)-Cl(1)	86.7(2)
O(2)-Ti(1)-Cl(2)	93.4(2)	O(1)-Ti(1)-Cl(2)	89.8(2)
N(2)-Ti(1)-Cl(2)	83.0(2)	N(1)-Ti(1)-Cl(2)	83.1(2)
Cl(1)-Ti(1)-Cl(2)	167.00(7)	C(1)-O(1)-Ti(1)	137.2(4)
C(28)-O(2)-Ti(1)	139.2(4)	C(7)-N(1)-C(14)	122.5(6)
C(7)-N(1)-Ti(1)	127.1(5)	C(14)-N(1)-Ti(1)	110.2(4)
C(16)-N(2)-C(15)	118.9(5)	C(16)-N(2)-Ti(1)	127.0(4)
C(15)-N(2)-Ti(1)	113.8(4)	O(1)-C(1)-C(2)	117.8(6)
C(3)-C(2)-C(1)	119.4(5)	C(2)-C(3)-C(4)	120.5(5)
C(1)-C(6)-C(7)	122.7(4)	N(1)-C(7)-C(6)	121.0(4)
N(1)-C(7)-C(8)	121.4(4)	C(6)-C(7)-C(8)	117.6(4)
C(1S)-C(2S)-C(2S)#1	106.4(4)	C(1S)#1-O(1S)-C(1S)	124.2(8)

Symmetry transformations used to generate equivalent atoms: #1 -x+1, y, -z+1/2

Table 17 Selected bond lengths [Å] and bond angles [°] for [Ti(SLPNDM)Cl_2.THF]

Ti(1)-O(2)	1.840(2)	Ti(1)-O(1)	1.831(2)
Ti(1)-N(2)	2.166(3)	Ti(1)-N(1)	2.170(3)
Ti(1)-Cl(1)	2.3512(12)	Ti(1)-Cl(2)	2.3695(13)
O(1)-C(1)	1.348(4)	O(2)-C(19)	1.343(4)
N(1)-C(7)	1.285(4)	N(1)-C(8)	1.487(4)
N(2)-C(13)	1.286(4)	N(2)-C(12)	1.477(4)
C(1)-C(2)	1.379(5)	C(1)-C(6)	1.403(5)
O(2)-Ti(1)-O(1)	109.93(10)	O(2)-Ti(1)-N(2)	85.53(11)
O(1)-Ti(1)-N(2)	163.03(11)	O(2)-Ti(1)-N(1)	163.61(11)
O(1)-Ti(1)-N(1)	84.99(11)	N(2)-Ti(1)-N(1)	80.65(11)
O(1)-Ti(1)-Cl(2)	97.10(8)	O(2)-Ti(1)-Cl(2)	87.06(8)
N(2)-Ti(1)-Cl(2)	90.45(9)	N(1)-Ti(1)-Cl(2)	84.30(8)
O(1)-Ti(1)-Cl(1)	87.01(8)	O(2)-Ti(1)-Cl(1)	95.46(8)
N(2)-Ti(1)-Cl(1)	84.51(9)	N(1)-Ti(1)-Cl(1)	91.96(8)
Cl(2)-Ti(1)-Cl(1)	174.16(5)	Cl(1)-O(1)-Ti(1)	136.3(2)
C(19)-O(2)-Ti(1)	132.8(2)	C(7)-N(1)-C(8)	117.4(3)
C(7)-N(1)-Ti(1)	123.6(2)	C(8)-N(1)-Ti(1)	118.7(2)
C(13)-N(2)-Ti(1)	122.4(2)	C(12)-N(2)-Ti(1)	119.6(2)
O(1)-C(1)-C(2)	120.2(3)	O(1)-C(1)-C(6)	119.4(3)
C(2)-C(1)-C(6)	120.0(3)	C(3)-C(2)-C(1)	120.1(4)

Table 18 Selected bond lengths [Å] and bond angles [°] for [Zr(SLPNDM)Cl_2(THF)]

Zr(1)-O(2)	2.002(5)	Zr(1)-O(1)	2.010(6)
Zr(1)-N(1)	2.360(6)	Zr(1)-O(3)	2.369(5)
Zr(1)-N(2)	2.382(6)	Zr(1)-Cl(2)	2.487(3)
Zr(1)-Cl(1)	2.521(2)	N(1)-C(7)	1.278(10)
N(1)-C(8)	1.495(10)	N(2)-C(13)	1.290(10)
N(2)-C(12)	1.465(10)	O(1)-C(1)	1.331(9)
O(2)-C(19)	1.336(9)	C(1)-C(2)	1.389(10)
C(1)-C(6)	1.393(9)	C(2)-C(3)	1.383(10)
O(2)-Zr(1)-O(1)	119.2(2)	O(2)-Zr(1)-N(1)	156.7(2)
O(1)-Zr(1)-N(1)	77.9(2)	O(2)-Zr(1)-O(3)	73.2(2)
O(1)-Zr(1)-O(3)	70.6(2)	N(1)-Zr(1)-O(3)	129.7(2)
O(2)-Zr(1)-N(2)	78.1(2)	O(1)-Zr(1)-N(2)	152.5(2)
N(1)-Zr(1)-N(2)	80.5(2)	O(3)-Zr(1)-N(2)	137.0(2)
O(2)-Zr(1)-Cl(2)	103.3(2)	O(1)-Zr(1)-Cl(2)	112.4(2)
N(1)-Zr(1)-Cl(2)	81.8(2)	O(3)-Zr(1)-Cl(2)	75.6(2)
N(2)-Zr(1)-Cl(2)	80.8(2)	O(2)-Zr(1)-Cl(1)	84.1(2)
O(1)-Zr(1)-Cl(1)	81.6(2)	N(1)-Zr(1)-Cl(1)	83.2(2)
O(3)-Zr(1)-Cl(1)	127.6(2)	N(2)-Zr(1)-Cl(1)	79.2(2)
Cl(2)-Zr(1)-Cl(1)	156.67(8)	C(7)-N(1)-C(8)	113.5(7)
C(7)-N(1)-Zr(1)	123.9(6)	C(8)-N(1)-Zr(1)	122.6(5)
C(13)-N(2)-C(12)	113.5(7)	C(13)-N(2)-Zr(1)	123.2(6)
C(12)-N(2)-Zr(1)	123.3(5)	C(1)-O(1)-Zr(1)	137.7(5)
C(19)-O(2)-Zr(1)	138.1(5)	O(1)-C(1)-C(2)	120.7(7)
O(1)-C(1)-C(6)	118.8(7)	C(4)-C(3)-C(2)	121.9(8)

Table 19 Selected bond lengths [Å] and bond angles [°] for [Ti(ETCycH)Cl_2].$CHCl_3$

Ti(1)-O(2)	1.828(5)	Ti(1)-O(1)	1.794(5)
Ti(1)-N(2)	2.202(6)	Ti(1)-N(1)	2.182(6)
Ti(1)-Cl(1)	2.323(2)	Ti(1)-Cl(2)	2.390(3)
O(1)-C(1)	1.361(8)	O(2)-C(24)	1.349(8)
N(1)-C(10)	1.512(8)	N(1)-C(7)	1.302(7)
N(2)-C(15)	1.467(8)	N(2)-C(16)	1.483(8)
C(1)-C(2)	1.387(9)	C(1)-C(6)	1.414(9)
O(2)-Ti(1)-O(1)	99.5(2)	O(2)-Ti(1)-N(2)	81.1(2)
O(1)-Ti(1)-N(2)	158.9(2)	O(2)-Ti(1)-N(1)	98.7(2)
O(1)-Ti(1)-N(1)	82.6(2)	N(2)-Ti(1)-N(1)	76.5(2)
O(1)-Ti(1)-Cl(2)	98.4(2)	O(2)-Ti(1)-Cl(2)	162.0(2)
N(2)-Ti(1)-Cl(2)	81.7(2)	N(1)-Ti(1)-Cl(2)	82.2(2)
O(1)-Ti(1)-Cl(1)	101.4(2)	O(2)-Ti(1)-Cl(1)	91.0(2)
N(2)-Ti(1)-Cl(1)	99.7(2)	N(1)-Ti(1)-Cl(1)	168.8(2)
Cl(2)-Ti(1)-Cl(1)	86.90(9)	C(7)-N(1)-C(10)	117.9(6)
C(7)-N(1)-Ti(1)	123.6(5)	C(10)-N(1)-Ti(1)	113.8(4)
C(15)-N(2)-Ti(1)	109.4(4)	C(16)-N(2)-Ti(1)	110.1(4)
C(1)-O(1)-Ti(1)	138.9(5)	C(24)-O(2)-Ti(1)	138.7(5)
O(1)-C(1)-C(2)	119.0(7)	O(1)-C(1)-C(6)	120.2(7)
C(2)-C(1)-C(6)	120.9(7)	C(3)-C(2)-C(1)	121.9(7)
N(1)-C(7)-C(6)	121.6(6)	N(1)-C(7)-C(8)	123.1(7)

Table 20 Selected bond lengths [Å] and bond angles [°] for [Zr(omtaa)Cl_2.½THF]

Zr(1)-N(1)	2.156(7)	Zr(1)-N(2)	2.159(7)
Zr(1)-N(3)	2.160(7)	Zr(1)-N(4)	2.154(6)
Zr(1)-Cl(1)	2.498(3)	Zr(1)-Cl(2)	2.509(3)
N(1)-C(2)	1.496(10)	N(1)-C(26)	1.441(1)
N(2)-C(4)	1.362(10)	N(2)-C(6)	1.407(10)
N(3)-C(14)	1.328(10)	N(3)-C(13)	1.430(10)
N(4)-C(17)	1.338(10)	N(4)-C(19)	1.422(10)
C(1)-C(2)	1.496(10)	C(2)-C(3)	1.402(10)
C(3)-C(4)	1.370(10)	C(4)-C(5)	1.509(10)
C(6)-C(7)	1.420(10)	C(6)-C(13)	1.433(11)
C(7)-C(8)	1.392(11)	C(8)-C(10)	1.422(12)
C(10)-C(12)	1.389(11)	C(10)-C(11)	1.536(12)
N(1)-Zr(1)-N(2)	77.4(3)	N(1)-Zr(1)-N(3)	119.9(2)
N(1)-Zr(1)-N(4)	74.0(2)	N(3)-Zr(1)-N(2)	73.6(2)
N(4)-Zr(1)-N(2)	122.0(2)	N(3)-Zr(1)-N(4)	78.7(2)
N(1)-Zr(1)-Cl(1)	87.4(2)	N(2)-Zr(1)-Cl(1)	90.0(2)
N(3)-Zr(1)-Cl(1)	142.7(2)	N(4)-Zr(1)-Cl(1)	136.7(2)
N(1)-Zr(1)-Cl(2)	144.2(2)	N(2)-Zr(1)-Cl(2)	137.3(2)
N(3)-Zr(1)-Cl(2)	85.3(2)	N(4)-Zr(1)-Cl(2)	88.3(2)
C(2)-N(1)-C(26)	124.7(7)	C(2)-N(1)-Zr(1)	137.0(6)
C(26)-N(1)-Zr(1)	98.0(5)	Cl(1)-Zr(1)-Cl(2)	84.75(9)
C(4)-N(2)-Zr(1)	136.3(6)	C(6)-N(2)-Zr(1)	98.0(5)
C(13)-N(3)-Zr(1)	99.0(5)	C(14)-N(3)-Zr(1)	136.2(6)
C(17)-N(4)-Zr(1)	135.6(6)	C(19)-N(4)-Zr(1)	98.2(4)
N(1)-C(2)-C(3)	120.6(8)	C(1)-C(2)-C(3)	116.7(8)

Table 21 Selected bond lengths [Å] and bond angles [°] for $[Al(EtSALEN)MeAlMe_2]^+[AlCl_3Me]^-$

Al(1)-O(1)	1.846(7)	Al(1)-O(2)	1.875(7)
Al(1)-C(21)	1.908(12)	Al(1)-C(22)	1.936(11)
Al(1)-Al(2)	2.899(4)	Al(2)-O(1)	1.870(7)
Al(2)-O(2)	1.884(7)	Al(2)-C(24)	1.925(11)
Al(2)-N(2)	1.954(9)	Al(2)-N(1)	1.970(10)
Al(3)-C(23)	1.949(12)	Al(3)-Cl(11)	2.124(5)
Al(3)-Cl(13)	2.130(5)	Al(3)-Cl(12)	2.155(5)
O(1)-C(1)	1.377(12)	O(2)-C(20)	1.361(11)
N(1)-C(7)	1.307(13)	N(1)-C(10)	1.487(10)
N(2)-C(12)	1.288(14)	N(2)-C(11)	1.472(13)
C(1)-C(2)	1.37(2)	C(2)-C(3)	1.35(2)
O(1)-Al(1)-O(2)	77.5(3)	O(1)-Al(1)-C(21)	112.0(5)
O(2)-Al(1)-C(21)	115.0(5)	O(1)-Al(1)-C(22)	113.6(5)
O(2)-Al(1)-C(22)	109.8(5)	C(21)-Al(1)-C(21)	121.0(6)
O(1)-Al(2)-O(2)	76.7(3)	O(1)-Al(2)-C(24)	104.7(4)
O(2)-Al(2)-C(24)	115.7(4)	O(1)-Al(2)-N(2)	149.7(4)
O(2)-Al(2)-N(2)	87.8(3)	C(24)-Al(2)-N(2)	105.5(5)
O(1)-Al(2)-N(1)	88.2(3)	O(2)-Al(2)-N(1)	136.2(4)
C(24)-Al(2)-N(1)	107.8(5)	N(2)-Al(2)-N(1)	85.1(4)
C(1)-O(1)-Al(1)	131.4(6)	C(1)-O(1)-Al(2)	124.8(6)
C(20)-O(1)-Al(2)	128.0(6)	C(20)-O(2)-Al(2)	130.2(6)
C(7)-N(1)-C(10)	119.1(10)	C(7)-N(1)-Al(2)	128.3(8)
C(10)-N(1)-Al(2)	112.5(7)	C(12)-N(2)-C(11)	121.6(10)
C(11)-N(2)-Al(2)	107.5(7)	C(2)-C(1)-C(6)	121.3(10)
C(1)-C(2)-C(3)	119.8(12)	C(2)-C(3)-C(4)	121.9(14)

Table 22 Bond lengths [Å] and bond angles [°] for Mepy

N(1)-C(3)#1	1.339(2)	N(1)-C(3)	1.339(2)
N(2)-C(5)	1.452(3)	N(2)-C(4)	1.459(2)
N(3)-C(9)#1	1.386(4)	N(3)-C(9)	1.386(4)
N(3)-C(8)	1.517(4)	N(3)-C(8)#1	1.517(4)
N(3)-C(7)	1.519(4)	N(3)-C(7)#1	1.519(4)
C(1)-C(2)	1.378(2)	C(1)-C(2)#1	1.378(2)
C(2)-C(3)	1.385(2)	C(3)-C(4)	1.514(2)
C(5)-C(6)	1.512(14)	C(5)-C(10)#1	1.554(14)
C(6)-C(7)	1.526(14)	C(9)-C(10)	1.512(12)
C(5)-C(10)	1.554(14)		
C(3)#1-N(1)-C(3)	119.0(2)	C(5)-N(2)-C(4)	113.0(2)
C(9)#1-N(3)-C(9)	141.6(3)	C(9)#1-N(3)-C(8)	47.6(2)
C(9)-N(3)-C(8)	110.1(3)	C(9)#1-N(3)-C(8)#1	110.1(3)
C(9)-N(3)-C(8)#1	47.6(2)	C(8)-N(3)-C(8)#1	65.3(4)
C(9)#1-N(3)-C(7)	61.1(2)	C(9)-N(3)-C(7)	114.1(3)
C(8)-N(3)-C(7)	106.2(2)	C(8)#1-N(3)-C(7)	141.9(3)
C(9)#1-N(3)-C(7)#1	114.1(3)	C(9)-N(3)-C(7)#1	61.1(2)
C(8)-N(3)-C(7)#1	141.9(3)	C(8)#1-N(3)-C(7)#1	106.2(2)
C(7)-N(3)-C(7)#1	56.3(3)	C(2)#1-C(1)-C(2)	119.1(2)
C(1)-C(2)-C(3)	119.0(2)	N(1)-C(3)-C(2)	121.9(2)
N(1)-C(3)-C(4)	114.21(14)	C(2)-C(3)-C(4)	123.8(2)
N(2)-C(4)-C(3)	113.35(13)	N(2)-C(5)-C(6)	123.1(3)
N(2)-C(5)-C(10)#1	103.5(3)	C(6)-C(5)-C(10)#1	19.8(4)
C(5)-C(6)-C(7)	111.8(8)	N(3)-C(7)-C(6)	118.1(4)
N(3)-C(9)-C(10)	114.6(5)	C(9)-C(10)-C(5)#1	120.4(7)

Symmetry transformations used to generate equivalent atoms: #1 x, -y+1/2, z